ALLOY DESIGN

Edited by
S. RANGANATHAN
V. S. ARUNACHALAM
R. W. CAHN

INDIAN ACADEMY OF SCIENCES
Bangalore 560 080

ACADEMY PUBLICATIONS IN ENGINEERING SCIENCES

General Editor: R. Narasimha

Volume 1. The Aryabhata Project
Edited by U. R. Rao, K. Kasturirangan

Volume 2. Computer Simulation
Edited by N. Seshagiri, R. Narasimha

Volume 3. Rural Technology
Edited by A. K. N. Reddy

Volume 4. Alloy Design
Edited by S. Ranganathan, V. S. Arunachalam, R. W. Cahn

ALLOY DESIGN

Edited by

S. RANGANATHAN
Banaras Hindu University, Varanasi

V. S. ARUNACHALAM
Defence Metallurgical Research Laboratory, Hyderabad

R. W. CAHN
University of Sussex, U.K.

INDIAN ACADEMY OF SCIENCES
Bangalore 560 080

Reprinted from the Proceedings of the Indian Academy of Sciences,
Engineering Sciences,
Volume 3, pp 253–349, 1980
Volume 4, pp 1–56, 1981

Edited by S. Ranganathan, V. S. Arunachalam and R. W. Cahn and printed for the
Indian Academy of Sciences by Macmillan India Press, Madras 600 002, India

CONTENTS

Foreword

Science has been late in coming to metallurgy. Until the last century, empirical knowledge together with the metal craftsmanship accumulated over generations provided all the metals and alloys that society needed. The leap from the art to the science of alloy making came with the discovery of structure: structure within the atom, in the arrangements of atoms, and in the distribution of aggregates of atoms. In this hierarchy of structures, the metallurgist made microstructure his very own. With the experience accumulated over a century he began to find connections between structure and properties, and simultaneously, he began to understand how microstructure develops. In spite of this, the day is still far distant when we can confidently say that to know the structure is to know the properties, and vice versa! How quickly we reach this state of knowledge will depend on how well we can grasp, not only the details of structure at various levels, but also how they are linked to each other.

Together with the emergence of the possibility of ' designing ' alloys, technology has rapidly grown to envisage processes which occur under widely varying temperatures and aggressive environments. Steels—which for a long time appeared to have all the properties an engineer could ask for—were found to be inadequate for some uses. Thus nickel, titanium and zirconium alloys came into existence to meet some of the challenges posed by the designer. And now, our environmentalists and conservationists have rung a clear warning bell: technologies with inbuilt obsolescence must be on their way out. Materials must now not only be stronger, but more durable and last in service over longer periods. The optimum use of material for a given application requires that we reduce the factor of safety (an index of our ignorance) in design. A classic example is the emerging use of the fracture toughness criterion in materials specification, opening the way for the use of intrinsically defective materials with greater confidence.

This volume brings together a series of articles which cover comprehensively these various facets of the science of alloy design. Robert Cahn provides a historical perspective, while Burte and Gegel summarise the science of ' Metallurgical Synthesis '. Specific means of strengthening a metal through processing, alloying and microstructure control are then evaluated. One article is devoted to the development of steels. Finally, the application of these principles in the design of titanium and zirconium alloys in two critical technology areas, the nuclear and aerospace industries, is described.

We feel this to be an opportune moment to review and assess our understanding of the behaviour of crystalline materials: for this decade marks the transition to a totally new concept in the design of alloys—the use of amorphous structures for a

wide variety of applications. As presaged in one of the articles, understanding the properties of metallic glasses will increasingly occupy the attention of metallurgists and material scientists in the years to come.

S RANGANATHAN
V S ARUNACHALAM
R W CAHN
Special Editors

Alloy design: a historical perspective

R W CAHN
University of Sussex, Falmer, Brighton, U.K.

MS received 10 January 1980

Abstract. This paper presents a historical perspective of the progress of mankind from the bronze age to the present stage in alloy development. In particular, the last four decades have seen empiricism giving way to intelligent and informed design of alloys. A spectacular example from this decade is the design of metallic glasses with optimum magnetic properties in 1979.

Keywords. History of metallurgy; alloy design; microstructures.

The first age of high material civilization, after the crudities of neolithic man, is today known as the *bronze age*. The first metallic material used by man to make tools, weapons and priestly objects was an alloy—or rather a range of alloys incorporating mainly copper, tin and arsenic—not a more or less pure native metal. Copper would not have made much of a sword or kitchen knife and would have been impossible to cast into the convoluted dragons of a thin-walled Chinese funerary urn. Only man's (and woman's) vanity required the malleability and beauty of pure gold, and where gold was concerned, unauthorised alloying was apt to lead to the dishonest metallurgist's decapitation.

Other copper alloys were introduced long before the scientific era of metallurgy. Thus, in the early twelfth century AD, the German monk Theophilus, in the earliest European manuscript on the metallurgical arts, describes how to make a hard solder out of one part of copper and two parts of silver, so that a silver handle might be soldered on to a silver church chalice.

The *iron age* which followed the bronze age was a long period of very slow and wholly empirical development; we are still in the declining years of that age. C S Smith tells us that it was not till the late eighteenth century that the identity of carbon as the essential alloying element for quench-hardening was first recognised, and until that time the hardening and tempering of iron alloys was an erratic, rule-of-thumb affair, at any rate in Europe. The craftsmen of Japan, India and Mesopotamia developed steel swords of very high and consistent quality long before the Europeans did, but their skills were nevertheless wholly empirical. It needed a combination of coke-based ironmaking, steel converters with blast, exact chemical analysis and accurate thermal measurements to make possible the development of steels with consistent properties, and this combination was not complete until well into the nineteenth century. By this time the crucial processes of quenching and tempering were well understood and it at last ceased to be necessary to assess the progress of tempering in terms of interference colours formed on the steel surface during the reheating operation.

Some crucial developments which paved the way to alloy development as we understand it today came in just that decade, 1896–1906, which also turned physics upside down. Just after Röntgen had discovered x-rays and ushered in that remarkable decade, Roberts-Austen, building on the work of Osmond, in 1896 published the first true constitutional diagram of the iron-carbon system; Roozeboom the following year further improved it. Heycock and Neville in 1903 produced a superb constitutional diagram for the copper-tin system, and thereby opened the way to the subsequent great flood of constitutional work which is the bedrock of modern alloy design. To connoisseurs of the historical fitness of things it is satisfying that the first accurate constitutional diagrams referred to the two alloy types which were first used on a large scale by man.

Two of the earliest major alloys to be discovered came from this same period. Tungsten steel had first been made by Mushet in 1868, but drastic improvements in lathe cutting tool performance awaited the systematic researches by Taylor and White, in 1898, on the heat-treatment of high-tungsten steels. Again, in 1899 Barrett and Hadfield stumbled upon the low-hysteresis silicon-iron, which ever since then has been used to build electrical transformers.

Two further developments ushered in the modern era: one was the discovery of x-ray diffraction by von Laue and the other, the resolute turning of metallurgy away from a chemical to a physical orientation, largely the doing of Rosenhain. It is difficult now to realize that at the end of the nineteenth century, metallurgists were quite uncertain about the crystalline nature of metals and alloys. Osmond in 1900 was still inclined to believe that only ' grains ' with geometrically regular external shapes were truly crystalline, and Rosenhain was one of the main protagonists of the view that amorphousness was common in alloys, and especially at grain boundaries, slip bands and polished surfaces. ' Beta-iron ' (that is, alpha-iron above its Curie temperature) was thought by some, including Rosenhain, to be an amorphous form of iron. The American metallurgist Howe in 1902 at length considered the ' essence of crystalhood ' and took the modern view of the matter, without which the later studies of plastic deformation, recrystallisation and alloy phases would have been impossible.

We have now reached the period of modern scientific metallurgy. Practice still had a very long lead over understanding: to appreciate this, one has only to contemplate the discovery of age-hardening in duralumin. It was a German engineer, Wilms, who in 1906 stumbled upon age-hardening in an Al-Cu-Mn-Mg alloy: he had hoped to demonstrate solution-hardening but to his disappointment his freshly quenched alloy was very soft. Purely by chance, he discovered that it hardened with the passage of time. It was then another 13 years before Merica, Waltenberg and Scott in America demonstrated the decreasing solubility of copper in aluminium with falling temperature (most of the early phase diagrams from Tammann's school were rather rough and ready), and drew the conclusion that age-hardening must be associated with the delayed precipitation of a second phase, *albeit* invisible in the microscope. That phase was not detected till Guinier and Preston in 1937–38 found it by x-ray diffraction, and not seen in the microscope till the 1950's; but Merica's simple hypothesis of 1919, unconfirmed though it was for many years, sufficed to guide other metallurgists into the intelligent—and successful—search for other age-hardening alloys, such as Al/Mg_2Zn and Cu/Be. According to Mehl, no new age-hardening alloys were discovered during the years 1906–19, the period during which age-hardening had remained an empirical mystery. Nothing could demonstrate more clearly how crucial

is the formulation of a hypothesis, even an unconfirmed one, in both limiting the area of search and in providing a psychological stimulus for experimental scientists to search for further exemplars of the hypothesis. This is how most alloys are designed.

The first half of the present century saw the development and improvement of a range of industrial alloys on a basis which, while largely empirical, was generally related to the simultaneous determination of binary or ternary phase diagrams. The development of the Fe-Ni-Cr stainless steels by Brearley was a case in point, and the gradual improvement of high-speed tool steels, another. It is to be noted that sometimes the introduction of a new composition (which is what we normally mean by ' alloy development ') is inseparable from the invention of a new process for manufacturing the material. An early example of this was Coolidge's invention in 1910 of a process to make ductile tungsten filaments by powder metallurgy followed by drawing down of the sintered rods. The secret lay in the addition of ' dopants '—potassium, silicon and aluminium in minute but essential quantities—so that tungsten for lamp filaments is properly to be regarded as an alloy, dilute though it is. Not only were the dopants needed to render the tungsten more ductile, they also conferred long life on the filaments. Dutch metallurgists discovered later that a vital consequence of the presence of the dopants was to destabilise transverse grain boundaries and enhance longitudinal ones, which is what prevents the whitehot filament from sliding apart at a transverse boundary. Such lessons are never quite lost in metallurgical history: the recent introduction of directionally solidified turbine blades, containing only longitudinal grain boundaries, undoubtedly owed something to the early researches on tungsten filaments. The reason for the efficacy of the tungsten dopants was established only during the past decade, by high-resolution electron microscopy. Only now is it understood that rows of minute bubbles, generated by vaporisation of compounds formed by the dopants, are strung out during wire-drawing and it is these rows that stabilise longitudinal grain boundaries.

Quite generally, throughout this century, the electrical industry, always research-intensive in all its aspects, has been a prime mover in alloy improvement. Indeed, this attitude can be traced back to Matthiessen, the English physicist who in the 1860s measured the electrical conductivity of many alloy systems and first distinguished the effect of dissolved alloying additions from that due to second phases: thereby he gave his name to Matthiessen's Law. Much later, Bozorth at Bell Telephone Laboratories, Honda in Japan and others developed a large range of soft and hard magnetic alloys, including invars in which zero thermal expansion was clearly related to a shifting Curie temperature—an early example of conscious alloy design. A great deal of ingenuity went even into so humble a problem as developing alloys for telephone relay reeds. The electrical industry was also responsible for a major piece of alloy development when it improved Barrett's silicon-iron for transformer laminations, by conferring upon it a strong crystallographic texture; grain-oriented silicon-iron with the ' Goss ' texture involved a sophisticated combination of minor dopants with precisely controlled heat-treatment schedules. Generally, it is in the electrical industry that the crucial role of minor dopants was first established, so that the industry was psychologically prepared for the postwar years when silicon needed to be laced with parts per million of electrically active dopants in a precisely defined geometry.

Alloy development programmes such as that leading to grain-oriented silicon-iron

focussed attention on the importance of precisely defined heat-treatments. It is no exaggeration to say that systematic improvements in heat-treatment schedules can sometimes so improve the properties of a long-established alloy that it virtually becomes a new industrial material. A good illustration of this principle is work done in recent years at the Centre for the Design of Alloys at the University of California, Berkeley. It was shown that the fracture toughness, K_{IC}, of standard AISI 4340 steel can be increased by over 50% by increasing the austenitising temperature from 870° to 1200°C (but still slow-cooling to 870°C before quenching). The austenite grain size is of course increased, but this unfavourable factor is outweighed by the much increased amount of retained austenite after quenching; this is soft and so arrests advancing microcracks. A marageing steel can be greatly toughened by a similar strategy. It is perhaps desirable that the concept of ' alloy design ' should be broadened to cover not only chemical composition (including trace elements) but also all aspects of processing.

Two well-known examples of the use of minor additions to inhibit undesirable effects of an unavoidable processing step—namely, solidification—are the ' modification ' of cast aluminium-silicon alloys by the addition of traces of sodium, and the conversion of graphite in cast iron from flake to nodular form by the addition of magnesium to the melt. The fact that theorists are still arguing about the mode of action of the sodium, more than half a century after its introduction, does not diminish its utility.

The search for new age-hardening alloys after 1919 was perhaps the first period when the recognition of a correlation between a fundamental feature and a desirable property guided a search within manageable limits: the totality of all possible alloy systems was reduced to those compositions for which supersaturation and precipitation might be anticipated. After 1950, following the verification of the dislocation hypothesis and the apotheosis of the electron microscope and microprobe, this kind of rationally restricted empiricism became much more frequent. This really is what is meant by ' alloy design '; the notion of design *ab initio*, by pure cerebration without recourse to experiment, is not one ever entertained by serious metallurgists. The story of the discovery and steady improvement of superalloys for gas turbines is the most impressive illustration of this procedure. Once the symbiosis of γ and γ' was recognised as the central basis of superalloy constitution, and once dislocation theory had shown how lattice parameter mismatch and γ' particle size and spacing related to creep resistance, the way was open to an intelligent incremental process of alloy improvement, always guided by microscopy and x-ray diffraction. Alloys rarely spring fully formed from their originators' investigations; almost always it is a process of incremental improvement of constitution and microstructure, just as it is with engineers' macrostructures of all kinds.

Superplastic alloys have developed during the past decade in a similar way to superalloys: once it became clear that what is needed is a microstructure which is both very fine-scale and very stable, it became possible to proceed rationally in the search for alloys with these characteristics, whether they were aluminium alloys or steels.

Sometimes, insight into microstructural processes has enabled gifted metallurgists to design alloys in such a way as to develop desired properties by means of a novel approach. Perhaps the most original example of this was Zackay's invention of

TRIP (transformation-induced plasticity) steels at Berkeley a few years ago. Orowan and Irwin, 25 years earlier, had recognised that in the simple Griffith energy-balance approach to the spread of a crack under stress, one had to allow for the possibility that plastic deformation in the vicinity of the crack tip would absorb extra energy (raising the effective surface energy of the crack faces). Zackay saw that the energy required to bring about a localised martensite transformation could play the same role as the energy associated with plastic deformation, and he also knew that high stresses can enhance martensitic shear transformations. (This had become progressively clear ever since the discovery by Hadfield in the last century of his manganese steel, which was used for railway points because it hardened under impact). On the basis of these insights, Zackay designed a steel which was just stable against martensitic transformation at ambient temperature in the absence of stress, but did transform under the action of the high stress at a crack tip when the steel was loaded. The crack cannot then find the energy needed to allow it to proceed. The local transformation inhibits brittle fracture; another way of regarding it is that transformation induces local plasticity, indeed a martensite change constitutes plastic deformation. This approach is one way of resolving the ancient paradox which has so severely restricted the use of strong ceramics in engineering: high static fracture strength implies low toughness. Indeed, 'alloyed' zirconia has been developed that is toughened in a similar way to TRIP steel.

The electrical industry is not the only area of advanced technology that has fostered striking advances in alloys. The American space programme led to a need for ultrastrong and tough materials for rocket casings and this need did much to accelerate research on marageing steels, to quote just one example. The nuclear industry has created an entirely new category of need, namely, the development of alloys to withstand growth, swelling, creep and brittle fracture under bombardment by neutrons and fission fragments. The earliest example was the need to find ways of stopping metallic uranium rods from turning into long, slender snakes after irradiation or thermal cycling. (The behaviour of the earliest uranium fuel rods must have been profoundly alarming to the metallurgists of the Manhattan Project!) It turned out that the important thing was to get rid of crystallographic texture in the rods, without allowing the grain size to become too large. This could be achieved by rapid polymorphic transition by a process formally akin to the later process of zone-refining. To secure a microstructure that was both random and fine-grained, it was found necessary to 'adjust' the metal by doping it with small amounts of iron and aluminium.... yet another instance of the importance of trace alloying additions. That was 35 years ago. Today, one of the main battles is against void-swelling in structural alloys for fast reactors, and here the last three years have brought a flood of research on the strange process of non-equilibrium solute segregation to alloy surfaces in the presence of a vacancy flux brought on by irradiation. The latest findings suggest that the addition of small amounts of certain solutes such as silicon to nickel-base alloys can help to neutralise both the segregation of other solutes and the tendency to form voids which is linked with the vacancy flux. Doping may once again come to the rescue.

New production methods can offer new scope to alloy designers. The most promising instance is the development of rapid solidification processing: the rapid quenching of small melt droplets by spraying into helium offers scope for retaining large amounts of solute in metastable solid solution, and subsequent warm isostatic

pressing can make ready-shaped products out of such powders without causing undesired precipitation of second phases. This stage of alloy design is just now getting under way. A related, very recent field of research is the design of highly alloyed metallic glass strips so as to optimise magnetic properties. At the end of 1979, it appeared highly probable that such glasses will soon begin to displace the grain-oriented silicon-iron from the cores of electric distribution transformers. Three laboratories have independently established that a composition close to $Fe_{82}B_{12}Si_4C_2$ gives the best compromise between high magnetisation, high permeability, low hysteresis and low eddy current loss. When competing investigators independently design almost the identical complex alloy, then alloy design may be said to have come of age.

Select Bibliography

Aitchison L 1960 *A history of metals* (London: Edward Arnold and Interscience)

Cahn R W 1973 *Modern practice in the design of strong alloys*, Journal of Metals (AIME), February, p. 1 *Microstructure and the design of alloys*, Inst. of Metals, London, 1973

Decker R F 1973 Alloy design, using second phases, *Met. Trans.* **4** 2495

Mehl R F 1965 The historical development of physical metallurgy, in *Physical metallurgy*, ed. R W Cahn (Amsterdam: North-Holland Publishing Co.) p. 1

Parker E R & Zackay V F 1974 *Fundamentals of alloy design*, CRC Critical Reviews in Solid State Sciences, p. 591

Smith C S 1960 *A history of metallography* (Chicago: University Press)

Metallurgical synthesis

H M BURTE and H L GEGEL
Air Force Materials Laboratory, Wright-Patterson Air Force Base, Ohio 45433, USA

MS received 14 February 1980

Abstract. Materials science has matured to the point where it can begin to be employed with other sciences such as mechanics in an interdisciplinary mode to permit the total metallurgical synthesis of components. Research is needed on topics such as material behaviour modelling, process mechanics and interface effects. The potential for increased productivity, decreased response time and increased reliability is presented in this paper, as are the possibilities of controlled microstructural gradients leading to more efficient products.

Keywords. Metallurgy; microstructure; synthesis; processing maps; process model; constitutive equations; yield function; lubrication.

1. Introduction

The discipline of alloy design has been very active in recent years. During this time, considerable attention has been given to the roles of crystallography and microstructure in the prediction and rationalization of properties, and some attempts have also been made to relate mechanical properties to electronic bonding (Collings & Gegel 1975). We still do not possess the complete capability to specify composition and microstructure *ab initio* to achieve property goals, but great strides have been made (Jaffee 1973). However, the ability to create, in a controlled manner, the materials structure which will lead to desired properties, even where the former can be predicted, has received much less emphasis. This paper will briefly describe some approaches available to the alloy synthesizer, illustrate some roadblocks, and suggest some opportunities for research in the future.

2. Metallurgical synthesis

Historically speaking, the fundamental properties that are important in the design of alloys, have been studied separately and in an unrelated manner. Some of these are: (1) electronic effects, (2) thermophysics effects, (3) thermoeleastic effects, and (4) thermoplastic effects. The inter-relationship of these variables with structural features is shown in table 1. Several of the more important goals of materials science have been to predict the thermoplastic properties and the fracture behaviour as a function of composition and microstructure in a finished shape. Metallurgical synthesis, then, must create this finished shape with desired properties.

A convenient way to define and illustrate metallurgical synthesis in the broader

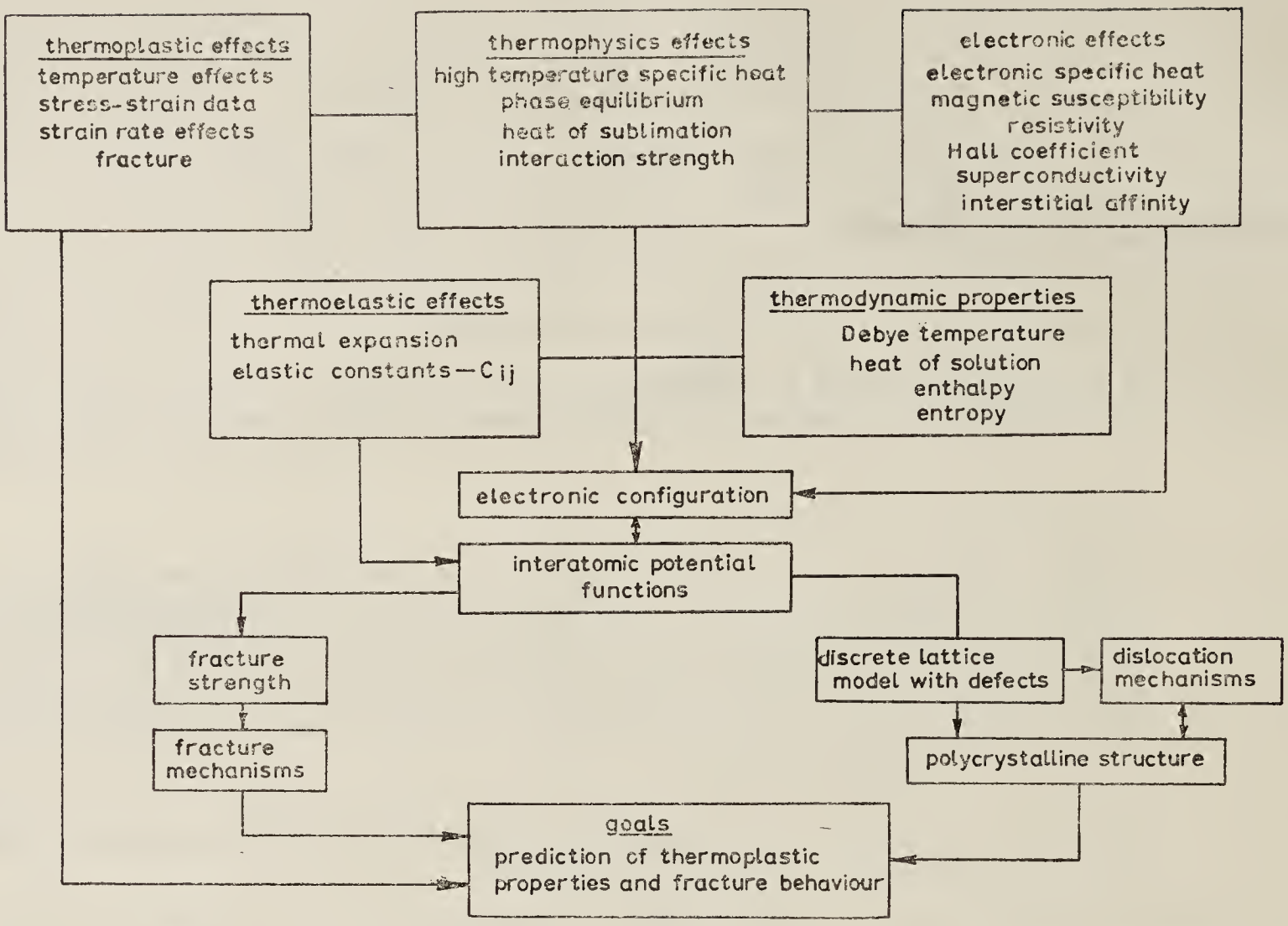

Table 2. The science of welding titanium (illustrative rather than all-inclusive)

Processing (synthesis)	Structure	Properties	Use
GTAW	Inclusion type and morphology	Yield strength	Wing box
PAW	Amount of beta phase	Bend radius	Spars, ribs
EBW	Alpha platelet size	Hardness	Landing gear
Pulsed current	Grain size	Ultimate strength	Turbine discs
Preheat	Dislocation content	Fracture toughness	Tubing
Post heat	Interstitial segregation	Corrosion resistance	Heat exchangers
Joint preparation	Pore size & distribution	Lap shear strength	Engine frames
Arc gas	Residual stress level		
Travel speed	Composition variations		
Heat input			
Filler composition			
Degree of constraint			

context of materials science starts with a conceptual framework suggested (Buessem 1963) to describe ceramic science, which can be modified and used for any area of materials science and technology (Ault & Burte 1966 and Burte 1978). Its application to titanium welding is illustrated in table 2. The engineering art of welding normally attempts to correlate preparation or processing conditions (including composition of input materials), with commonly measured properties. Processing conditions are modified until the desired or satisfactory properties are attained. The first step in converting this art to a science involves inserting knowledge of the materials structure between the processing conditions and properties. The familiar subjects of physical metallurgy, polymer physics, etc. are, of course, the areas of materials science which

are concerned with elucidating structure-property relationships, and this was the topic of table 1. Next, the definition of what properties to measure for the purpose of initial engineering design or to predict performance during actual service should be based on more than long experience or intuition. The expanding development and use of the science of fracture mechanics is a good example of such acitivity. Finally, given the knowledge of which structures can yield properties appropriate for the intended use, the goal of processing is to synthesize this structure. (The term ' synthesis,' although more familiar to the chemist dealing with polymeric materials than to the metallurgist or ceramist, is quite appropriate for all materials). Synthesis research is, in part, concerned with how to do this, and it can thus be differentiated from the other areas of materials science which involve structure $\leftrightarrow$ properties, or properties $\leftrightarrow$ use relationships.

In a more general sense, the goals of processing/synthesis are to:

(i) achieve the desired geometry (size, shape and tolerance) of a part or component with adequate defect control;
(ii) develop a controlled microstructure to yield the desired properties and in-service performance;
(iii) optimize economic aspects of production, including the conservation of materials and energy.

The term ' microstructure ' as used here includes the composition and its distribution, and the scale of structures may be on any level. Thus, metallurgical synthesis includes the creation of any desired structure—electronic, point defect, dislocation, grain, or macro—by control of composition and processing to achieve optimum properties in a metal or alloy.

Many engineers still think of ' processing ' primarily in terms of the first goal given above. Obtaining desired microstructures and properties is considered to be the function of subsequent and often unrelated post processing ' heat treatment.' Increasingly, as materials are developed and used whose properties are a function of their entire processing history, it will be necessary to consider goals (i) and (ii) *together*, to attempt a total synthesis of a component. The alloy synthesizer, in the future, must attempt to use processing to control and perhaps effect trade-offs or compromises between microstructures, absence of defects, and geometry, while also finding the economic optimum demanded by goal (iii). Metallurgical synthesis research attempts to provide the knowledge which will encourage concurrent attainment of these goals. To illustrate, for metal working operations such as extrusion, forging, rolling or sheet metal forming, it attempts to answer the following fundamental questions:

(i) What conditions does the forming process demand that the workpiece material withstand?
(ii) How does the workpiece material respond to the demands imposed by the process?

How can workability limits for a given material and process sequence be predicted so that the desired geometry can be obtained without gross defects? How can the environment of, and changes occurring to, each differential volume element of the

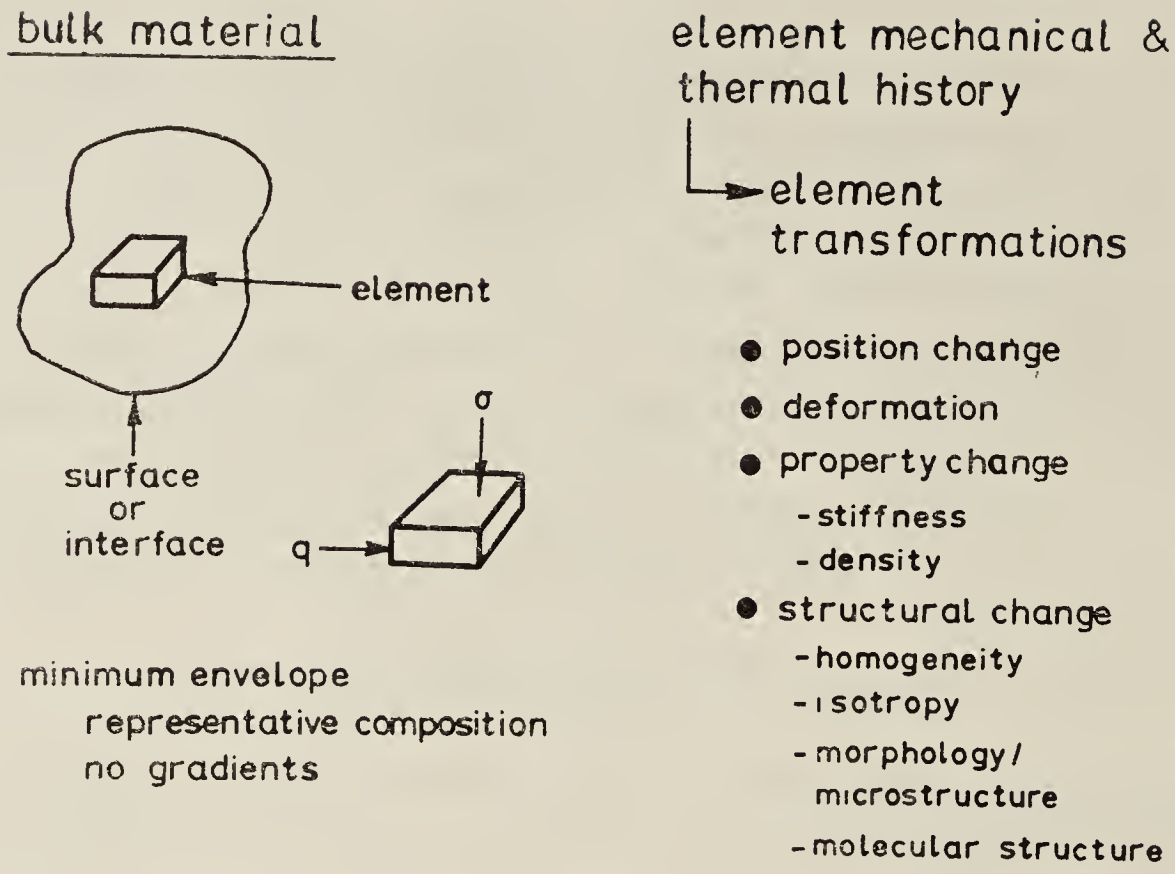

Figure 1. Each elemental volume, element of material must be tracked through the deformation zone to control microstructure/properties (F Kelley 1977, private communication)

material, as partially illustrated in figure 1, be tracked throughout the entire process to permit predicting and/or controlling the microstructure of the final product? Answering these questions can involve either theoretical analysis or empirical correlations, or most effective, a combination of these.

3. An illustration of metallurgical synthesis

To stimulate the interdisciplinary cooperation which will be necessary for effective metallurgical synthesis research it is desirable to identify some goals which cannot easily be attained within the current ' state-of-the-art.' These must be carefully selected so as to foster not only actual transition to use (and thus enthusiasm and support) but generic advances in the underlying science base. An example of such is an R & D programme to develop the technology base for demonstrating the feasibility for producing a dual property titanium alloy compressor disk (Burte & Gegel 1980). The specific goal, illustrated in figure 2, is to synthesise a disk that has different microstructures in the bore and rim regions, to emphasize low cycle fatigue (LCF) and burst strength (ultimate tensile strength, UTS) in the bore, and creep strength (without sacrificing fracture toughness) in the rim. The generic goal is the development and use of material lubrication and process models that will eventually be incorporated in an interactive computer program to allow designing a forging process that can produce such parts. Five areas which must be integrated are:

(i) Material behaviour modelling under conditions of processing,
(ii) Process mechanics,
(iii) Interface effects or boundary condition modelling,
(iv) Microstructure/property relationships in the finished shape, and
(v) The manufacturing system.

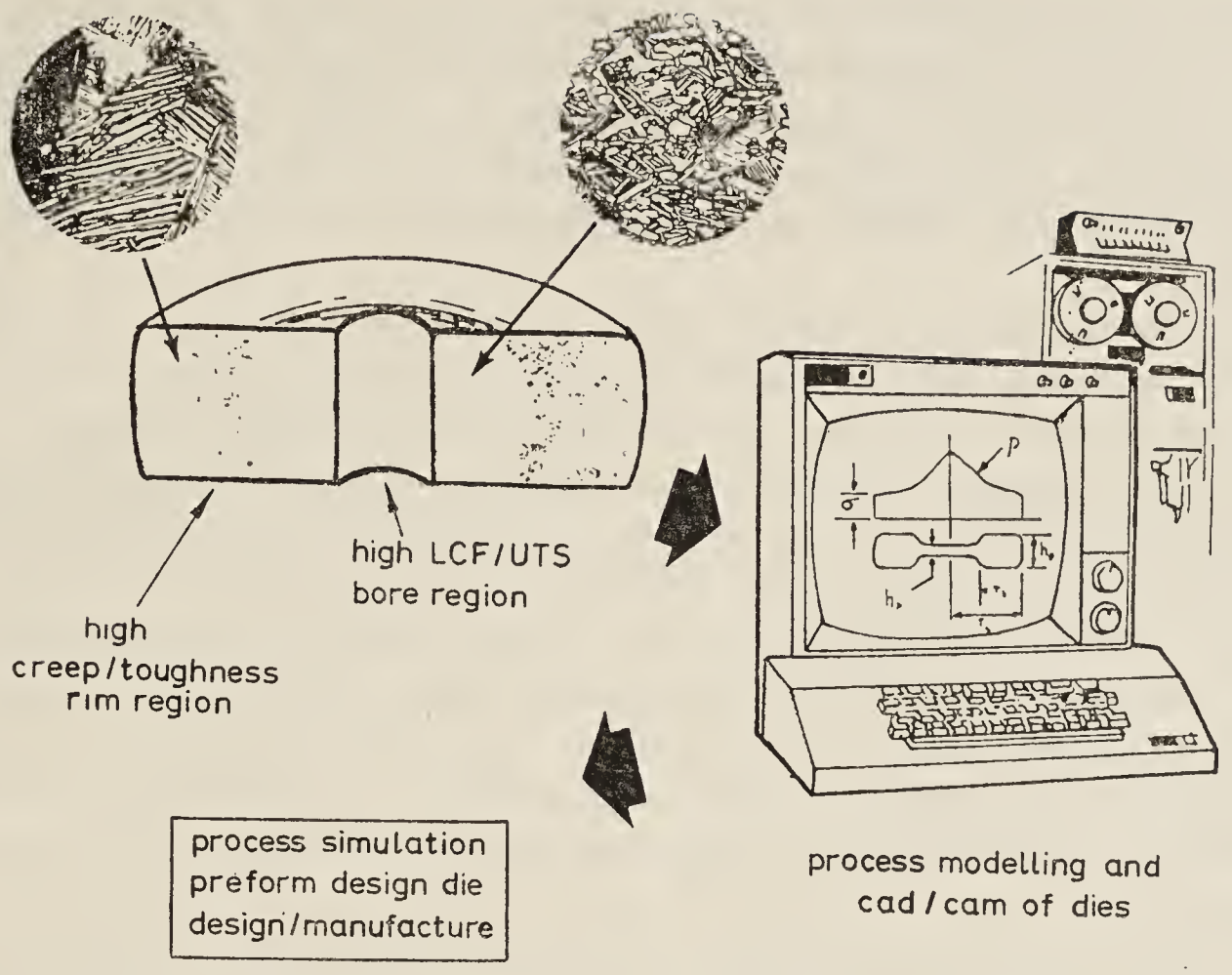

Figure 2. Air Force programme for a dual property titanium disk.

Material behaviour under actual processing conditions centres around the workpiece material's strain hardening behaviour, strain rate sensitivity, recrystallization, and phase transformation characteristics, and related sub-problems. It is concerned with quantitative relationships that make it possible to describe how a workpiece responds to the demands of the process and to predict whether or not a given geometry can be achieved without forming defects. Each bulk deformation process has different forming limit criteria, and empirical forming limit diagrams for forging are being developed. An analytical approach to predicting forming limit curves from constitutive equations is also being pursued, since it would increase the process design flexibility and control capability of the overall model. A significant research goal is the development of inelastic constitutive equations that contain evolutionary parameters to describe the current state of the system and microstructure. To verify these will then require reliable data, obtained under conditions of processing, on technological materials such as the multi-phase Ti-6Al-2Sn-4Zr-2Mo-.1Si (Ti-6242) alloy being considered.

Process mechanics attempts to describe the time-temperature-deformation path through the deformation zone; this influences the microstructure and the texture and thus the mechanical properties of the final disk. Since titanium alloys are anisotropic materials and have microstructures and phase transformation that can induce or trigger plastic instability phenomena, the effect of these must be introduced into the finite element or other numerical analysis routines normally used for such modelling. Some method for this which does not necessarily lead to a departure from standard procedures, as well as fast computational methods that will be feasible for the eventual interactive computer program, must be developed.

The boundary conditions for the process model are provided by the tool/workpiece interface. In forging, as with many other processes, the interface conditions although often controlling, are little known. Key areas for attention are effective

heat transfer coefficients between the workpiece and the tooling, and interface friction factors. Data and an understanding of the basic mechanisms must be sought, and an attempt must be made to develop a satisfactory interface model to contribute to the overall model. The generation of defects such as voids and shear bands is related to both friction and workability as well as the process variables of temperature and strain rate.

The material behaviour modelling must develop a series of processing-microstructure maps that can be used in conjunction with workability, process mechanics and interface descriptions to design a manufacturing process which will yield controlled microstructure gradients. Property-microstructure studies of specimens machined from sub-scale compressor disks will evaluate and guide progress toward this synthesis. A key to the process may be the design of forging preforms of appropriate starting geometries, perhaps themselves containing composite microstructures. For example, controlled thermal treatment of the preform might permit it to have an alpha+beta structure in the region that flows to form the bore, and a transformed beta structure in the region that flows to form the rim. In such a case, models with the capability to handle modular analyses of the various regions of the preform may be necessary.

Exercising a manufacturing system to design and produce a product to preset specifications is the test of feasibility. Included in this are the data generation capabilities, the interactive computer system, the primary deformation, heat treatment and handling equipment, and general process control.

4. General reasons for increased interest in metallurgical synthesis

Metallurgical synthesis offers the opportunity for new products and holds the key to solving many performance, production and economic problems. This is

Table 3. Why metallurgical synthesis

	○ Novel processing approaches often yield new materials or microstructure possibilities
New materials	○ Control uniformity and prevent defects during scale-up
	○ Realization of full potential of innovative new processes
	○ Novel processes may significantly reduce cost
	○ Flexible processes compatible with 'computational plenty'
Productivity	○ New process acceptability
	○ Reduce resources required for scale-up and/or debugging
	○ Reduce technological uncertainty inhibiting large capital investment
	○ Models for computer-aided manufacturing (and Cad/Cam optimization)
	○ Uniformity, reproducibility, absence of defects
Reliability	○ High performance materials used near their limits and where consequences of failure can be catastrophic
	○ Increasing impact of product liability concerns in 'normal' consumer products
	○ Controlled gradients ('one horse shay' components)
Response	○ Reduce time, cost and uncertainty of new process scale-up and/or application to a specific time oriented market
	○ Rapid response to market changes
	○ Rapid product customization

summarized in table 3 under the categories of yielding new materials, increasing productivity, contributing to reliability and permitting rapid response to market demands. Table 3 considers both aspects of metallurgical synthesis, the search for innovative new approaches and the activities which yield understanding and process models. These, of course, are not independent of each other, but in this paper, the emphasis is on the latter.

4.1 *New materials*

Metallurgical synthesis has the potential for creating novel approaches that often yield new materials or microstructural possibilities. The use of directional solidification to provide improved turbine blades or vanes with elongated grains running the length of the part, or potentially to grow single crystal blades or to develop ' eutectic composite ' microstructures are current examples. The enthusiasm generated by such innovative new possibilities quickly leads to attempts to transition from the laboratory to production to use—but this is often done in a very empirical way. At best there is some qualitative understanding of the phenomena involved and how different parameters interact; there is rarely a quantitative understanding or a model that can be used for quantitative predictions. As a result, it is often very difficult to control uniformity or prevent defect occurrence as the processes are scaled-up.

The use of chemical vapour deposition to produce coatings or free-standing parts had led to several examples where the transition from a small scale in the laboratory to large, more complex parts in production did not go smoothly and even led to projects being abandoned. The lack of a science base and the consequent need to proceed in an almost completely empirical manner proved to be too big a task for the resources available. The development of rapid solidified powders presents a new challenge where lack of a science base for further processing might hinder realization of their full potential. There is the intriguing possibility of preparing powders with novel, often metastable, microstructures which might be retained during further processing into parts, or used as the precursors to totally new microstructures in the final product. An empirical approach to finding the optimum processing conditions to yield geometry and absence from flaws at the lowest possible cost will involve exploring a matrix of N possibilities. The cost of this may be significant, but to also explore a variety of new microstructures which will be controlled or influenced by the flow and temperature etc of different consolidation and/or subsequent processing steps can easily generate a matrix of N^a, $a > 1$, possibilities. The cost of a purely empirical approach can now become so prohibitive as to inhibit development of the technology. An improved ability to model the processes involved, even approximately, should provide some guidelines to at least reduce the magnitude of the empirical task and help insure that the best possibilities are evaluated.

4.2 *Productivity*

Increasing the productivity of manufacturing processes is now an important factor in controlling inflation. According to Drucker (1974), transforming production from an experience-based to a knowledge-based technology would be a giant step toward enhancing productivity. Through the use of computer simulation, new processes may be fully developed, controlled and utilized to significantly reduce costs. For

example, there is much current interest in hot isostatic pressing (HIP) components to near finished dimensions, minimizing the cost of machining, and saving materials and energy. At present, either net shapes are not fully realized or many iterations are required to design the process due to the shape distortion that occurs because the powders do not shrink in an isotropic way. A current absence of analytical tools to predict the distortion hinders realization of the full benefit of the HIP process.

Modelling of new processes would reduce the resources required for scale-up and/or debugging. It would also reduce the technological uncertainty inhibiting large capital investment, making it easier for management to accept the risk of new processes. For example, ultra high speed metal removal is an interesting process that shows some feasibility for machining aluminium, but there is a current debate about the nature of the phenomena occurring in aluminium and whether they have the potential for reducing the cost of machining titanium, stainless steels or superalloys. A direct, empirical exploration of this for the difficult-to-machine metals would require constructing extremely expensive equipment. The current science base permits very little understanding of what is observed for aluminum or extrapolation from aluminum to other metals to help reduce the risk of such a decision. Even in familiar existing processes, there is bound to be considerable 'irrational' conservatism. Asking hard questions about what we are doing and why, and what would really be the effects of proposed changes, and the ability to use effective models to add credibility to the answers can help provide the necessary confidence.

Another active field for increasing productivity involves the application of computers to everything that happens in a factory. When applied to process control this obviously requires models of the processes. However, there is additional potential since 'integrated computer-aided manufacturing' may have its greatest impact in reducing the cost of overhead or secondary functions such as inventory control, purchasing, or process routing, thus offering the possibility of very flexible overall manufacturing systems. This presents the additional challenge to develop processes which will be compatible with such a system. Instead of one machine restricted to one process and a narrow range of products, there will be increased need for flexible 'machines' which can be quickly adapted to a variety of situations, and for the process models to support this.

4.3 *Reliability*

Increasingly, in many aspects of the technology which underlies modern society, materials are being used closer to their limits and the consequences of failure can be catastrophic. A jumbo jet, an energy generating or conversion plant, or an implant for prosthetic use in the human body are familiar examples. Even in low performance technology—in normal consumer products—demands for reliability have been rapidly growing in response to new laws, regulations and recent court decisions involving product liability. The role of reproducible, uniform, 'defect free' materials is obvious, and will undoubtedly impose requirements for improved processes to yield them. Process modelling, by permitting better process control, can increase the reliability of a product. In the case of a forging, the reliability might be determined by the absence of defects in the bulk of the material or by the probability of attaining a desired microstructure every time a component is fabricated. A related possibility involves the use of improved process control to yield different micro-

structures in different regions of a single component. The dual property disk described previously is a current example. Ideally, if all regions of components have their own optimum microstructures, maximum performance/efficiency can be combined with maximum lifetimes as in the famous ' one horse shay ' where everything wears out at the same time. Here is an area where process modelling can make a meaningful input to the widespread call for an increased conservation ethic in our society.

4.4 *Response*

As society becomes both increasingly complex and its rate of change increases, effective competition requires short response times to the demands of very diverse markets. To the extent that an improved process model can reduce the time and cost of manufacturing new products or introducing new processes, it can be a significant aid. Having the capability to simulate a production process on a computer will help to remove the uncertainty of new process scale-up, and can significantly reduce the time (and development cost) between product conception and production. Prior to gaining extensive production experience, economic models can predict the process conditions for minimum cost or minimum time. Should the market change suddenly or a need for rapid product customization occur, process models make it possible to accommodate these changes with a minimum of effort. Extrusion dies, for example, can now be designed in a matter of hours rather than weeks (Akgerman *et al* 1974), because CAD/CAM technology has eliminated the need for mechanical drafting, for model templates, for copy milling and for die tryout.

In the light of the above discussion, metallurgical synthesis should be recognized as an important component of technology. However, unlike other fields such as production and operations management, which are related to manufacturing, it has only recently begun to benefit from increased attention and activity.

5. Some areas where synthesis research is needed

In order to meet the generic goals of the ' dual property disk ' programme, it was necessary that a link between materials behaviour and mechanics be established. Such a disk will probably be forged by a controlled strain rate isothermal process using an alloy, Ti-6Al-2Sn-4Zr-2Mo-.1Si (Ti-6242), whose response to forging deformation is structure-sensitive and understanding the nature of its response to hot die conditions is therefore essential. The ability to achieve a near-net shape is strongly influenced by workpiece temperature, die temperature, and preform microstructure. Maximizing the hot workability and controlling the microstructure require adequate control of these variables. From a metallurgical synthesis point of view, the material variables must be understood and quantified so that the rate of energy input to the process can be balanced against the rate of energy dissipated by the material during metal flow. Otherwise, internal defects such as cavities or grain boundary cracks may form during forging, and these defects may lead to catastrophic failure in a service environment. The quantitative relationships that analytically describe the material behaviour, *i.e.*, the constitutive equations, processing-microstructure maps, failure maps, etc., provide the link between material response and process demands.

This quantitative knowledge will subsequently determine the nature of the process controls and the manufacturing systems.

5.1 *Constitutive equations*

Constitutive equations are essential for process simulation and microstructure control. They must be ' manageable ', that is they must be easily handled in finite element or equivalent numerical routines used to simulate metal flow, and they must be adequate to permit predictions of temperature, strain and strain rate fields by the process model. In addition, they must be sufficiently valid to permit extrapolation into temperature and strain rate space where accurate, direct experimental measurements of material properties are difficult.

The rate of deformation is an important parameter in almost every shape-making process, and it is necessary to characterize the material's response to it. Constitutive equations must be developed for each engineering material from experimental data that relate the true flow stress σ to the process variables, and, ideally, they should be capable of describing the structural changes that occur in an evolutionary way during deformation. The practical spectrum of strain rates is 10^{-4} s^{-1} to about 10^{3} s^{-1}. This range covers most processes, from superplastic forming to explosive forming, but excludes metal removal processes that can have strain rates in the deformation zone that are on the order of 10^{6} s^{-1}. Table 4 gives the ordinary range of deformation speeds for a number of common metalworking processes.

Many constitutive relationships have been employed in metalworking calculations; they are usually empirical equations that relate the flow stress to strain or strain rate, but rarely both. When strain and strain rate are considered together, they are often in terms of an empirical strain hardening law with a superposed power law creep rate factor $\dot{\epsilon}^{m}$. Some of the classical hardening laws are listed in table 5.

Table 4. Typical deformation speeds

Process	Range in ft/min	(m/min)
Tension test	0·0002 – 2	0·00006 – 0·61
Hydraulic extrusion stress	5 – 70	1.52 – 21·34
Tube drawing	10 – 100	3·05 – 30·5
Deep drawing of sheet	10 – 200	3·05 – 61
Sheet rolling	50 – 5,000	15·24 – 1524
Hammer forging	500 – 2,000	152·4 – 610
Charpy impact test	1,200	365·8
Drawing of fine wire	1,000 – 8,000	305 – 2438
Dynapak forging	4,000 – 10,000	1219 – 3048
Explosive forming	6,000 – 25,000	1829 – 7620

Table 5. Strain hardening laws

$\sigma = K\epsilon^{n}$	Holloman (1945)
$\sigma = \sigma_0 + K\epsilon^{n}$	Ludwik (1909)
$\sigma = K(\epsilon_0 + \epsilon)^{n}$	Swift (1952)
$\sigma = \sigma_s - (\sigma_s - \sigma_0) \exp(-\epsilon/\eta)$	Voce (1948)

The hardening law by Holloman is probably the most frequently used because of its simplicity. The exponent n is usually dependent on both strain and strain rate. The Ludwik and Swift equations include additional terms. These may describe the effects on strain hardening of a finite yield stress or the effects of pre-strain. The Voce hardening law includes a finite yield stress and a saturation stress σ_s. This model has been used (Kocks 1976) to describe the strain rate dependent strain hardening behaviour for high-purity aluminum and 304 stainless steel. Not all materials support the concept of a saturation stress, for example, 2024-0 aluminum alloy does not (Nagpal *et al* 1979). Investigations clearly show that the strain hardening coefficient and the strain rate sensitivity depend in general on both strain and strain rate. Thus, strain rate-independent strain hardening relationships are not sufficient and a more general approach is required to guide the development of constitutive relations for metallurgical synthesis applications. The desired hardening law should not only be capable of predicting the stress for a given temperature, strain rate and strain, but it must also accurately predict the tangent modulus.

These more general requirements lead to the phenomenological approach (Hart *et al* 1975) for developing constitutive equations. In this, the flow stress is expressed as a function of strain rate, absolute temperature, and one or more history-dependent parameters which characterize the current structure of the material and evolve with continuing deformation. These structure parameters partially determine the current mechanical properties, and strain hardening can be described in terms of the evolution of structure parameters with accumulated plastic strain. An important feature of this approach to characterizing the flow behaviour of materials is that the strain hardening coefficient γ and the strain sensitivity ν appear as state functions such that their dependence on stress, strain rate and temperature can be specified. This implies that the incremental stress-strain relationship

$$d \ln \sigma = \gamma \, d \ln \epsilon + \nu \, d \ln \dot{\epsilon} + \beta \, d \ln (1/T),$$

can be integrated for any known deformation path. This model has been applied to predict flow stress data at cold working temperatures, but it has yet to be tested at temperatures at which the substructure is continually being annihilated and reformed, as in hot working. Furthermore, it has been applied only to single-phase materials. Models of this sort would permit flow stress data at high strain rates (where adiabatic heating tends to lessen the validity of experimental data) to be extrapolated from low-strain rate, isothermal data.

5.2 *The yield function*

The experimental determination of the yield locus, flow rule and constitutive equations along various loading paths at hot working temperatures for multi-phase engineering alloys is an important area for investigation, because metalworking operations are never performed under uniaxial states of stress. Some method must be devised for extrapolating material data obtained under uniaxial loading conditions to whatever it would be for loading along other general stress and strain paths. The yield loci most often used are von Mises locus (for isotropic materials) and Hill's anisotropic generalization for materials with orthotropic physical symmetry (Hill 1948). The constructs for extrapolating materials data from one general strain path

to another are known as effective strain and effective stress, and, for these definitions to have meaning, the constitutive relation connecting the two must be the same irrespective of the loading path. Because anisotropy and constitutive relations are very sensitive to temperature (and microstructure), careful consideration of the metallurgical factors will be required.

5.3 *Processing maps*

One of the objectives of metallurgical synthesis is to produce a finished shape without defects, and, in order to accomplish this goal, an approach to display the ' defect generation ' mechanisms on processing maps which delineate the strain rate, effective strain and temperature regions within which flaws should not initiate is needed. Wedge cracking in grain boundaries (Grant 1968–1978 and Min & Raj 1978) and deformation and shear band types of discontinuities in the microstructure (Schectman & Elyon 1978) can strongly influence the durability of a product in service. Shear bands, for example, can provide an ' easy ' path for the propagation of cracks. The main problem, from the viewpoint of synthesizing a high quality component, is to design the metal forming process so that these types of flaws are avoided. An example of a processing map for aluminum which separates the region of cavitation,

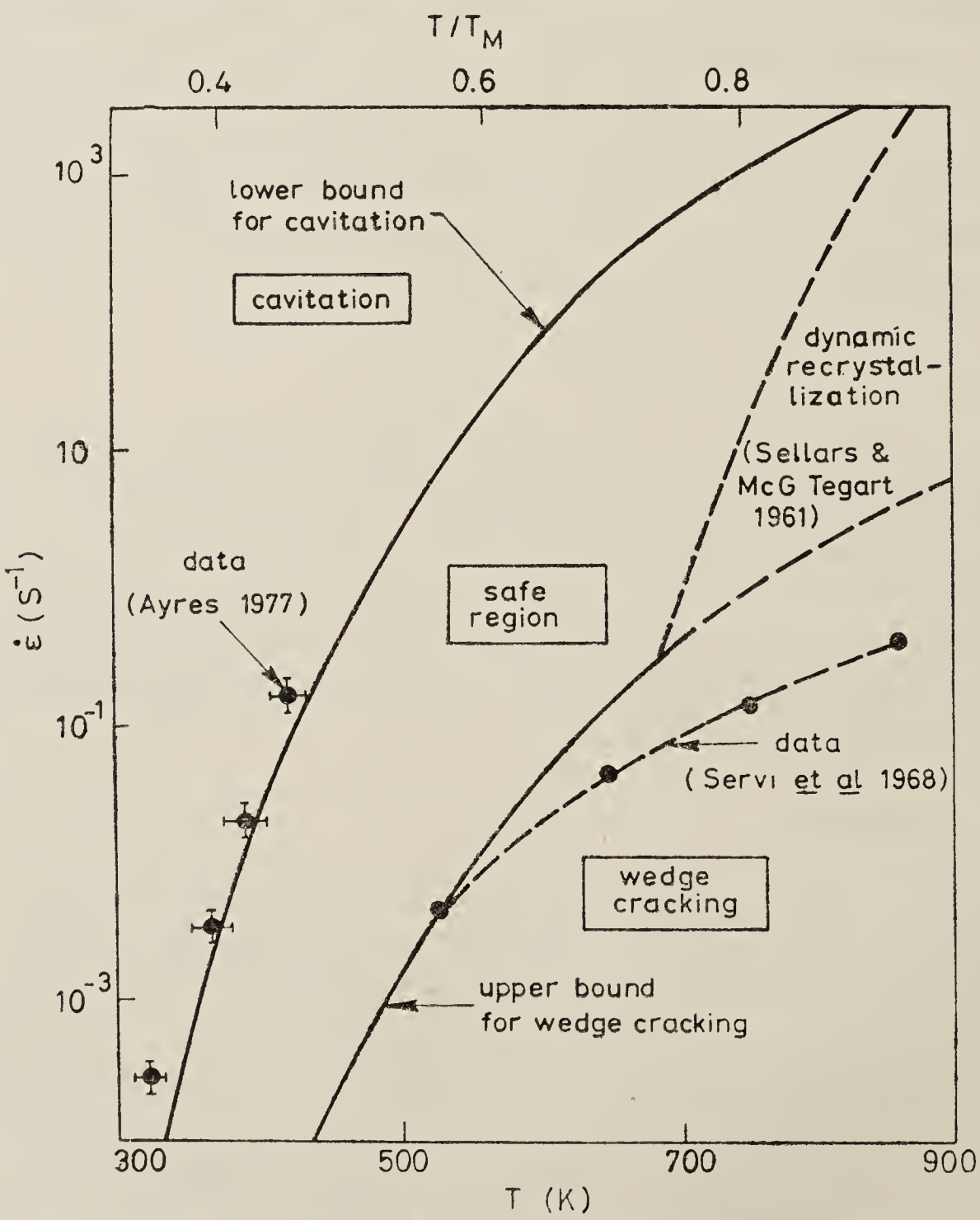

Figure 3. A processing map for aluminium which separates the region of cavitation, wedge cracking and dynamic crystallization (R Raj 1979, private communication)

wedge cracking and dynamic recrystallization is shown in figure 3. Another dimension to such processing maps would describe the changes in microstructure which can occur, and which must also be controlled to permit a total synthesis.

5.4 *Process modelling*

The mathematical analyses of metalworking processes are intended to provide the necessary information for proper design and control of the process. Therefore, the method of analyses must be capable of determining the effects of various parameters on metal flow characteristics. The process model provides the link between the materials science and mechanics part of metalworking. Computation efficiency, as well as solution accuracy, is an important, practical consideration. The major problem for practical metallurgical synthesis in industry is to develop an efficient analysis method that will take into account the dependence of material behaviour on the process variables, while providing a solution to the problem of non-steady-state heat transfer in a moving incompressible medium. Because the overall goal of metallurgical synthesis is to control both microstructures and properties, process models must be designed to accept microstructure and workability information. The challenge is to develop the concept of a general approximate method which combines the features of the upperbound method (Avitzur 1968), for efficiency of computation, and the finite-element method (Lee & Kobayashi 1970) for its accuracy.

5.5 *Lubrication*

The interface phenomena of friction, lubrication and die wear are of controlling importance in most metalworking processes such as forging, sheet metal forming and machining (Schey 1970). They deal with the effect of friction on forces, power requirements, strain and velocity distribution, and process limitations. Interface conditions also control heat transfer between the workpiece and the die or atmosphere. The lubricant must do these functions in addition to controlling the oxidation of the die and workpiece material. There is need for research to develop simple models for evaluating the interface conditions, and the data should be presented in a form that can be used as a boundary condition for the process models. Lubricants should also be studied in terms of their chemical composition, so the role of additives can be understood in terms of the functions the lubricant plays in a particular process.

6. Conclusions

(i) The knowledge needed for controlled synthesis of both the microstructure and the geometry which the alloy designer and the component designer specifies, can be developed, and represents a fruitful area for interdisciplinary cooperation.
(ii) Metallurgical synthesis research cannot be effectively accomplished in isolation; it must be done in relation to real situations and real problems. The definition of meaningful possibilities for near-term application can help.

References

Akgerman N, Altan T & Subramanian T L 1974 *Manufacturing methods for computerized forging process for high strength materials* (AFML-TR-284: Available NTIS)

Ault G M & Burte H M 1966 *Oxide dispersion strengthening* Vol. 47 Metallurgical Society Conferences (New York: Gordon and Breach Science Publishers) pp. 47-50

Avitzur B 1968 *Metal forming: processes and analysis* (New York: McGraw Hill)

Ayres R A 1977 *Met. Trans.* **A8** 487

Buessem W R 1963 *Physics and chemistry of ceramics* ed. C. Klengsberg (New York: Gordon and Breach Science Publishers) p. 14

Burte H M 1978 *Rapid solidification processing, principles and technologies* eds R Mehrabian, B H Kear and M Cohen (Baton Rouge: Claitor's Press) pp. 393-396

Burte H M & Gegel H L 1980 *Process modelling: fundamentals and applications to metals* eds T Altan, H M Burte, H L Gegel and A Male (Metals Park: American Society for Metals) p. 1

Collings E W & Gegel H L 1975 *Physics of solid solution strengthening* eds E W Collings and H L Gegel (New York: Plenum Press)

Drucker P F 1974 *Management—tasks, responsibilities and practices* (New York: Harper and Row Publishers) pp. 32-33, 68-70, 177

Grant N J 1971 *Fracture* (ed. H Liebowitz) (New York and London: Academic Press) Vol. 3

Hart E W Li C Y, Yamada H & Wire G L 1975 in *Constitutive relations in plasticity* (ed. A S Argon) (Massachusetts: MIT Press) p. 149

Hill R 1948 *Proc. R. Soc. (London)* **A193** 281

Holloman J H 1945 *Trans. AIME* **162** 268

Jaffee R I 1973 *Titanium science and technology* Vol. 3 eds H M Burte and R I Jaffee (New York: Plenum Press) p. 1665

Kocks U F 1976 *ASME J. Eng. Mat. Tech.* **98** 76

Lee C H & Kobayashi S 1970 *Int. J. Mech. Sci.* **12** 349

Ludwik P 1909 *Elemente der technologischen mechanik* (Berlin: Julius Springer)

Min B K & Raj R 1978 *Acta Met.* **26** 1551

Nagpal V, Shabel B S, Thomas, Jr. J F & Gegel H L 1979 *7th North American Metalworking Research Conference* (Dearborn: Society of Manufacturing Engineers) p. 172

Schectman D & Elyon D 1978 *Met. Trans.* **A9** 1018

Schey J 1970 *Metal deformation processes: friction and lubrication* ed J Schey (New York: Marcel Dekker Inc.) p. 1

Sellars C M & McG Tegart W J 1961-62 *J. Inst. Met.* **90** 21

Servi I S & Grant N J 1951 *J. Met.* **3** 917

Stuwe H P 1966 *Proc. of Conference on Deformation Under Hot Working Conditions* (University of Sheffield: Dept. of Metallurgy) p. 1

Swift H W 1952 *J. Mech. Phys. Solids* **1** 1

Voce E 1948 *J. Inst. Metals* **74** 537

Strengthening mechanisms in alloys

T BALAKRISHNA BHAT and V S ARUNACHALAM
Defence Metallurgical Research Laboratory, Kanchanbagh P.O., Hyderabad 500 258

MS received 2 August 1980

Abstract. Metals can be strengthened by methods appropriately combined to meet the operating conditions. In this 'alloy design', effort, we are guided by semi-quantitative relations that have been developed over the years and which relate the efficacy of the strengthening methods to the deformation modes. In this paper, the basic concepts are expanded with specific reference to dislocation glide, diffusional creep, grain boundary sliding and high strain rate deformation.

Keywords. Strengthening mechanisms; dislocation glide; dislocation climb; solution strengthening; precipitation strengthening; grain refinement; cell refinement; grain alignment.

1. Introduction

The term ' alloy design ' may sound presumptuous as most of the commercial alloys of today are not products of deliberate design and development. It should not sound so any more, as there are now clear demands for materials with specific properties tailored to meet some specific applications. The materials engineer of today is better qualified to deal with such requirements as there is an improved understanding of the theoretical base for materials design and a variety of appropriate processing techniques available to synthesise them (Burte & Gegel 1980) accordingly. There is no one single route for designing materials, as property requirements vary. Designing for a radiation environment calls for optimising properties different from those required for designing a load-bearing structure. Materials thus have to be designed keeping their end applications in view.

Most of the metals and alloys used in engineering are load-bearing. This implies that these materials should have the necessary strength not to yield or fracture under load and retain their strength in service. It is the object of this paper to review the various strengthening mechanisms that can be effectively utilised to make metals and alloys meet the service requirements.

Strengthening of metals is necessary because metals are invariably weak due to the nature of metallic bonding, which is diffuse and non-directional, and also because of a large number of lattice defects. An important defect, dislocation, has high mobility because of the long-range periodicity of metallic lattices and the small translation vectors as compared to the spacing of planes on which they move (Cottrell 1966). Changing the nature of metallic bonding or the crystal structure to increase strengthis not easy and cannot be recommended as it would lead to brittle solids.

A list of symbols appears at the end of the paper

Strengthening efforts should therefore be directed towards strengthening the lattice against the easy movement of lattice defects. We shall first discuss the various flow processes that occur in metals and alloys and consider a number of strengthening mechanisms that can make this flow difficult. We shall also consider strengthening against high-temperature deformation and against large strain-rate effects.

It is important to emphasise that strengthening a metal is only one part of alloy design. The other is concerned with the building up of resistance to fracture. This in fact sets an upper limit for strengthening as increase in strength is generally accompanied by a reduction in ductility and fracture resistance (Tien 1975). Thus an upper limit to strength is imposed by other mechanical property requirements as well. While some strengthening methods, though very effective, bring in this limit too rapidly, others are more moderate. We have to optimise the various strengthening methods to evolve a successful strategy.

2. Plastic flow in metals and alloys

2.1 *Deformation mechanism maps*

Plastic flow occurs by a variety of mechanisms, their relative importance changing with temperature and applied stress. An elegant way to represent these flow properties is by deformation mechanism maps (Weertman 1968; Ashby 1972a, 1973; Mohammed & Langdon 1974; Frost & Ashby 1975). These maps graphically depict the response of a metal or an alloy to applied stress in terms of its shear modulus and homologous temperature. Various zones in the map characterising particular flow processes are determined by analysing the strain rate equations for different flow processes and evaluating the predominant one. A typical deformation mechanism map is shown in figure 1 for iron (adapted from Ashby 1972a; Lindholm 1974; Hockett & Zukas 1974; Oxley 1974). At very high stresses the flow is determined by the theoretical strength of the crystal ($0{\cdot}06G$, where G is the shear modulus), athermal viscosity or twinning stresses. At high temperatures and low stresses, the flow is diffusional. An important area between these two extremes is governed by dislocation flow which falls in the range of usual temperatures and stresses in engineering applications.

2.2 *Resistance to dislocation induced flow*

Dislocation flow depends on some of the intrinsic properties of the host material, such as, elastic modulus E, diffusion coefficients D, and the crystal structure. This is because the energy of a dislocation is proportional to its modulus and the square of the Burgers vector b and its mobility at elevated temperatures is determined by the diffusion coefficients. As E, b and to a major extent, D are determined by the choice of the material they cannot be made to vary significantly by design. It is therefore necessary to seek other options available for reducing the dislocation mobility. This can be achieved by making the dislocation interact with the stress fields of other dislocations, sub-boundaries, grain boundaries, solute atoms and precipitates. These interactions, according to Fleischer & Hibbard (1973), can be ' gradual ' or 'rapid ' depending on the intensity of hardening. Rapid hardening has high $d\tau/df$ where $d\tau$

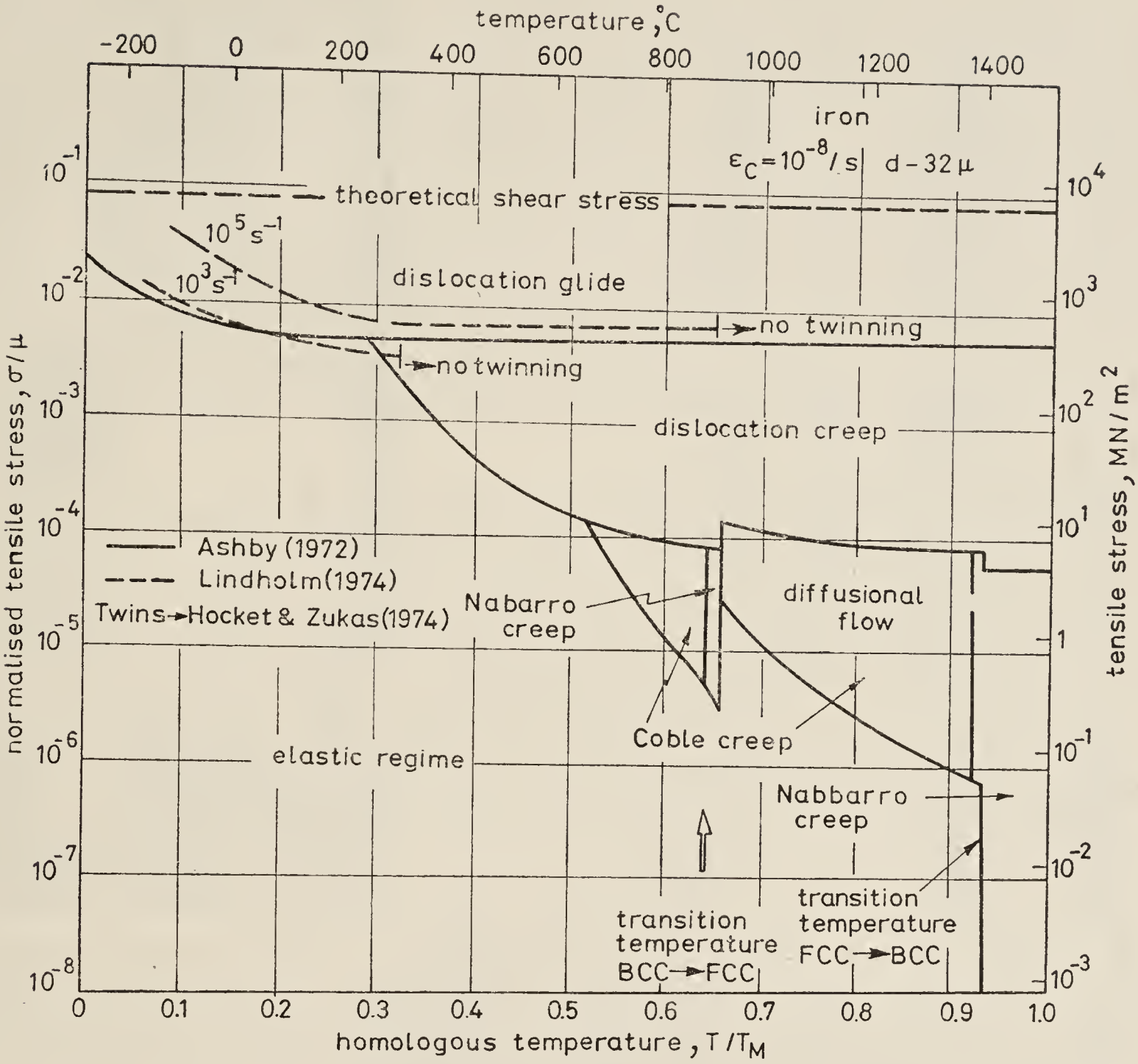

Figure 1. Deformation mechanism map for iron.

is the strength increment and df is increment in concentration of obstacles. Gradual hardening has only low $d\tau/df$ values. Table 1 summarises the characteristics of various obstacles to dislocation motion. The effectiveness of a specific obstacle is dependent on stress and temperature as well as on the density of other obstacles. An alloy designer has to combine several of these together to subdue the dominant deformation mechanism prevailing at the particular range of stress and temperature.

2.3 *Strengthening due to sub and grain boundaries*

Dislocation cells, sub-boundaries and grain boundaries are effective strengtheners at low temperatures. However dislocation cells generated by cold work alone are not very useful because of poor ductility. This disadvantage can be overcome when the cold-worked structure is slightly annealed to produce well-developed dislocation sub-structures. The matrix is then devoid of dislocations except in boundaries or cell walls, where they are arranged in low-energy configurations. The interaction of dislocations with these walls does not drastically reduce the ductility and this route can effectively be utilised for strengthening. The increase in strength due to stable sub-structure is proportional to D^{-1} (D is cell size) (Embury 1972; Takeuchi & Argon

Table 1. Mechanisms for strength and some of their characteristics

Obstacle	Strength of the interaction $d\tau/df$	Approximate formulae for strength and some examples	Work hardening rate and some values	Effect of temperature	Limiting factors
1	2	3	4	5	6
1. Substitutional atoms or interstitials at symmetric sites	Weak; $G/10$ to $G/100$	$\alpha_1 \sqrt{f}\,(1+\alpha_2 \sqrt{f})$ (Kocks *et al* 1976) for Ti/Sn $\alpha_1/G \sim 0{\cdot}01$, $\alpha_2/G \sim 10$ (figure 2)	Raises the saturation stress	Rapid drop with an apparent athermal breaking off at intermediate temperatures $\Delta F = 1/5\ Gb^3$	Cost, solubility, segregation, weight penalty intermetallic formation
2. Interstitials in bcc, or strongly bonding interstitials	$1 - 10G$ strong	$\alpha_1 \sqrt{f}$ (Kocks *et al* 1976) for Ti—0 $\alpha_1/G \sim 0{\cdot}1$ (figure 2)	—	Large temperature dependence $\Delta F = (1/5 - 1/10\ Gb^3)$	Embrittlement
3. Grain boundaries, dislocations cells, two phase structures	$G/2 - G/200$	$\alpha Gb \sqrt{\rho}$ (dislocation strengthening) $KL^{-1/2}$ or KL^{-1} (grain or interface strengthening) for Fe (Embury 1972) $\alpha \sim 0{\cdot}2m$, $G = 8{\cdot}3 \times 10^4\ MNm^2$, $b \sim 2{\cdot}5 \times 10^{-10}m$ if $\rho = 10^{16}m^{-2}$ $\Delta\sigma = 415\ MNm^{-2}$ $K \sim 0{\cdot}6\ MNm^{-3/2}$ if grain size changes from $10^{-3}m$ to $10^{-6}m$, the strength would increase by $582\ MNm^{-2}$	$\frac{1}{G}\frac{d\tau}{d\gamma^{1/2}}$ $\sim 1/2 - 1$	$1/2\ Gb^3$, weakly sensitive, can work upto $0{\cdot}4 - 0{\cdot}5$ TM	Coarsening, instability at elevated temperatures or in fatigue
4. Dispersoids	$G/10$	$0{\cdot}81\ Gb/L$ (Foreman & Makin 1966)	$1/G\ d\tau/d\gamma^{1/2} < (bf/2r)^{1/2}$ for $f = 0{\cdot}01$, $r = 200b$ $1/G\ d\tau/d\gamma^{1/2} = 1/2$ (Ashby 1970)	Strengths partly available even to high temperature; $\Delta F > Gb^3$	Ductility reductions, inhomogeneity of dispersion
5. Precipitates	$G/100 - G/200$	See table 2	No work hardening when cut, otherwise behaves like dispersoids	$\Delta F > Gb^3$	Solubility and coarsening at elevated temperatures, slip concentrations in fatigue, ductility reductions with large misfits.
6. Ordering	$\Delta\tau \sim \gamma_{APB}/b$ $\sim G/100$	γ_{APB}/b	$\frac{1}{G}\frac{d\tau}{d\gamma}$ $\sim 0{\cdot}1$ to $0{\cdot}3$ for ordered Fe-Co $\sim 0{\cdot}3$ Marcinkowski 1974)	Weakly sensitive to temperature below disordering temperature. Strength may increase with temperature (e.g. in Ni_3Al)	Embrittlement

1976). There is a ' memory effect ' in these sub-structures on the mode of deformation employed to develop them. When the stress systems are altered, the sub cells developed during processing turn unstable and ' dissolve ' causing flow instabilities. This should be borne in mind when dislocation cells are thought of as a strengthening route (Pattanaik *et al* 1974). However, sub-boundaries can be stabilised by second phase particles, voids, or even by solutes (Rama Rao 1978; Kutumba Rao *et al* 1975). The boundaries developed as a result of deformation-processing in the presence of dispersed particles have high stability and can be a source of useful strength over a range of temperatures. This coupled with grain refinement has led to the development of commercially viable processes under the generic name, ' thermo-mechanical processing '. High strength low alloy (HSLA) steels are products of such a processing.

Strengthening due to grain boundaries is similar to sub-boundary strengthening except that the strength increment ($\Delta\sigma$) is generally proportional to $d^{-1/2}$ (d is the grain size) according to the Hall-Petch equation: $\Delta\sigma = Kd^{-1/2}$ (Hall 1951; Petch 1953; Embury 1972; Margolin & Stanescu 1975). The proportionality constant K is found to vary with strain and temperature and is derived to be equal to $M^2\, r^{1/2}\, \tau_c$, where M is the Taylor orientation factor, r, the distance between the head of the pile-up and dislocation source and τ_c, the critical shear stress necessary to activate a dislocation source in the next grain (Armstrong *et al* 1962). However, recent experiments suggest that the Hall-Petch equation is not universally valid and the reasons for this are not clear (Hutchinson & Pascoe 1972; Morris *et al* 1976) and further work in this area is desirable.

Grain sizes can be reduced to micron and sub-micron levels by controlled micro-alloying additions followed by thermomechanical processing. Finely distributed insoluble particles can also inhibit grain growth. Fine grains generated as a result of thermomechanical processing are stable in many alloy systems (*e.g.* HSLA steels) and are capable of providing increase in strength upto intermediate temperatures.

It is worth pointing out that both sub-boundary and grain boundary strengthening are the only mechanisms which do not (Cottrell 1966) affect ductility and are therefore attractive for the designer. Figure 2 shows the relative hardening efficiencies of grain and cell boundaries as against various solute elements on a ' weight or volume percent ' basis. This figure was generated by assuming the boundary thickness to be around 5b and a sub-boundary wall thickness of about 20b and calculating the volume fraction of the boundary phase as the obstacle density. The grain or cell boundary route stands out as the most rapidly hardening mechanism.

A novel approach to strength, for some metallic systems at least, is to turn them glassy. This is achieved by appropriate choice of alloying additions and cooling these rapidly to prevent the onset of crystallisation. The resulting structure can be considered to contain only disordered grain boundary structures. This is known to provide high strength and some attempts are being made to evolve a theory for understanding their behaviour (Ramachandra Rao 1980 private communication; Cahn 1980).

2.4 *Precipitation hardening*

Alloying to precipitate a second phase is perhaps the most effective and successful strengthening route. The second phase particles can be incorporated by precipitation

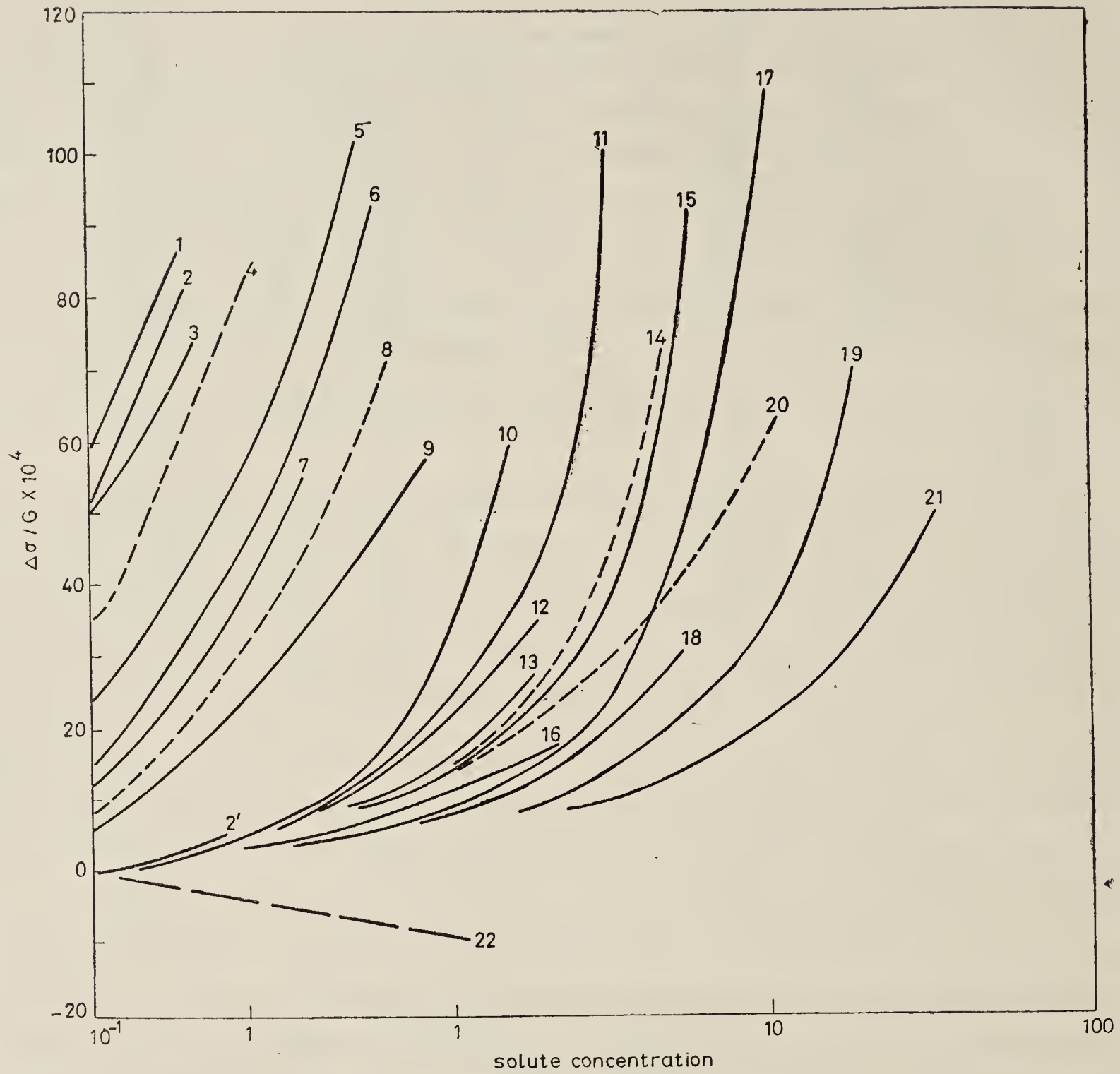

Figure 2. Effect of solutes, precipitates, dispersoids, grain or cell boundaries on strength. (Explanation to the curves are given in the table below)

Curve No.	Material	Strengthening element	Reference
1	bcc iron at 300°K	Grain boundary	Embury (1972)
2	Ti at 300°K	Grain boundary	Jaffee (1973)
2′	Ti at 450°K	Grain boundary	Jaffee (1973)
3	Ti	N	Tyson (1970); Everhart (1954)
5	Fe	Cells	Morrisson (1966); Takeuchi & Argon (1976)
6	Ni	Grain boundary	Embury (1972)
7	Fe	P	Pickering (1978)
9	Ti	Fe	Everhart (1954)
10	Ti	Mo	Everhart (1954)
11	Ti	V	Everhart (1954)
12	Fe	Si	Pickering (1978)
13	Ni	ThO_2	Sims & Hagel (1972)
15	Ti	Al	Solonia & Kuraeva (1973)
16	Fe	Mn	Pickering (1973)
17	Ti at 873°K	Sn	Solonia & Kuraeva (1973)
18	Ni	Al	Decker (1969)
19	Ni	Mo	Decker (1969); Pelloux & Grant (1968)
21	Ni	Cr	Decker (1969)
22	Fe	Cr	Pickering (1978)
8	$Kf^{1/2}$		
14	Kf		
20	$Kf^{2/3}$		

Table 2. Dislocation-particle interactions

mechanism & order of magnitude	effective resisting force/ 2E		activation energy F_0/Gb^3	represent-ation of force	typical formula	example	comparison of experiment with theory
	edge dislocation	screw dislocation					
core energy $\Delta F_{core} = F_{dis}/100$	$(2/\Delta F/F)^{1/2}$ 0.2	same 0.1	$W/\Delta F_{dis}$ $(W/b)/200$	—	—	strong compounds	—
modulus differences $\Delta G \sim G/2$	$\left[4\lvert\Delta G/G\rvert - 2(\Delta G/G)^2\right]^{1/2}$ 1	$\left[2\lvert\Delta G/G\rvert - (\Delta G/G)^2\right]^{1/2}$ 0.1	$\Delta G . b^2 \omega$ $W/2b$		$\frac{8Gb}{L}\left(1-\frac{E_1^2}{E_2^2}\right)^{1/2}$	Fe – Cu	$E_{Cu}/E_{Fe}=0.6; G_{Fe}=8.3\times10^4\,MN\,m^{-2}$ $1/L=1.2\times10^3$ Å $\Delta\tau = 475\,MN\,m^{-2}$ $\Delta\tau_{experiment}=500\,MN\,m^{-2}$ (Russell & Brown 1972)
interface step $\gamma_{int}\sim Gb/100$ $\gamma_{void}\sim Gb/10$	$(2b\gamma_{int}/E)^{1/2}$ 0.3 0.8	$b\gamma_{int}/E$ 0.02 0.2	$2bW\gamma_{int}$ $(W/b)/50$ $(W/b)/5$		—	Al – Cu Cu – Be (Brown & Ham 1972)	—
Orowan loop	strong	strong	W^2/L		$0.8Gb/L$	overaged alloys dispersion strengthened alloys	Cu-BeO (Hirsch-Humphreys 1970) $b=2.5$ Å, $L=2333$ Å $(\Delta\tau/G)_{theoretical}=0.858$ $(\Delta\tau/G)_{experimental}=0.9$
solid solutions	—	—	0.5	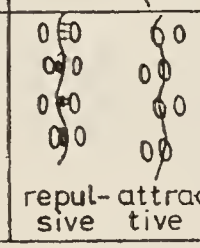	$\alpha_1(\sqrt{f}+\alpha_2\sqrt{f})$ (Kocks et.al. 1976)	Ni – Mo Ti – C Ti – Fe	the concentration dependence of $f^{1/2}$ is observed at low concentration and f' at high concentration

Table 2. (Contd.)

mechanism & order of magnitude	effective resisting force/ 2E		activation energy F_o/Gb^3	represent-ation of force	typical formula	example	comparison of experiment with theory
	edge dislocation	screw dislocation					
friction stress $G/100 = \tau_{ele}$	τ_{ele} b W/2E W/b x 100	same same	$\frac{\pi}{4} W^2 b$ $(W/b)^2/100$	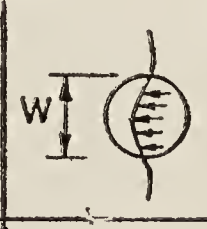	—	Al–Si	—
disordering $\gamma_{APB} = Gb/100$	γ_{APB} x W/2E (W/b)/100	same	$\frac{\pi}{4} W^2 \gamma_{APB}$ $(W/b)^2/100$	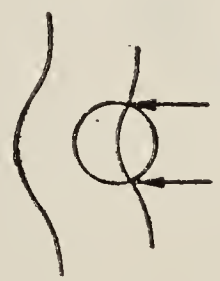	$\gamma_{APB}/2b - \frac{Gb}{W}$ $+K(\tau_p+\tau_m)$		nickel base alloy : mar M–200 $\gamma_{APB}=164 N m^{-1}$, $G=8.3\times10^4$ MN m^{-2} W=2500 Å, b=2.53 Å $\gamma_{APB}/2b = 325$ MN m^{-2} $-Gb/W = \frac{84 MN m^{-2}}{241 MN m^{-2}}$ experimental value=380 MN m^{-2}
misfit strains $\lvert\varepsilon\rvert = 1/100$	$\lvert\varepsilon\rvert$ GbW (w/b)/50	small	$GbW^2 \lvert\varepsilon\rvert$ $(w/b)^2/100$		$\frac{3.6 (Wf)^{1/2} \lvert\varepsilon\rvert^{3/2}}{b}$	copper–cobalt Al–Zn	—

of unstable solutes from solution. The strength of interaction between dislocations and second phase particles is determined by the particle size and volume fraction and by the nature of the particles themselves. Table 2 summarises various parameters which determine this interaction, both for obstacles that are cut or bypassed.

The modulus differences (soft particle strengthening, solute clusters *e.g.* Cu in Fe, Russell & Brown 1972), antiphase boundary energy or the stacking fault energy (superalloys, γ' in γ, Sims & Hagel 1972) and to a somewhat smaller extent, the misfit strains (Al-Cu alloys, Brown & Ham 1972) are usually the important factors for strengthening. On the other hand, the interface step energy and the core energy differences only lead to marginal strength benefits (Kocks *et al* 1973). Lattice mismatch, though a potent strengthener, adversely affects ductility. Lattice mismatch, in addition, enhances, the precipitate coarsening rate at elevated temperatures. Mismatch therefore is kept to a minimum in many alloy systems in spite of its rapid strengthening potential.

An interesting feature of precipitation-hardened systems is the variation of strength with precipitate size (figure 3, Mitchell 1966; Decker 1969). The strength at first increases and then gradually decreases with increasing particle size, even though the volume fraction of particles and hence the antiphase boundary energy, stacking fault energy or misfit strain energy all remain constant. In the cutting region, with increasing particle size, the particle dislocation interaction becomes stronger, forcing the dislocations to adopt increasing curvatures before being cut. This increases the

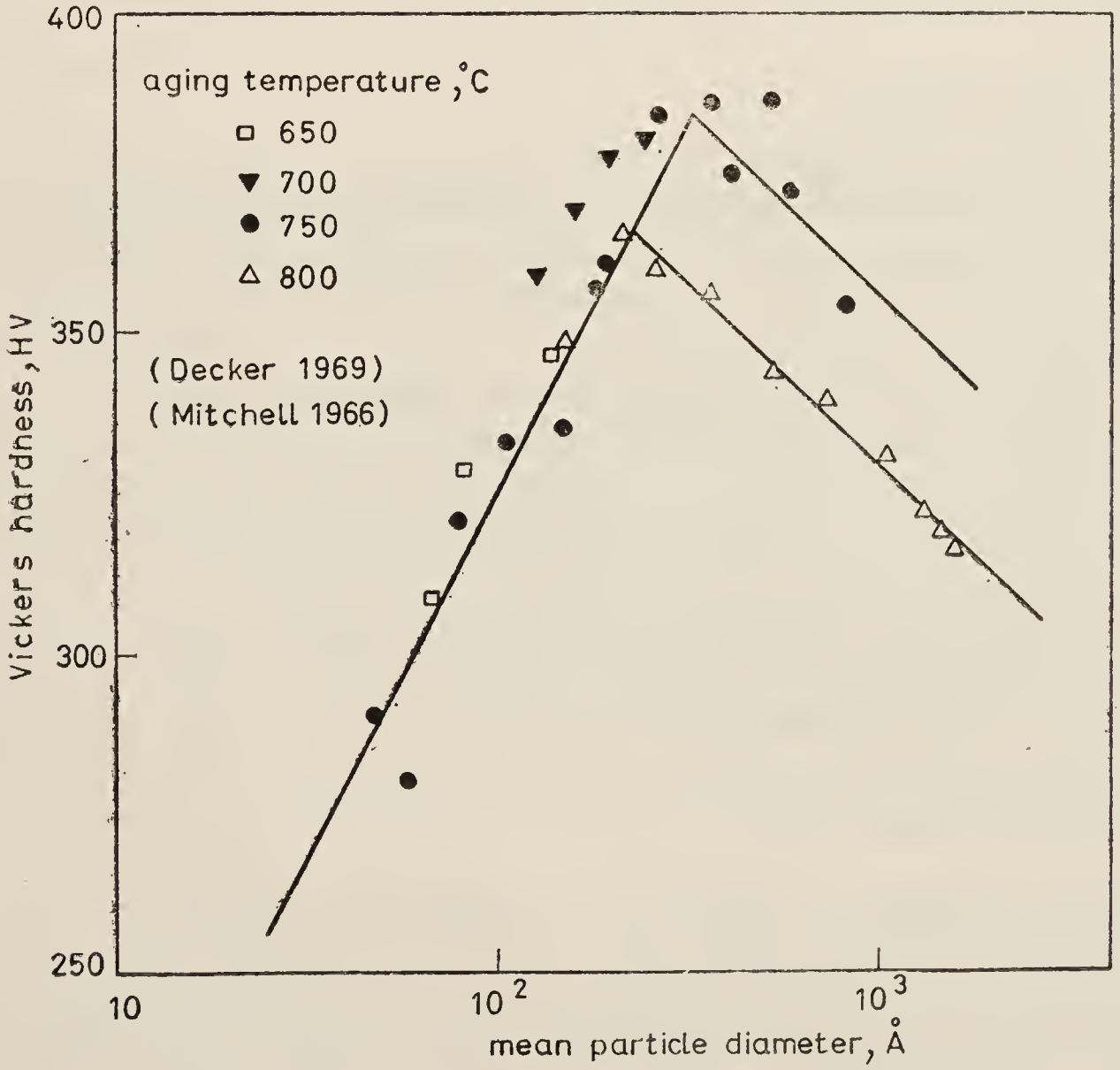

Figure 3. Effect of precipitate size on strength of the alloy.

average number of obstacles per unit length of dislocation and hence the strength. With further increases in particle size, the random spacing continues to increase and a stage is reached where particles can no longer be cut but have to be looped by the dislocation. The strength then falls according to the Orowan equation: $\Delta\sigma \sim Gb/(L\text{-}d)$ (Foreman & Makin 1966, 1967).

Orowan looping is a predominant deformation mechanism when particles are strong and when they are widely spaced. Even though the yield strength is lower in looping than when the particles are cut (figure 3), the material work hardens rapidly with strain due to dislocation foresting, and develops strength with deformation. The associated deformation is also more homogeneous. The influence of precipitate shape on strength has not received much attention so far. It is known however, that thin precipitates are powerful strengtheners. In fact the rapid grain boundary strengthening possibly arises from the almost infinite thinness of the boundaries.

Precipitation hardening often displays a temperature dependence that is not expected at first glance from such large obstacles. There could be many reasons for this anomaly. Dislocations can climb over the particles with increasing rapidity at elevated temperatures. The precipitates themselves tend to coarsen with time at elevated temperature (Ostwald ripening). Besides, dislocation interaction with particles can cause directional growth of the precipitates (Carry & Strudel 1976) facilitating the dislocations to find weaker channels to creep. For strength at elevated temperatures, it is therefore essential to choose only those precipitates which remain uniform and stable. If the particle distribution is non-uniform, dislocations would increasingly concentrate their activity in weaker zones once they could climb to reach there.

2.5 *Two-phase hardening*

There is an important class of alloys intermediate between precipitation hardening and grain size strengthening. The microstructures of these alloys contain an intimate mixture of two or more phases. Microstructures under this category include eutectic, eutectoidal, and other transformation structures. A typical microstructure is shown in figure 4 (plate 1) (Banerjee 1980 unpublished). Such alloys derive their strength from the fine structure of the colonies and the increase in strength shows a Hall-Petch type relationship to the colony size, the exponent ranging from $-\frac{1}{2}$ to -1 (Embury 1972), suggesting that the strength arises partly from an Orowan type interaction and partly from the Hall-Petch interaction.

A special feature of two-phase strengthening is that the composite exhibits good ductility and energy-absorbing characteristics even if one of the phases is brittle (Manganon & Thomas 1970) and hence deserves intensive study.

2.6 *Solution hardening*

This method is perhaps the oldest and was successfully practised by alchemists for developing bronzes, brasses and golden ornaments. In solution hardening, the host atoms are either replaced by solute atoms or the solutes occupy interstitial sites in the lattice. In explaining the mechanism of solid solution strengthening, Labusch (1972), Labusch *et al* (1975) and Haasen (1979) have shown that the effect of mismatch strain for solutes could be significant while Stern (1975) and Collings & Gegel

(1975) emphasise the importance of chemical and electrical effects. Similarly while Labusch (1970) emphasises the importance of dielastic interaction, Riddhagni & Asimov (1968) find it to be negligible. The solution-strengthening problem, being atomistic in scale, is outside the regime of normal microstructure-mechanical property rationale and is to some extent less understood.

Figure 2 shows the influence of increasing solute concentration (f) for several solutes on the strength of Fe, Ni and Ti. The strength of interaction varies over at least three orders of magnitude. Some elements cause rapid hardening, others only gradual. The rapid hardening by carbon in Fe is usually attributed to the asymmetry of distortion at the tetragonal site (Fleischer & Hibbard 1973). Ti is rapidly strengthened by interstitials such as O, C, N which has been attributed to the strong bonding effect (Tyson 1975). Strengthening in a fcc lattice like nickel is gradual and is governed mostly by size mismatch (Stoloff 1972) and lowered stacking fault energy (Gerold & Hartman 1968). The alloy with lower stacking fault energy is stronger as dislocations get extended into wider partials which have to be constricted before they can cross-slip over obstacles or interact with other dislocations to produce plastic deformation. Also plotted in figure 2 are two types of curves: (i) curves representing hypothetical Orowan type interaction by solute clusters, which gives $f^{1/2}$ dependence and (ii) curves showing f^1 dependence. For rapid-hardening solutes $f^{1/2}$ dependence correlates well, while for slow hardening solutes at higher concentrations, the f^1 function fits better. Inflexible dislocations arising out of a large number of solutes with weak force constants give rise to f^1 dependence (Gerold 1979).

2.7 *Order strengthening*

The atomic order in alloys can lead to significant strengthening (Marcinkowski 1974; Westbrook 1974) giving higher yield strength, creep strength, as well as work hardening coefficient. The strength increment essentially arises due to dislocation interactions with domain boundaries and dislocations leaving a trail of antiphase domain boundaries. Increased work hardening rate (3–4 times higher than that for disordered alloys) is usually attributed to the accumulation of multipoles that are not annihilated owing to difficult cross slip of superdislocations. In non-cubic crystals these can arise from an interaction of dislocations with axial domain walls (Arunachalam & Cahn 1974). The decreased cross slip is beneficial to fatigue and creep properties (Marcinkowski 1974).

The strength of many two-phase alloys is due to the ordered intermetallic precipitates in them: $Ni_3Al(\gamma')$ in nickel base alloys, Ni_3Mo in maraging steels and $CuAl_2$/ Mg Zn_2/Al_2Cu, in Mg, Cu alloys. A major drawback associated with order-strengthening (like many other modes of rapid strengthening) is the accompanying embrittlement. Structural application of fully order-strengthened materials depends on improving their ductility.

3. Strengths at high temperatures

At elevated temperatures materials deform by creep energized by a variety of diffusional and thermally activated processes. Strengthening at high temperatures should

therefore be directed towards slowing down these processes. The efficacy of a particular strengthening mechanism can be gauged from its effect on the various parameters in the relevant creep equation.

3.1 *Strengthening against diffusional flow*

Diffusional flow in polycrystalline materials occurs by flow of matter from grain boundaries under compression to boundaries in tension (Nabarro 1948; Ashby 1969; Herring 1970; Coble 1971; Raj & Ashby 1971, 1972; Burton 1972; Harris 1973; Ashby 1973; Burton & Beere 1978). This flow can occur either through grain boundaries (Coble creep) or through the bulk (Nabarro-Herring creep), the total flow being represented by a creep equation:

$$\dot{\epsilon} = A\ [(\sigma_a - \sigma_b)/G]\ (\Omega/KTd^2)\ D_{\text{eff}},$$

$$D_{\text{eff}} = D_v\ [1 + (\pi\ \delta\ D_b/d\ D_v)],$$

where A = a constant, σ_a = the applied stress, σ_b = the back stress that pins down the vacancy sources and sinks, Ω = the atomic volume, G the shear modulus, D_v = volume diffusion coefficient, d = the grain size, δ = the boundary thickness, K=Boltzmann constant and T=temperature in K.

Creep can be minimised by reducing D_{eff} or increasing σ_b. The effective diffuson coefficient D_{eff} can to some extent be reduced by alloying with heavy elements (Mo in Ti; W, Mo in Ni, Mo in steels), or elements that bind vacancies (Si in Ti). The back stress σ_b which opposes the grain boundary vacancy sources and sinks can be imposed on a polycrystalline array by incorporating a fine dispersion of stable inert particles in the material. More importantly, increasing the grain size (d) decreases the creep rate as $1/d^2$.

Polycrystals creep also by boundary sliding, with grains sliding past one another causing stress concentrations, which force the necessary local accommodation by diffusional flow, cavitation, or by dislocation creep. It is particularly important to suppress this mode as most of the high temperature alloys ultimately fail by shear and parting at grain boundaries (Perry 1974). The creep rate that can be attributed to sliding in a polycrystal can be empirically written to be (Raj & Ashby 1972; Gifkins 1977; Wilcox & Clauer 1972, 1966; Ashby 1972 b):

$\dot{\epsilon}$ = $C\ (DGb/KT)\ (b/d)^m\ [(\sigma_a - \sigma_b)/b]^n\ (L^2/r^3)\ (f\ (1/d,\ \theta)$
$\dot{\epsilon}$ = the strain rate due to sliding
C = a constant,
b = the Burgers vector,
D_b = the effective diffusion coefficient at the boundary zone,
d = the grain size,
σ_a = the applied stress,
σ_b = the back stress to moving boundary defects,
n = 1–3 (usually about 2) (Gifkins 1977, 1978)
m = $\sim 1 - 1{\cdot}5$ (Gates & Horton 1977),
L = the particle spacing at grain boundaries,

r = size of particles at grain boundaries,
$1/d$ = the grain aspect ratio,
θ = the orientation of the grain alignment with respect to stress.

The tendency to slide is lowered by increasing the grain size, incorporating stable particles at the boundaries, and more powerfully by growing grains of large $1/d$, aligned along the stress axis. Directionally solidified microstructures, such as those shown in figure 5 (plate 1), strengthened with precipitates, ideally fit into this requirement (Tiwari & Hema Reddy 1979, unpublished work) and provide excellent creep properties (figure 6). By suppressing boundary sliding, we, in effect, convert a polycrystal into a 'single crystal'. Better still would be to go in for single crystals with no boundaries to worry about.

3.2 *Strengthening against dislocation creep*

All obstacles become increasingly transparent to dislocation motion at elevated temperatures. Dislocations assisted by diffusional processes climb or cross-slip over these obstacles. The flow rate by such a process can be given by an approximate equation of the form (Bird *et al* 1969; Kocks *et al* 1973; Ashby 1973; Balakrishna Bhat & Arunachalam 1977; Takeuchi & Argon 1976):

$$\dot{\epsilon} = A\ [(\sigma_a - \sigma_b)/G]^n\ (DGb/KT),$$

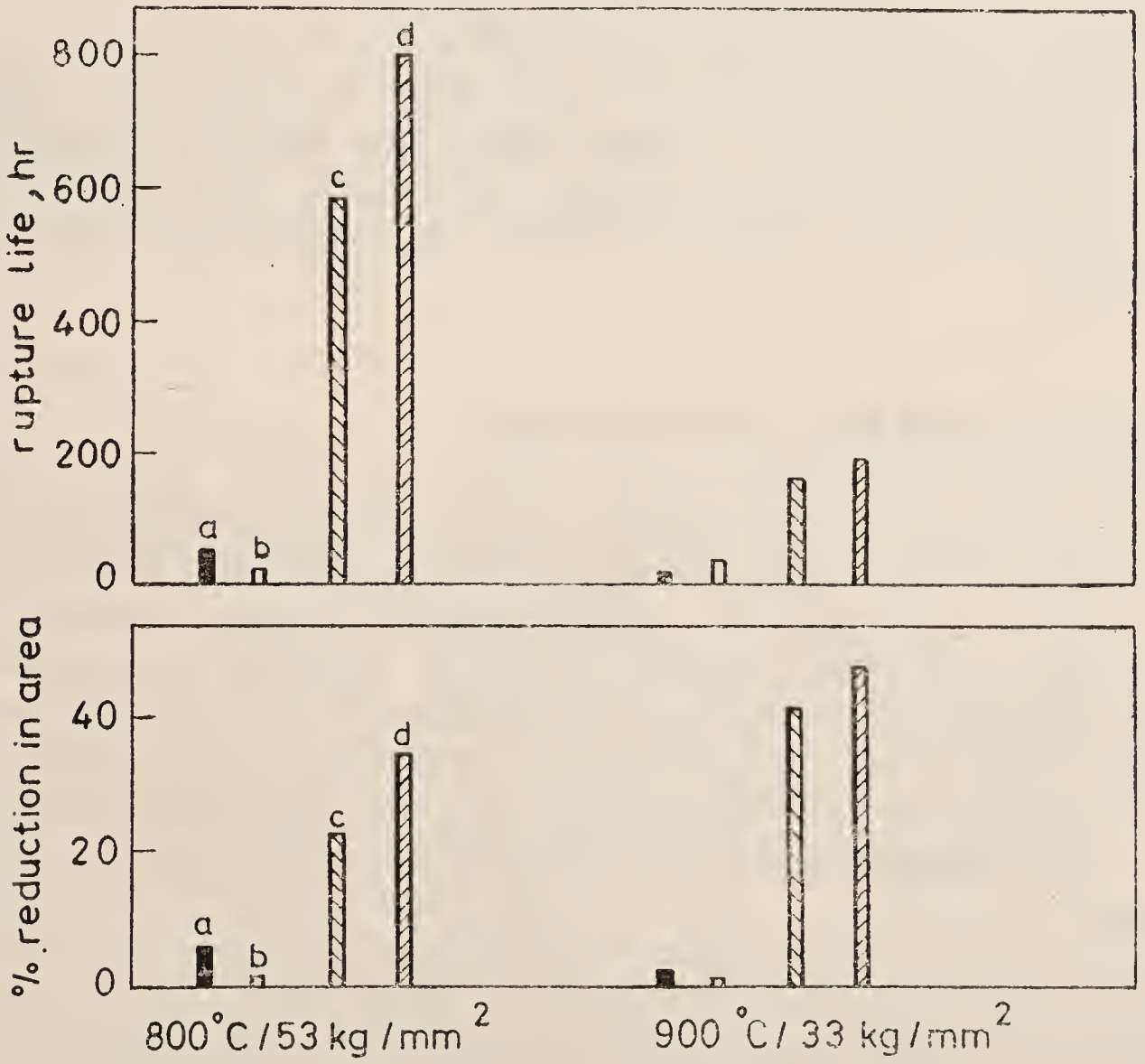

Figure 6. Creep properties of directionally solidified ZHS-6K compared against as cast properties (Hema Reddy & Tiwari, private communication). **(a)** Investment cast. **(b)** Investment cast plus heat-treated. **(c)** Directionally solidified. **(d)** Directionally solidified plus heat treated.

where the terms have their meanings as defined in previous sections. In this case the diffusion coefficient D is given by, $D \doteq D_v f_v + D_c f_c$, where f_v and f_c are the fraction of atom sites associated with bulk and core diffusion respectively; D_v is the volume diffusion coefficient and D_c the core diffusion coefficient.

It is essential to subdue dislocation creep for it is generally too rapid. We can attempt to decrease dislocation creep through many routes. D can be reduced a little by alloying. Some alloying elements segregate to dislocations (Si in Ti, Kehoe & Broomfield 1973) and form dragging obstacles. This leads to a reduced creep rate. Many elements in solution decrease stacking fault energy (Gallagher 1970). The dislocation reactions then become slower (Ashby 1973; Sastry *et al* 1974; Mohammed & Langdon 1974; Bird *et al* 1969) and the parameter A in the creep equation is reduced. The separated partials could climb together by nucleation of jog pairs. However, such nucleation has a large energy barrier and would be extremely slow (Baluffi & Granato 1979). Hence the separated partials will have to be constricted before climb or cross slip, an event which effectively introduces a back stress (σ_b) to dislocation motion. Stable particles can strongly reduce creep by providing a back stress which the dislocations must first overcome before creeping and interacting with other dislocations. The back stress has been calculated to be around 0·5 σ Orowan (Brown & Ham 1972) and recent calculations by Lagneborg & Bergman (1976) have suggested that this back stress is not constant but varies with applied stress. The back stress arises from the extra line lengths of dislocations that have to be created to form the climb configuration. The presence of this back stress explains the excellent creep resistance of nickel base superalloys. The back stress that is responsible for subdued creep also explains the anomalously high values of activation energy and stress exponents in the creep rate equation for these materials. Table 3 shows how incorporation of back stress in the creep equation brings down both θ and n values in line with the observed values for precipitate free systems (Balakrishna Bhat 1980; Lund & Nix 1975; Parker & Wilshire 1975).

4. Strengthening against high rates of deformation

There are some applications where the materials are required to stand up to localized impulsive forces, as for instance when they are hit by high velocity projectiles.

A parameter that is important for such an application is plastic modulus, $\partial\sigma/\partial\epsilon$, a function related to the work hardening coefficient. This parameter determines the spread of deformation in the bulk since plastic deformation waves propagate with a speed V_p given by $V_p = \{(\partial\sigma/\partial\epsilon)\rho\}^{1/2}$ (Cottrell 1966; Johnson 1972). High ' plastic modulus ' ensures that deformation rapidly spreads over a large volume which prevents strain localization and leads to the protection of the material against fracture. There are a number of ways of increasing this modulus; fine grain size, presence of fine non-deformable particles and solid solution alloying all increases this coefficient or shift the limit of work hardening to higher strain values. Precipitation hardening is not all that effective for this purpose as the precipitates are generally cut at high stresses and therefore do not lead to an increase in the work hardening. At strain rates between 10^3 to 10^4 s^{-1}, phonon drag has been claimed to be an energy dissipation mechanism (Klahn *et al* 1970; Kumar 1970). It is not clear how import-

Table 3. Incorporation of back stress in the creep equation removes the apparent anomaly in activation energies

Material	Temperature (°K)	n	Q app K mole^{-1}	Correction to Q due to variation of elastic modulus, K. cal, mole^{-1}	Correction to Q due to variation of back stress K. cal, mole^{-1}	Q real cal mole^{-1}
TD Nickel	1174	4	768	40	444	284
(Wilcox and	1218	4	768	43	442	283
Clauer 1966)	1343	4	980	56	650	274
Dispersion	977	4	640	9	238	392
strengthened	1200	4	810	45	434	331
superalloy	1311	4	835	72	406	357

ant this effect is in dislocation flow (Grenato 1973). More important than this is to combat adiabatic effects (figure 7, plate 2) (Balakrishna Bhat 1979; Tirupataiah & Raju 1980a unpublished work; Tirupataiah & Raju 1980) and to ensure that localized softening does not take place by adiabatic heating. This can be achieved only by choosing compositions of high melting point and avoiding inhomogenities which could otherwise localize flow. Increased ductility is also essential and this can be ensured by choosing systems with fcc structures or hcp structures with low c/a values (Kawata & Kuriyama 1974). Another exotic approach is to choose systems where the high stresses induce phase transformation, thus providing an energy dissipation mechanism. This has been attempted in some selected ceramic systems and in TRIP steels.

At high strain rates, the dislocation density can reach very high values which are not seen during normal rates of deformation. To provide strengthening, the obstacle density should therefore be high enough to match the increased dislocation density. Viewed from this angle, most of the strengthening mechanisms are ineffective and solute hardening may perhaps be the best.

5. Conclusions

Metals can be strengthened in a variety of ways appropriately combined to design alloys that can stand up to the major operating deformation mechanisms. There exist semi-quantitative relations to assess the efficacy of these strengthening routes, which can be used to guide us in alloy design.

Some of these techniques are well-understood and are being effectively used, while a few others deserve a better in-depth study so that they can also be utilised effectively. Newly emerging processing techniques provide challenges to the alloy designer to use them to synthesise alloys with still better properties. It is this challenge that makes alloy design intellectually stimulating and technically rewarding.

The authors thank Drs M L Bhatia, R Sivakumar, S N Tiwari and D Banerjee for discussions during the preparation of the manuscript and Dr D Banerjee, Shri Y Tirupataiah, Dr K R Raju and Shri M Hema Reddy for permission to cite their unpublished results.

List of symbols

A	constant in phenomenological relation
b	Burgers vector
c	constant
D	diffusion coefficient
D_b	boundary diffusion coefficient
D_v	volume diffusion coefficient
D_{eff}	effective diffusion coefficient
E	effective line tension
F_{dis}	energy per unit length of dislocation
f_c	fraction of sites associated with core diffusion
f_v	fraction of sites associated with volume diffusion
ΔF	activation free enthalpy
ΔF_{dis}	difference between high energy and low energy positions of the dislocation
G	shear modulus
k	Boltzman constant
K	Hall-Petch coefficient, a constant
L	obstacle spacing
m	exponent for $(1/d)$ for boundary sliding
n	stress exponent
r	particle radius
T	absolute temperature
w	obstacle width
$1/d$	aspect ratio
$\alpha_1, \alpha_2, \alpha_3$	constants
γ	surface energy
γ_{APB}	antiphase boundary energy
ϵ	strain
$\dot{\epsilon}$	strain rate
$\Delta\sigma$	strength increment
δ	boundary thickness
σ_a	applied stress
σ_b	back stress
ρ	dislocation density
τ	shear stress
τ_c	critical stress
τ_{ele}	element glide resistance
$\partial\tau/\partial\gamma$	variation of shear strength with strain

References

Armstrong R W, Codd I, Douthwaite R M & Petch N J 1962 *Philos. Mag.* **7** 45
Arunachalam V S & Cahn R W 1974 *Ordered alloys*, Proc. III Bolton Landing Conf. (New York: Claitors Pub. Dn.) p. 215
Ashby M F 1969 *Scr. Metall.* **3** 837
Ashby M F 1970 *Strength of metals and alloys* (Asilomar: Am. Soc. Met.) Vol. 2, p. 507
Ashby M F 1972a *Acta Metall.* **20** 887

Ashby M F 1972b *Surface Sci.* **31** 498
Ashby M F 1973 Microstructure and design of alloys, Proc. III Int. Conf. *Strength of metals and alloys* (London: Inst. Metals) Vol. 2, p. 8
Balakrishna Bhat T & Arunachalam V S 1977 *J. Mater. Sci.* **12** 2241
Balakrishna Bhat T 1980 *Effect of second phase on microstructural development and properties*, Ph.D thesis (to be submitted), Indian Institute of Technology, Madras
Baluffi R W & Granato A V 1979 Dislocations, vacancies and interstitials in *Dislocations in solids* ed. FRN Nabarro (Amsterdam: North Holland Pub. Co.) Vol. 4, p. 1-133
Bird J E, Mukherjee A K & Dorn J E 1969 *Quantitative relation between properties and microstructure* eds D G Brandon & A Rosen (Jerusalem: Israel Univ. Press)
Brown L M & Ham R K 1972 in *Strengthening methods in crystals* eds A Kelly & R B Nicholson (Amsterdam: Elsevier) p. 12
Burte H M & Gegel H L 1980 *Proc. Indian Acad. Sci.* (*Engg. Sci.*) **3** 261 (this issue)
Burton B 1972 *Mater. Sci. Eng.* **11** 255
Burton B & Beere W B 1978 *Metal Sci.* **12** 71
Cahn R W 1980 *Contemp. Phys.* **21** 43
Carry C & Strudel J L 1976 *Strength of metals and alloys*, Proc. IV Int. Conf. Nancy, France, Laboratoire de Physique du Solide, Vol. 1, p. 324
Coble R L 1971 *J. Appl. Phys.* **34** 1679
Collings E W & Gegel H L 1975 in *Physics of solid solution strengthening* eds E W Colling & H L Gegel (New York: Plenum) p. 147
Cottrell A H 1966 *The mechanical properties of matter* (New York: John Wiley)
Decker R F 1969 *Steel strengthening mechanism*, Proc. Symp. Zurich
Decker R F 1973 *Metall. Trans.* **4** 2495
Embury J D 1972 *Strengthening methods in crystals* eds A Kelly & R V Nicholson (Amsterdam: Elsevier) p. 331
Everhart J L 1954 *Titanium and titanium alloys* (New York: Rheinhold Pub. Corpn.)
Fleischer R L & Hibbard W R 1973 in *The relations between microstructure and mechanical properties of metals*, NPL Symp., London, HMSO, Vol. 1, p. 261
Foreman A T E & Makin M J 1966 *Philos. Mag.* **14** 911
Foreman A T E & Makin M J 1967 *Can. J. Phys.* **45** 511
Frost H J & Ashby M F 1975 in *Fundamental aspects of structural alloy design* eds R I Jaffee & B A Wilcox (New York: Plenum) p. 27
Gallagher P C J 1970 *Metall. Trans.* **1** 2429
Gates R S & Horton C A P 1977 *Mater. Sci. Eng.* **27** 105
Gerold V 1979 Precipitation hardening in *Dislocations in solids* eds FRN Nabarro (Amsterdam: North Holland) Vol. 4, p. 222
Gerold V & Haberkorn H 1966 *Phys. Status Solidi* **16** 675
Gerold V & Hartman K 1968 *Strength of metals and alloys*, Proc. Int. Conf., *Suppl. to Trans. Jpn Inst. Met.* **9** 34
Gifkins R C 1977 *Matall. Trans.* **A8** 1507
Gifkins R C 1978 *J. Mater. Sci.* **13** 1926
Gleiter H & Hortbogen E 1967 *Mater. Sci. Eng.* **2** 285
Grenato A V 1973 in *Metallurgical effects at high strain rates* eds R W Rohde, B M Butcher, J R Holland & C H Karnes (New York: Plenum) p. 255
Grilhe J, Boisson M, Seshan K & Goboriand R J 1977 *Philos. Mag.* **36** 923
Haasen P 1979 Solid solution strengthening in *Dislocations in solids* ed F R N Nabarro (Amsterdam: North Holland Publ. Co.) p. 115
Hall E O 1951 *Proc. R. Soc.* (*London*) **B64** 747
Harris J E 1973 *Metal. Sci. J.* **7** 1
Herring C 1970 *J. Appl. Phys.* **21** 437
Hirsch P B & Kelly A 1965 *Philos. Mag.* **12** 881
Hockett J E & Zukas E G 1974 *Mechanical properties at high rates of strain*, Proc. Conf. (London & Bristol: Oxford Pub. Inst. of Physics) p. 53
Humphreys H J, Hirsch P B & Gould D 1970 *Strength of metals and alloys* Proc. II Int. Conf., Asilomar (Asilomar: Am. Soc. Met.) p. 550
Hutchinson M M & Pascoe R T 1972 *Met. Sci. J.* **6** 90

Jaffee R I 1973 *Titanium science and technology* eds R I Jaffee & H M Burte (New York: Plenum) **3** 1654
Johnson W 1972 *Impact strength of materials* (England: Edward Arnold)
Kawata K & Kuriyama S 1974 *Mechanical properties of materials at high rate of strain* (Oxford: Inst. of Phys.; London, Bristol: Inst. of Phys.) p. 215
Kehoe M & Broomfield R W 1973 *Titanium science and technology* eds R I Jaffee & Burte H M (New York: Plenum)
Klahn D, Mukherjee A K & Dorn J E 1970 *Strength of metals and alloys* Proc. II Int. Conf., Asilomar (Asilomar Am. Soc. Met) p. 949
Kocks U F, Argon A S & Ashby M F 1973 Thermodynamics and kinetics of slip in *Progress in materials science* eds B Chalmers, J W Christian & T B Massalski (New York: Pergamon) p. 423
Kocks U F, Labusch R & Schwarz R B 1974 *Strength of metals and alloys* Proc. IV Int. Conf., Nancy, (Asilomar: Am. Soc. Met.) Vol. 1, p. 275
Kumar A 1970 *Strength of metals and alloys*, Proc. II Int. Conf., Asilomar (Asilomar: Am. Soc. Met.) p. 1001
Kutumba Rao V V P, Taplin D M R & Rama Rao P 1975 *Metall. Trans.* **A6** 77
Labusch R 1970 *Phys. Status Solidi* **41** 659
Labusch R 1972 *Acta Metall.* **20** 917
Labusch R, Ahearn I, Grange G & Haasen P 1975 *Rate processes in plastic deformation of materials* (Ohio, Metals Park: Am. Soc. Met.) p. 226
Lagneborg R & Bergman B 1976 *Metal Sci.* **10** 20
Lindholm U S 1974 *Mechanical properties of materials at high rates of strain* (London & Bristol: Inst. of Phys.) p. 3
Lund R W & Nix W D 1975 *Metall. Trans.* **A6** 1329
Manganon P L & Thomas G 1970 *Metall. Trans.* **11** 113
Marcinkowski M J 1974 in *Order-disorder transformations in alloys* Proc. Int. Symp., Tubingen, Germany (Berlin: Springer Verlag) p. 364
Margolin H & Stanescu M S 1975 *Acta Metall.* **23** 1411
McElroy S & Zkopiak Z C 1972 *Int. Metal. Rev.* **17** 175
Mitchell W I 1966 *Z. Metallk.* **57** 586
Mohammed F A & Langdon T G 1974 *Acta Metall.* **22** 779
Morris L R, Sang H & Moore D M 1976 *Strength of metals and alloys*, Proc. IV Int., Conf., Nancy, (Nancy, edt. Laboratoire de Physique du Solide) Vol. 1, p. 131
Nabarro F R N 1948 *Strength of solids*, Rep. on Conf., (London: Phys. Soc.) p. 75
Nicholson R B 1971 *Effects of second phase particles on the mechanical properties of steels* (London: Iron & Steel Inst.)
Oxley P L B 1974 in *Mechanical properties at high rates of strain*, Proc. Conf., (Oxford: Inst. of Phys.) p. 378
Parker J D & Wilshire B 1975 *Metal Sci.* **9** 248
Pattanaik S, Bhatia M L & Arunachalam V S 1974 *Trans. Indian Inst. Met.* **27** 227
Pelloux M N & Grant N J 1960 *Trans. TMS, AIME* **218** 232
Perry A J 1974 *J. Mater. Sci.* **9** 1016
Petch N J 1953 *J. Iron Steel Inst.* **174** 25
Petty G R 1974 *Physical metallurgy of engineering materials* (England: George Allen and Unwin Limited) p. 103
Pickering F B 1978 *Physical metallurgy and the design of steels* (England: Appl. Sci. Publ., Barking)
Raj R & Ashby M F 1971 *Metall. Trans.* **2** 1113
Raj R & Ashby M F 1972 *Metall. Trans.* **3** 1937
Rama Rao P 1978 *Trans. Indian Inst. Met.* **31** 239
Riddhagni B R & Asimov R M 1968 *J. Appl. Phys.* **39** 4144, 5169
Russell K C & Brown L M 1972 *Acta Metall.* **20** 969
Sastry D H, Luton M J & Jonas J J 1974 *Philos. Mag.* **30** 115
Sims C T & Hagel W C 1972 *Superalloys* (New York: Wiley Interscience)
Solonia O P & Kuraeva V P 1973 *Titanium science and technology* eds R I Jaffee & H M Burte (New York: Plenum) Vol. 4, p. 2156

Stern E A 1975 in *Physics of solid solutions strengthening* eds E W D Collings & H L Gegel (New York: Plenum) p. 183
Stoloff N S 1972 in *Superalloys* eds C T Sims & W C Hagel (New York: Wiley Interscience) p. 105
Takeuchi S & Argon A S 1976 *J. Mater. Sci.* **11** 1542
Thompson A W, Baskes M I & Flanagan W F 1973 *Acta Metall.* **21** 1017
Tien J K 1975 in *Fundamental aspects of structural alloy design* eds R I Jaffee & B A Wilcox (New York: Plenum) p. 27
Tirupataiah Y & Raju K R 1980 Technical Report MPG 80-02, Defence Metallurgical Res. Lab., Hyderabad
Tyson W R 1975 in *The physics of solid solution strengthening* eds E W Collings & H L Gegel (New) York: Plenum) p. 47
Weertman J 1968 *Trans. Am. Soc. Met.* **61** 681
Weertman J 1975 in *Rate processes in plastic deformation of materials* ed. Amiya Mukherjee (ASM p. 315
Westbrook J R 1970 *Ordered alloy*, III Bolton Landing Conf. (New York: Claitors Pub. Dn.)
Wilcox B A & Clauer A H 1966 *Trans. TMS AIME* **236** 570
Wilcox B A & Clauer A H 1972 *Acta Metall.* **20** 743

Plate 1

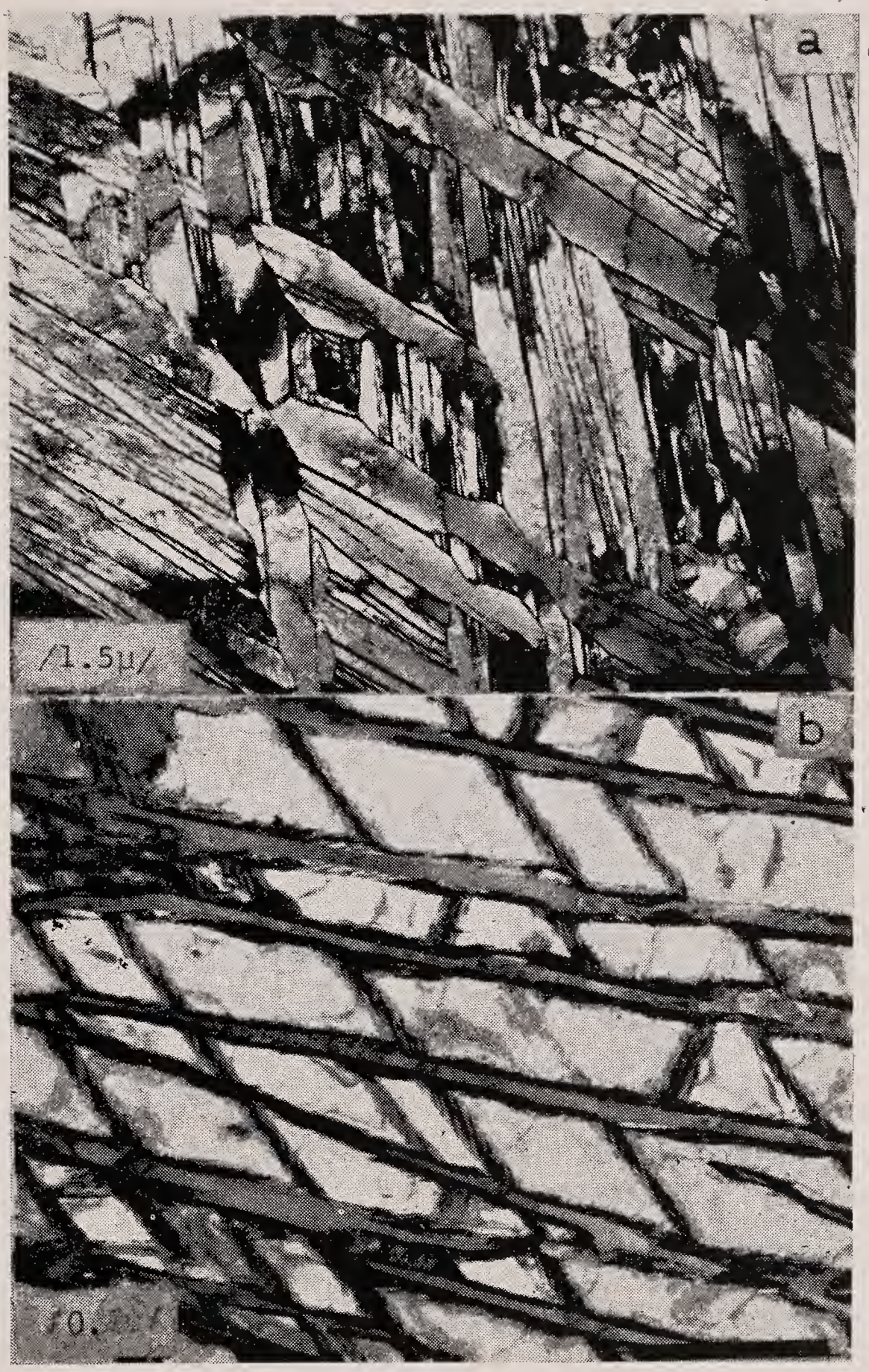

Figure 4. Two-phase structure in a typical titanium alloy.

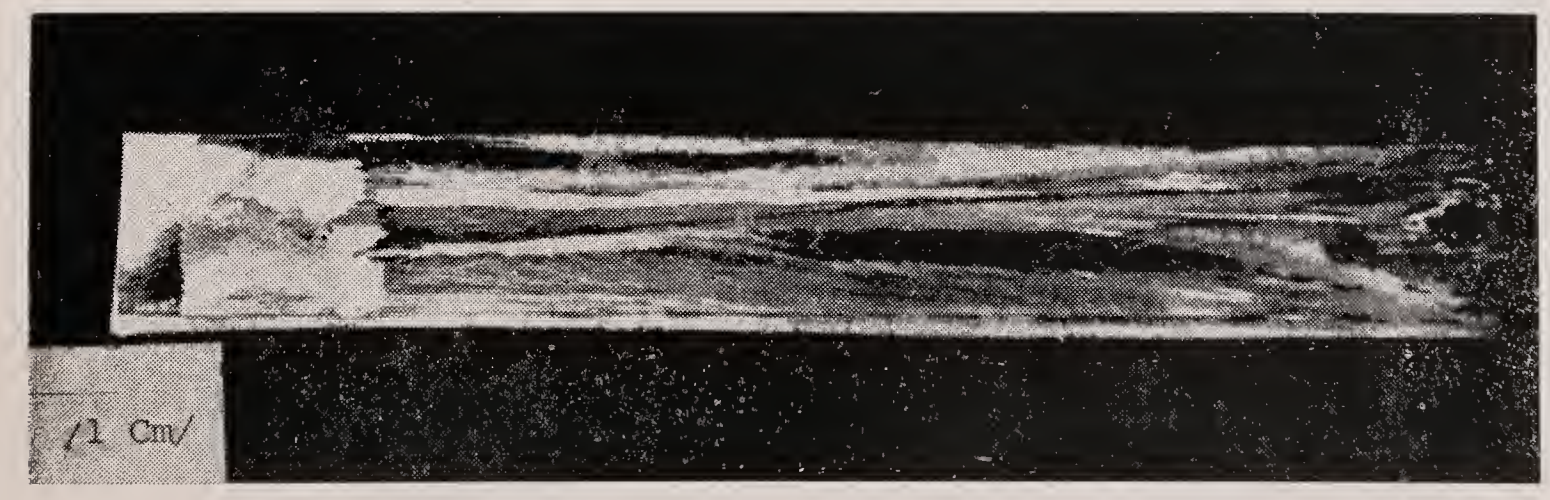

Figure 5. Directionally solidified ZHS-6K alloy.

Plate 2

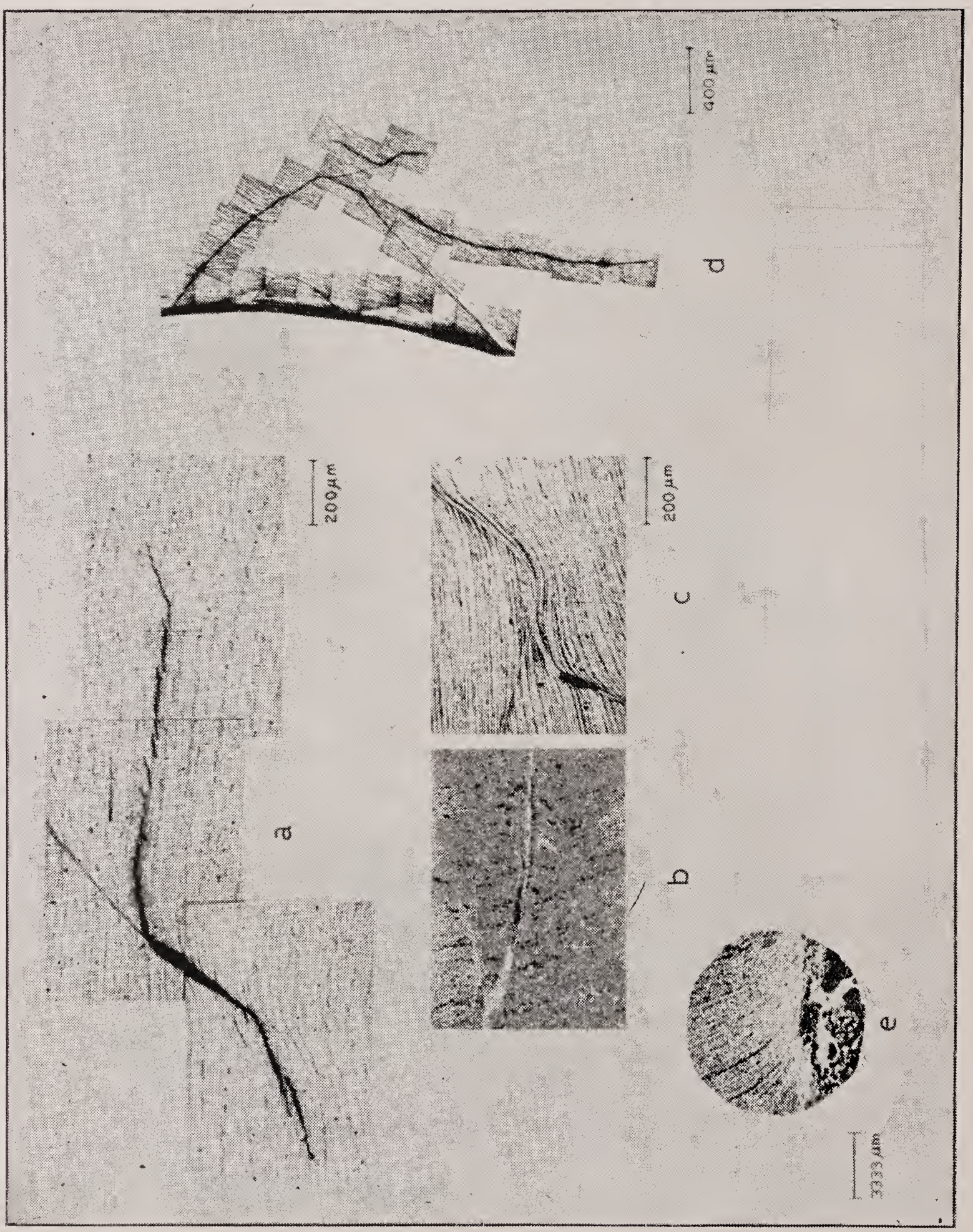

Figure 7. Adiabatic shear bands in steel with associated cracking failure.

Strengthening against creep

M L BHATIA
Defence Metallurgical Research Laboratory, Hyderabad 500 258

MS received 8 October 1980

Abstract. Strengthening alloys against creep deformation involves strengthening against dislocation glide and climb, and grain-boundary sliding. The rationale behind various techniques currently used for strengthening are discussed, especially with reference to Ni-base superalloys. Although one should try and minimize sliding by increasing grain-boundary viscosity, the grains should not be over-strengthened to minimize problems due to creep cavitation.

Keywords. Creep; strengthening mechanism; dislocation glide; dislocation climb; grain boundary sliding; precipitation hardening; recovery; solution strengthening; grain boundary viscosity; cavitation; superalloys.

1. Introduction

Time-dependent deformation of a structure under stress is known as creep. Creep can come about by dislocation movement at all temperatures. In addition grain-boundary sliding contributes to strain and the formation of cavities at temperatures above 0·5 T_m, T_m being the melting point of the base metal on the absolute scale.

When a material is loaded at a particular stress, it work-hardens and the deformation rate comes down. Upto $\sim 0{\cdot}1\ T_m$, no recovery processes are available and creep rate comes down with time, leading to logarithmic creep. Since creep rates in logarithmic creep soon become very slow, it is important only in very high-precision components, wherein locked-up stresses would impair dimensional accuracy (McLean 1962). Between 0·1 and 0·3 T_m, though some recovery processes come into play and creep rate does not come down as rapidly as in logarithmic creep, it is not a temperature regime in which the creep phenomenon causes serious problems. Thus, we shall mainly concern ourselves with the creep problem encountered by engineers; and this happens to be operative above 0·3 T_m, where recovery processes lead to a steady-state creep rate. Such a creep behaviour is known as recovery creep.

The intrinsic properties one has to consider for deciding the base metal for a particular application are its modulus, melting point, diffusivity and stacking fault energy. These have been adequately discussed (Ashby 1973). The metal base one would choose would be dictated by the operating temperature, stress, environment, and of course, cost. We shall not go into these aspects of choosing a metal base, but once a metal has been chosen, consider how it can be made resistant to creep under given operating conditions.

In this article we shall review our understanding of how different alloying elements and microstructures affect the high-temperature properties of an alloy. We shall do this in detail for Ni-base superalloys which play the most important role in gas turbines and have helped in understanding the various strengthening mechanisms.

We shall also outline some facets of alloy behaviour that need further understanding. which will help us design tailor-made alloys with lesser empiricism.

The basic problem in the use of alloys at elevated temperatures is to enable them to withstand deformation loads, and to ensure that they do not undergo surface degradation in the environment they are used in. The first problem can be tackled in two ways:

(i) By providing obstacles to the movement of dislocations and minimizing grain-boundary (GB) sliding.
(ii) By making a strong phase share a large fraction of the total load, so that the stress on the matrix is low (fibre strengthening). This method of strengthening will not be considered here.

One of the major problems in using the above two approaches is that of microstructural stability under operating temperatures, stresses, and temperature and stress cycles that a component is subjected to. Resistance to environmental degradation can be provided by alloying elements which form protective adherent oxide with low diffusivity for anionic and cationic species. Quite often an alloy is developed with mechanical properties in view, and then it does not have adequate resistance to environmental degradation. Under these circumstances the alloys are suitably coated to withstand such degradation.

2. Alloy strengthening against dislocation movement

There are a wide variety of obstacles that can be used to restrict the movement of dislocations. Unfortunately some of these like radiation-hardening and grain boundaries are useful only at low temperatures. This is because radiation-hardening anneals out at temperatures below 0·3 T_m (Finniston 1958-59). The grain boundaries cannot be used as obstacles at temperatures above 0·5 T_m, since they start to slide past each other and contribute to strain and generation of cavities leading to accelerated flow and fracture under creep. In addition, grain boundaries are responsible for diffusional flow. Thus grain boundaries are a source of weakness and have to be strengthened at temperatures above 0·5 T_m.

Another important low-temperature strengthening mechanism is substructure strengthening. Although successful attempts have been made to use substructure strengthening against creep at temperatures above 0·5 T_m in pure metals, specially those with low stacking fault energies (SFE) (Shorshorov 1973), this strengthening mechanism is unlikely to be useful in commercial alloys because of the instability of substructure under the combined action of stress and temperature. In fact, the presence of unstable substructure can lead to a larger mobile dislocation density leading to a higher creep strain and lower rupture life (Pattanaik *et al* 1974; Lloyd & McElroy 1974; Doble 1967).

The other strengthening mechanisms which are useful at low temperatures and are of interest at high temperatures are solid solution strengthening and second-phase particle strengthening. Before we consider the applications of these strengthening mechanisms we shall briefly consider some elementary concepts of creep deformation at temperatures above 0·4 T_m (recovery creep).

2.1 *Recovery creep*

Most engineering alloys used at high temperatures show small primary creep strains and spend a large fraction of their life in the steady-state creep regime (Grant & Mullendore 1965). In view of this observation we shall mainly concern ourselves with understanding how the steady state creep strain rate, $\dot{\gamma}$, can be minimized. The structure being deformed develops an increased dislocation density with time, which is responsible for slowing down the primary creep rate. Thereafter the alloy is expected to develop a dislocation structure which is typical of stress and temperature during steady-state creep. Cross-slip and climb are two possible recovery mechanisms, but since the edge dislocations cannot be eliminated by cross-slip, the important recovery mechanism which is responsible for maintaining a constant dislocation structure is the climb of dislocations during steady-state creep (McLean 1962). Deformation during steady-state creep comes about by glide between obstacles, and climb of dislocations, so that they are freed from the obstacles holding them. The creep rate can now be visualized to be either glide-controlled (viscous creep) or climb-controlled (recovery creep), depending upon which of these two steps is slower. During viscous creep the internal stress τ_{disl} due to dislocation structure, is expected to be less than τ_{app}, the applied stress (Dutton 1970). Thus, the dislocations can be considered to glide under the influence of effective stress, $\tau_{\text{eff}} = \tau_{\text{app}} - \tau_{\text{disl}}$. During climb-controlled recovery creep, the effective stress on dislocations is expected to approach zero so that $\tau_{\text{app}} = \tau_{\text{disl}}$. It is important to distinguish between viscous creep and climb-controlled recovery creep as the operating mechanism, since alloying elements influence glide and climb differently, *e.g.* climb rate is expected to be a strong function of the stacking fault energy (SFE) of the matrix whereas the glide rate is not (Sherby & Burke 1967).

Steady-state strain rate, γ is given by a formula of the form (Ashby 1973; Sherby & Burke 1967).

$$\dot{\gamma} = \frac{A\, D_{\text{eff}}\, G\, b}{kT} f(\text{SFE})\, (\tau_{\text{app}}/G)^n, \tag{1}$$

where A and n are material constants, D_{eff} is the effective diffusion coefficient and takes into consideration relative contributions due to volume diffusion and dislocation core diffusion, f(SFE) is a function of the SFE of the material, G is the shear modulus, b is Burger's vector of dislocation, and k and T have their usual significance.

Values of $n = 3$ have been found for some solid solution alloys and are ascribed to viscous creep. According to a simplistic model (Bird *et al* 1969) $n = 3$ for viscous creep can be rationalized on the assumption that mobile dislocation density ρ_m is proportional to $(\tau_{\text{app}})^2$, and their velocity v is proportional to τ_{app}. Thus $\dot{\gamma} = \rho_m\, bv$, gives a value of $n = 3$. However, one would expect ρ_m to be a function of τ_{disl} and τ_{eff}, and v to be a function of τ_{eff}. Simple dependence of $\dot{\gamma}$ on τ_{app} can arise only if τ_{eff} is $\alpha\ \tau_{\text{app}}$. In an alloy which is supposed to deform by viscous creep, this simple proportionality has not been found (Oikawa & Karashima 1974).

Values of n between 4 and 5 have been found for a large number of pure metals

at temperatures above 0·5 T_m and activation energy in such cases corresponds to that for self diffusion. The creep process under these circumstances has been unambiguously identified as climb-controlled recovery creep (Bird *et al* 1969). Values of n between 4 and 5 are best understood if one considers

$$\dot{\gamma} = d\gamma/dt = (d\tau/dt)/(d\tau/d\gamma) = \dot{r}/h, \tag{2}$$

where $\dot{r}$ is the recovery rate and h is the hardening rate. The stress dependence of $\dot{\gamma}$ arises mainly from stress dependence of $\dot{r}$ (McLean 1962; Watanabe & Karashima 1970). Now, if one considers $\dot{r}$, as due to the growth of the dislocation network by the climb process, $\dot{\gamma} \propto (\tau_{\text{disl}})^3$ in the absence of stress (Friedel 1964). The presence of stress is known to accelerate the recovery process (Thornton & Cahn 1961). The climb rate in the presence of stress is expected to be further enhanced by a factor which is proportional to the normal stress, which in turn is proportional to τ_{app}. Since $\tau_{\text{app}} = \tau_{\text{disl}}$, the value of $n = 4$ is easily understood.

2.1a *Solid solution strengthening* Aspects of solid solution strengthening at ambient temperatures are reasonably well understood. The strengthening due to solutes is expected to be proportional to the distortion of the matrix, as judged by change in lattice parameter (Mott & Nabarro 1948). Thus 10 at.% W and 30 at.% Cr produce a similar change in the lattice parameter of Ni and lead to a similar increase in flow stress. Increase in flow stress is also proportional to ΔN_v for the same distortion of the matrix (Decker 1968) where ΔN_v is the difference between the electron vacancy number of the solvent and the solute. The dependence of flow stress on ΔN_v has been attributed to the differences in the modulus of solute and solvent (Fleischer 1963), and to a decreased SFE (Beeston *et al* 1968).

Regarding the contribution of solutes to creep resistance, not much data correlating creep with the nature of the solute exists. The contribution of solutes towards increased modulus G (Stoloff 1972), in increasing the creep resistance, (*via* equation (1)) is doubtful, since G does not seem to vary with increasing solute content (INCO 1977). The direct contribution of solutes to flow due to the distortion of the matrix, or due to the modulus difference between solvent and solute atoms is unlikely to be important (McLean 1962). This can be easily understood to be the situation for climb-controlled recovery creep. According to McLean, solutes reduce creep rate by hindering climb, possibly through their influence on SFE. In support of these views, one could cite results which show that there is no significant difference in stress rupture at 815°C, (0·6 T_m), between Ni-10 at.% W and Ni-10 at.% Cr alloys (Pelloux & Grant 1967). If distortion of the matrix and glide were important considerations, there would have been significant differences. On the other hand, the ΔN_v contribution is likely to be identical for both W and Cr (Stoloff 1972) and thus they both would similarly influence the creep life. In view of the importance of SFE on creep behaviour, it would be useful to have reliable data on the effect of different solutes on SFE. Cobalt is supposed to be added to Ni-base superalloys because it is supposed to reduce the SFE (Stoloff 1972). However Cr has been shown to be twice as effective in reducing the SFE as Co (Beeston & France 1968). In addition, the SFE of Ni-Co alloys is expected to increase with increasing temperature (Ericsson 1966). The reason for Co addition may be its unusual influence on Al

and Ti solubility in Ni-Cr alloys (Heslop 1964). It decreases the solubility of Ti and Al at lower temperatures, thus increasing the volume fraction of the γ' phase; in addition it reduces the γ' solvus temperature, thus increasing the temperature range in which the alloys can be hot-worked.

2.1b *Second-phase particle strengthening* The decrease in creep rate brought about by addition of alloying elements which go into solid solution is insignificant compared to the decrease effected by the presence of second-phase particles. For example, single-phase Ni-20 Cr decreases the creep rate of Ni by a factor of 10^2 at 750°C, addition of 3·5% (Al+Ti) which form 15–20% volume fraction of the γ' phase, further reduces the creep rate of Ni-20 Cr by a factor of 10^6 (Threadgill & Wilshire 1974).

Nickel-base superalloys expected to resist deformation at high temperatures are two-phase alloys, consisting of fcc (γ) matrix, strengthened either by γ' Ni_3 (Al, Ti) or oxide dispersions. γ' is obtained by precipitation from a supersaturated solid solution and forms uniformly throughout the matrix. γ' being deformable, rather larger volume fractions of this phase can be incorporated without making the alloy brittle. Oxide-dispersion strengthened alloys contain oxides with high free-energy of formation and are incorporated into the matrix by the powder metallurgy route. Large volume fractions of oxide dispersions cannot be incorporated without making the alloy brittle (Hosford 1973). γ'-strengthened alloys have superior strength and creep resistance characteristics below $\sim$ 1000°C because of the large volume fraction of finely spaced γ'. The poorer properties of γ'-strengthened alloys at higher temperature is due to drop in the strength of γ' with increasing temperature, and because of their rapid coarsening. Dispersion-strengthened alloys are superior at higher temperatures where the dispersoids are stabler. If superior mechanical properties are required over a wide temperature range, the superalloys can be strengthened by both the γ' particles and the oxide dispersions (Benjamin & Bomford 1974).

Before we discuss the creep behaviour of superalloys, we would briefly like to consider the mechanical behaviour of γ' (Ni_3Al). Ni_3Al has a superlattice with Cu_3Au type structure and remains ordered upto very close to its melting point, 1385°C. Figure 1 (Thornton *et al* 1970) shows the flow stress of Ni_3Al at different temperatures and strains. The flow stress of Ni_3Al remains unchanged over a large temperature range if one considers the flow stress at a strain of 10^{-6}. However, flow stress at higher strains becomes a function of temperature and shows a maximum at 700°C. Thornton *et al* attribute this behaviour to increasing (100) slip with increasing temperature, and increased work-hardening due to interaction of (111) and (100) slip. The softening above 700°C has been attributed to recovery.

We shall not discuss the behaviour of two-phase alloys in short-time tensile tests. This behaviour has been adequately reviewed (Kelley & Nicholson 1963; Stoloff 1972). We would like to mention that alloys containing non-deformable oxide dispersions yield by the Orowan-looping mechanism. In the γ'-strengthened alloys, when the interparticle spacing is small, the particle is cut before the stress required for looping is reached (Balakrishna Bhat & Arunachalam 1980). When the particle is cut, the flow stress is a function mainly of coherency strains, and antiphase boundary energy. In addition the flow stress depends upon differences in elastic moduli between γ and γ', and particle matrix surface energy.

The increased resistance to creep in two-phase alloys has been considered to arise

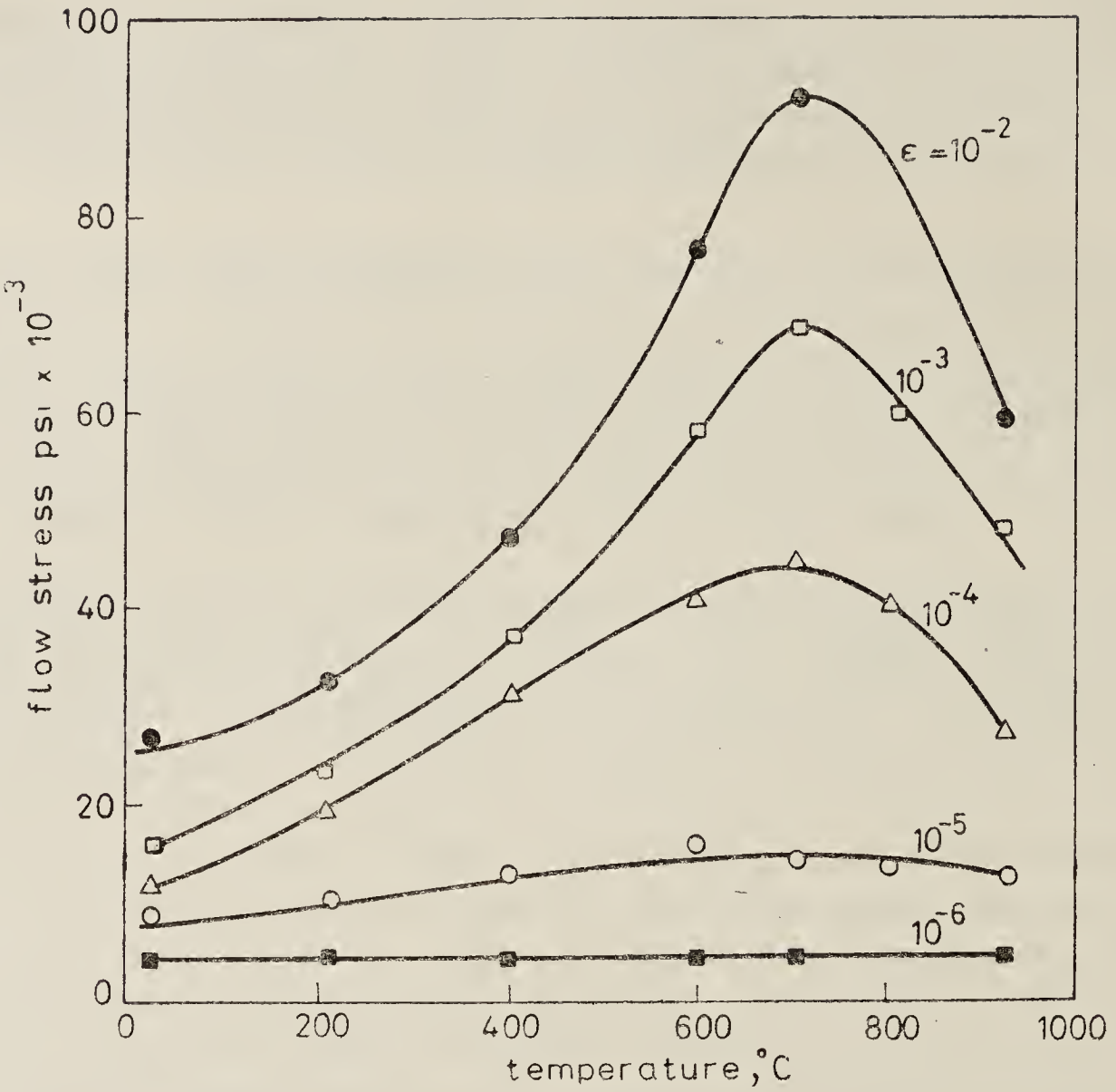

Figure 1. Increase in flow stress of γ' (Ni_3Al) with temperature measured at various strain levels. After Thornton *et al* (1970)

from threshold stress, the stress below which climb will not take place. The concept of threshold stress was first proposed by Brown & Ham (1971) and they considered it to arise from increased dislocation length, which has to be supplied by stress, as the dislocation overcomes the particle by climb. According to recent estimates (Shewfelt & Brown 1977) the threshold stress is expected to be 0·4 (Orowan stress). In view of the concept of threshold stress (τ_ρ), equation (1), is modified by replacing τ_{app} by $(\tau_{app} - \tau_\rho)$. This concept has been used by Balakrishna Bhat & Arunachalam (1977) to explain the high values of n. They have also been able to explain the high values of n at low stresses and lower values at higher stresses found for dispersion-hardened alloys (Lund & Nix 1976). This agreement with data for disperison-hardened alloys seems to be reasonably good.

However, the values of n found for precipitation-hardened alloys, at temperatures about 750°C are similar to those found for climb-controlled creep of single-phase alloys; figure 2 (Ferrari 1976) at low stresses. Only at high stresses n increases. This kind of behaviour has been explained (Balakrishna Bhat & Arunachalam 1977) by the concept of τ_ρ varying with τ_{app} such that $\tau_\rho \propto \tau_{app}$ (Lagneborg 1973), thus at low stresses, when τ_{app} is substituted by $\tau_{app} - \tau_\rho$, the same value of n results. At higher stresses τ_ρ attains a constant value and thus high values of n are obtained.

The understanding of deformation behaviour of precipitation-hardened superalloys at low stresses is important since this is the regime in which most superalloys are used.

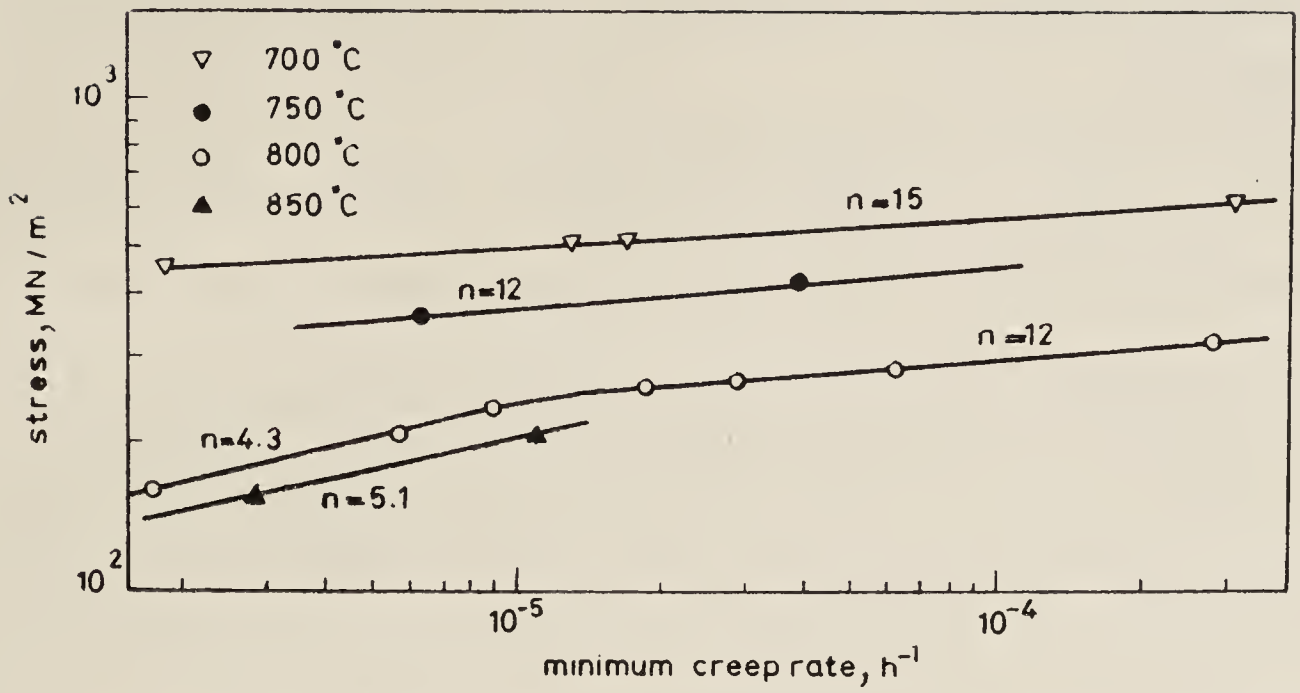

Figure 2. Variation of n with stress and temperature for a Ni-base superalloy. Low values of n are observed at 800 and 850°C, only at low strain rates.

The creep of precipitation-hardened alloys has been considered to be controlled by particles being overcome by climb at low stresses. Creep has been so considered, since the applied stress is considerably less than 0·2% proof stress of the alloy, which is dictated by the 0·2% proof stress of the particle. However if we consider figure 1, we know that the particles are very weak at low strains. Now the increase in flow stress at high strains comes about due to increased work-hardening of the particles. However, it is possible that if the experiments are carried out at temperatures above 750°C, recovery effects soften the particles, so that their strength continues to be low. Thus cutting would be possible at stresses considerably below 0·2% proof stress. At high strain rates the work-hardening rate would predominate over the recovery rate, the particle strength and the alloy strength would go up and the particles would have to be overcome by climb. Thus the concept of threshold stress would become applicable at high stresses and strain rates.

In the light of the above discussion, we consider the three following mechanisms:

(a) At low stresses, and low strain rates, and high temperatures, the particles remain soft by recovery and are cut. In this regime the creep rate is determined either by viscous creep or climb-controlled recovery creep through the particle. The alloy is expected to behave like a solid solution alloy. Low values of n would result, accompanied by high Q (corresponding to diffusion in γ'). Although experimental evidence exists for this mechanism being operative (Decker 1968), surprisingly it has been ignored (Threadgill & Wilshire 1974; Balakrishna Bhat & Arunachalam 1977; Lagneborg 1973; Evans & Harrison 1979), in explaining the values of n and Q found in this regime. Most authors try and explain the values of n in terms of mechanism (b). Mechanism (a) is likely to be the most important creep mechanism in actual use in superalloys. Values of n and Q in the range in which this mechanism is applicable should be the same as for values for γ'; $n=4{\cdot}5$ and $Q=150$ Kcals/mol (Stoloff & Davies 1967).

(b) At intermediate stresses and strain rates, the particles are harder and are overcome by climb. The concept of the threshold stress applies, and high values of n, accompanied by low values of Q result (corresponding to diffusion in the matrix). The transition from mechanism (a) to (b) would take place at lower strain rates as

the temperature is lowered. The properties of γ' are not important when this mechanism is operative.

(c) At higher stresses (0·2% proof stress), the particles are still harder, but the stresses are high enough to overcome by cutting or looping. Again the concept of threshold stress applies, accompanied by high n and low Q. This mechanism is unlikely to be important, at the stresses and temperatures at which superalloys are used.

The first mechanism would be inoperative at low temperatures and high values of n have been reported at low temperatures (figure 2). The data of Dennison & Stevens (1970) show values of $n=8$ at stresses below 55 kg/mm^2 for the alloy P.E. 16 at 650°C, and $n=11$ at stresses above 63 kg/mm^2 and possibly corresponds to mechanism (b) and (c) listed above. The data of Evans & Harrison (1979) show all the three regions of n for Nimonic-90 at 850°C (figure 3). Further support for the views expressed above is the high values of Q at high temperatures, and the low values at low temperatures (Heslop 1962–63, Leverant & Kear 1970, Dennison *et al* 1978). Also Tipler *et al* (1978) and Decker (1968), clearly show cutting of the particles under creep conditions at temperature above 800°C, at stresses of the order of 0·25 to 0·3 of the 0·2% proof stresses in support of mechanism (a).

In view of the importance of mechanism (a), the properties of γ' become important in determining the creep behaviour of precipitation-hardened superalloys. Thus γ' should have a low SFE and should be strengthened by slow diffusing solutes to decrease the creep rate.

3. Design against GB sliding and its consequences

At high temperatures, grain boundaries become glissile, and grains across the boundaries can slide past each other. The grains then become incompatible with each other

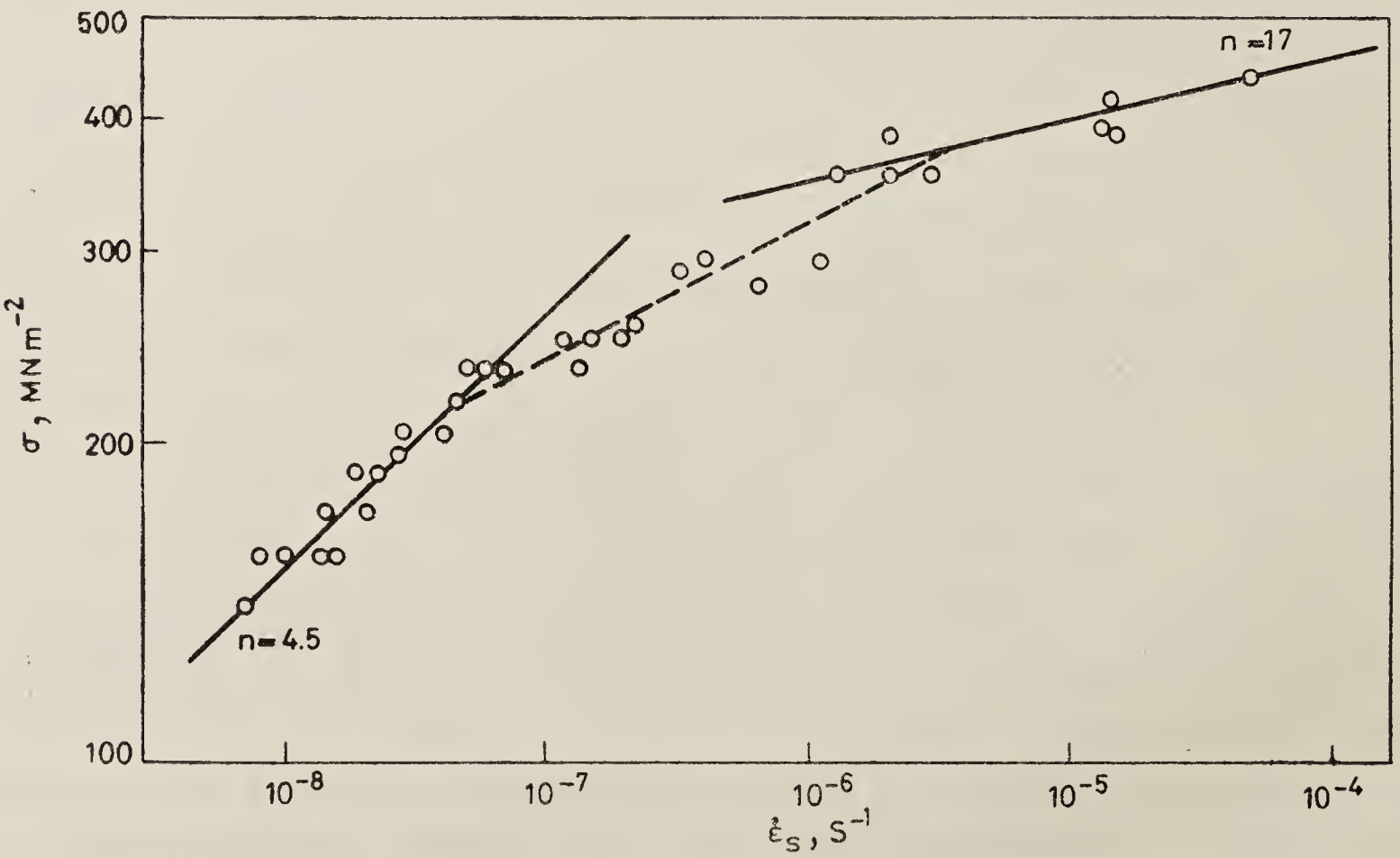

Figure 3. Variation of secondary creep rate of Nimonic-90 with applied stress showing three different values of n corresponding to different mechanisms by which particles are overcome by dislocations.

leading to failures with low ductilities, unless the incompatibilities created by sliding are accommodated in one way or another.

3.1 *Grain size and shape control to minimize GB sliding*

Grain-boundary sliding is a nuisance, which is best avoided by not having grain boundaries, *i.e.*, by using single crystals. Although one can use single crystals for exotic applications, the cost of growing single crystals does not justify the use of single crystals for more mundane applications. The next best one can do is to use directionally aligned grains, with grain boundaries parallel to operating stress axis, so that there is no shear stress on the grain boundaries. This can be achieved by directional solidification or by recrystallization (Allen 1972; Bhatia & Cahn 1978). This concept has been used to improve the performance of turbine blades and vanes for aero-engines and tungsten filament lamps.

The techniques mentioned above for avoiding sliding are too expensive or too impractical for most applications. Thus, one has to learn to live with grain boundaries, despite the incompatibility problems created by their sliding.

Naively one can think of minimizing the contribution of sliding by minimizing the area of grain boundaries, *i.e.*, by increasing the grain size. This has its pitfalls, specially if the component dimension approaches grain size (Richards 1968), since a single sliding displacement can lead to component failure.

3.2 *Influence of boundary segregation, boundary humps and second phase particles on GB sliding*

An important method by which the ill effects of sliding can be minimized is by making sliding more difficult, *i.e.*, by increasing the viscosity of the grain boundaries, since the displacement rate across a single grain boundary is inversely proportional to its viscosity. The intrinsic viscosity of a flat grain boundary is given by (Ashby 1972):

$$\eta_B^i = (kT/8bD_B), \tag{3}$$

where b is the atom size and D_B is the grain boundary diffusion coefficient. Thus the intrinsic viscosity of a grain boundary can be increased by decreasing D_B. According to a model developed by Li (1963) grain boundaries are visualized as regions with porosity. The lower the porosity of the grain boundary the lower the diffusivity. One can then understand that better filling up of this porosity can come about by putting in solute atoms which are over-size and under-size relative to matrix atoms. These solutes would segregate to the grain boundaries leading to a decrease in grain boundary porosity. This could be the rationale for the addition of trace quantities of B, Zr, Mg to Ni-base superalloys to suppress sliding and its attendant evils. The quantity of the element added seems to be critical, since larger amounts lead to the precipitation of undesirable brittle phases at the grain boundary (Tewari & Hemareddy 1980).

Equation (3) above was given for the viscosity of a flat, atomically smooth grain boundary. But grain boundaries are rarely so smooth, they generally contain ledges and humps. Obviously, these deviations would lead to an increase in viscosity. Raj

and Ashby (1971) give the following expressions for the viscosity of a grain boundary with ledges or humps of height h,

$$\eta_B = (kTh^2/8b^3D_B). \tag{4}$$

Equation (4) was derived by assuming that boundary diffusion is the dominant mode of transport of matter. Thus deviations from the planarity of height h increase the boundary viscosity by (h^2/b^2). This can have a remarkable influence on grain boundary viscosity and the concept has been used to minimize sliding effects by heat-treatments which would give zig-zag boundaries (Betteridge & Heslop 1974) with a large value of h.

Another important method by which grain boundary viscosity can be increased is by putting particles on grain boundaries. Although this method is widely used, its use can be self-defeating if the matrix/particle or grain-boundary/particle interface strength is not high, so that decohesion at the interface comes about as stress concentrations build up due to the various accommodation processes discussed below. The boundary viscosity when the particles do not decohere is given by:

$$\eta_B = kT\, A_f a^2/8b^3\, D_B, \tag{5}$$

where A_f is the area fraction of second phase particles at the grain boundaries and a is the particle diameter, D_B in this case is the diffusion coefficient along particle matrix interface. According to Raj & Ashby (1971), the above expression is valid for particles upto $\sim$ 1000 Å diameter, when interphase boundary diffusion is the dominant transport mode. In such cases, for the same volume fraction of second-phase particles, the boundary viscosity increases with the size of the particles. Thus the justification for using coarse carbide particles in Ni base alloys. The boundary viscosity becomes independent of particle diameter as it approaches 10 μ, when the matrix diffusion becomes a dominant transport mechanism.

A comparison of equations (4) and (5) shows that humps of the order of the size of second phase particles are equally effective in increasing the grain boundary viscosity. In addition, the grain boundary humps do not suffer from dangers of decohesion as particles do. However, in order to make the humps stable against grain boundary migration, which would tend to even out the humps, one requires particles to pin the grain boundaries (Gladman 1966; Bhatia 1969). For Ni-base alloys the particles needed to prevent grain migration need not be brittle carbides, but could be reasonably ductile γ'. The above discussion throws some light on the controversy regarding the necessity of having grain boundary carbides to minimize sliding (Weaver 1959-60; Gibbons & Hopkins 1971; Perry 1974).

Another important concept regarding the role of particles on the grain boundaries is that they introduce a kind of threshold stress before sliding can take place (Horton 1972; Hornbogen 1973). This is akin to the critical resolved shear stress in the matrix. However, since the interparticle spacings are large the critical resolved shear stress for sliding is small.

3.3 *Accommodation processes for GB sliding*

Now we shall consider various processes for accommodating incompatibilities

created by sliding; figure 4 (Edward & Ashby 1979). The accommodation can be purely elastic, when the elastic stresses set up by sliding balance the applied shear stress. It can be diffusional, leading to diffusional flow (Nabarro-Herring creep and Coble creep). The incompatibilities can be accommodated by plastic flow, leading to non-uniform creep. However, in a large number of applications, the temperatures and operative stresses are such that incompatibilities due to sliding are not fully accommodated by the processes mentioned above. In such cases, cavitation (r-type, or nearly equiaxed cavities) or triple-point cracking (W-type cavities), occurs at grain boundaries roughly perpendicular to the tensile axis. Since a majority of creep failures are due to the formation of cavities, which lead to failure with low ductilities, it is important to understand growth of cavities. Before doing so, we shall briefly mention the influence of other accommodation processes on creep.

When sliding is accommodated elastically, elastic stresses build up at asperities, or steps, or at other grain boundaries at triple points. The stresses so built up balance the applied stress and sliding stops. This accommodation process is likely to be important at low temperatures and low stresses; at higher temperatures and stresses, diffusional and plastic accommodation processes will come into play to take care of larger sliding displacement. In case sliding is fully accommodated elastically, the total sliding displacement is likely to be insignificant according to Raj & Ashby

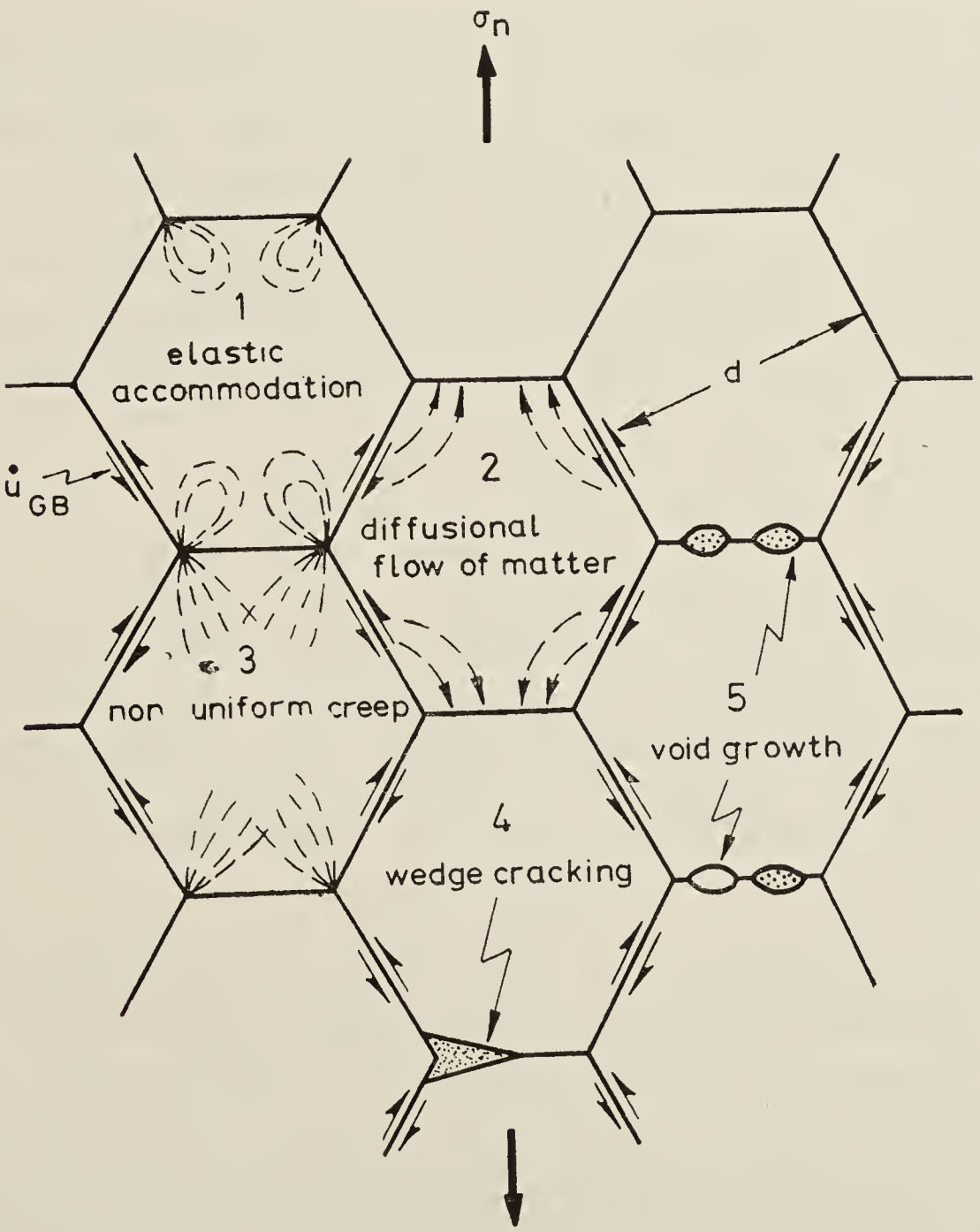

Figure 4. Various ways in which grain boundary sliding can be accommodated (grains 1, 2 and 3). If it is not accommodated triple point cracking (grain 4) or cavitation (grain 5) results. (After Edward & Ashby 1979).

(1971). Thus, the alloy designer need not worry himself about the contribution of this deformation mode to overall creep rate. However, according to Raj & Ashby's analysis considerable stress concentration can build up during elastic accommodation of sliding. In fact, according to the analysis of various accommodation processes done by Ashby and his coworkers, the maximum stress concentration is generated by elastic accommodation, and this could play an important role in the nucleation of cavities. This mode of generation of cavities would be important at relatively low temperatures and high stress (not high enough to initiate plastic accommodation).

When grain-boundary sliding is fully accommodated by diffusional flow, the deformation rate is dictated by stress-directed diffusion of vacancies from grain boundary regions in tension to other regions in compression. The stresses that develop during sliding due to normal displacement of boundaries are of magnitudes such that the flux of atoms exactly compensates these displacements. The stress-directed diffusion which can take place *via* grain boundaries (Coble creep) is important at relatively lower temperatures. At higher temperatures, diffusion through bulk becomes important (Nabarro-Herring creep). Without going into mathematical analysis (Raj & Ashby 1971), from the general considerations mentioned earlier, the sliding rate can be minimized by increasing the grain size and having elongated grains parallel to the stress axis. These are methods used to strengthen against diffusion creep.

As mentioned earlier, second-phase particles slow down sliding by virtue of their influence on grain boundary viscosity. Raj & Ashby (1971) analyzed this situation, and since diffusional accommodation across the particles requires diffusion over considerably smaller distances, compared to diffusional accommodation across grain boundaries, they conclude that from macroscopic considerations, diffusion creep should not be influenced by a dispersion of second-phase particles, but should be dictated by grain size. However, Raj & Ashby point out that from microscopic considerations, second-phase particles could introduce a threshold stress, below which no diffusion creep takes place. According to them, threshhold stress is supposed to arise due to difficulty in absorption and emission of vacancies at the grain boundaries, when the boundaries contain particles. This is so, if the absorption or emission of vacancies is expected to take place by climb of grain boundary dislocations, which requires a threshold stress in the manner in which it is required for climb inside grains containing second-phase particles. Threshold stress for diffusion creep has been observed for dispersion-hardened systems (Ashby 1969). An alternate way of looking at the threshold stress for diffusion creep would be that of Horton (1972) and Hornbogen (1973), according to whom there is a threshold stress below which sliding cannot take place and hence diffusion creep also cannot take place.

When sliding is accommodated plastically, it leads to non-uniform flow, the plastic flow being concentrated in the region of the grain boundary. An important concept to take into consideration in the case of plastic accommodation, is that of transition strain rate, developed by Crossman & Ashby (1975). Transition strain rate is defined as that strain rate at which the strain rate due to grain-boundary sliding is equal to strain rate due to grains in the absence of grain boundaries. Below this strain rate, grain-boundary sliding makes a significant contribution to the overall strain rate, and leads to stress concentration on the grain boundary triple junctions, the normal stresses being approximately four times the shear stress. Above this transition strain

rate, *i.e.*, at stresses above those corresponding to the transition strain rate, since the grain interior deformation rate increases with (stress)^4, and the grain-boundary sliding rate increases as (stress)^1, the contribution of grain-boundary sliding to overall strain decreases, and so do the stress concentrations that arise due to sliding. Figure 5 shows schematically how the transition strain rate varies for grain boundaries with different viscosities, and grains with different resistances to creep. According to the discussion above, high viscosity of grain boundaries is desirable under any operating condition.

3.4 *Optimization of grain strength to minimize the consequences of sliding*

Let us consider a component which can withstand the strain rates corresponding to low viscosity GB and high viscosity GB of figure 5. We would like to know grain strength and GB viscosity requirement when the component is operating at the lower stress shown in figure 5.

If the alloy has low grain strength and low viscosity as shown in figure 5, we are going to be operating below the transition strain rate with the attendant problems of grain-boundary sliding. However if the alloy has the low grain strength and the high grain boundary viscosity shown in the figure, we shall operate at strain rates above the transition, thus mimimizing problems due to grain-boundary sliding. In case our alloy has high viscosity grain boundaries, and the grain strength is also high, we shall again be operating at strain rates below transition, which is not desirable. In fact, under these conditions, plastic accommodation may not be possible, because of the very high strength of the grain, and if the temperature is not high enough for diffusional accommodation, we would end up with cavitation or triple junction cracking. However, if the component is operating at the higher stress shown in the figure, using low grain strength would lead to high creep rates, and any of the two viscosities would do, if the higher strain rate in the component is permissible. However if the

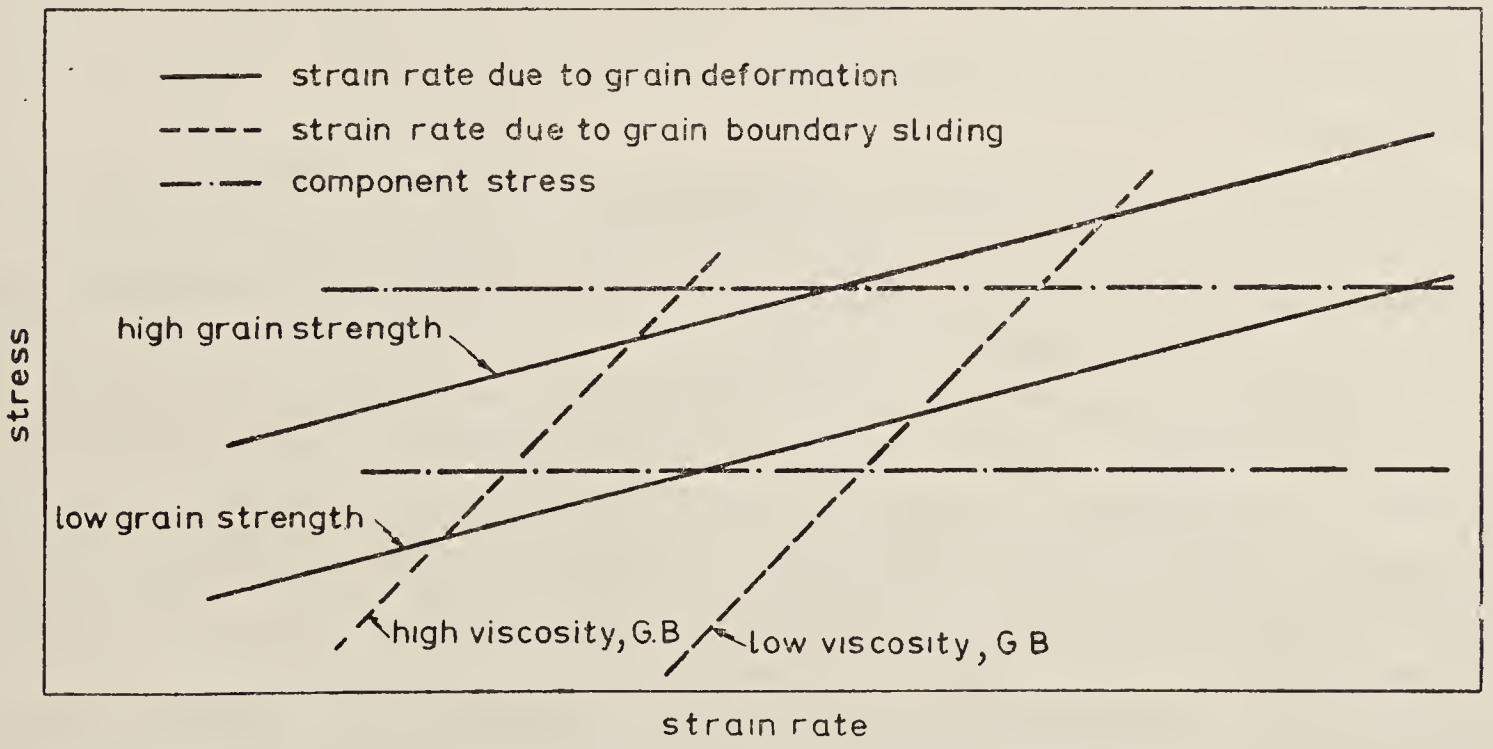

Figure 5. Schematic representation of relationship between applied stress and strain rate for grain deformation ($n = 4$) and grain boundary sliding ($n = 1$). Component stresses considered in the discussion are also shown. Transition strain rate for any combination of grain boundary viscosity and grain strength is given by intersection of relevant stress/strain rate plots.

strain rate has to be kept within limits, we should be selecting grain boundaries with high viscosities, and grains with high strength.

In brief, we can summarize that for applications under any operating stress, the grain-boundary viscosity should be as high as possible, and the grain strength should be such that the grains flow at the operating stresses. Overstrengthening the grains against flow, when the operating stresses do not require such strengths, is undesirable.

3.5 *Optimization of GB structure against cavitation*

Engineering components deforming under creep conditions would have significantly higher rupture life, if the ductilities of the components were comparable to ductilities in short-time tensile tests. Rupture-ductility and life are generally limited by cavitation and the formation of triple point cracks. A large number of papers (see Perry 1974) have dealt with the problem of cavities forming at grain boundaries normal to the tensile stress, whereas the sliding displacements are expected to be more prominent at boundaries inclined at 45° to the tensile axis. Figure 4 due to Edward & Ashby (1979), shows that one need not be intrigued by the formation of cavities at boundaries normal to the tensile axis, when the sliding is taking place at inclined boundaries. The nucleation of cavities at the boundaries normal to the stress axis is due to the non-accommodation of sliding displacement, as shown in figure 4. The growth of cavities can take place by deformation or by diffusion (Edward & Ashby 1979; Pavinich & Raj 1977).

We have already considered the usefulness of having oversize and undersize solutes segregating to grain boundaries and decreasing the sliding rate by virtue of their influence on boundary diffusivity. We have considered the usefulness of coarser second-phase particles on the grain boundaries to decrease the sliding rate. We have also considered how humps in the grain boundaries can be more useful than carbide particles in suppressing sliding in Ni base superalloys. However, although the concept of humps on the grain boundaries has been used to increase ductility and rupture life in some cases, the alloys more often rely on second-phase particles to suppress grain-boundary sliding. Thus, we shall now consider the nature of second-phase particles and structure in the vicinity of grain boundaries to minimize sliding and cavitation.

Cavities are known to nucleate at second-phase particles (Pavinich & Raj 1977; Fleck *et al* 1975). As discussed earlier, the cavity nucleation can come about by decohesion at the second-phase particles, owing to high stress concentration generated by various accommodation processes. One of the methods by which one can minimize decohesion tendency at the particle/matrix interface is by decreasing the energy of this interface. $M_{23}C_6$, the grain boundary carbide in some Ni-base alloys, precipitates intergranularly as plates (Piearcy & Smashey 1967). Although the plate morphology of $M_{23}C_6$ has to be avoided to minimize stress concentration, it is a pointer towards the existence of low energy interface (Aaronson *et al* 1970), which is to be preferred.

Precipitation heat-treatments in some Ni-base superalloys are so adjusted, that one ends up with a γ'-envelope around the carbides at the grain boundaries. Could this again be due to the low energy of the carbide/γ'-interface? The answer to this question, and better optimization of precipitate/matrix interface energy will have to await interface energy measurement.

Another microstructural variable that can influence creep rate and rupture-ductility is the precipitate-denuded zones near grain boundaries. There has been controversy regarding the optimum width of this zone. According to some investigators it should be narrow (Heslop 1972), while others believe that it should be relatively wide (Venkiteswaran *et al* 1973). If we consider figure 5 we see the usefulness of the precipitate-free zone, which would have lower strength, allowing accommodation of grain-boundary sliding. Its width should depend upon operating stress, and grain strength. If the operating stress leads to grain flow at a strain rate above the transition strain rate one needs no precipitate-free zones for accommodation of grain-boundary sliding. However, if the operating stress is considerably lower than this, one would need a reasonable width of precipitate-free zone to accommodate sliding.

4. Conclusions

Alloys can be strengthened against creep by strengthening the grains against dislocation glide and climb, and by making grain-boundary sliding more difficult. Grains can be strengthened by addition of solid solution elements which decrease SFE. Very effective strengthening of grains can be provided by a dispersion of second-phase particles. Contributions due to grain-boundary sliding can be minimized by having coarse and columnar grains, by decreasing grain-boundary diffusivity, and by having humps and second-phase particles on the grain boundaries. The particle/matrix interface energy should be low to avoid decohesion leading to cavity nucleation. The grain-boundary viscosity should be maximized for all operating stresses, but the grains should not be overstrengthened.

References

Aaronson H I, Laird C & Kinsman K R 1970 *Phase transformations* (Ohio: Am. Soc. of Metals) p. 313

Allen R E 1972 *Superalloys* Proc. II Int. Conf. (Columbus, Ohio: Metals and Ceramic Infn. Centre) Rep. 72-10

Ashby M F 1969 *Scr. Metall.* **3** 837

Ashby M F 1972 *Surface Sci.* **31** 498

Ashby M F 1973 *The microstructure and design of alloys*, Proc. III Int. Conf. on Strength of Metals and Alloys (London: Institute of Metals) Vol. 2, p. 8

Balakrishna Bhat T & Arunachalam V S 1977 *J. Mater. Sci.* **12** 2241

Balakrishna Bhat T & Arunachalam V S 1980 *Proc. Indian Acad. Sci.* (*Engg. Sci.*) **3** 275 (this issue)

Beeston B E P, Dillamore I L & Smallman R E 1968 *Metal Sci.* **2** 12

Beeston B E P & France G K 1968 *J. Inst. Met.* **96** 105

Benjamin J S & Bomford M J 1974 *Metall. Trans.* **5** 615

Betteridge W & Heslop J 1974 *The nimonic alloys* (London: Edward Arnold)

Bhatia M L 1969 *Influence of porosity on recrystallisation* D. Phil Thesis, University of Sussex, UK

Bhatia M L & Cahn R W 1978 *Proc. R. Soc.* (*London*) **A362** 341

Bird J E, Mukherjee A K and Dorn J E 1969 *Quantitative relationship between properties and microstructure* eds D G Brandon & A Rosen (Jerusalem: Israel Univ. Press)

Brown L M & Ham R K 1971 *Strengthening methods in crystals* eds A Kelly & R B Nicholson, (Amsterdam: Elsevier) p. 12

Crossman F W & Ashby M S 1975 *Acta Metall.* **23** 425

Decker R F 1968 *Steel strengthening mechanisms*, Proc. Symp. Zurich, (Zurich: Climax Molybdenum Corpn.), p. 1

Dennison J P & Stevens R 1970 *Scr. Metall.* **4** 421
Dennison J P, Holmes P D & Wilshire B 1978 *Mater. Sci. Engg.* **33** 35
Doble G S 1967 *The effect of deformation on dispersion-hardened alloys* Ph.D Thesis, Case Western Reserve Univ., USA
Dutton R 1970 *Scr. Metall.* **4** 247
Edward G H & Ashby M F 1979 *Acta Metall.* **27** 1505
Ericsson T 1966 *Acta Metall.* **14** 853
Evans W J & Harrison G F 1979 *Mater. Sci. Engg.* **37** 271
Evans W J & Harrison G F 1979 *Metal. Sci.* **13** 346
Ferrari A 1976 *Superalloys: Metallurgy and manufacture*, III Int. Symp. Seven Springs, Pennsylvania, eds B H Kear *et al* (Lousiana: Claitors Pub. Div.) p. 201
Finniston H M 1958-59 *J. Inst. Met.* **87** 360
Fleck R G, Taplin D M R & Beevers C J 1975 *Acta Metall.* **23** 415
Fleischer R L 1963 *Acta Metall.* **11** 203
Friedel J 1964 *Dislocations* (London: Pergamon) p. 278
Gladman T 1966 *Proc. R. Soc.* (*London*) **A294** 298
Gibbons T B & Hopkins B E 1971 *Metal Sci.* **5** 233
Grant N J & Mullendore A W 1965 *Deformation fracture at elevated temperatures* (Cambridge, Mass: MIT Press)
Heslop J 1962-73 *J. Inst. Met.* **91** 28
Heslop J 1964 *Cobalt* **24** 128
Hornbogen E 1973 *The microstructure and design of alloys* Proc. III Int. Conf. on Strength of Metals and Alloys (London: Inst. of Met.) Vol. 2, p. 108
Horton C A P 1972 *Acta Metall.* **20** 477
Hosford W F 1973 *The microstructure and design of alloys*, Proc. III Int. Conf. on Strength of Metals and Alloys (London: Inst. of Met.) Vol. 2, p. 8
INCO 1977 *Data book on high temperature high strength nickel base alloys* (London: INCO Europe Ltd.) p. 4439
Kelley A & Nicholson R B 1963 *Prog. Mater. Sci.* **10** 3
Lagneborg R 1973 *Scr. Metall.* **7** 605
Leverant G R & Kear B H 1970 *Metall. Trans.* **1** 491
Li J C M 1963 *Recovery and recrystallisation of metals* (New York: John Wiley)
Lloyd D J & McElroy S 1974 *Acta Metall.* **22** 339
Lund R W & Nix W D 1976 *Acta Metall.* **24** 469
McLean D 1962 *Mechanical properties of metals* (New York: John Wiley)
Mott N F & Nabarro F R W 1948 *Strength of solids*, Report of Conf. (London: Physical Soc.) p. 1
Oikawa H & Karashima S 1974 *Mechanical behaviour of materials* Proc. Symp., Kyoto, (Japan: Soc. of Mater. Sci.) ab. II, p. 169
Pattanaik S, Bhatia M L & Arunachalam V S 1974 *Trans. Indian Inst. Met.* **27** 227
Pavinich W & Raj R 1977 *Metall. Trans.* **A8** 1917
Pelloux R M N & Grant N J 1967 *Trans. AIME* **218** 232
Perry A J 1974 *J. Mater. Sci.* **9** 1016
Piercey B J & Smashey R 1967 *Trans. AIME* **239** 451
Raj R & Ashby M F 1971 *Metall. Trans.* **2** 1113
Richards E G 1968 *J. Inst. Met.* **96** 365
Sherby O D & Burke J E 1967 *Prog. Mater. Sci.* **13** 323
Shewfelt R S W & Brown L M 1977 *Philos. Mag.* **35** 945
Shorshorov M Kh 1973 *The microstructure and design of alloys*, Proc. III Int. Conf. on Strength of Metals and Alloys (London: Inst. of Met.) Vol. 2, p. 43
Stoloff N S 1972 *Superalloys* eds C T Sims & W C Hagel (New York: John Wiley) p. 79
Tewari S N & Hemareddy M 1980 Unpublished work
Tipler H R, Davidson J H & Lindblom Y 1978 *High temperature alloys for gas turbine*, Liege Conf., eds. D Coutsouradis *et al* (London: Appl. Sci. Publ.) p. 359
Thornton P H & Cahn R W 1961 *J. Inst. Met.* **89** 153
Thornton P H, Davies R H & Johnston T L 1970 *Metall. Trans.* **1** 207

Threadgill P L & Wilshire B 1974 *Creep strength in steel and high temperature alloys* (London: Metals Soc.) p. 217
Venkiteswaran P K, Bright M W A & Taplin D M R 1973 *Mater. Sci. Engg.* **11** 255
Watanabe T & Karashima S 1970 *Metal. Sci.* **4** 52
Weaver C W 1959-60 *J. Inst. Met.* **88** 462

Alloy design for fracture resistance

Y V R K PRASAD and P RAMA RAO*
Department of Metallurgy, Indian Institute of Science Bangalore 560012, India
*Department ot Metallurgical Engineering, Banaras Hindu University, Varanasi 221005, India

MS received 10 March 1981

Abstract. Several methods for improving the strength of metallic materials are available and correlations between strength and various microstructural features have been established. The purpose of this paper is to review parallel developments favouring improved fracture resistance. Resistance to fracture in monotonic loading, cyclic loading and when fracture is environment-aided have been considered in steels, aluminium alloys and anisotropic materials. Finally, the question of optimising alloy behaviour is discussed.

Keywords. Fracture resistance; microstructural design; cleavage fracture; ductile fracture; fracture toughness; fatigue fracture; fatigue crack growth rates; low cycle fatigue; stress corrosion cracking; optimisation.

1. Introduction

Materials engineering came into being when it was realised that it is possible to control the properties of solid materials by controlling their internal microstructures. Of considerable technological significance is the work which brought out the role played by a variety of microstructural features such as grain boundaries and second-phase particles in arresting the motion of dislocations and thereby contributing to substantial strengthening of solids. This work dominated the concern of the materials scientist during the two decades following the discovery of dislocations and the advent of the transmission electron microscope. During the seventies, attention was turned to a parallel problem namely improvement in resistance of materials to fracture. In the same way that stopping *dislocations* was the concern in strengthening materials against deformation processes, the materials engineer's interest is currently focussed on means to arrest the spreading of *cracks* and other such flaws in order to render the materials more fracture-resistant. In this endeavour, as before, microstructural control is an available and important aid. It is the purpose of this paper to indicate how this is so for metals and alloys.

It has been seen that when a metal is strengthened against one particular mode of deformation, sometimes there is consequential impairment of its resistance to another type of deformation. A classical example is that of refinement of grain size, which enhances resistance against dislocation glide. but causes the metal to be more prone to grain-boundary sliding and diffusion creep. It has become necessary now also to examine what fracture processes arise due to particular means of alloy strengthening. Further, a variety of fracture processes occur beeause of loading

and environmental conditions. It is necessary therefore to examine whether any deleterious effects fracture modes occur when microstructures are modified to develop resistance against one particular type of failure. This aspect will also be dealt with in this paper.

2. Fracture resistance in monotonic loading

It is well established that of metallic materials can be strengthened by the following means (Bhat & Arunachalam 1981): (a) solute addition, (b) refinement of grain size, (c) incorporation of second phase particles, (d) dislocations, (e) phase transformation and (f) texture control.

We shall consider the effects of these strengthening processes on the fracture tendencies of metals and alloys with the help of appropriate examples. In order to do this, it would have been useful to deduce expressions correlating parameters reflecting fracture resistance and other material mechanical properties whose relationships to microstructural features are clearly established. Unfortunately, no such clear-cut expressions based on rigorous treatment of the fracture process are available. Even so we shall present below a few correlations which, though incomplete, do contain clues useful for the present discussion.

The ductile-to-brittle transition temperature has been used as a measure of the fracture toughness of the material especially prior to the adoption of the mechanics approach and the development of the K_{Ic} concept. Using a combination of a dislocation mechanism for crack nucleation, the Griffith criterion and the Hall-Petch analysis for grain size dependence of strength, Smallman (1963) has deduced the following ' ductile-to-brittle transition equation ':

$$(\sigma_i d^{1/2} + k_y)\, k_y = \psi\, \gamma\, \mu, \tag{1}$$

where σ_i is the friction stress obtainable from the Hall-Petch intercept, d the polycrystal grain size, k_y the Hall-Petch slope, ψ, a constant dependent on the stress state, μ the shear modulus and γ the fracture surface energy. Features that raise the left hand side of the above equation enhance the impact transition temperature (*i.e.*, brittleness) and *vice versa.*

An important relation for fracture stress (σ_f) as has been given by Cottrell (1957) is applicable when cleavage fracture occurs and is:

$$\sigma_f \approx \frac{4\,\mu\,\gamma_w}{k_y}\, d^{-1/2}, \tag{2}$$

where γ_w is the plastic work done around a crack as it moves through the crystal.

Fracture toughness, now clearly understood as the resistance of a material to crack propagation in structures containing defects of varying size and geometry, is represented in linear elastic fracture mechanics by the parameter K_{Ic}. K_{Ic} is the critical stress intensity factor at which fast fracture occurs and is determined under plane-strain conditions and mode I (crack opening mode) of crack propagation. Hahn & Rosenfield (1968) have related K_{Ic} to tensile properties, which is another useful correlation given below:

$$K_{\mathrm{Ic}} = n\,(2E\,\sigma_y\,\epsilon_f / 3)^{1/2}, \tag{3}$$

where n is the monotonic strain-hardening exponent, E the Young's modulus and ϵ_f the true fracture strain in uniaxial tension.

Another useful correlation is due to Krafft (1964), especially relevant to the ductile fracture situation typified in scanning electron micrographs by the appearance of dimples, namely

$$K_{\mathrm{Ic}} \approx En\,(2\pi\,d_T)^{1/2}, \tag{4}$$

where d_T is the 'process zone size' which has been shown to correspond to the diameter of an equiaxed microvoid, which in turn depends on the particle (or inclusion) spacing.

With the help of the above correlations it becomes possible to see generally the influence of many of the microstructural parameters on fracture resistance. These correlations have a bearing on the following discussion on the development of fracture resistance in alloys and is presented in a sequence parallel to the strengthening effects listed above. We shall base many of the observations on steels and aluminium alloys and refer to anisotropic materials such as titanium and magnesium alloys only when the influence of crystallographic texture is considered.

2.1 *Effect of solutes*

The effect of solutes on the fracture toughness of steels has not been as systematically studied as their contribution to flow stress in ferritepearlite steels and austenitic steels (Pickering & Gladman 1963; Dyson & Holmes 1970). A general observation, however, is that substitutional solutes which show appreciable strengthening increase the impact transition temperature. This can be understood in terms of the solute effect in raising σ_i in equation (1). The effect of interstitial solutes, carbon and nitrogen, is even more detrimental to fracture toughness and the impact transition temperature. These interstitials significantly raise σ_i as well as k_y in equation (1) and one of the cardinal principles of the design of tough steels is to have the lowest possible interstitial content. The example of carbon-free ultra-high strength maraging steels which are characterised by superior fracture toughness substantiates this view. Among the various solute additions to iron alloys there is at least one element, namely nickel, whose addition is not detrimental to toughness. The reason for this is not clear but may lie in the effect of nickel on stacking fault energy (SFE) and thus on the propensity to deformation twinning. It is also noteworthy that manganese is a favoured addition when high fracture toughness is desired (*e.g.* rail steels and steels for low temperature applications) possibly because of the beneficial effect of manganese in lowering the transformation temperature and causing refinement of the ferrite grain size and pearlite colony size.

This discussion will not be complete unless we mention the interacting effects of solute elements between themselves and with other defects. Frequently substitutional solutes can form insoluble stable compounds such as TiC and TiN by combining with the interstitial elements. Some degree of precipitation may occur but it is more interesting to note that such second phases often pin down grain boundaries and aid grain refinement (*e.g.* aluminium as a grain refiner in steel) when a marked improvement in toughness occurs. Interactions of solutes with dislocations (line

defects) are known to cause strain ageing with considerable strengthening but with attendant loss of ductility. Segregation of metalloid atoms such as antimony, phosphorous and tin to grain boundaries (planar defects) can also result in severe embrittlement. In an important contribution Jokl *et al* (1980) have recently explained this drastic embrittlement on the basis of a new concept that the plastic work (γ_p) is a function of the ideal work of fracture (γ) and a small decrease in γ due to grain boundary segregation results in a large reduction in γ_p. Although grain boundary embrittlement may be solved by the addition of other elements *e.g.* carbon in molybdenum reduces embrittling oxygen coverage of grain boundaries (Arun Kumar 1981), an easy remedy to temper as well as to strain-age embrittlement at present seems to be the avoidance of the concerned temperature range of exposure.

2.2 *Effect of grain size*

Equation (2) given above was the first to demonstrate the inverse dependence of fracture stress on grain size ($\sigma_f \propto d^{-1/2}$) for cleavage fracture. The importance of the celebrated data obtained by Low (1954) lies not only in the verification of equation (2) but also in showing the greater sensitivity of σ_f than σ_y to grain size resulting in intersection of σ_f and σ_y plots as a function of $d^{-1/2}$. The implications of this are as follows: for large grain sizes greater than the intersection grain size, fracture occurs when $\sigma = \sigma_y = \sigma_F$. However at smaller grain sizes, $\sigma_f > \sigma_y$ and *strain hardening* is required before the fracture stress level is reached, the extent of strain hardening required being greater as grain size decreases and the ratio (σ_f/σ_y) increases. On this basis as well as on the basis of equation (1), one can readily understand the depression of ductile-to-brittle transition temperature with decreasing grain size. It may, however, be noted that although in the transition range the grain size has a marked effect, below the transition temperature the grain size has no great effect on fracture toughness.

Schwalbe (1977) has deduced a formula for K_{Ic} in terms of grain size which is

$$K_{Ic} = 3\ \sigma_{cl}\ d^{1/2}\ (\sigma_{cl}/\sigma_y) \tag{5}$$

where σ_{cl} is cleavage fracture stress expressed (Rosenfield *et al* 1977) as $\sigma_{cl} = 343 + 103\ d^{-1/2}$. d is the ferrite grain size and this formula has been found to fit measured K_{Ic} values in several steels. It is interesting to note that σ_y is influenced by temperature, deformation rate, grain size, alloying and heat treatment whereas σ_{cl} depends mainly on ferrite grain size.

A more detailed analysis of grain size dependence of K_{Ic} is due to Armstrong (1977) who has deduced a Hall-Petch type of relation, which is so well-established in the yield stress dependence of grain size. Emphasizing that both for yielding and fracture the critical action of a stress concentration is involved, Armstrong (1977) has shown that

$$K_{Ic} = \left[C\left(\frac{\pi\ s\ a\ e}{a+s}\right)^{1/2} \right] [\sigma_f + k_y\ d^{-1/2}], \tag{6}$$

where s is a critical plastic zone size at the tip of a crack of size a. For

$$\frac{s}{a} > 1{\cdot}0, \left(\frac{s\,a\,e}{a+s}\right)^{1/2} \approx s^{1/2}.$$

C, a numerical constant has been found to be $(8/\pi)^{1/2}$ for plane strain deformation. The Hall-Petch like plots of K_{Ic} have now been experimentally obtained for ferrite grain size as well as prior austenite grain size (Stonesifer & Armstrong 1977; Joshi *et al* 1977). The comparison shows that the ferrite grain size effect is the larger of the two influences pointing to the important inference that the strong or weak fracture toughness dependence on grain size matches the corresponding strong or weak effect for the yield stress-grain size correlation. The Hall-petch type plot for K_{Ic} of variously-treated aluminium alloys has also been demonstrated (Armstrong 1977). More data of this type will be invaluable in understanding the significance of the Hall-Petch type correlation for K_{Ic} *versus* $d^{-1/2}$.

There is a general significance deducible from the results obtained for fracture stress, the impact transition temperature and K_{Ic} with refinement of grain size which was succinctly expressed more than 250 years ago by Réaumur (quoted by Armstrong 1977) that the quality of a steel is established by the fineness of its microstructure. This general statement is vindicated by observations of increased fracture toughness with refinement in the scale of a variety of transformation products and serves as an unfailing guideline in the design of tough steels. An outstanding product that has resulted from an awareness of this observation is the high strength low alloy steel (Cohen 1975; Raghavan & Ramaswamy 1981).

2.3 *Effect of second-phase particles*

A microstructure-fracture toughness correlation that has received much attention is has to do with the presence of inclusions in steels. Birkle *et al* (1966) have shown that at constant strength level, K_{Ic} is enhanced by a factor of 1·5 with reduction of sulphur content from 0·049 to 0·008 wt % in an AISI 4340 ultrahigh strength low-alloy steel. A reciprocal type of relationship between toughness and volume fraction of inclusions shown by Baker (1974) for non-metallic inclusions in steel is generally valid for all systems containing a dispersion of second-phase particles. A similar result has been obtained for the fracture toughness of aluminium alloys (Mulhearn & Rosenthal 1971). A measurable parameter that incorporates many of the inclusion characteristics, namely volume fraction, shape and size that contribute to the effect of inclusions on toughness is the total projected length of inclusions per unit area. In a random array of elliptical inclusions with semi-axes p, q, r and a total volume fraction of f, the total inclusion projection (P) on a section normal to the r-axis and in the direction of p is given by:

$$P = 2\,f\,v/3\,\pi\,p, \tag{7}$$

where v is the aspect ratio of the inclusions. It has been shown (Baker 1974) that for various deformed type I and type III MnS systems, a single plot showing monotonic decrease of short transverse toughness with increase in P is obtained despite large differences in volume fraction, aspect ratio and size.

The importance of inclusions and other second-phase particles in metallic materials arises from the fact that ductile fracture initiation occurs at these dispersoids. Equation (4) depicts the general observation that K_{Ic} increases with inclusion spacing. An interesting situation concerns inclusion deformation and fracture behaviour during *processing* of alloys. A typical instance is the work of Baker (1974) who found decreasing toughness with increasing hot deformation of steel. This is explained in terms of decreasing distance between MnS inclusions as a result of working. These inclusions are unbonded to the matrix and during deformation the interface parts and the particles elongate *decreasing* inter-inclusion distance. Consequently the overall toughness is lowered in much the same way as in the effect of increasing volume fraction of inclusions. An opposite trend of results has been obtained by Ashok (1976) in the case of $CuAl_2$ particles in an Al-6 wt % Cu alloy. These particles are strongly bonded to the matrix and during hot rolling, particle fracture rather than interface parting occurs. Considering also that grain elongation takes place, the result is an *increase* in inter-particle distance. The particle redistribution during deformation causes improvement in fracture toughness. A noteworthy feature is that hard, brittle particles should be distributed as homogeneously as possible since inhomogeneities cause small local particle spacings which are also deleterious and result in weak crack paths. There is also the effect of alignment of inclusions which can occur during processing, which is invariably responsible for reduction in toughness in the transverse and especially the short transverse direction. The problem of anisotropy is minimised by cross-rolling or addition of rare earth metals such as cerium (Luyckz *et al* 1970). Similarly calcium is used to globularise oxides and minimise anisotropy in toughness (Hilty & Popp 1969).

At constant volume fraction f of the second-phase particles, the mean particle distance λ and the particle size λ^* are interrelated:

$$\lambda = \lambda^* (2/3f)^{1/2} (1-f). \tag{8}$$

Even so there is evidence to suggest (Schwalbe 1977) that refinement in the size of particles (important for void nucleation) has a greater beneficial effect on K_{Ic} than increasing inter-particle distance (important for void growth). The size effect arises because the larger the particle, the greater the probability that it will contain a flaw, and also the greater the probability that interfacial decohesion may occur due to blockage of slip bands (McEvily 1978). Removal of large-sized inclusions using secondary remelting processes such as electroslag refining or vacuum arc remelting has been shown to result in doubling K_{Ic} at constant strength of AISI 4340 steel (Hebsur *et al* 1980a).

Besides the size, shape, orientation and distribution of second phase particles, their type is also of considerable importance. Sulphide inclusions are more deleterious than carbides while carbides are more harmful than intermetallic precipitates. The superior fracture toughness of maraging steels, compared with ultrahigh strength quenched and tempered low alloy steels, is attributable to the presence in the former steels of a finer distribution of fracture-resistant intermetallic precipitates in comparison with coarser and more brittle carbides in the latter.

In the high strength aluminium alloys, because of the fcc structure of the matrix material, the problem of ductile-to-brittle transition does not exist. There is a general loss of fracture toughness, however, when yield strength is increased by the precipitation

reactions due to a decrease in resistance to ductile rupture. The attention therefore is mainly on particle dispersions. These in aluminium alloys can be divided into three categories: (a) coarse insoluble intermetallic particles formed during solidification due to the ineivtable presence of iron and silicon; (b) intermetallic particles formed during solid state precipitation due to added elements namely chromium, manganese or zirconium, and (c) precipitates developing during ageing such as GP zones, transition and equilibrium precipitates. The coarse intermetallics of category (a) do not contribute to strength but because they are brittle, provide preferential crack paths. A reduction in iron and silicon contents results in substantial improvement in fracture toughness (Staley 1978). The particles of category (b) do not also influence strength except indirectly through their retarding effect on recrystallisation during processing. Systematic studies of their effect on fracture toughness are lacking. Limited data available on Al-Zn-Mg-Cu alloys suggest that manganese containing intermetallics (*e.g.* Al_{20} Mn_3 Cu) are more detrimental than those containing zirconium (*e.g.* Zr Al_3) or chromium (Al_{12} Mg_2 Cr). The general effect of precipitates (category (c) particles) is to enhance strength with concurrent reduction in fracture toughness. When fracture is of the transgranular precipitate type (those that form during underageing or those that develop during overageing), the precipitate has no distinguishable effect on the combination of strength and toughness except during quenching or ageing treatments, which promote intergranular fracture lower toughness (Staley 1975; Kirman 1971).

2.4 *Effect of dislocations*

In steels, higher dislocation densities can arise due to cold work, quenching strains or strains resulting from low transformation temperatures. Finer initial grain size provides higher work-hardening rates with attendant increase in dislocation densities during straining. The effects of alloying elements on stacking fault energy are also important in the way dislocation densities and work hardening rates are. If the recovery and recrystallisation temperatures are exceeded during working, annealing out of dislocations occurs, the noteworthy aspect being the formation of subgrains in warm-worked alloys.

In general, an increase in dislocation density causes a decrease in tensile ductility and increase in impact transition temperature. It appears that uniformly distributed dislocations are less detrimental to toughness than dislocation arrays (Pickering 1978). Again unlocked dislocations are less harmful to toughness than are dislocations locked by precipitates or solute atmospheres (strain ageing is known to result in loss of ductility and toughness). Systematic work on the effect of subgrains on fracture toughness parameters is not available.

In duralumin-type age-hardenable alloys, the introduction of cold work as an intermediate treatment during quenching and subsequent ageing has been tried. In underaged and peakaged tempers and low levels of cold work, toughness increments and strength decrements have been observed. Higher levels of cold work in naturally-aged tempers have provided superior combinations of strength and toughness while the same in average tempers causes poorer combinations of strength and toughness (Staley 1978).

2.5 *Effect of transformation*

The use of high resolution electron microscopy is undoubtedly a major development

in the characterisation of the various microstructural elements and thereby in our understanding of the effect of heat treatment on the fracture toughness behaviour of steels. The transformed products in steels exhibit a bewildering variety and it is only in recent years that a clear picture has emerged although quantitative correlations of fracture toughness parameters and microstructural features are not yet available.

Let us first consider ferrite-pearlite microstructures. It has been observed that in medium-high carbon steels, reduction in ferrite grain size and pearlite colony size improves fracture toughness. Increasing the volume fraction of pearlite by increasing the carbon content, markedly decreases the maximum uniform strain, total strain at fracture, increases the impact transition temperature and lowers the ductile Charpy shelf energy. The morphology of pearlite has complex effects. A decrease in the interlamellar spacing impairs toughness possibly because of its positive effect on strength. However, the simultaneously observed decrease in the pearlite-cementite plate thickness improves impact resistance because thinner carbide plates can bend rather than crack and initiate cleavage fracture (Pickering 1978). Because of these opposing effects, an optimum pearlite interlamellar spacing can be found to result in the highest impact toughness.

On the basis of fairly extensive studies of various ultrahigh strength steels, namely quenched and tempered steels of the AISI 4340 class, maraging steels and TRIP (transformation-induced plasticity) steels (Fe-0.3C-12Ni-9Cr-2Mn) the following conclusions emerge about microstructure-fracture toughness relations (Zackay 1975):

(a) free ferrite, whether present as separate grains or as platelets in upper bainite lowers toughness;
(b) lower bainite and tempered martensite free from lath boundary films of carbides provide high toughness;
(c) the substructure of martensite is important too; dislocated martensite being tougher than twinned martensite;
(d) the presence of retained austenite films around martensite laths substantially improves fracture toughness; and
(e) the production of strain-induced martensite of suitable chemical composition in TRIP steels at an appropriate rate relaxes triaxiality and raises in an overall sense the fracture energy resulting in the highest strength and toughness combinations in ferrous systems.

The effect of higher austenitising temperatures (1200°C instead of the conventional 870°C) employed in the case of AISI 4340 steel provides an extremely interesting situation. A systematic trend of increasing plane-strain fracture toughness (K_{Ic}) and decreasing Charpy V-notch energy is observed as the austenitising temperature is raised while the yield strength remains unaffected. It is important to realise that low austenitising temperatures result in small austenite grain size but a large fraction of brittle undissolved carbides. Higher austenitising temperatures lead to greater dissolution of carbides but cause an increase in austenite grain size. Using these observations, Ritchie & Horn (1978) have explained the apparent paradox by associating a reduction in critical fracture strain with the decrease in Charpy V-notch energy and an increase in characteristic distance for ductile fracture, due to dissolution of void initiating particles, with the increase in sharp-crack fracture toughness.

2.6 *Effect of crystallographic texture*

In anisotropic materials such as titanium alloys, zirconium alloys and magnesium alloys, the fracture behaviour is sensitively dependent on the crystallographic texture. The effect of texture on fracture toughness is complicated and depends upon whether ductility or strength dominates in contributing to the energy consumed during fracture. In commercial titanium sheets, Frederick & Hanna (1970) reported that the fracture toughness is higher in the longitudinal direction than in the transverse direction. This is attributed to the easy $\{10\bar{1}0\}\ \langle 11\bar{2}0\rangle$ slip in the longitudinal specimens facilitated by the duplex type of texture (ideal and (0002) peaks at transvere direction) present in the sheets. In Ti-6Al-4V sheets (Parkinson 1972) the texture consists of basal poles parallel to the transverse direction. This gives rise to higher transverse strength and hence higher transverse fracture toughness under plane-stress conditions (as in thin sheets). However, in thicker sheets, as the plane-strain conditions are approached, there is a shift to higher longitudinal values. Here ductility dominates the fracture process. Recent work of Bowen (1978) on thick plates of highly textured Ti-6Al-4V showed that high values of fracture toughness are obtained in longitudinal specimens with the direction of crack propagation aligned in the short transverse direction. In general, the K_{Ic} values are found to be higher when the crystallographic deformation mode $\{10\bar{1}0\}\ \langle 11\bar{2}0\rangle$ or $\{11\bar{2}2\}\ \langle 11\bar{2}3\rangle$ slip was parallel to the planes of maximum shear stress for plane-strain conditions. The Charpy impact values also showed a similar trend.

In polycrystalline magnesium, the low temperature fracture stress is highly texture-dependent and considerable improvement in fracture stress can be achieved by having strong basal pole intensities parallel to the sheet normal (Wilson 1966). These results indicate that the fracture process in magnesium materials is texture-dependent and further work on these lines is needed on commercial magnesium alloys.

3. Fracture resistance in cyclic loading

In classical terminology, the fatigue ratio (fatigue limit or fatigue strength at high endurances/ultimate tensile strength) has been used as a rough guide to the fatigue strength of materials. Laird (1976) has plotted averages of scatter bands for fatigue ratio of various alloy systems as a function of ultimate tensile strength normalised with respect to Young's modulus. This plot forcefully brings out the existence of a great deal of similarity in the fatigue behaviour of several engineering alloys. It turns out that fcc copper and aluminium alloys are somewhat inferior to steels and titanium alloys. The reason for this has been traced to the occurrence of strain ageing in the latter two systems. The generally lower cyclic strength, as compared with monotonic strength is due to, as has been clearly established now, the formation of persistent slip bands in pure metals and single phase alloys and work-softened bands in poly-phase alloys. Microstructural design for fatigue resistance must essentially aim at combating the tendency towards such instabilities. A general observation also is that in moderately strong alloys, decreasing SFE through solute addition and increasing cyclic hardening at the crack tip have been found to maximise plastic work involved in opening the crack tip at each cycle and thus to high fatigue resistance (Laird 1976). In anisotropic materials, the fatigue life and fatigue crack growth rates are widely

different in longitudinal and transverse directions. In Ti-6Al-4V alloy tested in the longitudinal direction, the smooth bar fatigue limit is higher (Larson & Zarkades 1976) and the fatigue crack growth rates are smaller (Bowen 1976). The differences are again related to the texture-dependent plastic deformation processes that cause fatigue crack initiation and propagation.

3.1 *Fatigue crack propagation studies*

Fatigue crack propagation (FCP) studies have been carried out extensively in recent times. These studies have assumed great practical significance because they determine the growth potential of subcritical (often preexisting in practice) flaws to critical dimensions to failure. It is usual to plot, on a log-log basis, the variation of FCP rate da/dN as a function of the alternating stress intensity ΔK. A sigmoidal plot is commonly obtained which is divisible into three regimes: Regime I at values of $da/dN \lesssim 5\times10^{-6}$mm/cycle in which the prime interest has been in the threshold value ΔK_{th} below which the crack stops growing; Regime II up to da/dN values of about 5×10^{-4} mm/cycle in which linearity is observed and the expression $da/dN = C(\Delta k)^m$, where C and m are material constants, is applicable (if the initial and final crack lengths at which the crack becomes unstable are known then the safe number of cycles can be estimated by solving for dN and integrating). Regime III at still greater da/dN values corresponds to accelerated growth rates up to final fracture. The microstructural effects can be discussed with reference to these three regimes.

FCP behaviour in region I is strongly sensitive to microstructure. At such low crack growth rates ($<10^{-6}$ mm/cycle *i.e.*, about an interatomic spacing per cycle) it has proved difficult to relate microstructural effects directly to changes in fracture modes because the scale of plasticity approaches the order of the microstructural size. However, efforts in this direction are vigorously continuing (Ritchie 1979; Scarlin 1979; Taira *et al* 1979; Gerberich & Moody 1979). We shall limit ourselves to briefly cataloguing the observed effects.

In low strength ferritic-pearlitic steels, ΔK_{th} values decrease markedly with increasing yield strength. In ultrahigh strength martensitic steels, increasing cyclic yield strength led to significant increase in near-threshold propagation rates and reduction in ΔK_{th}. Thus cylic softening can be regarded as very beneficial to improving region I behaviour.

While refining grain size can be helpful in raising the fatigue limit (especially in low stacking fault energy materials), improved resistance to near-threshold crack propagation has been observed with coarser grain sizes in low strength steels (Masounave & Baflon 1976; Gerberich & Moody 1979; Yokobori 1979) and titanium alloys (Robinson & Beevers 1973). However contrasting behaviour has been observed in the case of high strength steels (Ritchie 1979).

Results of the effect of particles in regime I FCP are also available. In the case of medium strength pearlitic rail steel, decreasing the volume fraction of inclusions led to marked increases in the fatigue limit with however no systematic effect on ΔK_{th}. In strong low-alloy steels, Hebsur *et al* (1980 a,b) have observed substantial lowering of FCP in region I as a consequence of electroslag refining. In aluminium alloys (Knott & Pickard 1977) underaged structures have better near-threshold resistance

than peak and overaged structures whereas in tempered martensitic steels, spheroidised structures offer by far the best resistance (Ritchie 1977a).

A particularly striking effect of microstructure has been observed (Suzuki & McEvily 1979) in AISI 1018 mild steel. By suitable heat-treatment procedures, duplex microstructures where the martensitic phase is continuous and encapsulates the ferritic phase were found to increase strength ($\sigma_y = 450$ MPa) and threshold intensity ($\Delta K_{th} = 20$ MN/m$^{-3/2}$) in contrast to the microstructures in which the ferritic phase surrounds the martensite (σ_y) $= 290$ MPa and $\Delta K_{th} = 10$ MN/m$^{3/2}$). This appears to be a promising way of improving the FCP resistance of low carbon steels.

Comparisons at constant strength have been made in an ultrahigh strength steel (Ritchie 1979) between isothermally transformed structures containing an interlath network of retained austenite within a lower bainite-tempered martensite matrix and quenched and tempered fully martensitic structures containing no austenite. The beneficial effect of austenite is thus brought out once again and this may be due to with the interacting environmental effects which are important in region I (see also the following section). In the same steel, impurity-induced embrittlement (temper embrittlement) gave rise to vastly accelerated growth rates and a reduction in ΔK_{th} by almost 30% (Ritchie 1977b).

In regime II, where fatigue fracture often occurs by a transgranular ductile striation mechanism, there are several investigations to suggest that FCP is unaffected by microstructure (Ritchie 1977a), at least in steels. This is perhaps a singular instance where in regard to mechanical behaviour, microstructure plays no part. Although this view has prevailed, there are attempts to investigate this aspect with greater care. A recent contribution by Yokobori (1979) on the basis of dimensional analysis and comparison of mathematical equations suggests that, for the case without mean stress, the following equation is appropriate:

$$da/dN = B(\Delta K/\sqrt{S}\,\sigma_c)^{n^*}, \tag{9}$$

where σ_c and S are constants with dimensions of stress and length respectively. Yokobori (1979) has found that B and $\sqrt{s}\,\sigma_c$ are nearly independent of monotonic yield strength but n^* increases with increasing ferrite grain diameter in a low carbon steel. The plots for different grain size intersect at $\ln \Delta K = \ln \sqrt{s}\,\sigma_c$. The effect of microstructural features, other than grain size on n^*, has not yet been investigated but Yokobori's result is pioneering insofar as microstructual influence in region II FCP in steels is concerned.

In aluminium alloys, experimental evidence is gathering in favour of microstructural influence on FCP in regime II (Hahn & Simon 1972; Raju 1980). Raju (1980) has emphasized on the basis of analysis of *da/dN versus* ΔK as well as *versus* plastic zone size and a strength correla-parameter, that in order to extract the microstructural effect, comparisons have to be made at constant yield strength. A clear and marked influence of microstructure in regime II emerges in the case of alpha-beta titanium alloys. Data have been recently gathered and analysed in terms of interacting environmental effects and alternate microscopic fracture modes (Gerberich & Moody 1979).

In stage III, the fatigue crack growth rate is rapid since the maximum stress intensity approached K_{Ic} and the failure is microstructure-controlled. The fracture features in this stage resemble the static modes such as cleavage, intergranular and fibrous

fracture. All the microstructural parameters that affect K_{Ic} will also influence the stage III FCP. For example, the removal of non-metallic inclusions in alloy steels improves the K_{Ic} and also reduces the FCP rates in stage III (Hebsur *et al* 1980 a,b). Similarly in aluminium alloys, the resistance to FCP in stage III is nearly doubled by decreasing the volume fraction of intermetallic particles (Staley 1978). Additional resistance to FCP may be obtained by having a larger dispersoid spacing.

3.2 *Low cycle fatigue*

Cyclic stress-strain response has attracted large-scale response because of its relevance to designing alloys for fatigue resistance. Cyclic plastic strain-controlled low cycle fatigue (LCF) has been systematically studied for this purpose (Rama Rao 1978; Gandhi *et al* 1979) as also because for components containing a notch, plasticity near the notch root experiences a plastic strain controlled condition. In principle any component subjected to a start-stop operation constitutes an instance of LCF. A model for FCP discussed in the foregoing section which incorporates LCF properties has been suggested by Antolovich & Saxena (1975). A distinction between LCF and high cycle fatigue (HCF) is made in terms of transition fatigue life (N_{tr}) below which the elastic-plastic strain situation obtains while above N_{tr}, purely elastic strain controlled fatigue occurs. N_{tr} is structure-sensitive decreasing, with increasing strength in steels (Laird 1976).

On the basis of dislocation substructures developed during LCF, a distinction is made between metals and alloys in terms of planar slip and wavy slip materials. When SFE is low, narrow straight surface slip bands and planar dislocation structures occur. In contrast, high SFE materials develop wavy slip bands and dislocation cell structures. An important observation is that the cyclic stress-strain curve is independent of prior treatment for wavy slip metals (Laird 1976).

The influence of microstructural variations on LCF may be illustrated by the work of Malakondaiah & Rama Rao (1977) on an age-hardenable high-strength aluminium alloy which was subjected to LCF following several thermal and thermomechanical treatments after solutionizing. It was found that the overaged alloy showed the best fatigue resistance and the underaged alloy the least with the other treatments following in between the two. Data indicated a good correlation between the observed variation in fatigue life and the fatigue hardening exponent n' arising from the relationship between the stable stress range $\Delta\sigma$ and the plastic strain range $\Delta\epsilon_p$ namely,

$$\Delta\sigma = k'\Delta\epsilon_p^{n'}$$

where k' is another constant. The interpretation of the observed correlation between n' and fatigue life is the following. For a strong material such as the aluminium alloy RR58, inherently capable of resisting stress concentrations, an enhancement in n' raises material resistance to strain concentrations by bringing about an enhanced degree of strain homogenisation. Thus in n' we have a satisfactory index to characterise the material microstructure in the context of LCF. Tomkins' (1968) life-predictive equations corroborate this idea. The overaged alloy contains coarse, uniformly distributed impenetrable particles which resist disordering by the to-and-fro passage of dislocations and represents the best microstructure for LCF resistance.

Laird (1976) has also pointed out that in precipitation-hardened alloys localised softening can be prevented by choosing either an overaged microstructure of the type described above or large precipitate plates interspersed with smaller more close spaced precipitates.

4. Resistance to environment-aided fracture

Metals and alloys undergo spontaneous fracture when subjected to the conjoint action of a corrosive environment and tensile stress. This is generally referred to as stress corrosion cracking (SCC). Environment-aided fracture can also occur due to hdyrogen embrittlement and this type of fracture is not discussed here. The susceptibility to SCC is represented in terms of time-to-failure under constant load in the presence of an environment, or more recently in terms of a threshold stress intensity for stress corrosion crack propagation, K_{Iscc}, below which SCC does not occur. The susceptibility to SCC depends on a large number of factors which may be electrochemical, metallurgical or mechanical in nature. When materials are strengthened by any of the several microstructural variations described above, the SCC susceptibility is also affected. The considerations involved in the alloy design for SCC resistance are discussed below.

The strengthening achieved by alloying leads to an increased susceptibility to SCC. This could be due to a preferential segregation of alloying elements in the microstructure providing anodic areas for corrosion crack initiation or due to a lowering of SFE which promotes the formation of planar arrays of dislocations. For example, the addition of zinc or aluminium to copper decreases the SFE and also promotes the transgranular stress corrosion crack propagation (Swann & Embury 1965). On the other hand, the addition of nickel to 18% chromium steel increases SFE and also improves the resistance to SCC. Further, the additions of minor alloying elements like nitrogen and phosphorous to stainless steel decrease its resistance to SCC since they tend to promote the formation of planar dislocation arrays. Thus the SCC susceptibility of solid solution-strengthened materials is related to the dislocation substructure through SFE provided segregations are eliminated.

The SCC susceptibility is also influenced by grain size, the resistance being greater in fine-grained materials (Parkins 1964). The materials strengthened by grain refinement will therefore be resistant to SCC and the time-to-SCC failure is related to the grain size through a Hall-Petch type relation (Sudhaker Nayak 1980).

Dispersed-particle strengthening does not influence the SCC behaviour of materials but some of the precipitation-hardened materials are prone to SCC. The most important example of this type is the Al-Zn-Mg alloy (Kelley & Nicholson 1963). If these alloys are heat-treated in the conventional way, preferential precipitation of $MgZn_2$ occurs along grain boundaries which promotes intergranular SCC. However, a recent study (Poulose *et al* 1974) has shown that the stress corrosion crack velocity is reduced by overaging the alloy to give a large volume fraction of the precipitate at the grain boundary. This is at the expense of some loss in toughness. Another example of intergranular SCC caused by grain boundary precipitation is the sensitised stainless steel. In this case also, resistance to SCC may be obtained by solution treatment or stabilization with titanium or columbium. Thus SCC considerations are important in precipitation-hardened materials.

Strengthening by cold work makes the material prone to SCC since the high dislocation density enhances the rate of corrosion reactions, and the residual stresses aid the stress corrosion crack propagation. From the SCC viewpoint, therefore, this strengthening method is not favourable.

The susceptibility of materials strengthened by transformation depends on the microstructure developed, and high resistance to SCC can be obtained by suitable heat treatments. For example, in the 300-M steel, it is shown (Ritchie *et al* 1978) that high SCC resistance may be obtained by isothermal transformation at 250°C when compared with the conventional oil quench from 870°C. This is interpreted in terms of the beneficial role of retained austenite in increasing the resistance to SCC.

In anisotropic materials, texture significantly affects stress corrosion failure. This arises from the fact that the nucleation of stress corrosion cracks as well as their propagation are partly crystallographic in nature. Recent work on titanium and Ti-6Al-4V sheet materials (Sudhaker Nayak *et al* 1980 a,b) has shown that stress corrosion crack initiation can be avoided by having a texture that provides a close-packed crystallographic plane like $\{10\bar{1}1\}$ or $\{11\bar{2}2\}$ to be parallel to the crack initiating surface. This texture is achieved in cold-rolled titanium and in annealed longitudinal specimens of titanium to some extent. The texture dependence of stress corrosion crack propagation was examined by Fager & Spurr (1968) and Boyer & Spurr (1978). The susceptibility to SCC is highest if the texture is such that the maximum stress is applied to the basal plane which is close to the cracking plane. This occurs in the transverse specimens of titanium alloys with $\{0002\}$ poles at the transverse direction (TD). The resistance to SCC can thus be improved if the texture is such that the basal planes are not stressed. This condition is met in the longitudinal specimens of Ti-6Al-4V with $\{0002\}$ peak at TD and in this case, an unusual crack branching tendency is observed (Larson & Zarkades 1974). As the textures and deformation modes are essentially similar in titanium and zirconium materials, the above considerations hold good for zirconium materials also. A recent study (Adams *et al* 1978) supports this conclusion.

5. Optimisation of mechanical behaviour

The ideal alloy for structural applications at ambient temperatures is one which possesses the best combination of strength, fracture toughness, fatigue resistance and resistance to environmental embrittling phenomena such as stress corrosion. It is instructive to examine whether for a given material it is possible to arrive at a composition and microstructure which results in such optimum mechanical behaviour.

We have seen that the various strengthening mechanisms do not influence fracture resistance even in monotonic loading in an identical fashion. The discussion in § 2 has indicated that frequently fracture toughness is impaired when strength improvement is promoted. The outstanding exception is the case of grain size refinement which favours increased strength as well as fracture toughness and simultaneously lowers impact transition temperature. Recent work on FCP indicates that grain size refinement in a low carbon steel lowers crack propagation rates in region II. However, there are observations pointing to a deleterious effect of finer grain size in FCP in region I and at threshold. Insofar as SCC is concerned, finer grain size once again is a desirable feature. It is not uncommon to encounter conflicting effects

when fracture resistance in differing situations is considered. For instance strain ageing which results in locked dislocations impairs fracture resistance in monotonic loading but is regarded as beneficial in cyclic loading. Similarly, alloying to reduce SFE improves fatigue resistance in general by mitigating microstructural instability but is very harmful from the viewpoint of SCC resistance.

In view of the wealth of information available on AISI 4340 type ultrahigh strength quenched and tempered low alloy steels, we are in a position to raise the question in this case whether there exists a microstructural condition which displays optimum response to deformation and the variety of fracture conditions we have dealt with. The composition and the established heat treatment provide ultrahigh levels of strength ($>$ 1250 MPa) in this steel. An innovative procedure to modify the microstructure further is to employ higher austenitising temperatures. Such a treatment causes, besides better dissolution of carbides, retention of austenite in the form of enveloping films around martensite laths. This results in substantial improvement of fracture toughness without detriment to strength. Further, the presence of retained-austenite films has been seen to enhance SCC resistance and ΔK_{th} in FCP which is sensitive to environmental effects. Alas! the higher austenitising temperature and the resulting microstructure markedly lower Charpy V-notch energy, which is an important engineering consideration. Further, the overall fatigue resistance is also adversely affected because regions of soft retained austenite induce strain localisation during cyclic deformation. It appears therefore that on the basis of the present state of the knowledge of alloy behaviour the best one can do is to choose a microstructure appropriate to the specific application but it is simply impossible to aim at optimisation of mechanical behaviour from the viewpoints of strength and fracture resistance under varying loading and environmental conditions. This conclusion is reinforced when we realise that even for steel, for which sub-stantial data are available, we have not brought into consideration the requirements of easy processing and acceptable mechanical behaviour at elevated temperatures (Bhatia 1980). Although it seems daunting to set such optimisation as a goal, undoubtedly the alloy designer must feel stimulated and inspired by the existence of such a challenge.

References

Adams B L, Baty D L & Murty K L 1978 *Scr. Metall.* **12** 1151

Antolovich S D & Saxena A 1975 *Eng. Fract. Mech.* **7** 649

Antolovich S D & Saxena A 1975 *Metall. Trans.* **46** 741

Armstrong R W 1977 *Fracture 1977* (ed. D M R Taplin) (Waterloo: University Press) Vol. 4 p. 83

Arun Kumar 1981 *Strengthening mechanisms in solids*, Proc. Dept. Atomic Energy Symp., Suratkal

Ashok S 1976 Ph.D. Thesis, University of Cambridge, England

Baker T J 1974 *Inclusions and their effects on steel properties*, Proc. Conf., University of Leeds, U K

Bhat T B & Arunachalam V S 1980 *Proc. Indian Acad. Sci.* (*Engg. Sci.*) **3** 275 (this issue)

Bhatia M L 1980 *Proc. Indian Acad. Sci.* (*Engg. Sci.*) **3** 297 (this issue)

Birkle A J, Wei R P & Pellisier G E 1966 *Trans. ASM* **59** 981

Bowen A W 1976 *Texture and the properties of materials*, Proc. 4th Int. Conference on texture (eds. G J Davies, I L Dillamore, R C Hudd and J S Kallend) (London: The Metals Society) p. 218

Bowen A W 1978 *Acta Metall.* **26** 1423

Boyer R R & Spurr W F 1978 *Metall. Trans.* **A9** 1443

Cohen M 1975 *Microalloying 1975*, Proc. Int. Symp. HSLA Steels, Washington D.C.

Cottrell A H 1957 *Trans. Met. Soc. AIME* **212** 192
Dyson D J & Holmes D 1970 *J. Iron Steel Inst.* **208** 469
Fager D N & Spurr W F 1968 *Trans. ASM* **61** 263
Frederick S F & Hanna W D 1970 *Metall. Trans.* **1** 347
Gandhi C, Vakil Singh & Rama Rao P 1979 *Trans. Indian Inst. Met.* **32** 122
Gerberick W W & Moody N R 1979 ASTM STP 675 p. 292
Hahn G T & Rosenfield A R 1968 ASTM STP 432 p. 5
Hahn G T & Simon R 1972 Symposium on fracture and fatigue, Washington D C
Hebsur M G, Abraham K P & Prasad Y V R K 1980a *Eng. Fract. Mech.* **13** 851
Hebsur M G, Abraham K P & Prasad Y V R K 1980b *Int. J. Fatigue* **2** 147
Hilty D C & Popp V T 1969 *AIME Elec. Furn. Conf. Proc.* **27** 52
Jokl M L, Vitek V & McMahon Jr C J 1980 *Acta Metall.* **28** 1479
Joshi A L, Mallik A K & Banerjee S 1977 *Trans. Indian Inst. Met.* **30** 405
Kelly A & Nicholson R B 1963 *Prog. Mater. Sci.* **10** 151
Kirman I 1971 *Metall. Trans.* **2** 1761
Knott J F & Pickard A C 1977 *Met. Sci.* **11** 399
Krafft J M 1964 *Appl. Mater. Res.* 88
Laird C 1976 *Alloy design and microstructural design* (eds J K Tien and G S Ansell) (London: Academic Press) p. 175
Larson F & Zarkades A 1974 Properties of textured titanium alloys, MCIC-74-20, Batelle Columbus Laboratories, Ohio, USA
Larson F & Zarkades A 1976 *Texture and properties of materials*, Proc. 4th Int. Conf. on Texture (ed G J Davies) (London: The Metals Society), p. 210
Low J R 1954 *Relation of properties to microstructure* (Metals Park, Ohio: ASM) p. 163
Luyckz L, Bell J R, McLean A & Korchynsky M 1970 *Metall. Trans.* **1** 3341
Malakondaiah G & Rama Rao P 1977 *Fracture 1977* (ed D M R Taplin) (Waterloo: University Press) Vol. 1, p. 741
Masounave J & Baflon J P 1976 *Mechanical behaviour of materials* Proc. 2nd Int. Conf. (Metals Park, Ohio: ASM) p. 636
McEvily A J 1978 *Fracture mechanics* Proc. 10th Symp. Naval Structure Mechanics, Washington D C p. 229
Mulherin J H & Rosenthal H 1971 *Metall. Trans.* **2** 427
Parkins R N 1964 *Metall. Rev.* **9** 209
Parkinson F L 1972 Titanium alloy 6A1-4V sheet DOT/SST Rep. No. FAA-SS-72-01, Boeing Co., Seattle, USA
Pickering F B 1978 *Physical metallurgy and the design of steels*, (London: Butterworths) p. 32
Pickering F B & Gladman T 1963 Iron and Steel Institute Spec. Rep. No. 81 p. 10
Poulose P K, Morral J E & McEvily A J 1974 *Metall. Trans.* **5** 1393
Raju K N 1980 *Energy balance considerations in brittle fracture and fatigue crack growth* Ph.D. Thesis, Indian Institute of Science, Bangalore
Rama Rao P 1978 *Trans. Indian Inst. Met.* **31** 239
Ramaswamy V & Raghavan V 1981 *Proc. Indian Acad. Sci.* (*Engg. Sci.*) (to appear)
Ritchie R O 1977a *Metall. Sci.* **11** 368
Ritchie R O 1977b *Metall. Trans.* **A8** 1131
Ritchie R O 1979 *Int. Metall. Rev.* **5 & 6** 205
Ritchie R O, Cedeno M H C, Zackay V F & Parker E R 1978 *Metall. Trans.* **A9** 35
Ritchie R O & Horn R M 1978 *Metall. Trans.* **A9** 331
Robinson J L & Beevers C J 1973 *Metall. Sci.* **7** 153
Rosenfield A R, Hahn G T & Embury J D 1977 *Metall. Trans.* **3** 2797
Scarlin R B 1979 ASTM STP 675 p. 396
Schwalbe K H 1977 *Eng. Fract. Mech.* **9** 795
Smallman R E 1963 *Modern physical metallurgy* (London: Butterworths) p. 339
Staley J T 1975 ASTM STP 605 p. 71
Staley J T 1978 *Fracture mechanics*, Proc. 10th Symp. Naval Structural Mechanics, Washington, p. 671
Stonesifer F R & Armstrong R W 1977 *Fracture 1977* (ed D M R Taplin) (Waterloo: University Press) Vol. **2**, p. 1

Sudhaker Nayak H V 1980 *Texture-dependent stress corrosion failure commercial titanium and Ti-6Al-4V alloy sheets in methanol-bromine solution* Ph.D. Thesis, Indian Institute of Science, Bangalore

Sudhaker Nayak H V, Vasu K I & Prasad Y V R K 1980a *J. Mater. Sci.* **15** 1265

Sudhaker Nayak H V, Vasu K I & Prasad Y V R K 1980b *Res. Mechanica* (in press)

Suzuki H & McEvily A J 1979 *Metall. Trans.* **A10** 475

Swann P R & Embury J D 1965 *High strength materials* (ed V F Zackay) (New York: John Wiley) p. 327

Taira S, Tanaka K & Hoshina 1979 ASTM STP 675 p. 135

Tomkins B 1968 *Philos. Mag.* **18** 1041

Wilson D V 1966 *J. Inst. Met.* **94** 84

Yokobori T 1979 ASTM STP 675 p. 683

Zackay V F 1975 40th Meeting of the Structures and Materials Panel, Brussels, Belgium

Microstructural synthesis

S RANGANATHAN and P RAMACHANDRARAO
Centre of Advanced Study in Metallurgy, Department of Metallurgical Engineering, Banaras Hindu University, Varanasi 221 005

MS received 16 February 1981

Abstract. This paper outlines the different routes available for the synthesis of strong microstructures with emphasis on recent developments. Strong microstructures may be obtained from the melt by rapid solidification, whereby large extensions in solid solubility may be achieved, grain size refined and metastable phases precipitated. It is also possible to produce metallic glasses possessing a remarkable combination of properties. Partial crystallization of these glasses adds another dimension to possible microstructures. The conventional route of solid state transformations has been made more exciting with our increased understanding of spinodal decomposition, ordering and martensitic transformations.

Keywords. Rapid solidification; metallic glasses; spinodal decomposition; ordering; martensites.

1. Introduction

The evolution of microstructure is a fascinating theme in physical metallurgy both for its intrinsic scientific interest and its possible technological applications. As our understanding of the relation between microstructure and properties has expanded, it becomes crucial to be able to produce the desired microstructure in a given alloy. Conventionally this has been done through heat treatments in the solid state. In recent years the desirability of combining mechanical and thermal treatments has been realized. It is now possible to view the problem of the design of microstructures on a rational basis. This review highlights recent developments in the production of strong microstructures from the liquid state, *via* the glassy state or from the solid state. For earlier work the reviews by Nicholson & Davies (1971), Nicholson (1971), Davies (1971) and Decker (1973) may be consulted.

2. Strong microstructures from the melt

The last few decades have seen remarkable progress in controlling the microstructures that can be developed from the molten state. Notable attempts in this direction include the now well-established techniques for controlled solidification of eutectics (Hogan *et al* 1971; Weatherly 1975), the fast emerging field of rheocasting (Flemings *et al* 1976), highly promising methods for casting of melts with uniformly dispersed insoluble second phase particles (Mehrabian *et al* 1974), laser glazing (Breinen *et al* 1976), production and compacting of powders by rapidly solidifying droplets (Cebulak *et al* 1976) and the synthesis of flakes, wires, tapes etc., from the melt by processes

which generate cooling rates of the order of 10^5–10^9 Ks^{-1} (Pond *et al* 1976). Solidification at such spectacular cooling rates enables development of stronger alloys by simultaneously bringing into play a variety of strengthening mechanisms involving refinement in grain size, enhanced solid solubility, modification of phase transformations and dispersion of fine precipitates (Honeycombe 1978). The progress made so far is highlighted and a forecast of the possible developments in this novel area of research is made.

2.1 *Rapid solidification*

Techniques for rapid solidification are now well established and have been critically reviewed in the past (Anantharaman & Suryanarayana 1971; Jones 1973). The many factors that control the rate of solidification and its measurement or estimation have been comprehensively discussed by Jones (1976a). The present section is devoted to the constitution and microstructural features of rapidly-solidified alloys and their role in the development of stronger alloys.

2.2 *Microstructural features*

The spectacular cooling rates involved in rapid solidification lead to considerable kinetic undercooling of the melt (Loehberg & Muller 1970). In several alloys, the drastic undercooling so attained is sufficient to suppress nucleation and leads to the formation of metallic glasses. These novel species of metallic materials are discussed in § 3. In a number of cases, however, a spectrum of microstructures ranging from diffusionlessly or massively solidified regions to the more common but considerably refined dendritic or cellular growth can be noticed (figure 1, plates 1 and 2). The overall microstructure of the foil with particular reference to shapes of grains, relative predominance of equiaxed, columnar and dendritic structures has received some attention (Ramachandrarao & Anantharaman 1968a). Kattamis *et al* (1973) studied the influence of process variables such as melt temperature, piston velocity, surface condition of the plattens etc., on the microstructure of Fe-Ni alloys quenched by the piston-and-anvil technique. They observed that quenching undercooled droplets results in a highly cored dendritic structure in the central regions of the foil under the combined influence of undercooling, rapid cooling and intense fluid flow. In the case of many melt-spun or gun-quenched alloys, particularly those based on aluminium, a characteristic microstructure comprising of two sets of parallel grains meeting along a common boundary is often noticed (figure 2, plate 2). Such a grain morphology had earlier been attributed to heat transfer along the plane of the foil. A recent study (Chattopadhyay *et al* 1980) has shown that grains on either side of a common boundary are in twin orientation and that the central boundary is itself a trace of a (111) twin plane. The boundaries separating the elongated grains in each set were shown to be traces of (001) planes. The occurrence of grains with such twin orientation was rationalised in terms of Eady and Hogan's model (Eady & Hogan 1974) for the growth of twinned dendrites stabilised at the high growth rates by non-equilibrium solute trapping at the solid-liquid interface.

2.3 *Grain size strengthening*

The variety of microstructural features in rapidly solidified alloys produced under the combined influence of undercooling, solute diffusion rates, heat transfer conditions etc., makes it difficult, in many cases, to give meaningful grain size values. Early experiments utilising x-ray line breadth analysis on a few metals and alloys have shown that the coherently scattering domain size can be of the order of 1000 Å or less (Ramachandrarao & Anantharaman 1968b). No significant contributions to line breadth arise due to residual strains in gun-quenched alloys while the piston-and-anvil technique may introduce some small strains. Subsequent electron metallographic studies have shown that the grain size can be as low as 30 Å with or without dislocation substructure or vacancy clusters (Boswell & Chadwick 1977; Jones 1976b).

Boswell & Chadwick (1977) attempted to determine the mean grain diameter ($\bar{d}$) in rapidly solidified foils by considering homogeneous steady state nucleation rate per unit volume (I) and isotropic linear growth rate (G) at the prevalent reduced undercooling

$$\Delta T_r = \frac{T_m - T}{T_m}$$

below the equilibrium freezing temperature T_m. According to Johnson & Mehl (1939) $\bar{d}$ is related to I and G by

$$\bar{d} = (GI)^{1/4}. \tag{1}$$

The mean grain diameters calculated by Boswell and Chadwick on the assumption of isothermal solidification and equation (1) were found to be about four times as large as those detected experimentally. The discrepancy can be corrected only by reducing the free energy required to form a critical nucleus from the usually accepted value of 50–70 kT to about 40 kT, where k is the Boltzman constant. Consideration of nonisothermal solidification enabled these authors to evaluate the cooling rate dependence of $\bar{d}$. Since the cooling rate is a function of the thickness of the foil, the procedures developed enable the correlation of grain size as a function of foil thickness to be made. Boswell and Chadwick further showed that $\bar{d}$ (in μm) in aluminium can be related to the cooling rate R by the expression

$$\bar{d} = 1{\cdot}75 \times 10^7 \times R^{-0.9}. \tag{2}$$

The foregoing discussion assumes homogeneous nucleation. The probable role of solute elements in grain refining *via* the formation of an inoculant phase has also been investigated in chill-cast Al-Zr alloys. It has been observed that grain refinement occurs abruptly beyond a cooling rate-dependent critical concentration of zirconium (Ohashi & Ichikawa 1973). Increasing the cooling rate pushes the limiting value of solute concentration to higher values. The abrupt incidence of grain refinement has been attributed to the formation of a cubic phase Al_3Zr, when the prevalent cooling rate does not permit the retention of all the zirconium in solid solution. It thus becomes necessary to separate the contributions of cooling rate and

inoculant to grain refinement in certain alloys. Sahin & Jones (1978) have shown that the cooling rate alone can cause a refinement in grain size from 0·9 mm at 800 K s^{-1} to 2·5 μm at 10^6 K s^{-1} in an Al-0·4 at % Zr alloy.

An immediate consequence of the fine grain size in the as-quenched microstructure is a remarkable enhancement in strength of the material. Data is relatively scarce at the extremely small grain sizes obtained by rapid solidification to test the Hall-Petch relationship between grain size and strength. However, extrapolations from tests on conventionally processed materials with larger grain sizes appear to be valid. In this context, the results of Inokuti & Cantor (1977) on rapidly solidified pure iron are of interest. They observed that rapidly solidified pure iron can be wholly ferritic, wholly martensitic or a mixture of both. The presence of equiaxed bcc grains of ~ 4 μm size was shown to be a result of the massive transformation of austenite. The martensitic structure consisted of packets of ~ 4 μm size with the martensite plate width being $\sim 0{\cdot}3$ μm. The microhardness of the quenched samples ranged from 250 kg mm^{-2} for the ferritic structure to 700 kg mm^{-2} for the martensitic structure. When the average grain size of the sample was ~ 27 μm in an isolated sample the hardness was only 129 kg mm^{-2}. These results lie on the hardness *vs* (grain size)$^{-1/2}$ plot extrapolated from the solid state quenched specimen data and suggest that the Hall-Petch relationship is valid down to 4 μm grain size.

As pointed out earlier, in several cases, the as-solidified structure consists of several cells within the fine grains. Wood & Honeycombe (1976) have shown that often a large number of adjacent grains have low angle grain boundaries indicating that they are cell or dendritic boundaries. In view of this, they contend that the cell size should be the true parameter in establishing the Hall-Petch relationship for rapidly solidified alloys. There is, however, little doubt that the fine grain size achieved by rapid solidification and frequently stabilized by grain-boundary precipitation by a stable or metastable phase has a significant impact on the strength of rapidly solidified alloys.

2.4 *Solid-solution strengthening*

One of the notable results of rapid solidification has been the metastable extension of mutual solid solubility limits in many binary systems. Such extensions, besides validating the Hume-Rothery conditions for solid solubility, prove to be of immense significance in the development of newer aluminium alloys. Aluminium-based systems exemplify the possibilities in a remarkable way (Anantharaman *et al* 1977; Jones 1978). Perusal of table 1 shows that only seven elements dissolve $1>$ at.% in aluminium under equilibrium conditions. On rapid solidification, however, the number increases to 19; thus opening up immense possibilities for solution-and precipitation-strengthened aluminium alloy development. In this section, we shall deal with solid-solution strengthening in rapidly solidified alloys.

Fontaine (1976) has analysed the hardening effect due to various transition elements in the aluminium matrix on the basis of the interaction of solute atoms with dislocations. The interaction can be elastic because of the size difference between solute and solvent atoms and electrostatic because of their valence difference. Fontaine's analysis has shown that the increment in hardness

$$\Delta = H_v - H_v\,(Al) = K\mu\,(\eta c)^{4/3}, \tag{3}$$

Table 1. Equilibrium and metastable solid solubilities in aluminium binary alloys (for references see Anantharaman *et al* 1977)

Solute	Maximum solid solubility in equilibrium	At. % Metastable
Ag	23·8	40·00
Au	0·04	0·14
Ca	<0·01	<0·01
Ce	~0·01	1·90
Co	<0·01	5·00
Cr	0·38	>6·00
Cu	2·50	18·00
Fe	0·03	4·40
Ga	8·80	65·00
Ge	2·80	33·00
Mg	18·90	>36·80
Mn	0·70	>9·00
Mo	0·07	1·00
Ni	0·02	7·70
Pd	0·00	>10·00
Pt	<0·01	2·20
Si	1·59	16·00
Sn	0·02	0·26
Ti	0·74	2·00
V	0·2	2·00
W	0·02	1·90
Zn	49·5	43·50
Zr	0·08	1·50

where η is the fractional difference in atomic size, c is the atom fraction of solute and μ is the shear modulus. K is a proportionality constant and was found to be ~ 79. Cr, Mn, Cu and Zr increase the hardness of the aluminium matrix according to equation (3) while elements like Fe, Co and Ni lead to considerably greater hardening than predicted. Fontaine has attributed the discrepancy in the behaviour of Fe, Co and Ni to their clustering tendency in the aluminium matrix. The clustering occurs on a scale too fine to be readily detected by electron metallography. Small angle x-ray scattering studies indicate clusters of ~ 20 Å size (Bonefacie *et al* 1975). Such clusters can lead to considerable strengthening and enhance microhardness. The analysis implicitly assumes equality of grain size in various alloys or ignores the effect of grain size. Sahin & Jones (1978) have calculated that in the case of an Al-2·7 at.% Zr alloy the fine grain size can itself lead to about 250 MPa increment in the hardness of otherwise pure aluminium. It is hoped that high-resolution electron metallographic analysis of various alloys with controlled grain size will establish the validity or otherwise of Fontaine's analysis.

Tool steels have been an obvious choice for study by rapid solidification since a considerable fraction of expensive alloying elements is not taken into solution in conventional heat treatment because of the stability of their carbides. In the case of the T and M-series of tool steels, for example, rapid quenching has favoured the retention of significant amounts of austenite as a result of its supersaturation with alloying elements and consequent lowering of M_s temperature. An attendant feature

has been the near complete suppression of carbides and retention of a bcc phase as well. Rayment & Cantor (1978) have concluded that at the highest cooling rates attainable the bcc phase is δ-ferrite retained at room temperature, while at intermediate cooling rates it forms and transforms to austenite (but not martensite). Further reduction in the cooling rate enables austenite to form martensite. In T1 steel, no carbide was detected while the molybdenum-bearing steels showed the presence of δ M_6C-type carbide. A comparison of the tempering behaviour of the solid-state-quenched and liquid quenched tool steels shows that the peak hardness attained is reached at a higher temperature in the latter and also has a higher value. X-ray studies show that the increase in hardness is essentially due to the transformation of austenite to martensite with the process being completed at about 700°C. Solid-solution strengthening thus appears to play a major role in rapidly solidified tool steels.

2.5 *Dispersion strengthening*

The foregoing account of the microstructural and defect characteristics of rapidly solidified alloys shows that the fine grain size, reduction in the scale of segregation and retention of vacancies play a dominant role in establishing the final microstructure. All these contribute to and affect the ageing behaviour of liquid-quenched alloys by providing grain boundaries for heterogeneous nucleation of precipitates with an enhanced tendency for nucleation. Age-hardening has been observed in a number of aluminium alloys containing transition elements whose solid solubility has been considerably extended by rapid solidification. Such alloys, particularly those having Fe in solution, have high strengths even at high temperatures and indicate that dispersion hardening is taking place. An even distribution of metallic inclusion has been considered responsible for the improved fatigue and stress rupture life of a commercial 2024 alloy processed by liquid-quenching techniques. For more details regarding the variety of aluminium alloys amenable to strengthening by dispersion, the excellent review by Jones (1978) can be consulted.

In the case of monotectic systems, it is possible to obtain a fine distribution of one phase in the other by rapid solidification. The recent work of Chattopadhyay & Ramachandrarao (1980) has shown that a variety of morphologies ranging from single phase to arranged dispersion of cadmium particles in an aluminium matrix can be obtained (figure 3 plate 3). Electron metallography has shown that the single phase decomposes by the formation of spherical Guinier-Preston (GP) zones and the associated strengthening is being investigated.

2.6 *Development of alloys by melt-quenching methods*

The fundamental requirement of rapid solidification *i.e.* good and effective contact between the liquid and a heat sink, imposes several restrictions on the technique and limits the possible geometries of the product. The gun-and melt-extraction techniques produce flakes of small size while melt-spinning can give rise to continuous or discontinuous tapes. Such products can be handled only by consolidation techniques. The immense possibilities of microstructural control associated with rapid solidification have, however, spurred notable activity in fine powder production by gas atomisation, metal spraying by gas and plasma torches and solidification *in situ* of

thin layers by laser glazing. The processing of flakes obtained by rapid solidification has followed conventional routes of rolling, forging and pressing after suitable compaction and cladding. Hot isostatic pressing of such starting material is finding increased application (Grant 1978).

Notable progress has been made in developing super alloys, aluminium-base alloys, tool steels and titanium alloys by these routes. Progress made till recently has been summarised by Grant (1978). It was pointed out that several production gas turbine engines are now based on the use of turbine disks made from rapidly solidified alloy powders. Besides aluminium alloys containing transition elements, development of 2024 alloy with lithium additions has been found to be extremely noteworthy (Sankaran & Grant 1980). Addition of lithium reduces the density of the alloy by about 3% and increases the Young's modulus by 6%. Lithium additions also significantly improve the fatigue strength (at 10^7 cycles) to ultimate tensile strength ratio as well as the strength and ductility of 2024 alloy. Rapid coarsening of the strengthening precipitate δ' leads to a loss of strength at elevated temperatures. Such a loss can be prevented by the addition of cadmium.

3. Strong microstructures via the glassy state

A new era in physical metallurgy was ushered in by Duwez *et al* (1960) when they quenched Au-Si eutectic alloy from the melt and produced a metallic glass. The introduction of bulk production techniques such as melt spinning in the early 1970s led to intensive studies of these novel materials. They can be used in the glassy state or can be precursors to the partially crystallized or the fully crystallized state. Thus new types of microstructures have become available to the alloy designer (Ramachandrarao *et al* 1980).

3.1 *Metallic glasses*

There has been a steady increase over the years in the number of systems amenable for glass formation. The criteria for easy glass formation have been evolved on the basis of thermodynamic, kinetic and processing factors (Polk & Giessen 1978). Two major classifications are noble or transition metal-metalloid (*e.g.* Pd-Si, Fe-P-C, Ni-P-B) and metal-metal glasses (*e.g.* Ni-Nb, Cu-Zr).

In principle it is expected that every liquid would form a glass upon cooling, if a critical cooling rate to prevent crystallization is exceeded (Cohen & Turnbull 1959). A possible guiding factor is the reduced melting temperature defined as

$$\tau_m = kT_m/\Delta H_v,$$

where T_m is the melting point and ΔH_v is the heat of vaporization. The glass-forming tendency increases with decreasing τ_m. It is also possible to achieve correlation of the glass-forming tendency with appreciable differences in the size of the component atoms, valence and electronegativity. A predictive approach based on the compositional dependence of the strain energy of mixing liquid metals has been developed by Ramachandrarao (1980). Another indication of a valence electron effect comes from the observation that crystalline equilibrium phases are found at

the composition of many metallic glasses. These phases have usually topologically close-packed crystal structures. Elements of such close packing bear a strong resemblance to the random close packing in the glass.

Metallic glasses exhibit exceptional strengths and hardnesses. The ratio of Young's modulus-to-yield strength is typically around 50 and exceeds the value for conventional crystalline materials. The plane-strain fracture toughness for Fe- and Ni-based metallic glasses is ~ 40 kg/mm$^{3/2}$ and is again better than those for steels of comparable yield strength (Davis 1978). Such an attractive combination of properties provides a strong incentive for overcoming the limitations provided by specimen size.

3.2 *Partially crystallized microstructures*

The ceramic engineer has long known the advantages of partially crystallizing ceramic glasses. Glass ceramics find a wide variety of applications, the most familiar being pyro-ceram used in ovenware. The metallurgist is now following this route.

A typical example of a partially crystallized Metglas 2826 ($F_{40}Ni_{14}B_6$) is shown in figure 4 (plate 3). Detailed studies of the kinetics of crystallization of a number of Fe-Ni based alloys are available (Ranganathan *et al* 1980). The mechanical properties of partially crystallized alloys have been determined in Cu-Zr alloys (Freed & Vander Sande 1980) and crystallization appears to be detrimental. However there is an indication that with suitable changes in composition, improvements can be effected.

Another possible area of application is in superconductivity. A number of titanium, niobium, molybdenum and tungsten-based amorphous alloys exhibit superconductivity (Inoue *et al* 1980). However, flux-pinning forces are characteristically weak in these materials. The sample T_c can be increased by introducing crystalline particles. Clemens *et al* (1980) have demonstrated this for Mo-Ru-Si-B glass and found that the critical current density is increased by two or three orders of magnitude. As-quenched amorphous alloys are flexible and readily fabricated into superconducting lines, transformers and magnets. The heat treatment of the component can then be carried out to alter the microstructure and achieve the optimum properties.

4. Strong microstructures from the solid state

Phase transformations have been used from time immemorial for producing high strength materials. Their applications to steels (Ramaswamy & Raghavan 1981), titanium alloys (Banerjee & Krishnan 1981) and zirconium alloys (Krishnan & Asundi 1981) are illustrated separately. In this section spinodal decomposition, order-hardening and martensitic transformation are treated from the microstructural point of view. All three transformations are the objects of current and intensive investigations.

4.1 *Spinodal decomposition*

In spinodal decomposition a small excursion occurs in composition variation but is spread throughout the material. With time the composition variation is amplified. The theory of this mode of decomposition of a supersaturated solid solution is well

understood because of the classic investigations of Hillert (1961) and Cahn (1968). It has become a transformation of practical importance, as it has been realized that it permits us to introduce a homogeneous and fine distribution of second-phase particles. Butler & Thomas (1970) made extensive use of the transmission electron microscope to document the changes that take place in the Cu-Ni-Fe system with ageing. An example of the microstructure produced in Co-Ti-Nb alloys in presented in figure 5 (plate 4) (Singh *et al* 1980). It is readily seen that the distribution of Co_3Ti particles is truly homogeneous and truly oblivious to the presence of grain boundaries.

During the later stages of ageing the precipitating phases have compositions approaching the equilibrium ones. At this stage, the elastic strains become sufficiently large and lead to a loss of coherency by the generation of interfacial misfit dislocations. These dislocations are often sessile. Thomas (1977) has argued that the interfaces can then be considered similar to grain boundaries. Thus this transformation presents a unique route for the synthesis of a microstructure, periodic in dimensions and periodic in the distribution of dislocations.

4.2 *Order hardening*

The increase in the strength of alloys with the progress of ordering is an attractive concept in the development and design of alloys. While its full potential is yet to be realized in practice, there are several significant contributions in this area (Stoloff & Davies 1971).

In isostructurally-ordered alloys such as Cu_3Au, peak strength occurs at a critical domain size. The interaction of superdislocations with matrix dislocations and antiphase boundaries leads to an increase in flow stress. When the ordered alloy has a different structure such as in Cu-Au a near doubling of strength occurs (Arunachalam & Cahn 1967). This extra hardening has been attributed to the change in lattice symmetry, leading to substantial misfit stresses.

Mishra (1980) has carried out an extensive study of order hardening in a series of Ni-Mo and Ni-W alloys. The domain sizes were evaluated by both transmission electron microscopy and polarized light metallography. It was established that domain size played a crucial role in the order-strengthening of Ni_4Mo and Ni_4W. Domain growth and coalescence at later stages led to softening.

The ageing temperature plays an important role in the mode of transformation. This may be illustrated with reference to Ni-20%W. At relatively high temperatures ($>940°C$) a heterogeneous mode prevailed. Perpendicular twins formed. New domains are nucleated near grain boundaries (figure 6, plate 5). At lower temperatures ($<830°C$) homogeneous nucleation occurred, leading to a mosaic structure (figure 7, plate 5). Thus it is possible to vary the microstructure in the ordered alloys by suitable changes in the heat treatment schedule.

4.3 *Martensitic transformations*

As in spinodal decomposition and ordering, martensitic transformation can also produce a relatively uniform microstructure. The two major classes of martensites that occur in steels are lath and plate martensites (Marder & Marder 1969; Nishiyama 1978). The former is found in plain carbon and low-alloy steels of low

carbon content as well as in certain high-alloy steels like marageing steels and martensitic stainless steels. In these cases an austenite grain transforms into several packets, each packet containing blocks of several orientations. The blocks form laths within themselves. The plate martensites are lenticular with characteristic midribs. These plates are either fully or partially twinned.

The strength of the martensite has been attributed to interstitial solid solution, the internal structure of martensite and the size of martensite packets or plates. Norstroem (1976) reported that substitutional solid-solution strengthening, packet boundaries (high angle), lath boundaries (low angle) and dislocation densities within the laths are the main factors contributing to the yield strength of martensite. The toughness values of steels with twinned martensite substructure were invariably lower when compared to steels in which the substructure consisted of martensite lath.

Thomas (1977) has used the above considerations to arrive at guidelines for designing strong, tough steels based on the martensitic transformation. By ensuring M_s to be above 350°C through suitable adjustment of the carbon content and alloying elements, it is possible to obtain dislocated martensite with minimal twinning. Secondly a composite structure wherein the martensite is surrounded by a continuous thin film of austenite enhances the toughness values at high strength. High resolution electron microscopy has proved a powerful tool in discriminating between bands of interlath martensite and cementite.

The martensitic transformation can also be exploited to strengthen softer phases. An example is the duplex austenitic-martensitic stainless steels. Singh *et al* (1981) have investigated 304 stainless steels. It is possible to produce by deformation two varieties of martensites (bcc and hcp) in varying amounts. Tempering leads to changes in the relative amounts of these phases. A wide variety of microstructures can thus again be produced in the same alloy. An excellent survey of the possibilities in steels, which form the most complex groups of alloys, has been given by Honeycombe (1981).

References

Anantharaman T R & Suryanarayana C 1971 *J. Mater. Sci.* **6** 1111

Anantharaman T R, Ramachandrarao P, Suryanarayana C, Lele S & Chattopadhyay K 1977 *Trans. Indian Inst. Met.* **30** 423

Arunachalam V S & Cahn R W 1967 *J. Mater. Sci.* **2** 876

Banerjee D & Krishnan R V 1981 *Proc. Indian Acad. Sci.* (*Engg. Sci.*) Vol. 4 (to appear)

Bonefacie A, Kerenovic M, Kirin A & Kunstelj D 1975 *J. Mater. Sci.* **10** 243

Boswell P G & Chadwick G A 1977 *Scr. Met.* **11** 459

Breinan E M, Kear B H, Banas C M & Greenwald L E 1976 *Super alloys: Metallurgy and manufacture* (Baton Rouge USA: Claiter's Publishing Division) p 435

Butler E D & Thomas G 1970 *Acta Metall.* **18** 347

Cahn J W 1968 *Trans. Met. Soc. AIME* **28** 258

Cebulak W S *et al* 1976 *Met. Engg. Q.* **16** 4

Chattopadhyay K & Ramachandrarao P 1980 *J. Mater. Sci.* **15** 685

Chattopadhyay K, Lele S & Ramachandrarao P 1980 *J. Cryst. Growth* **19** 229

Clemens B M, Johnson W L & Bennett J 1980 *J. Appl. Phys.* **51** 1116

Cohen M H & Turnbull D 1959 *J. Chem. Phys.* **31** 1164

Davies G T 1971 in *Strengthening methods in crystals* eds. A Kelley and R B Nicholson (Barking: Applied Science) p. 485

Davis L A 1978 in *Metallic glasses* (Ohio: American Society for Metals) p. 190

Decker R F 1973 *Metall. Trans* **4** 2495
Duwez P, Willens R H & Klement W 1960 *J. Appl. Phys.* **31** 1136
Eady J A & Hogan L M 1974 *J. Cryst. Growth* **23** 129
Flemings M C, Riek R G & Young K P 1976 *AFS Int. Cast Met. J.* **1** 11
Fontaine A 1976 in *Rapidly quenched metals* eds N J Grant and B C Giersen (Cambridge: Mass: M.I.T. Press) p. 163
Freed R L & Vander Sande J B 1980 *Acta Metall.* **28** 103
Grant N J 1978 in *Rapidly quenched metals* III ed. B. Cantor (London: The Metals Society) Vol. 2, p, 172
Hillert M 1961 *Acta Metall.* **9** 525
Hogan L M, Kraft R W & Lemkey F D 1971 *Adv. Mater. Sci.* **5** 114
Honeycomb R W K 1978 in *Rapidly quenched metals* III ed. B Cantor (London: The Metals Society) Vol. 1, p. 73
Honeycombe R W K 1981 *Steels: Microstructure and properties* (London: Edward Arnold)
Inokuti Y & Cantor B 1977 *J. Mater. Sci.* **12** 946
Inoue A, Suryanarayana C, Masumoto T & Hoshi A 1980 *Sci. Rep. Res. Inst. Tohoku Univ.* **A28** 182
Johnson W A & Mehl R F 1939 *Trans Met. Soc. AIME* **135** 416
Jones H 1973 *Rep. Prog. Phys.* **36** 1425
Jones H 1976a in *Rapidly quenched metals* eds N J Grant and B C Giersen (Cambridge, Mass: M.I.T. Press)
Jones H 1976b in *Vacancies '76* (London: The Metals Society) p. 175
Jones H 1978 *Aluminium* **54** 274
Kattamis T Z, Bronson W E & Mehrabian R 1973 *J. Cryst. Growth* **19** 229
Krishnan R & Asundi M K 1981 *Proc. Indian Acad. Sci.* (*Engg. Sci.*) Vol. 4 (to appear)
Loehberg K & Mueller N 1970 *Fizika* **2** (Suppl 2) 4
Marder J M & Marder A R 1969 *Trans. ASM* **60** 651
Mehrabian R, Riek R G & Flemings M C 1974 *Metall. Trans.* **5** 1899
Mishra N S 1980 *Microstructural studies of ordering in Ni-Mo and Ni-W alloys* Ph.D. Thesis, Banaras Hindu University
Nicholson R B 1971 in *Strengthening methods in solids* eds A Kelly and R B Nicholson (Amsterdam: Elsevier)
Nicholson R B & Davies G J 1971 in *Strengthening methods in solids* eds A Kelly and R B Nicholson (Amsterdam: Elsevier)
Nishiyama Z 1978 *Martensitic transformation* (New York: Academic Press)
Norstroem L A 1976 *Scand. J. Metall.* **5** 159
Ohashi T & Ichikawa R 1973 *Z. Metallkde* **64** 517
Polk D E & Giessen B C 1978 in *Metallic glasses* (Ohio: American Society for Metals) p.1
Pond R B Sr., Maringer R E & Mobley C E 1976 in *New trends in materials processing* (Ohio: American Society for Metals) p. 128
Ramachandrarao P 1980 *Z. Metallkde* **71** 172
Ramachandrarao P & Anantharaman T R 1968a *Trans. Met. Soc. AIME* **245** 890
Ramachandrarao P & Anantharaman T R 1968b *Trans. Met. Soc. AIME* **245** 892
Ramachandrarao P, Ranganathan S & Anantharaman T R 1980 *Bull. Mater. Sci.* **2** 17
Ramaswamy V & Raghavan V 1981 *Proc. Indian Acad. Sci.* (*Engg. Sci.*) Vol. 4 (to appear)
Ranganathan S, Claus J C, Tiwari R S & Heimendahl M V 1980 *Proc. Int. Conf. on Metallic Glasses: Science and Technology* (Budapest: Hungarian Academy of Sciences)
Rayment J J & Cantor B 1978 *Met. Sci.* **12** 155
Sahin E & Jones H 1978 in *Rapidly quenched metals* III ed. B Cantor (London: The Metals Society) Vol. 1, p. 138
Sankaran K K & Grant N J 1980 *Mater. Sci. Engg.* **44** 213
Singh J, Lele S & Ranganathan S 1980 *J. Mater. Sci.* **15** 2010
Singh J, Sarma D S & Ranganathan S 1981 (to be published)
Stoloff N S & Davies R G 1971 in *Strengthening methods in crystals* eds A Kelly and R B Nicholson (New York: Elsevier)

Thomas G 1977 in *Fundamental aspects of structural alloy design* eds R I Jaffee and B A Wilcox (New York: Plenum Press) p. 331

Weatherley G C 1975 in *Treatise on materials science and technology*, ed. H Herman (New York: Academic Press) Vol. 8, p. 121

Wood J V & Honeycombe R W K 1976 *Mater. Sci. Engg.* **23** 107

Plate 1

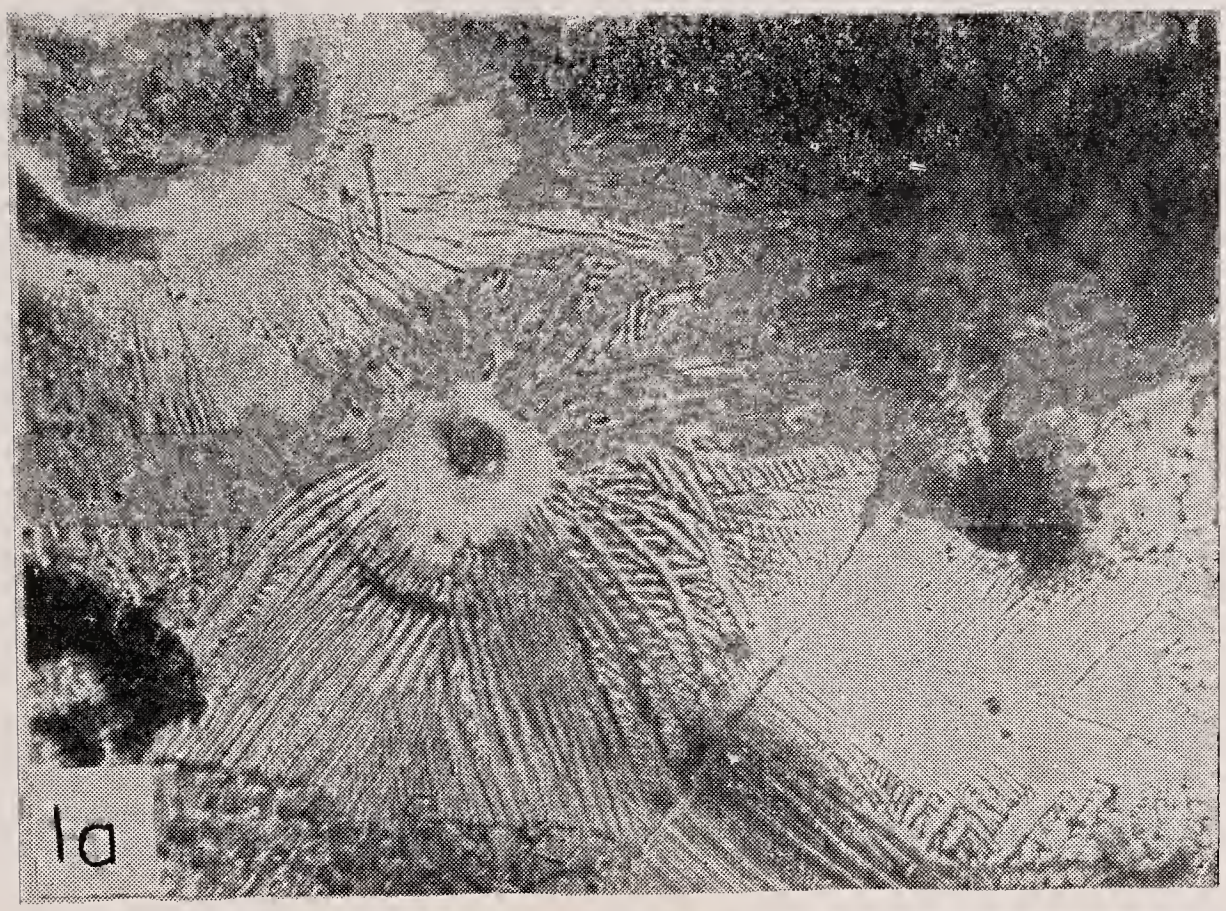

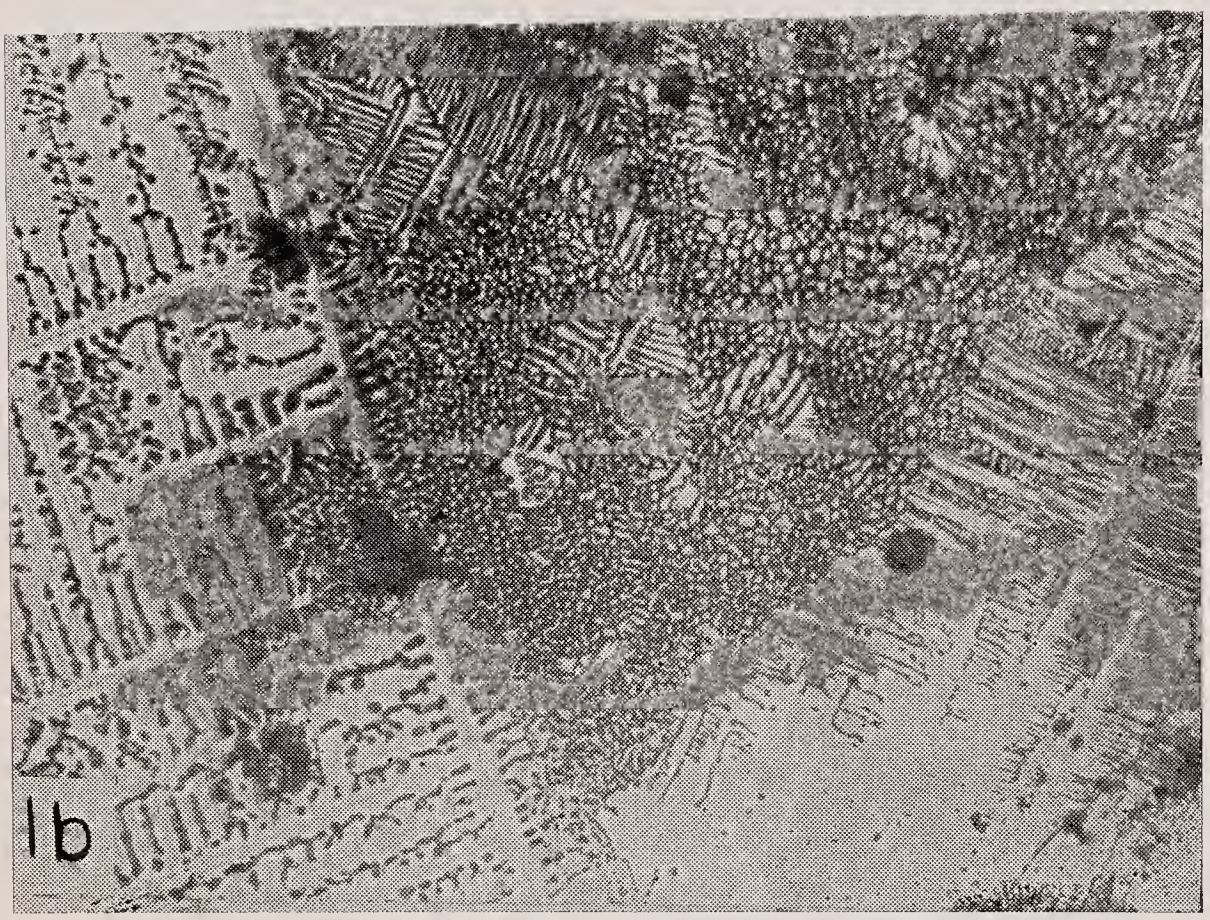

Figure 1. Microstructures in rapidly solidified Sn-0·7 at.% Pb Alloy. **a** Pre-dendritic regions 500 ×. **b.** Dendrites 100 ×.

Plate 2

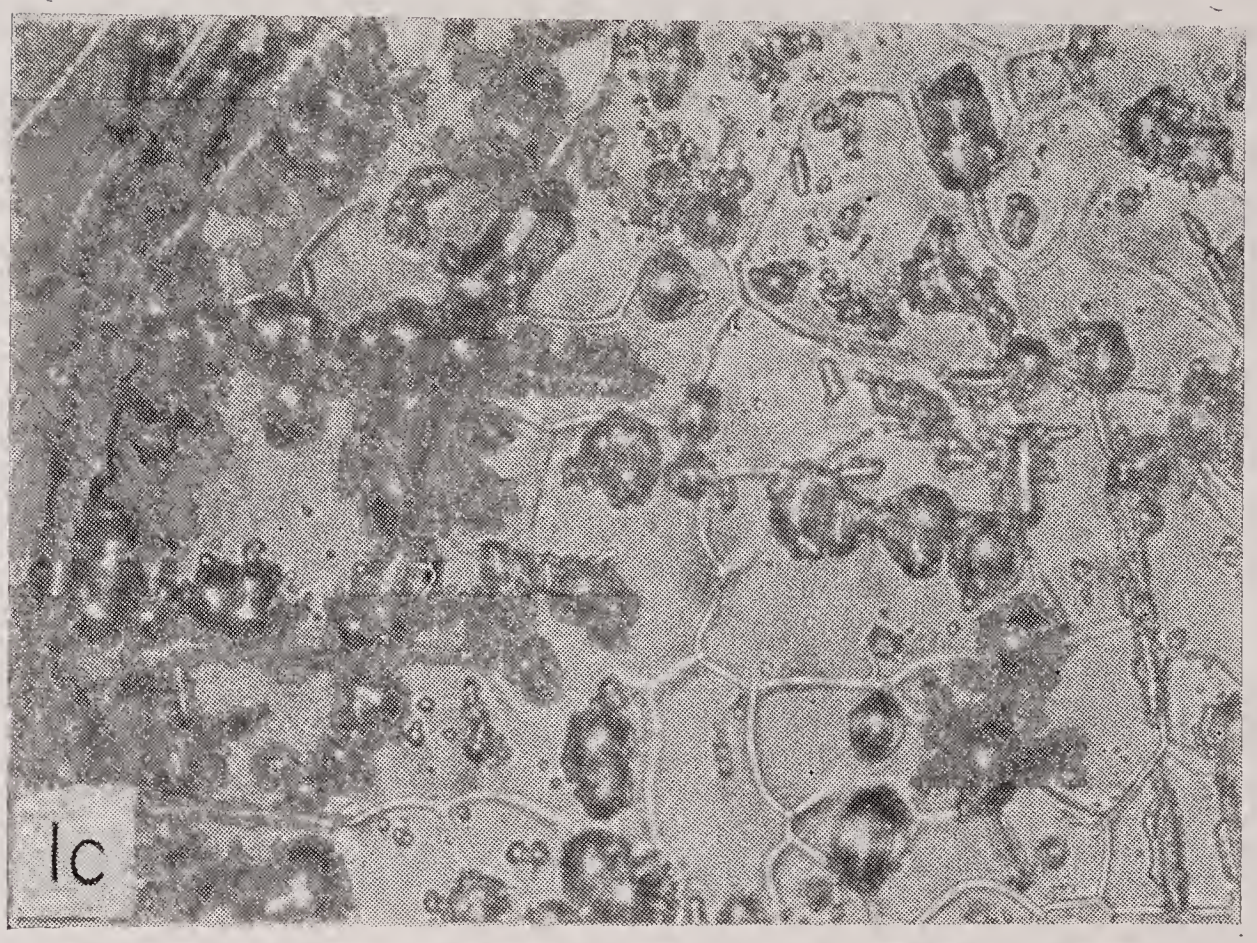

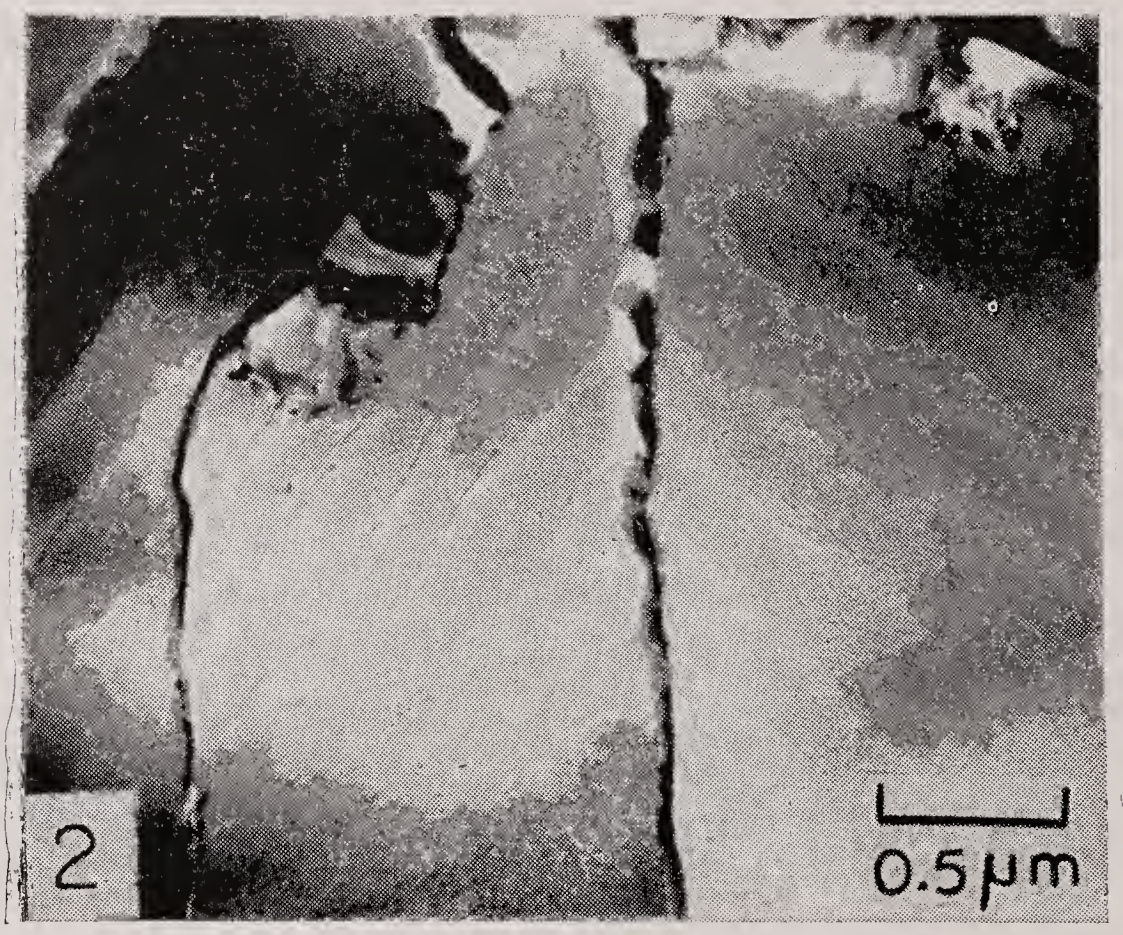

Figure 1c. Microstructures in rapidly solidified Sn-0·7 at.% Pb alloy. Granular regions with precipitates 1000 ×

Figure 2. Twinned dendrites in an Al-1·3 at.% Ni alloy

Plate 3

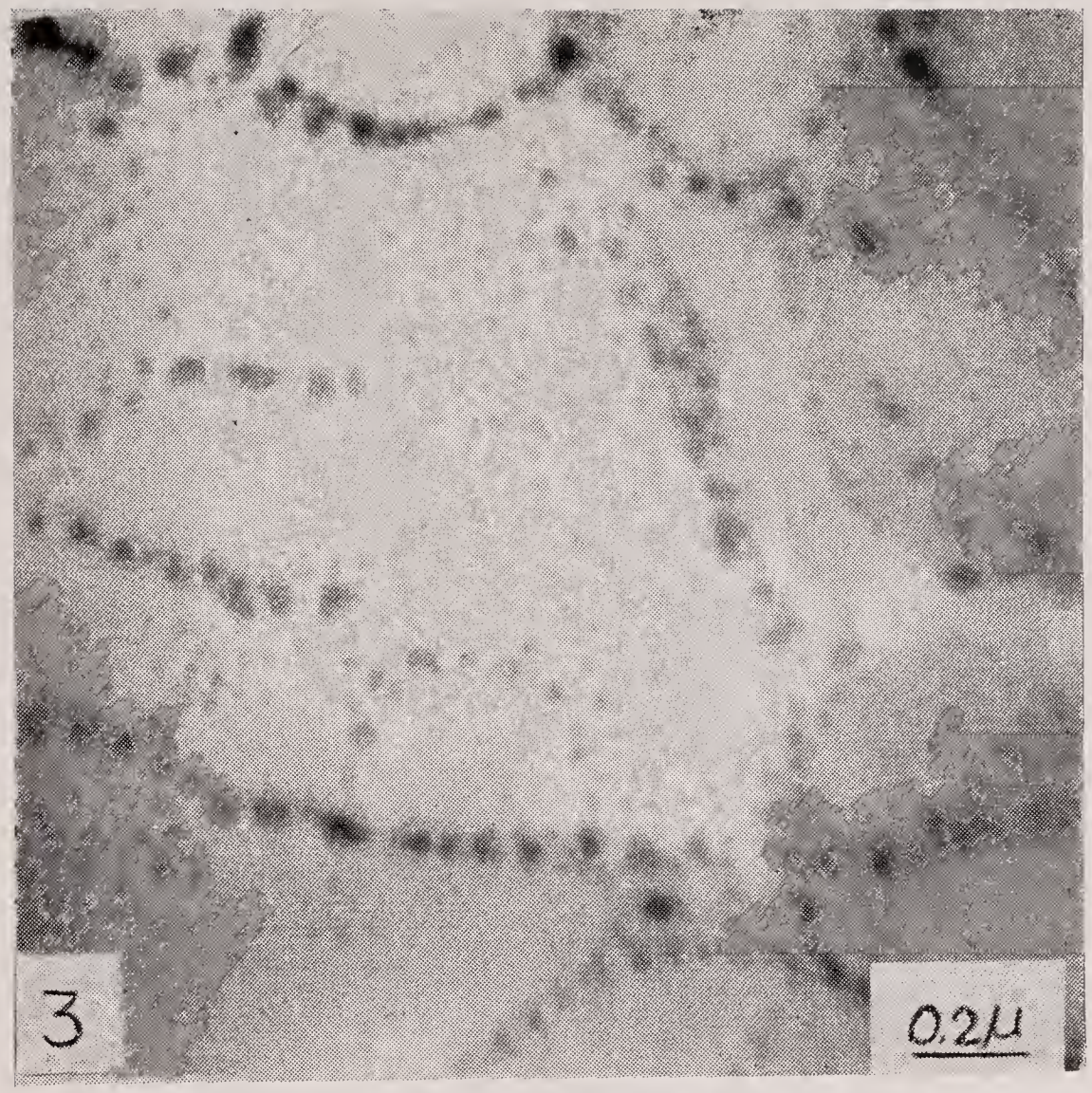

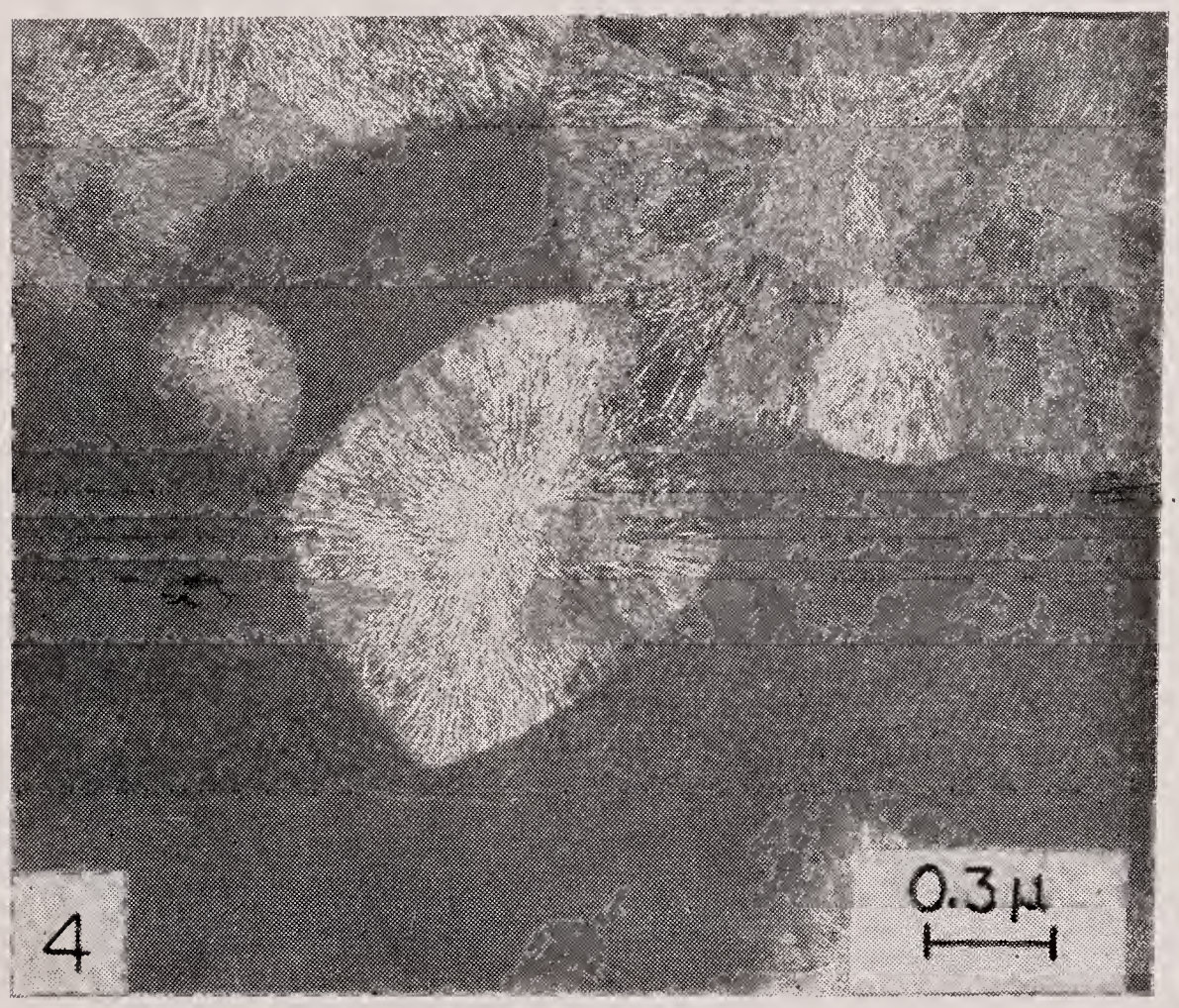

Figure 3. Fine distribution of Cd in the aluminium matrix of a hypomonotectic Al-Cd alloy

Figure 4. Partially crystallized Metglas-2826 aged at 623 K for 4 hr

Plate 4

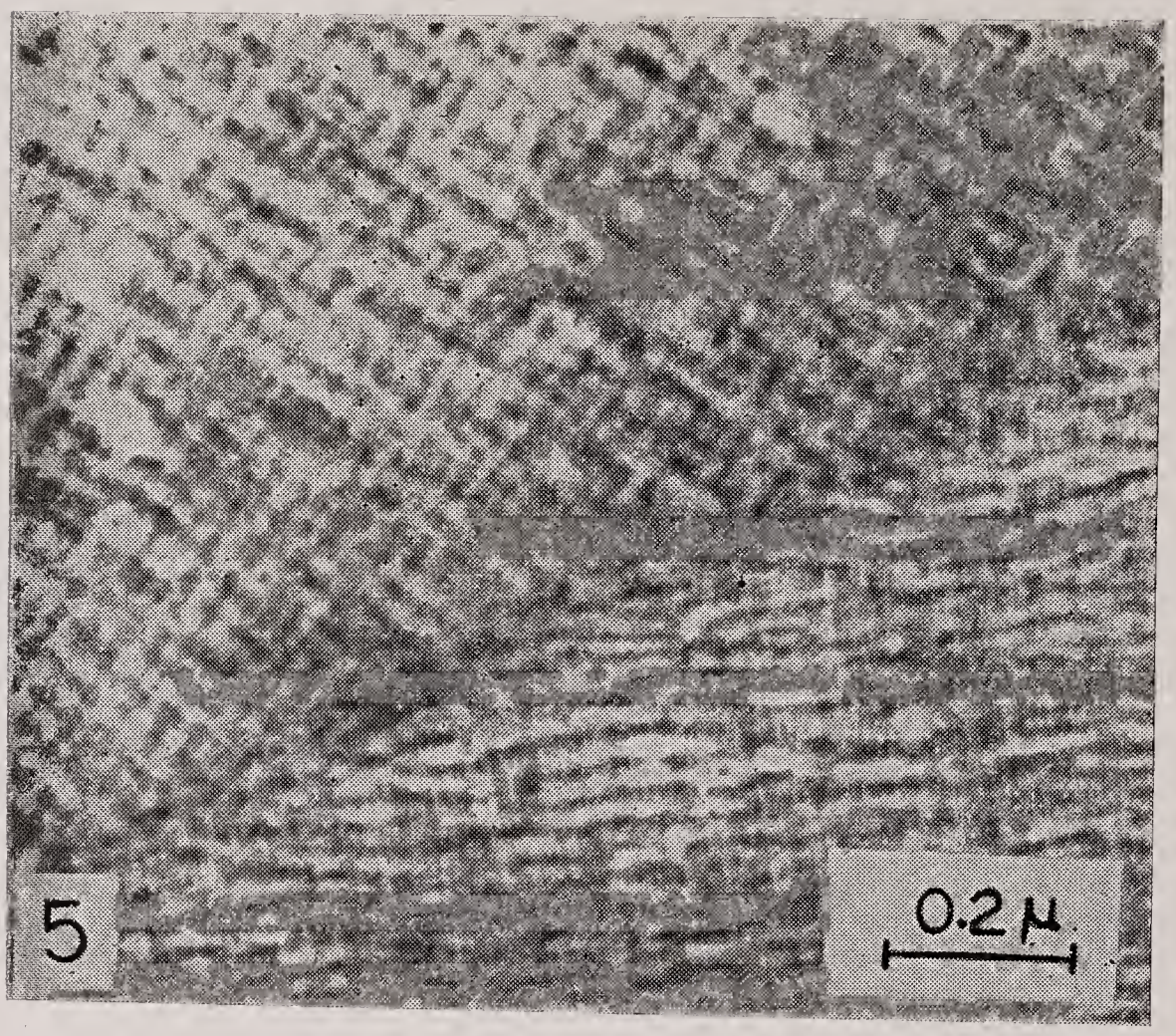

Figure 5. Co-3 wt % Ti-2 wt % Fe aged at 873 K for 96 hr. Spinodally transformed

Plate 5

Figure 6. Ni-20% W aged at 1213 K for 100 hr perpendicular twins
Figure 7. Ni-20% W aged at 1103 K for 30 min: Mosaic domain structure

New developments in carbon and alloy steels

V RAMASWAMY and V RAGHAVAN*
Steel Authority of India Limited, Research and Development Centre, Ranchi 834 002
*Department of Applied Mechanics, Indian Institute of Technology,
New Delhi 110 016

MS received 19 May 1980

Abstract. Recent developments in carbon and alloy steels outlined in this paper include those pertaining to low-carbon mild steels, high-strength low-alloy (HSLA) steels, dual-phase steels, low-carbon bainitic steels, ultrahigh strength steels and ferritic stainless steels. The factors that improve the cold-forming characteristics of low carbon sheets and strips are outlined. The physical metallurgy principles governing the ferrite grain refinement in HSLA steels are discussed, pointing out how it can be achieved by the controlled rolling process. The importance of sulphide shape control in imparting the necessary through-thickness ductility in HSLA steels is discussed and the various methods available for inclusion shape control are outlined. Improved formability coupled with adequate strength characterizes the dual-phase steels. Among the ultrahigh strength steels, two recent developments, *viz.* TRIP steels and maraging steels are outlined. It is pointed out how the improved formability of ferritic stainless steels is making them compete with the more expensive austenitic stainless steels. The scope for future developments in these steels is discussed at the end.

Keywords. Mild steels; alloy steels; stainless steels; new developments; high-strength low-alloy steels; dual phase steels; low-carbon bainitic steels; ultrahigh strength steels; ferritic stainless steels; cold-forming; sulphide shape control.

1. Introduction

In the past decade or so, considerable progress has been made in the development of newer varieties of carbon and alloy steels for specific end uses. This upsurge of interest has been brought about both by scientific advances, which have made available sophisticated instruments like the transmission electron microscope, the scanning electron microscope and the electron probe microanalyser, and by market trends which dictated the need to develop new high-strength steels with adequate toughness. These steels possess many desirable properties such as high yield strength, good weldability, adequate cold-forming ability and good fracture resistance.

The physical metallurgy principles governing alloy development and our increased knowledge of the interrelationship between microstructure and mechanical properties have enabled us to meet stringent property requirements in these steels. Considerable work has been carried out to quantify the contributions of the various strengthening methods involved in the development. For example, it is known that solid solution strengthening, grain-size refinement, dislocation strengthening, texture hardening, precipitation hardening and dispersion strengthening all contribute to the increase in the yield strength of high strength low alloy (HSLA) steels. It is the

purpose of this paper to review the new developments that have taken place in the controlled making, shaping and treating of these steels.

The steels that will be discussed here include low-carbon mild steels, high-strength low-alloy steels, dual-phase steels, low-carbon bainitic steels, ultra-high strength steels and ferritic stainless steels. While discussing HSLA steels, special attention is paid to the development of fine ferrite grain size and inclusion shape control. The discussion on ultra-high strength steels includes TRIP steels and maraging steels. Dual-phase steels are still in a promising state of development. The discussion on ferritic stainless steels points out how the newer steel-making techniques such as argon oxygen decarburization and vacuum-oxygen decarburization help in attaining improved formability and good corrosion resistance.

2. Low-carbon mild steels

2.1 *The basic composition*

Low-carbon mild steels are produced largely in the form of sheet or strip in cold-rolled or annealed condition. These steels invariably exhibit the discontinuous yield phenomenon and require a final temper rolling treatment to remove it. The basic composition is about 0·1% carbon and 0·3–0·4% manganese. The low carbon content is necessary to impart adequate formability. The manganese content is restricted to an amount which will form globular manganese sulphide (MnS) particles so as to prevent the formation of iron sulphide (FeS) films, which result in hot shortness. The sulphur content should also be kept low, to reduce the nonmetallic inclusion content for good cold formability.

2.2. *Cold forming characteristics*

The main cold forming processes are: deep drawing, stretch forming and bending. Great strides have been made in understanding the various factors which improve the ability of these steels to be cold formed (Blickwede 1968; Duckworth & Baird 1969; Pickering 1971). In order to get good cold-forming characteristics, it is essential to have:

(i) a high value of the plastic anisotropy parameter R,
(ii) a high value of the work-hardening exponent n,
(iii) high uniform elongation,
(iv) high elongation at fracture, and
(v) a low yield strength.

Aluminium-killed steels usually exhibit R values of 1·4 to 1·8, if processed under carefully controlled conditions. Aluminium content of 0·02–0·05% is very important in promoting the right texture to impart the necessary deep drawing characteristics. Finely dispersed aluminium nitride particles are believed to be responsible for the development of the preferable $\{111\}$ texture. It has been found difficult to produce rimming steels with R values consistently higher than 1·3, but open-coil annealing, which can remove the interstitials, has some possibilities (Blickwede 1968). Other

additions such as titanium (Blickwede 1968), copper (Rickett & Leslie 1959) and phosphorus (Wacquez & van Daele 1967) also impart high R values. Titanium can eliminate strain ageing tendencies when present in sufficient quantities to lock up all the carbon and nitrogen in the steel. It has also been shown that increasing the ferrite grain size increases the R value.

Among the other factors listed above, the work hardening exponent n increases with increasing grain size. The presence of second-phase particles such as sulphides, oxides and carbides decreases the elongation at fracture. The yield stress follows the well-known Hall-Petch relationship, increasing linearly with the reciprocal of the square root of the grain diameter. So, a low yield stress is obtained with a large grain size. However, the grain size cannot be increased beyond 50 μm or so, if the surface appearance of the sheet or strip is to be preserved.

3. High-strength low-alloy steels

During the last 15 years, great progress has been made in the development of HSLA steels. These steels satisfy requirements such as a high yield strength (for good load-bearing capability), formability, weldability, fatigue resistance, toughness and adequate corrosion resistance. High strength and formability are conflicting requirements and to balance all these properties, a quantitative knowledge of the property-structure correlations is essential. The development of these steels has been accomplished by controlled rolling practices and also by effective utilization of microalloying elements such as Nb, V and Ti (Pickering 1977). The steels developed by different steel companies abroad and by the Rourkela Steel Plant along with their mechanical properties are listed in table 1.

3.1 *Ferrite grain refinement*

The high yield strength of microalloyed steels is partly achieved by grain refinement of the polygonal ferrite matrix (Gray 1972). The ferrite grain size resulting from the transformation of austenite to ferrite strongly depends on the initial grain size of austenite as the ferrite grains nucleate at the austenite grain boundaries. A fine austenite grain size provides more potential nucleation sites for ferrite. Therefore, it is essential that a fine austenite grain size is maintained and grain growth is prevented. Microalloying elements such as Nb, V or Ti cause fine carbide particles to form (Gray & Yeo 1968; Gray 1973). These particles interact with the austenite grain boundaries and alter the grain coarsening characteristics of austenite. Any tendency of an austenite grain boundary to move away from a carbide particle leads to a local increase in the grain boundary energy. Consequently, these particles have a pinning effect on the migrating boundary, which slows down the rate of both recrystallization and grain growth of austenite during hot rolling. This retardation occurs at temperatures below about 1050°C. During rolling below this temperature, the austenite grains elongate in the rolling direction and remain in the elongated state, as ferrite grains nucleate at the grain boundaries. The ferrite nucleation is promoted, as the grain boundary area of the elongated grains is somewhat greater. In addition, the ferrite also nucleates within the deformed austenite grains (Priestner 1974). There is also some evidence for ferrite nucleation on the surfaces of the second phase

Table 1. Typical composition and mechanical properties of HSLA steels

Steel	Composition											Mechanical properties		
	C	Mn	P	S	Si	Al	Nb	V Min	Ni	N Min	Mo	Y. S MN m^{-2}	T. S MN m^{-2}	Elongation %
Van 80 (Jones & Laughlin USA)	0·18	1·5	0·04	0·025	0·6	0·02		0·05		0·005		550	655	18
Maxiform 80 (Republic Steel, USA)	0·09	1·6	0·015	0·03	0·6	0·02	0·06	—	—	—	—	550	620	18
Molycorp X-70 (USA)	0·04	1·69	0·016	0·01	0·02	—	0·06	—	—	—	0·25	545	665	31
August Thyssen Hutte (WG)	0·12	1·6	0·035	0·03	0·5	0·02	0·02	—	—	—	—	420	520	22
British Steel Hyplus 23 (UK)	0·18	1·40	0·05	0·05	0·5	—	0·10	—	—	—	—	355	494	20
Italsider X-70 (Italy)	0·05	1·45	0·02	0·014	0·02	—	0·045	—	0·3	—	0·2	500	628	36
Nippon Steel X-70 (Japan)	0·08	1·75	0·009	0·003	0·11	0·039	0·047	—	0·2	—	0·25	560	707	39
Rourkela Steel Plant (India)	0·14	1·0	0·03	0·03	0·06	—	0·03	—	—	—	—	420	550	22

particles. Thus, optimum ferrite grain refinement occurs in a steel containing fine deformed austenite grains with dispersions of fine second-phase particles. Heavy deformation and a low-finish rolling temperature are essential for effective grain refinement. The finishing temperature in controlled rolling is about 700–750°C, as compared to 900–950°C in the conventional rolling (Korchynsky & Stuart 1970). However, if too low a finish-rolling temperature is used, the transformed ferrite is deformed and incompletely recrystallized (Pickering 1977). This results in inferior properties, as the impact transition temperature is raised due to this, as shown in figure 1 (Melloy & Dennison 1973).

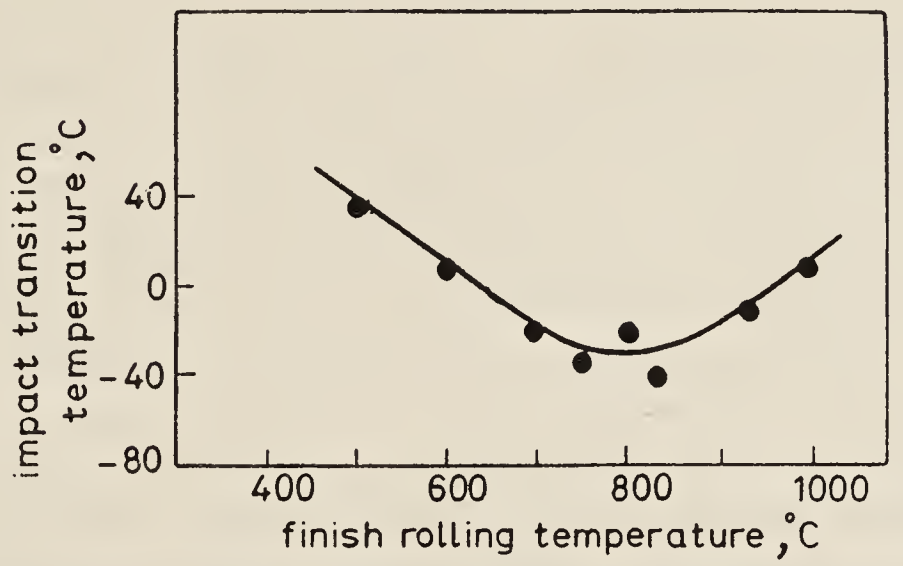

Figure 1. Effect of finish rolling temperature on the impact transition temperature of an HSLA steel.

In the earlier years, controlled rolling was done up to 12 mm thick plates. Considerable difficulty was experienced in controlled rolling of thicker plates. Due to the larger temperature difference between the surface and the centre of such thick plates, a mixed grain structure was obtained, the centre having the coarser grains. This resulted in inferior properties. The problem was overcome by adding more than one grain-refining microalloying element to the steel. Both niobium and vanadium were added to ensure that the grain size at the centre was also fine. The overall composition of the steel was suitably adjusted to preserve the good welding characteristics. HSLA steel plates of varying thicknesses are in commercial production in the Rourkela Steel Plant, using the controlled rolling practice.

Figure 2 (plate 1) is the optical micrograph of an HSLA steel depicting the fine ferrite grains. The thin-foil electron micrograph in figure 3 (plate 1) depicts row precipitates resulting from the precipitation of NbC at the austenite-ferrite interface during the transformation to ferrite. Table 2 summarizes the ferrite grain sizes obtained in different products through various production routes (Gladman *et al* 1977).

Table 2. Typical ferritic grain sizes obtained in various products

Product	Grain size μm
Thick plate	8 to 10
Thin plate	5
Normalized plate and bar	5
Strip	3 to 4
Best Laboratory normalized plate (1975)	3 to 4
Best Laboratory controlled rolled plate (1975)	1 to 2

3.2 *Contributions to strength and impact resistance*

So far, the discussion has been about how controlled rolling of high-strength steels gives fine ferrite grain size. Recently, using regression analysis, expressions have been derived to assess quantitatively the contributions to the strength of HSLA steels through various strengthening mechanisms that are operative. The yield stress σ_y of the controlled-rolled steel can be written as

$$\sigma_y = \sigma_i + k\, d^{-1/2} + \sigma_{ppt} + \sigma_{ss} + \sigma_{disl} + \sigma_{text},$$

where σ_i is the lattice friction stress, σ_{ppt} is the precipitation strengthening, σ_{ss} is the solid solution strengthening, σ_{disl} is the dislocation hardening, and, σ_{text} is the texture hardening. $k\, d^{-1/2}$ represents the grain size contribution to the yield strength, k is the Hall-Petch constant and d is the mean ferrite grain diameter. The fine grain size increases the yield strength, as the ferrite grain boundaries provide obstacles to dislocation motion. Nondeformable carbide particles can contribute effectively to the yield strength and this contribution can be evaluated using the Ashby-Orowan formula (Gladman *et al* 1971). The hardening contribution depends on the volume fraction and size of the carbide particles; it increases with increasing volume fraction and with decreasing particle size. Solid solution strengthening depends on the size difference between the solute and the solvent and the concentration of the solute, increasing with increasing size difference and solute concentration. It is possible to calculate reasonably accurate values for dislocation hardening (Little *et al* 1973) by measuring dislocation densities using the transmission electron microscope. Keh (1965) gave the following relationship between the flow stress σ_f and the square root of dislocation density ρ,

$$\sigma_f = \sigma_i + 0{\cdot}38\, G\, b\, \sqrt{\rho},$$

where G is the shear modulus of the matrix and b is the Burgers vector of the dislocations.

Morrison (1975) reported the following contributions to the yield strength of an HSLA steel of composition 0·13% C, 0·30% Si, 1·4% Mn and 0·03% Nb, commercially controlled-rolled to 9·5 mm thick plates at a finish rolling temperature of 650°C:

$$\sigma_y\,(550\ \mathrm{MN\ m^{-2}}) = \sigma_i\,(32) + \sigma_{ss}\,(135) + \sigma_{ppt}\,(35) + \sigma_{text}\,(45) + \sigma_{disl}\,(43) + kd^{-1/2}\,(260).$$

The dominant contribution of grain size to the yield strength is evident. The contribution from precipitation can be increased, if titanium is used in preference to niobium. Due to the greater solubility of titanium as compared to niobium, a higher degree of supersaturation is obtained, which promotes the formation of a larger volume fraction of carbide particles. The contributions to the strength of the crystallographic texture and the dislocation density become apparent only at low finish rolling temperatures, as illustrated in figure 4.

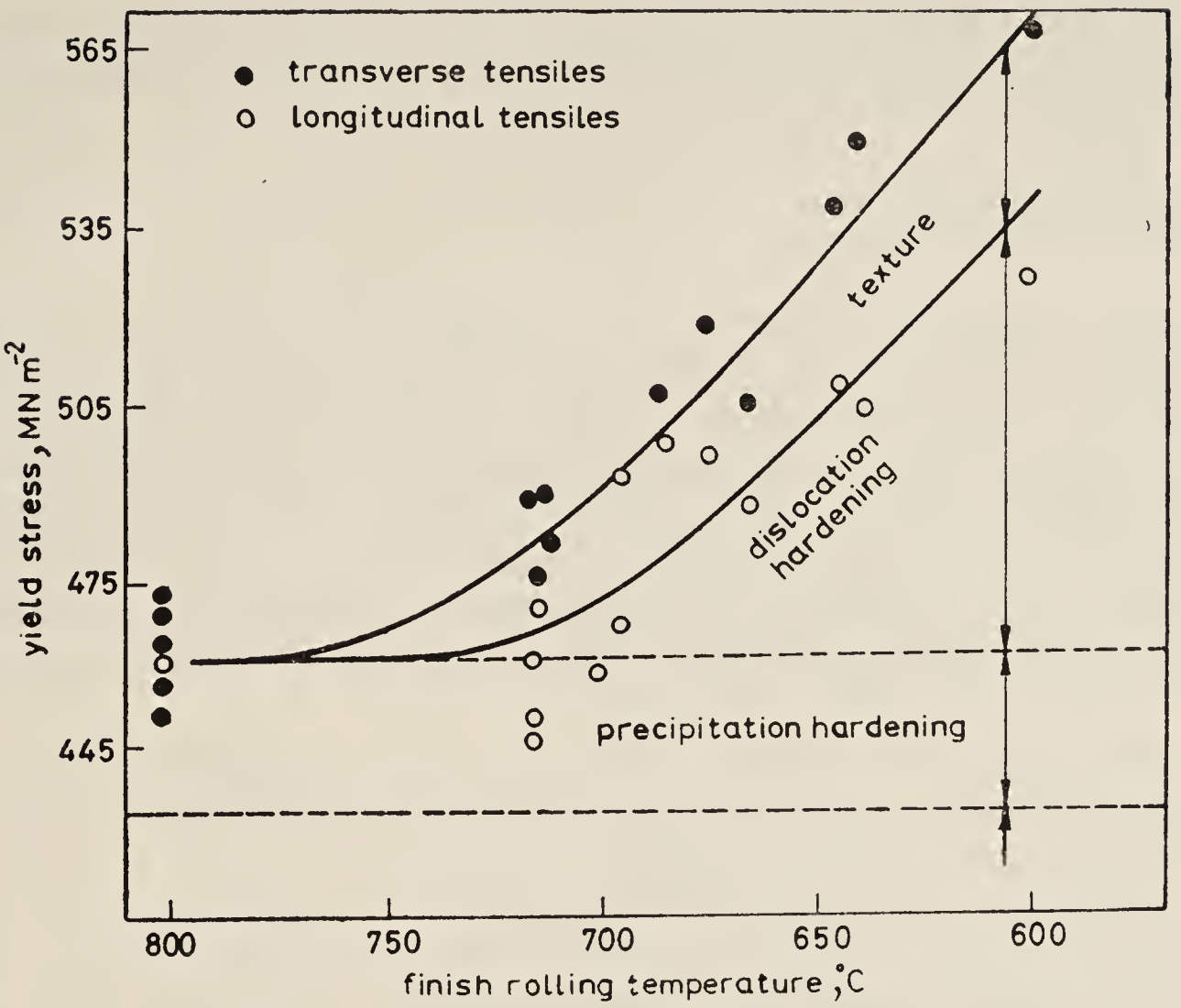

Figure 4. Variation of the yield strength of an HSLA steel as a function of finish rolling temperature.

Table 3 lists the changes in the impact transition temperature of a steel per 10 MN m^{-2} ($\sim$ 1 kgf/mm^2) increase in the yield stress, brought about by both microstructural and compositional parameters (Pickering 1978). It can be deduced from this table that, for obtaining a low-transition temperature, it is desirable to have a low-carbon,

Table 3. Effect of microstructural and compositional parameters on the impact transition temperature of mild steels

Parameter	Change in impact transition temperature °C per 10 MN m^{-2} increase in yield stress
Microstructural	
Pearlite	*
Dislocations	+ 4
Precipitation	+ 2·7
Grain refinement	− 6.7
Compositional	
Phosphorus	+ 35
Nitrogen	+ 20
Carbon	+ 6·7
Silicon	+ 5·3
Manganese	− 3·3
Aluminium**	− 18

*Does not increase the yield stress. 10% pearlite increases the impact transition temperature by 22°C.

**The effect of aluminium is through the removal of free nitrogen by forming aluminium nitride.

high-manganese, aluminium-killed and grain-refined steel. To avoid an undue increase in the hardenability of the steel, the manganese content is generally limited to about 1·5%.

3.3 *Inclusion shape control*

Nonmetallic inclusions are important in controlling the mechanical properties of HSLA steels. In particular, the total ductility at fracture and the charpy shelf energy are influenced by their volume fraction, shape and distribution. The inclusions provide sites for the nucleation of voids, which eventually grow, coalesce and cause fracture. The nucleation of such voids depends on the bonding at the inclusion-matrix interface and the ability of the inclusion to resist cracking. Under adverse circumstances, HSLA steels exhibit lack of through-thickness ductility (Little & Henderson 1971), lamellar tearing during welding (Farrar & Dolby 1971) and splitting during bending.

Hot-rolled steels show a marked anisotropy in the mechanical properties. This anisotropy is caused by an elongation of the inclusions into long flat ribbons. Elongated particles and discontinuous inclusion stringers such as alumina, calcium aluminate or spinel also cause low transverse ductility and premature ductile fracture. As manganese sulphide becomes more plastic than steel with decreasing temperature, the low finishing temperature during controlled rolling may trigger a highly undesirable distribution of sulphide inclusions. To improve the transverse properties, the stringer-type inclusions should be replaced by more isolated and less elongated oxides and sulphides. In most tonnage steels, there is a higher volume fraction of sulphides than oxides; so, controlling the sulphide shape is more important.

Calcium (Hilty & Poop 1969), zirconium (Mihelich *et al* 1971) or rare earth elements (Luyckx *et al* 1970) are added to modify the sulphide shape. These additions cause a decrease in the ability of the inclusions to plastically deform by altering their constitution. In their presence, the inclusions remain as rounded globules rather than deform into elongated particles during rolling.

Calcium additions globurize the alumina-type oxides by forming calcium aluminates and also cause the sulphides (mainly calcium sulphide) to associate with the oxides. Due to its very high vapour pressure, low solubility in steel and great reactivity, calcium is considered difficult to control (Pickering 1974). But recent developments such as injecting the calcium powder deep into the ladle through a plunger have overcome this problem (Forester *et al* 1974; Langhammer *et al* 1977). At present, calcium additions to modify inclusion shape is practised in many plants with good results.

Zirconium is added in sufficient amounts depending on the sulphur, nitrogen and oxygen content of the steel (Korchynsky & Stuart 1970; Arrowsmith 1974). Zirconium can dissolve in manganese sulphide and decrease its plasticity. Sufficient zirconium should be added such that a non-deformable zirconium-manganese sulphide is formed. Because of its great affinity for nitrogen, zirconium cannot be used as a sulphide modifier in steels, whose properties are enhanced by high nitrogen contents. Rare earths form a non-deformable sulphide or oxysulphide. Because of their high affinity for oxygen and sulphur, the amount of rare earths must be sufficient to combine with both these elements. It has been suggested that, for minimum costs, rare earths should be added to steels of an optimum sulphur level, about 0·01%.

The major effect of sulphide modifying additions is to increase the transverse and the through-thickness ductility and the charpy shelf energy to levels comparable to those obtained in the longitudinal direction. The anisotropy of these properties is minimized in this way. Figure 5 shows that the optimum rare-earth/sulphur ratio is 2·0 for minimum anisotropy. Figure 6 shows that the rare-earth additions are more effective than zirconium additions in reducing anisotropy.

3.4 *Uses of HSLA steels*

There are a variety of ways by which the high strength and good toughness properties of HSLA steels can be utilized. Even at a high strength level, HSLA steels possess superior fabricability and this allows high production rates. These steels are currently used for oil pipelines located at sub-zero temperatures. Their high fatigue strength, low cost and good weldability have made them attractive in truck

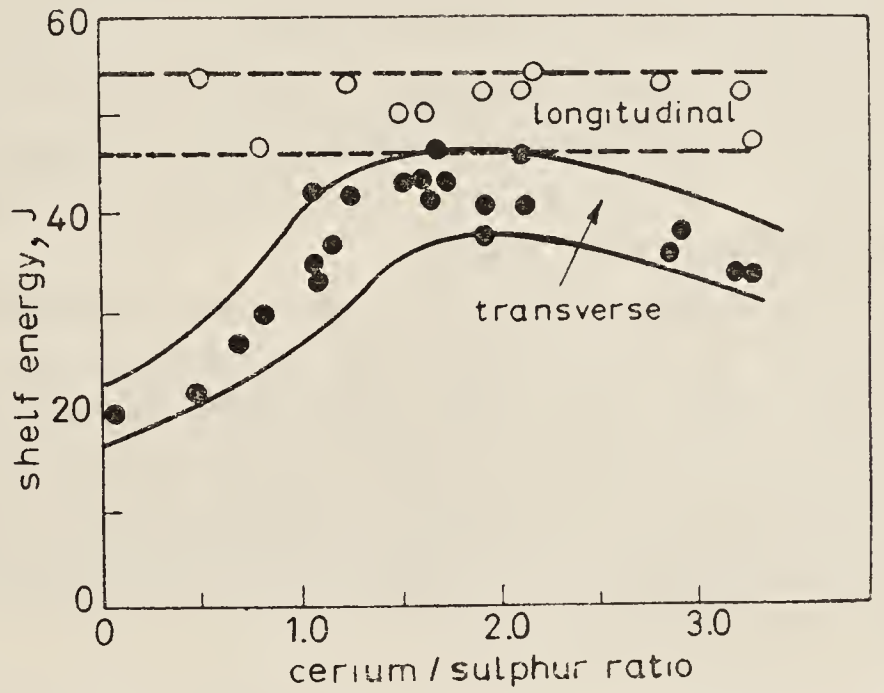

Figure 5. Effect of rare earth additions on longitudinal and transverse charpy shelf energy.

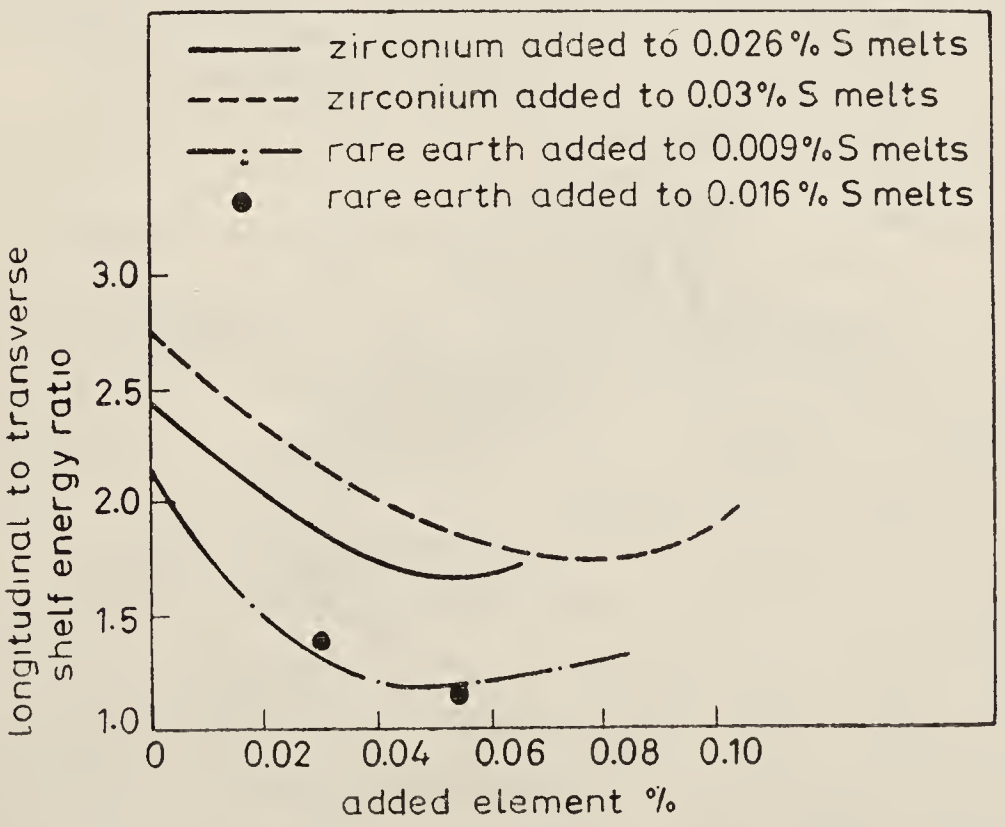

Figure 6. Effect of zirconium and rare earth additions on the anisotropy of charpy shelf energy.

and rail road applications. They are used for large land storage tanks, pipe fittings, valves, bridges, electric transmission poles, off-shore platforms and marine equipment. To meet safety regulations and weight reductions, HSLA steels are increasingly used in the automotive industry in USA, UK, Japan and West Germany.

4. Dual-phase steels

Very recently, dual-phase steels have attracted a good deal of attention among all the HSLA steels, as they offer the highest formability for a given strength level. As the name implies, dual-phase steels consist of a dispersion of two phases, martensite in a ferrite matrix. They are produced by annealing or holding in the two-phase region of austenite and ferrite in the Fe-C phase diagram and then cooling at a sufficiently fast rate to transform the austenite into martensite (Hayami & Furukawa 1977; Rashid 1976; Davies 1978).

The initially developed dual-phase steels were based on the conventional mild steel composition, namely, carbon, silicon and manganese. In these steels, after the annealing in the two-phase region, quenching is necessary to convert the austenite into martensite. Figure 7 compares the elongation-tensile strength relationships for dual-phase steels with those of HSLA steels. The advantage of higher percentage of elongation in the dual-phase steels is evident.

More recently, the composition of dual-phase steels has been modified so that it can be produced directly from the hot strip mill without requiring any further heat treatment (Coldren & Tither 1978). The composition of the low-carbon, low-alloy steel should be such that it exhibits the right transformation characteristics on continuous cooling. On processing through a conventional high speed hot strip mill, the desired ferrite-martensite structure should be obtained in the as-rolled coiled sheet. The required transformation characteristics are:

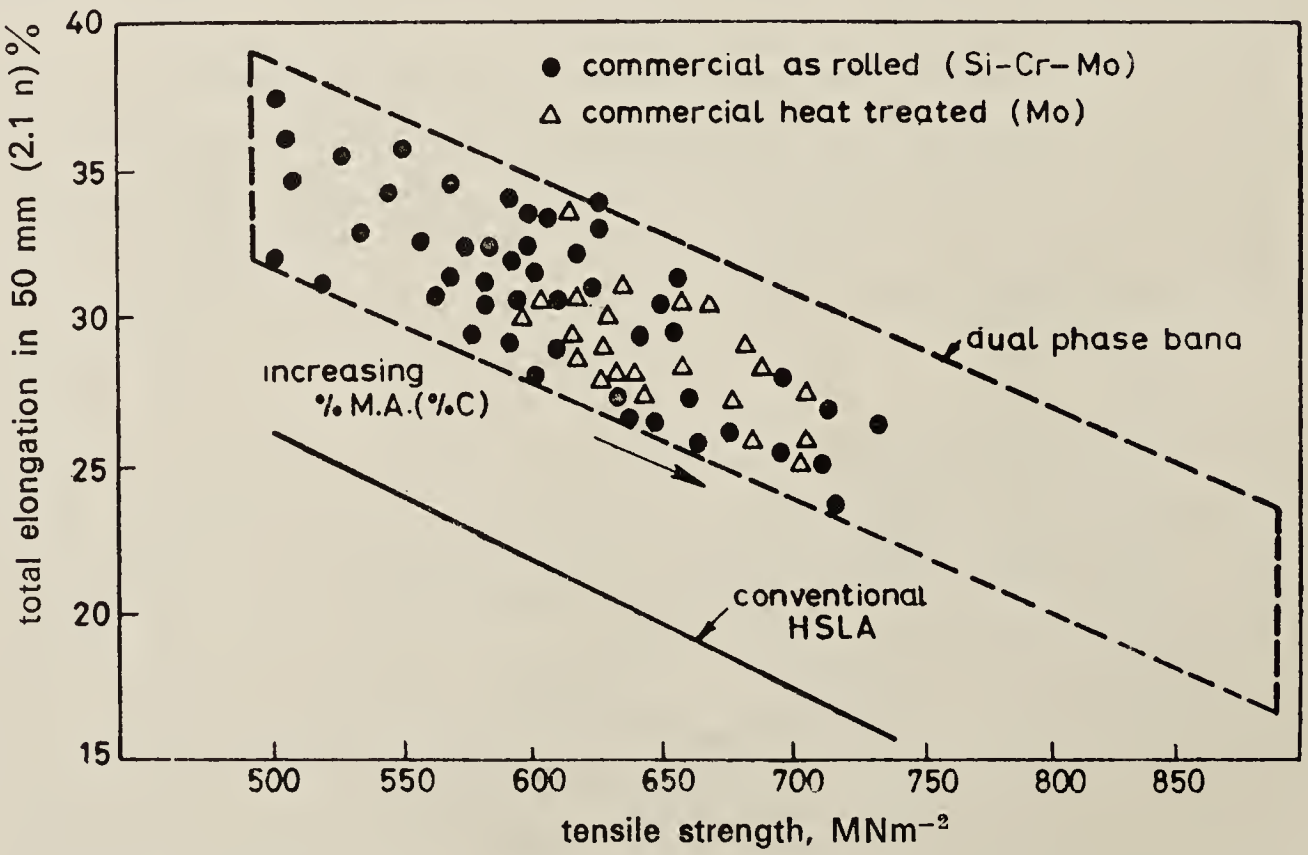

Figure 7. Comparison of the relationship between tensile strength and elongation of dual-phase steels and an HSLA steel.

(i) The ferrite C-curve should be elongated to yield substantial amounts of polygonal ferrite over a wide range of cooling rates;
(ii) the pearlite nose should be suppressed to avoid pearlite formation;
(iii) the pearlite finish temperature should be as high as possible to avoid pearlite formation during cooling to the coiling temperature of about 600°C; and
(iv) there should be a wide gap between the ferrite and the bainite transformation ranges, to provide a wide temperature range within which no transformation is possible.

A typical composition of the low-carbon, low-alloy steel is 0·06%C, 1·2% Mn, 0·9% Si, 0·6% Cr, 0·4% Mo and 0·04% Al, with additions of rare earth elements or zirconium for inclusion shape control. It may be noted that no carbide-forming microalloying elements are present in this steel. The as-rolled coiled product has a yield strength of 450 MN m^{-2}, a tensile strength of 680 MN m^{-2} and an elongation of 24%. This steel is not sensitive to variations in the coiling temperature. As such it is possible to produce this steel in the existing hot strip mills.

In the sheet form, dual-phase steels are finding increasing applications in the automotive industry in USA and Japan. They are also being fabricated into other shapes such as wheel spiders, engine mounts, tie rod couplings and cross members.

5. Low-carbon bainitic steels

In the last two decades, considerable amount of work has been carried out to obtain a wide range of strengths in low-carbon steels with a bainitic structure (Honeycombe and Pickering 1972). For example, in bainitic steels, the yield strengths can range from 450 MN m^{-2} ($\sim$ 45 kg/mm^2) to 900 MN m^{-2}, with adequate impact resistance. The bainitic steels have been developed with the following objectives (Pickering 1967):

(i) A bainitic structure produced by air cooling minimizes the economical and metallurgical disadvantages of quenching and tempering;
(ii) the use of low-carbon steels promotes good weldability and adequate formability;
(iii) a minimum variation in properties over a wide range of section sizes is obtained; and
(iv) an adequate toughness consistent with the strength level is achieved.

To meet the above objectives, it is essential that the polygonal ferrite formation should be retarded in relation to the bainite transformation. The nose of the ferrite C-curve in the isothermal transformation diagram should be pushed substantially to the right. This is brought about by very small quantities of boron in solution in the austenite. Boron is believed to segregate to the austenite grain boundaries and thereby retard the nucleation of ferrite at the boundary. The bainite transformation rate should not be retarded to any great extent, so that bainite is capable of forming over a wide range of cooling rates and thus the transformation to martensite is averted. A flat top of the bainite C-curve is essential, as schematically illustrated in figure 8. All these requirements are met in a steel with 0·10–0·15% carbon, 0·5% molybdenum, 0·7–1·0% manganese and 0·002% boron.

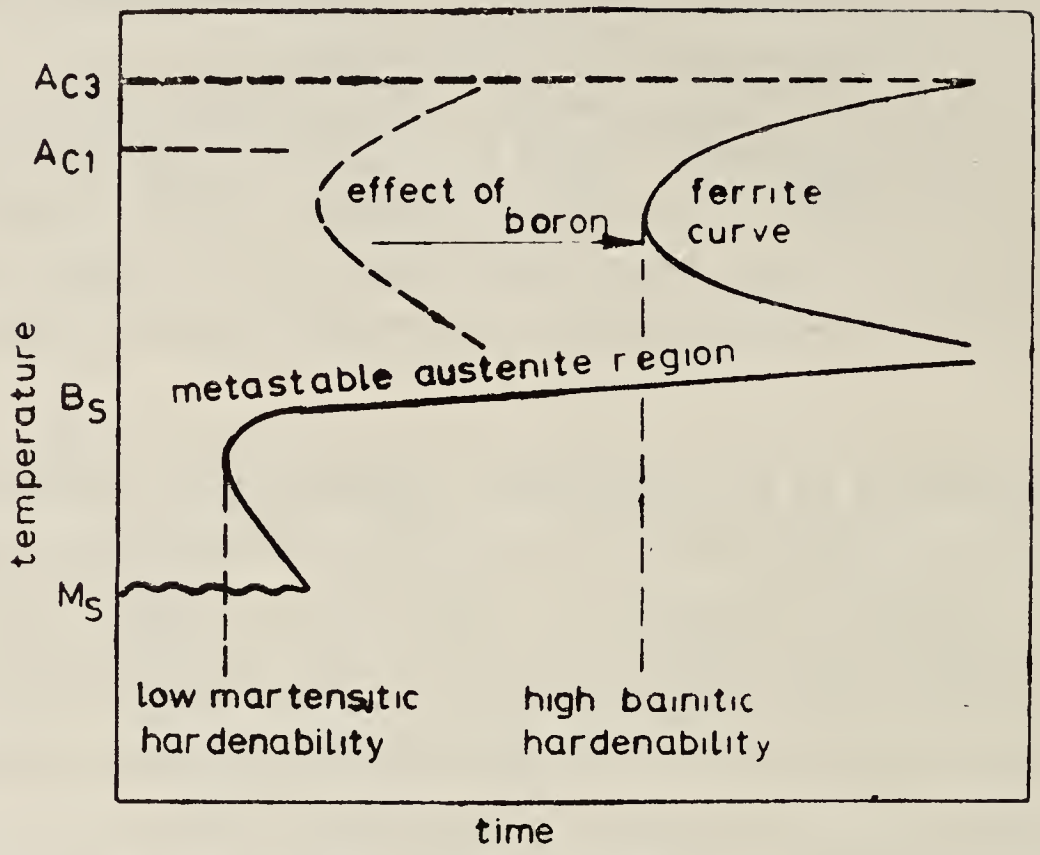

Figure 8. The effect of boron on the isothermal transformation diagram of a low-carbon bainitic steel.

The strengthening mechanisms in the low carbon bainitic steels are the following (Bush & Kelly 1971; Smith & Hehemann 1971):

(i) a fine bainite lath size, which increases the yield strength through the Hall-Petch relationship;
(ii) a high dislocation density within the bainitic laths which increases the flow stress. The dislocation density increases with decreasing bainite transformation temperature; and
(iii) a fine carbide dispersion which gives rise to precipitation hardening.

It is anticipated that low-carbon bainitic steels will have a potential market and that improvements will be forthcoming. Low-carbon steels (0·02–0·08% C) with manganese contents upto 4·5% have very attractive properties and may offer a more economical alternative to the complex and more highly-alloyed bainitic steels with expensive alloying elements (Durbin & Krake 1973; Terazawa *et al* 1971). The cooling rate required to produce the bainitic structure free from polygonal ferrite decreases with increasing manganese content. However, higher manganese contents create weld cracking problems (Pickering 1978).

The actual and potential applications of bainitic steels include pressure vessels, boilers, gas and oil pipelines, earth-moving equipment and engine mounts.

6. Ultra-high strength steels

In the previous sections, we have described steels with yield strengths of upto 750 MN m^{-2}. These steels possess relatively simple microstructures and involve inexpensive manufacturing routes. Ultrahigh strength steels may be defined as those having yield strengths greater than 1250 MN m^{-2}. Correspondingly, more complicated production routes are involved, with specific thermal or thermomechanical treatments. A large number of quenched-and-tempered steels are now known (May *et al* 1976).

We will limit our discussion here to two recent developments, in which a good understanding of the physical metallurgy principles involved has yielded successful results.

6.1 *TRIP steels*

The word TRIP stands for transformation induced plasticity (Zackay 1969). The composition of a TRIP steel is so adjusted that the martensitic start M_s temperature is below room temperature, but the deformation-induced martensitic start M_d temperature is above room temperature. First, the steel is deformed above the M_d temperature, where austenite is stable to deformations. Typically, the deformation given is heavy, ~80%. The deformation produces the right degree of metastability that permits the strain-induced transformation of austenite to martensite at small plastic strains at the operative service temperature, which is below M_d but above M_s. The plastic strain at the tip of a growing crack induces the phase transformation, which in turn increases the work hardening rate and enlarges the plastic zone size. Consequently, the fracture toughness of these steels turns out to be excellent.

A typical composition of the TRIP steels is 0·25% carbon, 2% manganese, 2% silicon, 8% nickel, 9% chromium and 4% molybdenum. After the appropriate thermomechanical treatment, this steel can achieve ayield strength of 1400 MN m^{-2}, an elongation of 50% and a fracture toughness (K_{Ic}) of 200 MN $m^{-3/2}$. The cost of TRIP steels is high and they are useful only in specialized applications, such as rocket vehicle skins, high-strength fasteners and cables (Dulis & Chandhok 1969).

6.2 *Maraging steels*

The development of maraging steels is another method of improving fracture toughness and ductility at a high level of strength. These steels are based on low-carbon high-alloy austenites, which transform on cooling to lath martensite, with a very high and uniform dislocation density. The base composition is typically Fe-18% Ni. 3–8% each of cobalt and molybdenum, with minor amounts of aluminium and titanium are added to the base composition. The function of these substitutional alloying elements is to form fine precipitates of intermetallic compounds on ageing. The compounds have been typically identified as Ni_3Mo and $Ni_3(A1Ti)$. These compounds precipitate at a relatively low ageing temperature, presumably aided by the high dislocation density in the lath martensitic structure (Kelly & Nicholson 1970). In some maraging steels, a bewildering variety of precipitates have been identified (Floreen 1968). But it is generally accepted that the two strengthening mechanisms involved are the formation of small ordered regions and the fine dispersion of precipitates of intermetallic compounds.

Maraging steels find applications where high strength combined with excellent toughness is required and where cost is not a major consideration. Typical applications include military bridges, rocket casings and other aerospace applications.

7. Ferritic stainless steels

The distinguishing properties of stainless steels are their excellent corrosion resistance,

high temperature creep strength and oxidation resistance. The fabrication characteristics from the point of view of both hot and cold working, adequate weldability and other mechanical and physical properties are the factors that must be considered in the selection of a stainless steel for a particular application.

The stainless steels comprise four major categories:

(i) martensitic stainless steels,
(ii) austenitic stainless steels,
(iii) ferritic stainless steels, and
(iv) controlled transformation stainless steels.

Martensitic stainless steels are oil-quenched or air-cooled to obtain the martensitic structure at room temperature. The carbon content in these steels may vary from 0·1 to 1·0%. Austenitic stainless steels have both chromium and nickel to ensure the presence of the austenitic phase at room temperature. They have a low carbon content to prevent the precipitation of chromium carbide at the grain boundaries and the consequent intergranular corrosion. Ferritic stainless steels have ferrite as the stable phase at all temperatures and so they cannot be heat-treated. Generally, the formability characteristics of ferritic steels is poor as compared to the austenitic steels. Controlled transformation stainless steels are those in which typically a precipitation process is suitably controlled to obtain the optimum mechanical properties.

During recent years, several new developments have taken place in all groups of stainless steels. As an example, it is intended here to outline the recent developments in ferritic stainless steels (Pickering 1976; Schmidt & Jarleborg 1974; Meditta & Ramaswamy 1976).

The composition and mechanical properties of some typical ferritic stainless steels are given in table 4. The formability characteristics of the conventional ferritic steels such as AISI 405, 430 and 446 are quite inferior. One of the major developments has been to improve the formability of ferritic stainless steels. This is achieved by improving the microcleanliness of the steels and by reducing the interstitial content. A reduction in the level of sulphur and silicon improves the microcleanliness (Bricker and Spaeder 1972; Davison 1974). By lowering the level of the interstitial elements such as carbon and nitrogen from 1000–2000 ppm to 50–150 ppm, it is possible to improve several properties including formability (Davison 1974). With the above reduction, the plastic anisotropy factor R is increased to 1·44, which is

Table 4. Typical compositions and mechanical properties of ferritic stainless steels

Designation	Composition (wt%)							Mechanical properties		
	C	Si	Mn	Cr	Al	Mo	Ti	Y.S. MN/m²	T.S. MN/m²	Elongation %
AISI 405	0·06	0·25	0·40	13·5	0.2		—	280–380	400–540	20–30
AISI 409	0·06	0·25	0·40	11·0	—	—	0·4	250–280	450–480	25–30
AISI 430	0·06	0·40	0·40	17·0	—	—	—	280–450	450–580	20–35
AISI 442	0·08	0·25	0·40	21·0				310–420	520–580	20–30
AISI 446	0·08	0·25	0·40	25·0				340	550	23
18–2	0·02	0·40	0·40	18·0	—	2·0	—	340	550	40
E-Brite 26–1	0·02	—	—	26·0	—	1·0	—	345–400	496–552	28–40

comparable to that of aluminium-killed low-carbon steel (see § 2.2). New production techniques such as argon-oxygen decarburization (AOD), vacuum-oxygen decarburization (VOD) and electron beam refining have made such improvements possible in the chemistry of the ferritic stainless steels. These minor but vital modifications in chemistry have been exploited by a number of steel companies and more than thirty new grades are now available. The latest in the series is called the extra low interstitial (ELI) stainless steel. The ELI grade has superior intergranular corrosion resistance, formability, weldability and resistance to ribbing (a surface defect caused by carbide bands) and roping (markings like those produced by discontinuous yielding, see § 2.1). Figure 9 depicts the decrease in the critical current density of a ferritic stainless steel for passivation, with reduction in carbon content. Current developments centre around the basic compositions of 18Cr-2Mo and 26Cr-1Mo. It is well known that molybdenum is particularly beneficial in imparting resistance to pitting corrosion in environments containing chloride ions.

By virtue of their low cost, ferritic stainless steels with improved properties are gradually replacing the more expensive austenitic stainless steels in a variety of applications. These include houseware such as washing machine tubs, transportation uses in passenger cars and railway coaches, applications in the chemical and food industry and in the nuclear and power industry.

8. Future developments

The key factor in the development of fine grained ferrite in HSLA steels has been the microalloy carbides precipitated during controlled rolling. The development of these steels has been mostly due to empirical work. If the underlying processes of nucleation and growth during precipitation and recrystallization and the mutual interaction between the two transformation processes are well understood, there is

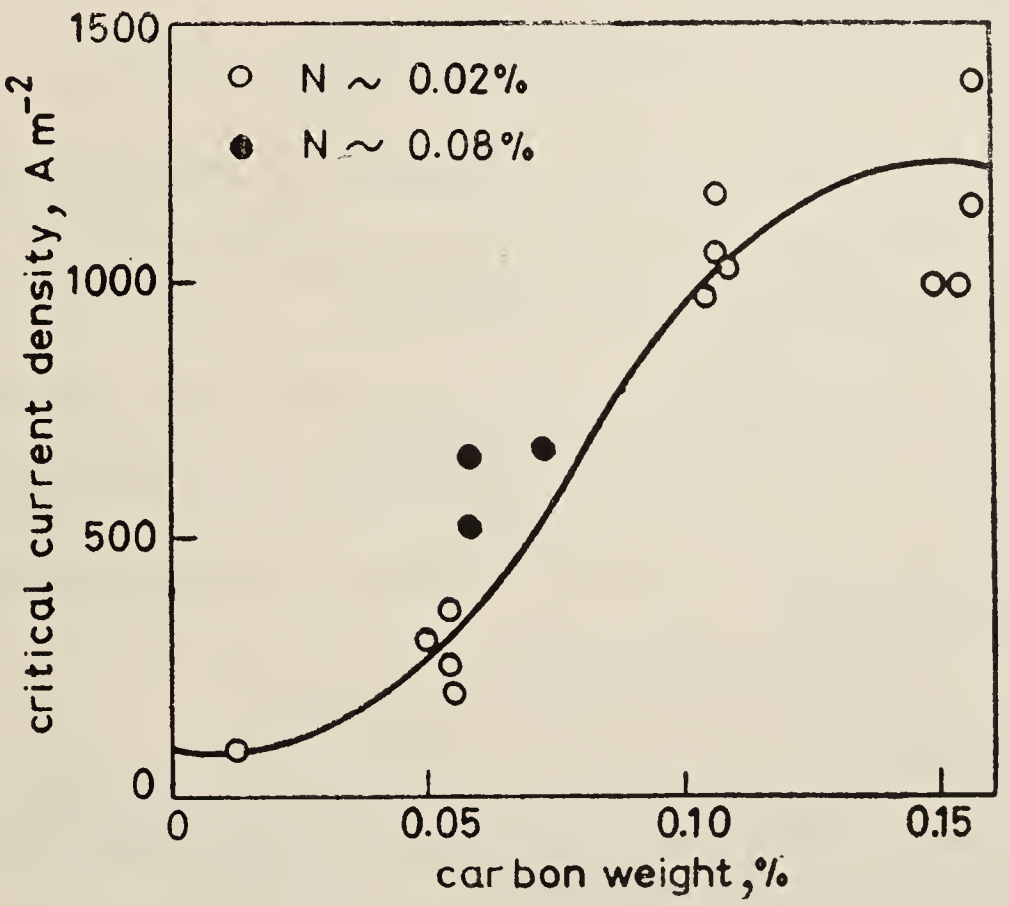

Figure 9. Effect of residual carbon on the critical current density for passivation of a ferritic stainless steel.

little doubt that ferrite grain sizes can be still further reduced (Deb & Raghavan 1981, to be published). Future work on dual-phase steels will be directed towards understanding the microstructural mechanisms that account for the enhanced ductility at the same strength level in these steels. Low-carbon bainitic steels will undoubtedly be developed on a larger scale to meet the demands for higher strengths. In the case of ultrahigh strength steels, future work needs to be on the size and spatial distribution of inclusions. The varying roles of cementite, alloy carbides and intermetallic compounds as precipitates need to be understood better, in order to elucidate the factors that contribute to the high fracture toughness.

It is hoped that metallurgists will fully apply the well-established physical metallurgy principles and use the sophisticated experimental tools that are available to them today, to meet the new challenges posed by the design engineers and to develop new steels for specific end uses.

References

Arrowsmith J M 1974 *Inclusions and their effects on steel properties* (London: Br. Steel Corpn.)
Blickwede D J 1968 *Trans. Am. Soc. Met.* **61** 653
Bricker K G & Spaeder G E 1972 *Metall. Engg. Q.* p. 1
Bush M E & Kelly P M 1971 *Acta Metall.* **19** 1363
Coldren A P & Tither G 1978 *J. Met.* **30** 6
Davies R G 1978 *Metall. Trans.* **A9** 671
Davison R M 1974 *Metall. Trans.* **5** 2287
Deb P & Raghavan V 1981 to be published
Duckworth W C & Baird J D 1969 *J. Iron Steel Inst.* **207** 861
Dulis E J & Chandhok V K 1969 *Met. Progress*, 101
Durbin M & Krake P R 1973 *Processing and properties of low carbon steels* (New York: AIME) p. 109
Farrar J C M & Dolby R E 1971 *Effect of second-phase particles on the mechanical properties of steels* (London: Iron & Steel Inst.) p. 71
Floreen S 1968 *Metall. Rev.* **13** 115
Floreen S & Speich G R 1964 *Trans. Am. Soc. Met.* **57** 714
Forester E, Klapdar W, Richter H, Rommerswinkel H, Spetzler E & Wendorff J 1974 Stahl and Eisen **94,** 11
Gladman T, Dulieu D & McIvor I D 1977 *Microalloying '75 Proceedings* (New York: Union Carbide Corp.) p 32
Gladman T, Holmer B & McIvor I D 1971 *The effect of second-phase particles on the mechanical properties of steels* (London: Iron & Steel Inst.) p. 68
Gray J M 1972 *Metall. Trans.* **3** 1495
Gray J M 1973 *Processing and properties of low carbon steels* (New York: AIME), p. 225
Gray J M & Yeo R B G 1968 *Trans. Am. Soc. Met.* **255** 61
Hayami S & Furukawa T 1977 *Microalloying '75 Proceedings* (New York: Union Carbide Corpn) p. 311
Hayami S, Furukawa T, Gondth H & Takechi H 1977 Paper presented at TMS-AIME Fall Meeting, Chicago, USA (Preprint)
Hilty D C & Poop V T 1969 *Trans. AIME* **67** 52
Honeycombe R W K & Pickering F B 1972 *Metall. Trans.* **3** 1099
Keh A S 1965 *Philos. Mag.* **12** 9
Kelly A & Nicholson R B 1970 *Strengthening methods in crystals* (Amsterdam: Elsevier)
Korchensky M & Stuart H 1970 *Low alloy high strength steels*, Proc. Symp., Scandinavian Conf., (Nuremberg: The Metallurgy Companies) p. 17
Langhammer H J, Abratis H & Patel P 1977 *Injection metallurgy*, SCANINJECT, Proc. Int. Conf., Lulea, Sweden, D13.1

Little J H, Chapman J A, Morrison W B & Minz B 1973 *Strength of metals and alloys*, Proc. III Int. Conf., (London: Iron & Steel Inst.) Vol. 2, p. 80
Little J A & Henderson W L M 1971 *Effect of second phase particles on the mechanical properties of steels* (London: Iron & Steel Inst.) p. 182
Luyckx L, Bell J R, McLean A & Korchynsky M 1970 *Metall. Trans.* **1** 3341
May M J, Gladman T & Walker E F 1976 *Philos. Trans. R. Soc.* **A282** 377
Mediratta S R and Ramaswamy V 1976 *Physical metallurgy of ferritic stainless steel*, Tool and Alloy Steels, p. 451
Melloy G E & Dennison J D 1973 *Strength of metals and alloys*, Proc. III Int. Conf., (London: Iron & Steel Inst. Vol. 1, p. 60
Mihelech J L, Bell J R & Korchynsky M 1971 *J. Iron Steel Inst.* **209** 469
Morrison W B & Chapman J A 1976 *Philos. Trans. R. Soc.* **A282** 289
Pickering F B 1967 *Transformation and hardenability in steels*, (Ann. Arbor: Climax Molybdenum Company) p. 109
Pickering F B 1971 *Toward improved toughness and ductility* (Kyoto: Climax Molybdenum Co.) p. 9
Pickering F B 1974 *Inclusions and their effect on steel properties*, (Leeds: Br. Stl. Corpn.) p. 3
Pickering F B 1977 *Microalloying, '75 Proceedings* (New York: Union Carbide Corpn.) p. 9
Pickering F B 1976 *Int. Metall. Rev.* p. 227
Pickering F B 1978 *Physical metallurgy and the design of steels* (London: Appl. Sci. Pub.)
Priestner R 1974 *Inclusions and their effect on steel properties* (Leeds: Br. Steel Corpn.) p. 4
Rashid M S 1976 SAE Preprint 760206
Rickett R L & Leslie W C 1959 *Trans. Am. Soc. Met.* **51** 310
Schmidt W & Jarleborg D 1974 *Ferritic stainless steels with* 17% *Cr* (Ann. Arbor: Climax Molybdenum Co.)
Smith D W & Hehemann R F 1971 *J. Iron Steel Inst.* **209** 406
Terazawa T, Higashiyama H & Sekino S 1971 *Towards improved ductility and toughness* (Kyoto: Climax Molybdenum Co.) p. 101
Wacquez & van Daele R 1967 *Sheet Metal Industries* **44** 21
Zackay V F 1969 *J. Iron Steel Inst.* **207** 894

Plate 1

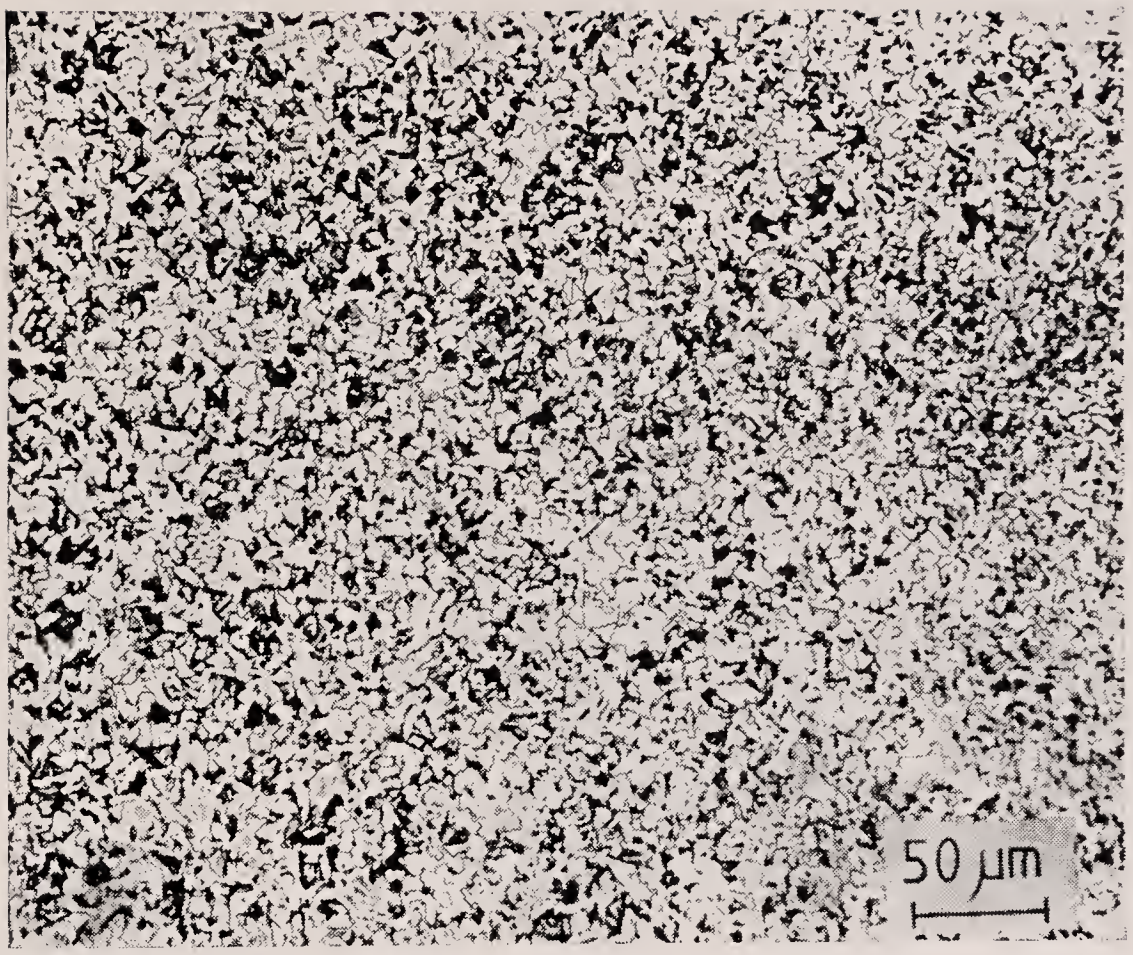

Figure 2. Light micrograph of an HSLA steel showing the fine ferrite grain size.

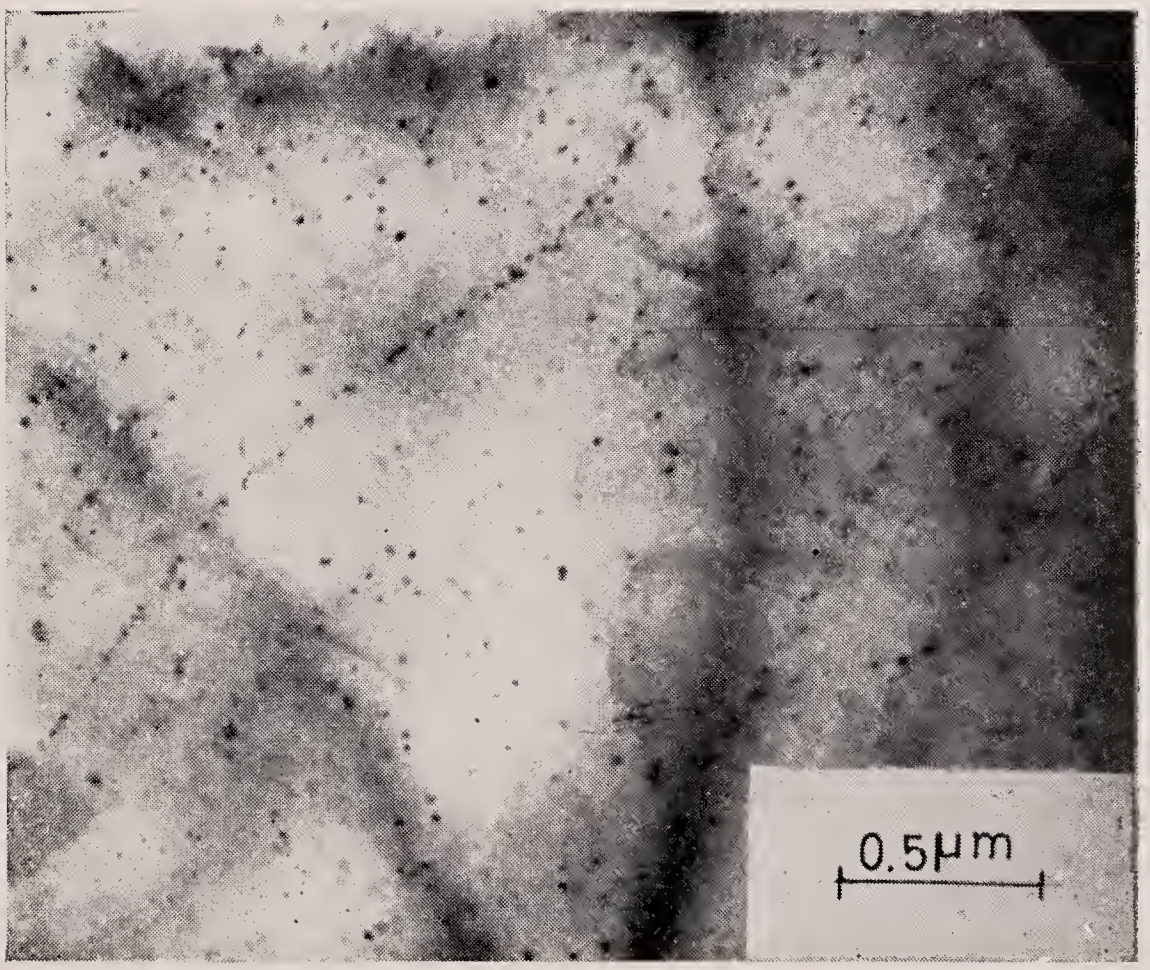

Figure 3. Thin foil transmission electron micrograph showing the row precipitation of NbC in an HSLA steel.

Challenges in alloy design: Titanium for the aerospace industry

D BANERJEE and R V KRISHNAN*
Defence Metallurgical Research Laboratory, Hyderabad 500 258
*Materials Science Division, National Aeronautical Laboratory, Bangalore 560 017

MS received 19 December 1980

Abstract. This review describes the principles governing the design of titanium alloys for engine and airframe applications in the aeronautical industry. The relationships between processing, microstructure and properties of the commonly used $\alpha+\beta$ titanium alloys are described in some detail. The 'state of science' is seen to be sufficiently advanced to enable the metallurgist to optimally design this class of alloys to meet specific requirements. The challenges to the alloy designer lie in increasing the temperature capability of titanium alloys, and in standardising processing techniques which will decrease the high manufacturing costs of components.

Keywords. Titanium alloys; processing; microstructure; property correlation; creep strength; structural applications

1. Introduction

The successes of the aerospace industry are responsible for a number of metals which were once considered exotic becoming commonplace. Titanium is one such metal. Its high specific strength, corrosion resistance and melting point render its alloys suitable to the variety of applications illustrated in figure 1. Another characteristic property—its tremendous affinity for oxygen—posed the major challenge to titanium technology. The problem of extraction was overcome when Kroll announced his chloride-reduction process: the oxide ore is converted to a tetrachloride which is then reduced by magnesium. Arc-melting in water-cooled copper crucibles, under inert atmospheres, made it possible to produce large quantities of clean alloy ingots. The oxidation loss of material during processing continues, however, to escalate titanium production costs to the present day.

By far the most prominent use of titanium alloys is directed to engine and airframe applications in the aeronautical industry. Understanding the principles of titanium metallurgy and their application to this end is now a major concern of the authors' laboratories. In this review, therefore, we restrict ourselves to this particular aspect of titanium alloy design. Our task will be to define as precisely as possible the interactions between the effect of alloying at the atomic and microstructural levels with a third variable, the processing technique used to impart the required form to the alloy.

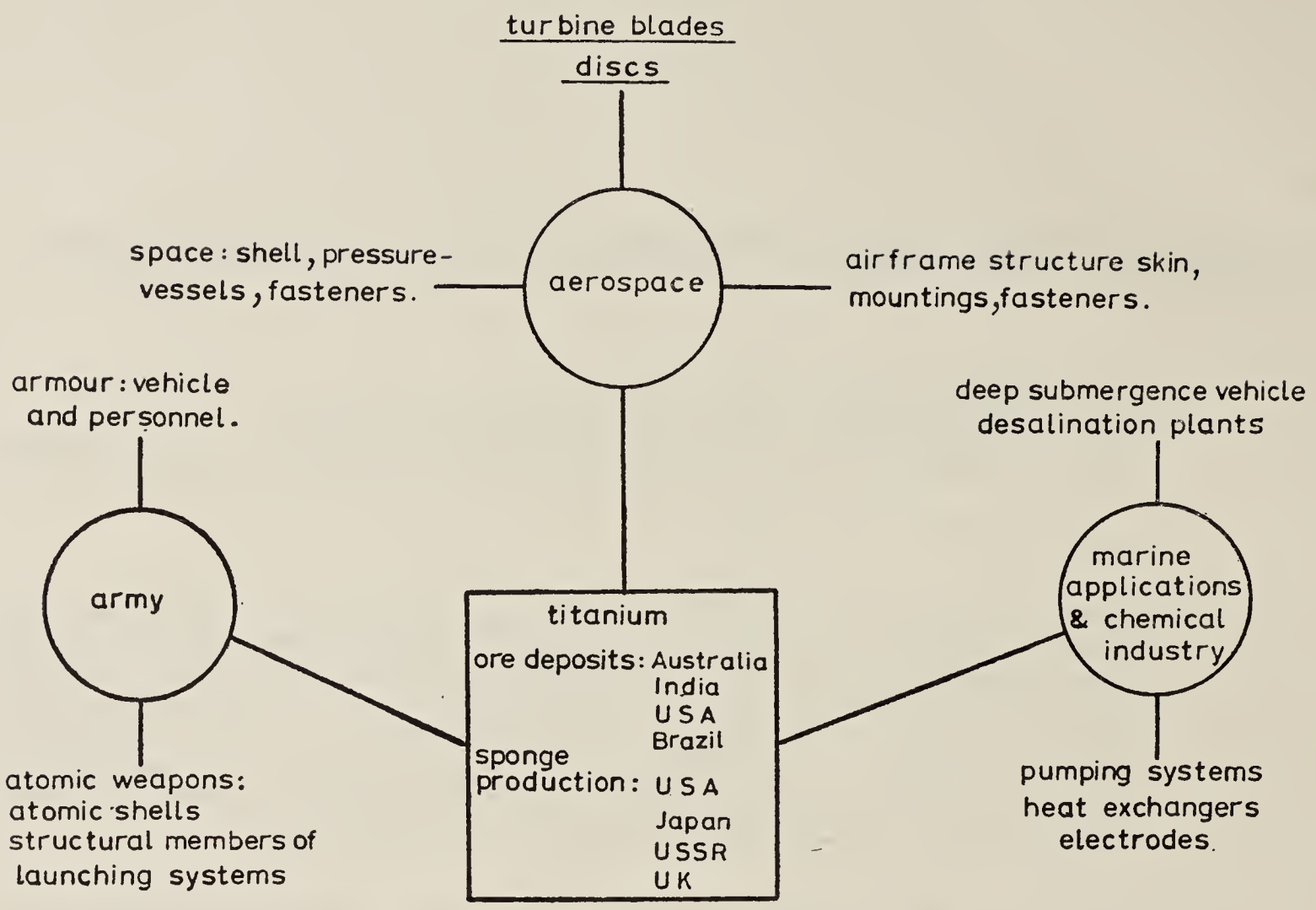

Figure 1. The applications of titanium alloys.

2. Basic considerations

Titanium exhibits two allotropic modifications: the low temperature form, α-Ti which has a hexagonal close-packed structure, and transforms to β, a body-centred cubic phase at 1155 K. The β structure is stable up to the melting point, 1941 K.

Alloying additions alter the relative stabilities of these two phases and, with few exceptions, introduce additional phases. This behaviour can be correlated with the group number of the element, to a first approximation. Thus alloying elements with less than 4 electrons/atom stabilise the α phase (Jaffee 1973). Those with an electron/atom (e/a) ratio equal to 4 are neutral to both α and β, while the β phase is stabilised by elements with an e/a greater than 4, including the transition elements. The tendency to form intermetallic compounds through a eutectoid transformation increases with positive deviation from an e/a ratio of 4. Of the interstitials, O, C and N stabilise α while H stabilises β. These features together with some typical phase diagrams are indicated in figure 2. Also pertinent to this discussion is the fact that the atomic size of titanium lies within $\pm$ 15% of the most common alloying elements.

Alloying additions will also alter the basic properties of each phase. Solid-solution strengthening of the α phase is of the order of 35–70 MN/m^2 per % of alloy addition while the β phase can be strengthened only by 14–30 MN/m^2 per % of alloy addition (Jaffee 1973; figure 2 of Bhat & Arunachalam 1980). The eutectoid formers are somewhat more effective in strengthening than the isomorphous elements, such as Mo, Nb or V. Of considerable importance is the fact that additions of β-stabilisers result in alloys of greater density than the base metal, while the addition of the most common α-stabiliser, aluminium, results in an alloy of lower density. The interstitials are generally kept to low levels as they lead to various types of embrittlement.

2.1 *Preliminary considerations in alloy design*

2.1*a Base structure* The specific properties required for the applications we are interested in (figure 3) provide guidelines for our choice of the base structure and composition of the alloy. The situation is unambiguous for the gas turbine alloy. The atomic mobility of alloying elements govern creep rates at high temperatures. The α phase, with its close-packed structure, naturally exhibits far lower diffusivities

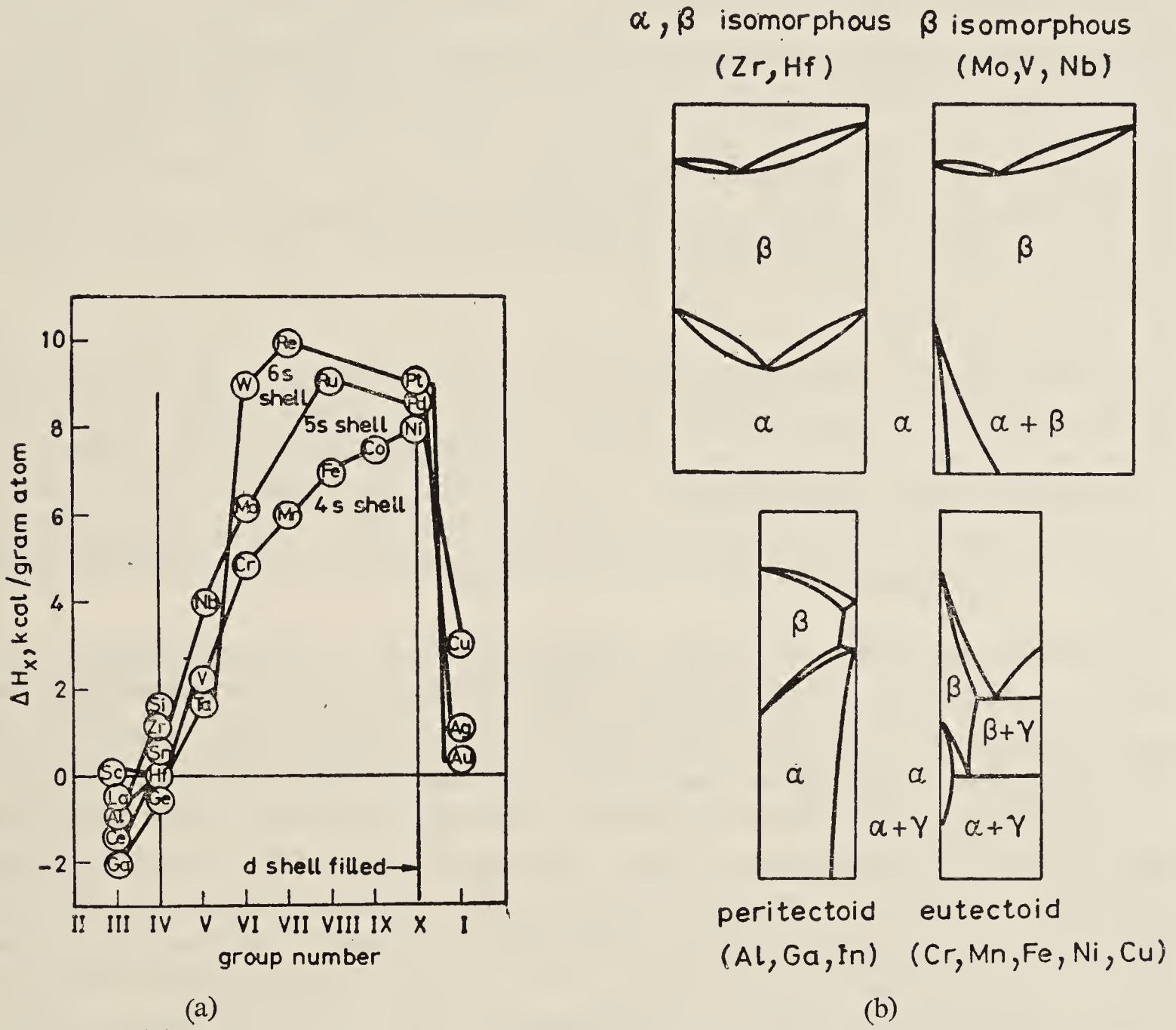

Figure 2. The effect of alloying elements on the stability of the α and β phases. **a.** after Jaffee (1973) shows the enthalpy of transfer of solute from β to α. **b.** after Kornilov (1970).

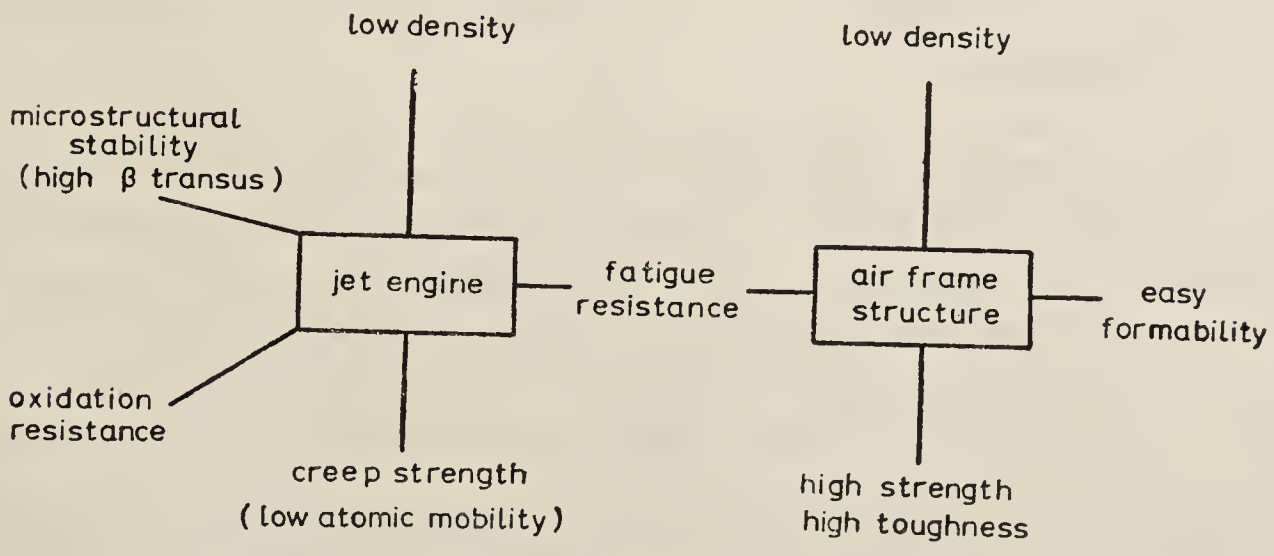

Figure 3. Property requirements of titanium alloys in aircraft applications.

than the β phase. (Metals with bcc structures are rarely used under creep environments except at low homologous temperatures.) This consideration is consistent with other requirements of low density and a high α/β transus. Thus high temperature titanium alloys are all ' near α ' alloys—they contain very low volume fractions of β.

The demands of the structural alloy are more conflicting. Since structural alloys can have complicated shapes with thin sections, deformability becomes a prime concern. The β phase has a large number of slip systems which are easily activated by any orientation of stress (Wood 1972) and forming operations are preferably done in the β phase field. Therefore it is advantageous to choose compositions with a low α/β transus, or those in which the β phase can be retained at room temperature. However, such compositions would also have high densities. The strength level which any given composition can attain may therefore be the deciding factor for a given application. In practice, structural alloys of titanium can be single phase α alloys, $\alpha+\beta$ alloys or high β alloys; a variety which simply reflects the nature of the problem.

2.1*b* *Microstructure* While the simple considerations outlined above determine the major constituent phase, strong alloys are usually two-phase structures. The two phases in commercial titanium alloys are the α and β phases, and the distribution and morphology of these phases determine to a great extent the properties of these alloys, as we shall see later. In this section we describe the variety of $\alpha+\beta$ microstructures which may be produced through various combinations of processing and heat treatment.

A fundamental feature of the $\beta\rightarrow\alpha$ transformation is the crystallography of the product α. Most often, the α phase forms with the classic Burgers relationship to the parent structure $(0001)_\alpha \| (110)_\beta$; $[11\bar{2}0]_\alpha \| [\bar{1}\bar{1}1]_\beta$, and this relationship holds for both the hexagonal martensite as well as the nucleation and growth product. In both cases the morphology of the α phase is plate-like, with the broad faces of the plate lying on or close to $(1\bar{1}00)$ (figures 4a, plate 1). Except in alloys with a high β-stabilising content, the β transforms to α on cooling through the transus. The structure formed when such an alloy is solutionised above the transus and cooled is shown in figure 4a (plate 1). Characteristic of this structure are the Burgers-related Widmanstatten α laths formed in colonies —each colony consisting of laths of the same Burgers variant —within the prior β grains. A strong tendency for α to nucleate initially at the prior β grain boundaries (grain boundary α or gb α) is also observed. The term ' transformed β ' (hereafter referred to as Tβ) is commonly used to denote a microstructural appearance of this kind*.

However, if the alloy is worked below the β transus, the α phase would nucleate during the process of plastic deformation and would contain a worked substructure. Subsequent annealing high in the $\alpha+\beta$ phase field results in the formation of a recrystallised structure of (i) equiaxed α if the hot reduction has been of sufficient magnitude ($>30\%$) (figure 4b, plate 1) and (ii) an α phase with high aspect ratio if the hot reduction is less than 30% (figure 4c, plate 1). The α phase formed in this manner is known as primary α (Pα). The cooling rate from the annealing temperature

*The term 'transformed β' makes no distinction as to the mechanism of the $\beta\rightarrow\alpha$ transformation —whether martensitic or nucleation and growth, or whether β is retained or not. It refers only to the acicular appearance of the α phase formed from β during cooling.

further determines the final microstructure. If the alloy is cooled very gradually the adjustment of the volume fraction to higher amounts of α occurs by the migration of the existing primary α/β interface (figure 4d, plate 1). Alternatively, rapid cooling results in the formation of α plates (secondary α) within the pre-existing β grains giving rise to a fraction of transformed β type structure (figure 4e, plate 1). The volume fractions of primary α and transformed β (for a given composition) in a $\alpha+\beta$ worked alloy may therefore be adjusted by the annealing temperature (below the α/β transus) and the subsequent cooling rate. We refer to this type of structure as ' primary α and transformed β' (Pα+Tβ).

More subtle adjustments in microstructure are achieved within the transformed β region. Quenching from the annealing temperature results in transformation of β to hexagonal martensite. The martensite may then be tempered to produce a β precipitate at the plate boundaries. Alternatively, the cooling rate can be decreased, with intermediate isothermal holds if necessary, to produce varying degrees of coarseness of ' secondary α ' plates in the transformed β region (figure 4f, plate 1).

Finally, if the β stabilising additions are much higher, the β phase may be retained at room temperature on rapid cooling through the transus. The resulting metastable β can then be aged to produce a fairly uniform distribution of acicular α on a much finer scale than achievable in the higher α alloys discussed above. A typical structure of this class is shown in figure 4g (plate 1).

3. $\alpha+\beta$ Titanium alloys—relationship of properties to microstructure

The mechanical properties of $\alpha+\beta$ titanium alloys are strongly microstructure-dependent, and for a given composition, microstructure may be tailored to suit a wide variety of requirements. In figure 5 (plate 2) we broadly relate various microstructural types (described in figure 4) to yield strength, ductility, fracture toughness, fatigue and creep resistance. $\alpha+\beta$ alloys constitute outstanding examples of two-phase mixtures in which both phases are ductile. Deformation and fracture in such a situation is necessarily complex. We review in this section the understanding gained over the last decade of the principles which govern the features illustrated in figure 5 (plate 2).

3.1 *Slip modes and void formation* (*Greenfield & Margolin* 1972)

Yield in two-phase materials is initiated by the weaker phase and proceeds by transfer of slip to other portions of the structure. The α phase deforms by prismatic, pyramidal or basal slip. The tendency for inhomogenous planar slip on these planes is enhanced in alloys containing aluminium, either through its effect on the stacking fault energy or due to the creation of short range order in the α lattice (J C Williams 1980, private communication). Since the basal plane of α and a (110) slip plane of β is parallel across a semicoherent interface between Burgers-related α and β (figure 4a, plate 1), such interfaces do not constitute significant barriers to slip at stresses above the yield stress. Strain incompatibility, on the other hand, can arise at incoherent α/β interfaces such as those associated with gbα in Tβ structures and Pα in Pα+Tβ structures (figures 4a–f, plate 1). Such interfaces constitute preferred sites for void nucleation, as well as growth.

3.2 *Yield strength and grain size* (*Jaffee* 1973; *Margolin et al* 1973)

The yield strength of a material is related to the grain size through the Hall-Petch relationship

$$\sigma_y = \sigma_0 + Kd^{-1/2},$$

where d, the effective grain size, is defined by the mean free path for slip in the structure.

In Tβ structures, Widmanstatten α/β interfaces do not constitute a barrier to slip. Slip planes can change direction across some colony boundaries (adjacent colonies may share a common basal plane through the crystallography of the Burgers relationship) and across all prior β grain boundaries. The yield strength is therefore controlled by prior β grain size and more weakly through the colony size.

Subtransus hot working and solution treatment breaks up the prior β grain structure. The mean free path for slip in the Pα+Tβ structure is therefore of the order of the Pα size, and such structures exhibit a higher yield strength than the Tβ class as indicated by figure 5 (plate 2). The strength of the individual units composing this structure also governs the overall yield strength. Refining the α distribution in the Tβ portion and increasing the volume fraction of this portion therefore enhances strength.

3.3 *Ductility and fracture toughness* (*Greenfield & Margolin* 1972; *Chesnutt et al* 1976; *Hall et al* 1972; *Hirth & Froes* 1977; *Hall & Hammond* 1978)

Incoherent α/β interfaces are preferred sites for void nucleation and growth. Therefore, the total area of such interfaces in a structure will influence ductility. Since crack propagation in ductile materials occurs by void nucleation and coalescence in the stressed region ahead of the crack tip, incoherent α/β interfaces also influence the crack path through the structure (and hence fracture toughness) in that they arrest and deviate cracks along the interface, provided that the α phase associated with the interface is sufficiently thick.

The opposing effects of primary α morphology on ductility and toughness are illustrated in figures 6a and b. A lenticular α morphology provides greater surface area for void formation; it however also increases crack path tortuosity. The greater work of plastic accommodation per unit volume for a tortuous crack path, together with lower stress intensities at a deviated crack tip, combine to promote toughness.

An optimized Pα+Tβ structure for strength, ductility and toughness may therefore consist of an equiaxed Pα morphology for ductility, a coarse secondary α fraction to promote toughness, and a fine secondary α fraction to provide strength (Hall *et al* 1972). Such a structure is shown in figure 5 (plate 2) and may be obtained by a processing schedule of the type indicated in figure 4f (plate 1).

A Tβ structure is associated with considerably higher fracture toughness. The crack path across such a structure is indicated in figure 6c, and seems to be governed by the formation of shear-bands or cleavage on the basal plane of the α phase ahead of the crack tip (Hall & Hammond 1978). The crystallographic nature of crack propagation in this structure results in long, deviated crack path portions of the order of the colony size, and hence a high toughness (figure 6c). The ductility of such a

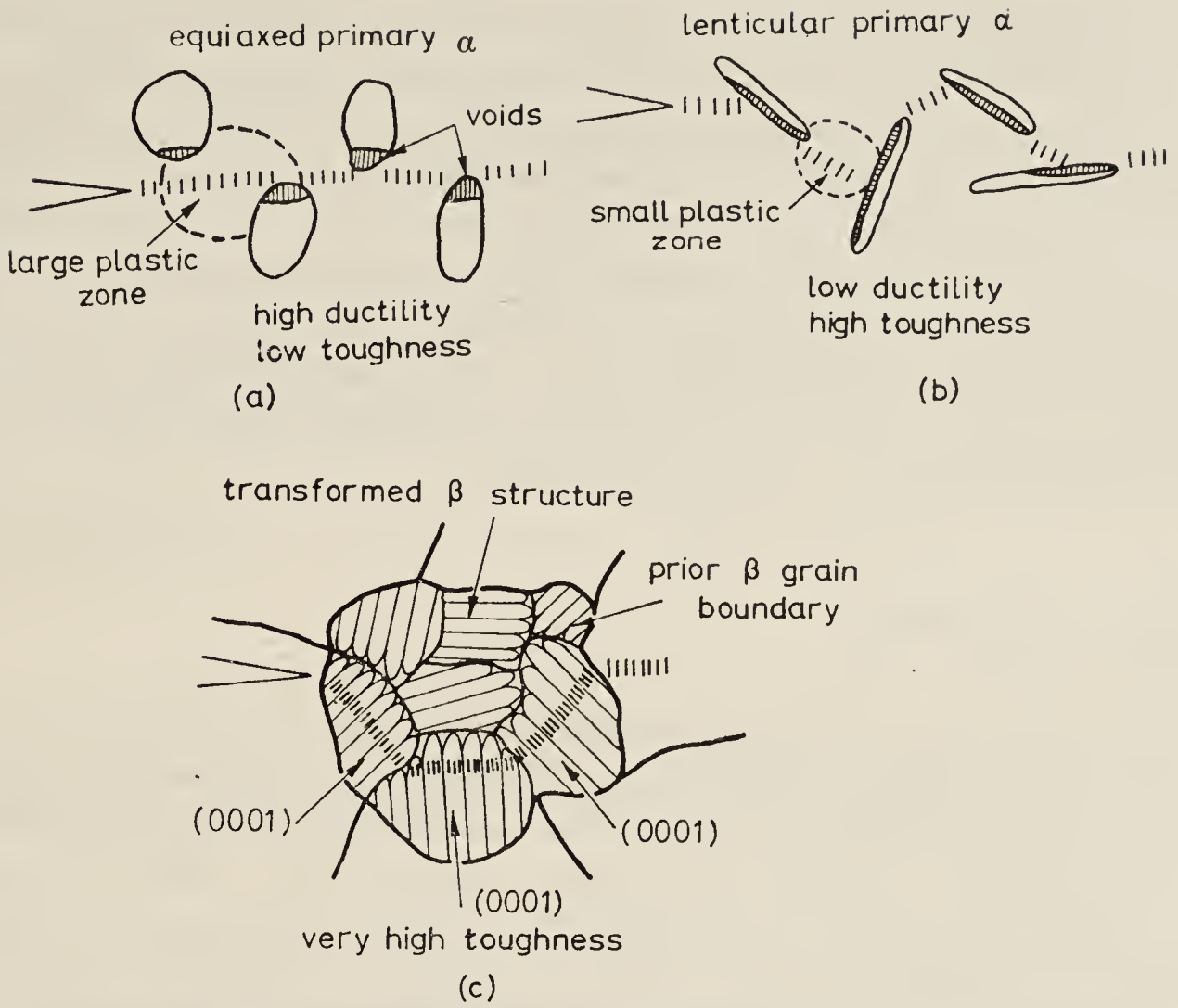

Figure 6. Crack path-microstructure relationships in $\alpha+\beta$ titanium alloys. (a and b after Hirth & Froes 1977). Hatched lines indicate the crack path.

structure, however, is controlled by the nature of gbα. A continuous gbα film coupled with a coarse prior β grain size allows rapid void growth across the structure. Optimized β solutionising temperature and time, and rapid cooling rates, promote the ductility of this class of structure.

3.4 *Fatigue and creep resistance*

Tβ structures exhibit superior fatigue (Yoder *et al* 1979) and creep properties (Eylon *et al* 1976) as compared to Pα+Tβ alloys. The increased fatigue performance can be attributed to the crystallographic nature of fatigue crack growth as described above. The causes underlying superior creep behaviour are more complex and will be dealt with in the subsequent section. From a microstructural point of view it appears that the large numbers of parallel, closely-spaced α/β interfaces (about a micron apart) present in this structure type may constitute a barrier to dislocation motion under creep conditions, and thus create a threshold stress below which creep cannot occur (Bhat & Arunachalam 1980). The larger effective grain size may also decrease grain boundary-related creep rates (Jaffee in Versnyder & Gell 1977).

3.5 *On α/β interfaces in titanium alloys*

The preceding discussion serves to emphasise the critical role α/β interfaces play in determining mechanical properties of such alloys. TEM studies of these interfaces have recently revealed highly complex structures (Rhodes & Williams 1975; Rhodes

& Paton 1979a; Banerjee 1979). Studies at DMRL (Banerjee 1979) for instance show that the β layer in a Tβ structure is sandwiched between thin layers of an fcc phase of a definite crystallography as illustrated in figure 7 (plate 3). The fcc phase has been suggested to be a hydride of titanium (Banerjee & Arunachalam 1980, under publication) or a transition phase forming during the $\beta \rightarrow \alpha$ transformation (Rhodes & Paton 1979a). Though some efforts have been made to evaluate the effect of the ' interface phase ' on properties (Rhodes & Paton 1979b), the results, we feel, are not conclusive. The clarification of the origin of this phase and its role in determining the mechanical properties of the $\alpha+\beta$ alloys will occupy the attention of titanium metallurgists for some time to come.

4. Designing against creep

A high degree of creep, fatigue and oxidation resistance is required of material to be utilised as compressor or turbine blades and discs in the demanding environment of an aircraft engine. Figure 8 compares the temperature range of use of present-day $\alpha+\beta$ titanium alloys—the upper limit being around 550°C—with other systems. In the first part of this chapter we discuss the design of these alloys against creep. However, the aim of the titanium alloy designer is to achieve the temperature capability of the nickel base alloys in use around 600–800°C—their replacement by titanium would result in enormous weight gains. Accordingly in the latter portion we outline possible approaches towards achieving this goal (Arunachalam & Banerjee 1980).

4.1 $\alpha+\beta$ *Creep-resistant alloys*

The last decade has seen the evolution of two criteria on which successful high temperature titanium alloy design is based. The first defines the framework within which the composition of the alloy may be manipulated: Rosenberg's α-equivalent (Rosenberg 1970); the second relates to structure: transformed β structures exhibit superior combinations of creep and fatigue properties (§ 3).

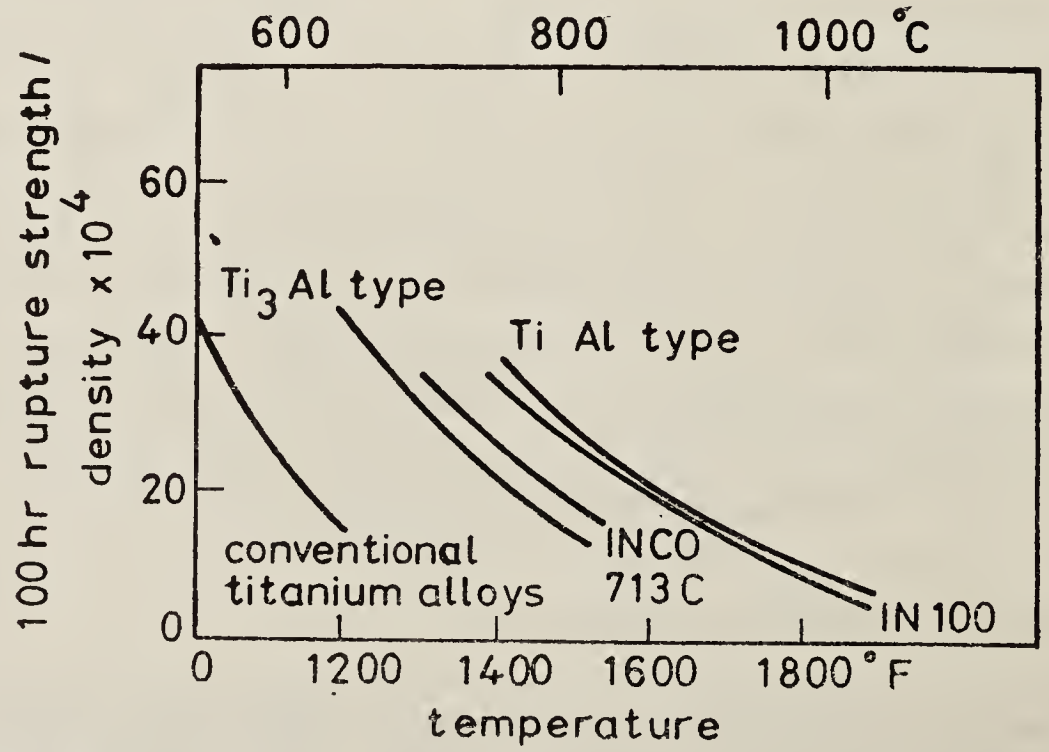

Figure 8. The temperature capability of titanium alloys (After Versnyder & Gell 1977.)

4.1*a Composition* We have seen that basic considerations require the matrix structure of an $\alpha+\beta$ creep-resistant alloy to be the α phase. This phase may be solid-solution strengthened by additions which either stabilise or are neutral to the α phase: Al, Zr and Sn. Aluminium, in addition, may lower the stacking fault energy of the α phase and therefore might contribute to creep strength. There however exists a limit to which these strengthening additions may be made in that beyond a critical value, the α phase decomposes to form fine precipitates of an embrittling compound, Ti_3Al. This limit is defined by an upper value of the 'α-equivalent' content of the alloy empirically arrived at by Rosenberg (1970).

$$\alpha\text{-equivalent} = \mathrm{Al} + \frac{\mathrm{Sn}}{5} + \frac{\mathrm{Zr}}{6} + 10\,(O) < 9\ (\mathrm{wt}\%),$$

where $O = O + C + 2N$ (Jaffee 1973).

Incorporation of a small volume fraction of β(5–10%) further strengthens the α phase. This is achieved by additions of Mo or Nb just above their solubility limit in α.

A potent, if rather unusual, way of strengthening this basic composition against creep is through the addition of small amounts of silicon. This element, because of its considerably smaller atomic size (—20%), interacts strongly with dislocations in α-titanium to provide an atmosphere drag (dynamic strain aging) below 720 K (Mahoney *et al* 1977). Above this temperature silicon precipitates as silicide on dislocations under stress.

Table 1 indicates typical commercial compositions of creep-resistant alloys and their respective properties.

4.1*b Heat treatment* The effect of heat-treatment on the creep behaviour of the transformed β structures can be extremely complex. Higher solution-treatment temperatures and faster cooling rates allow the retention of silicon in solid solution (and this is one reason why transformed β structures display superior creep

Table 1. Composition and properties of 'near—α' creep-resistant alloys (data from DF Neal 1976, private communication to V S Arunachalam)

Alloy	Al	Zr	Sn	Mo	Nb	Si	Bi	Ultimate tensile strength at room temp. MN/m^2	Creep:total plastic strain % after 100 hr at 773K and 300 MN/m^2
IMI 829	5·5	3	3·5	0·25	1	0·30	—	962	0·061
IMI 685	6	5	—	0·50	—	0·25	—	992	0·122
Ti-11	6	1·5	2	1	—	0·35	0·1	903	0·219
Ti-6242	6	4	2	2	—	—	—	1019	0·060
BT 9	6·5	1	—	3	—	0·25	—	—	—

properties). These treatments, however, also control the scale of the transformed β structure through parameters such as the prior β grain size, the colony size, and interlath spacing of α within a colony. The creep strain has been found to be minimal at an optimal cooling rate (Blenkinsop *et al* 1976) (figure 9, plate 4).

With increase in operating temperature the microstructure coarsens by spheroidisation of the retained β plates (Banerjee 1979); in addition, silicon is removed from the solid solution (Mahoney *et al* 1977), reducing its effectiveness in creep inhibition.

A clear quantitative understanding of the influence of these parameters on creep has not been achieved, but must be essential if the creep stability of high α alloys is to be improved. Towards this end, work is in progress (Rama Rao 1980, unpublished work) to draw up deformation mechanism maps of some commercial high temperature alloys such as IMI 685 (table 1) to clearly define the conditions of temperature and stress at which various creep mechanisms are dominant.

4.2 *Limitations of $\alpha+\beta$ alloys and alternative routes to higher temperature capability*

The present-day $\alpha+\beta$ alloys can be used to temperatures of only 550°C and their use above this temperature appears to be essentially limited by their creep stability. Two causes for this degradation can clearly be identified: the first is the loss in microstructural stability. This is essentially dependent on the operating point of the alloy as related to its β transus rather than its melting point. We have noted that the upper limit on the α-equivalent content prevents our achieving a higher β transus in such alloys. The second factor causing loss in creep properties appears to be the loss of silicon from the solid solution at high temperatures.

If there is then a limit to the temperature capability of the $\alpha+\beta$ alloys can one design creep-resistant alloys with an alternative second phase? Considerable work has been carried out over the last decade on alloys based on the intermetallics Ti_3Al and TiAl (Lipsitt *et al* 1975, 1980) in the TiAl system. These alloys offer significant high temperature strength advantages over the high α class and compare well with nickel base alloys (figure 8).

4.2*a* *$\alpha+Ti_3Al$ alloys* A possible second phase to strengthen α could be the intermetallic compound Ti_3Al (hexagonal, DO_{19}) which forms as a fine dispersion in the matrix in the range 7–12 wt% Al (figure 10a, plate 5). The structural analogy to the $\gamma+\gamma'$ system in Ni-base superalloys is readily apparent. These alloys possess attractive high temperature tensile strength (Gysler & Weissmann 1977) but are verybrittle. The cause of embrittlement has been clearly identified. Inhomogeneity and planarity of slip in high aluminium alloys is accentuated by the presence of fine, coherent ordered particles. The resulting high stresses at dislocation pile-ups lead to cracking (Lutjering & Weissmann 1970).

Lutjering & Weissmann (1970) have, however, shown that if the particle spacing is carefully adjusted so that dislocations bow out between the particles, the slip distribution becomes more homogeneous, and some ductility is gained. The problem is then one of retaining the right interparticle spacing at operating temperatures. This problem has two aspects: one pertains to the significant changes in volume fraction of Ti_3Al with temperature due to the shape of the $\alpha+Ti_3Al/\alpha$ solvus; and the other relates to coarsening rates of the Ti_3Al precipitates. Coarsening beyond the critical particle spacing would lead to strength decrements. While the latter is now being

evaluated (Mukherjee & Banerjee 1980, unpublished research), investigation on the effect of alloying additions on the slope of the solvus is also essential to arrive at suitable compositions which show a limited dependence of Ti_3Al volume fraction on temperature. We must remember that extensive work has already been carried out to ductilise TiAl alloys of this kind over the last decade, but no commercial composition is as yet available.

4.2*b Other dispersions* Inert dispersoids of oxides may also be considered as a strengthening second phase for the α matrix. In addition, oxide dispersoids may also be incorporated in the $\alpha+Ti_3Al$ system discussed above to activate secondary slip sources. The effect of yttria dispersoids on the recrystallisation of commercial and purity titanium has been evaluated (Krishnan *et al* 1976) (figure 10b, plate 5) and the dispersoids found to be ineffective in retarding recrystallisation. Some work on the effect of such dispersoids on the strength of titanium has also been reported (Sankaran *et al* 1980). It must be emphasised in this context that while such dispersoids are ' inert ' in most metals, the large solubility of oxygen in titanium does not justify this description; and it is precisely this large solubility which prevents the incorporation of large volume fractions of fine oxide dispersions in the structure by conventional routes. An exploratory experiment involving the rapid solidification of a titanium-erbium mixture by laser-glasing techniques appears to have been successful in this respect (Sastry 1980, private communication). However, the coarsening of such dispersoids is likely to remain a problem in the context of elevated temperature use. An optional dispersoid could be titanium carbide since carbon has a much lower solubility in titanium, but this possibility has received no attention so far.

5. Structural alloys

There exists an increasing demand for tough, high strength/weight ratio alloys for structural applications in aircraft such as skin, forgings and fastener components. Titanium alloy compositions used for such applications are listed in table 2 and may be seen to divide into three classes according to their composition: the α alloys, the $\alpha+\beta$ alloys and the metastable β alloys. The most common of these are the $\alpha+\beta$ alloys, the outstanding example being Ti-6Al-4V. The principles of design of this

Table 2. Composition and class of structural alloys of titanium

Category	Composition
α	Ti—5Al—2·5Sn
$\alpha+\beta$	Ti—6Al—V4
	Ti—6Al—6V—2Sn
	Ti—6Al—2Sn—4Zr—6Mo
	Ti—4·5Al—5Mo—1·5 Cr (CORONA 5)
Metastable β	Ti—13V—11Cr—3Al
	Ti—11·5Mo—6Zr—4·5Sn (βIII)
	Ti—8Mo—8V—2Fe—3Al
	Ti—3Al—8V—6Cr·4Mo—4Zr (βC)
	Ti—10V—2Fe—3Al

class of alloys have been comprehensively discussed in §§ 2 and 3, and are well illustrated in the recent development of the alloy CORONA 5 (Froes & Highberger 1980). Their disadvantages lie in that they are not cold formable and require working at fairly high temperatures. Moreover they exhibit poor hardenability over thick sections since the scale of microstructure (secondary α size) is sensitive to the cooling rate from the solutionising temperature.

For structural applications, therefore, the emphasis has shifted to the metastable β class. In this section we briefly describe the alloying and processing of this alloy type.

5.1 *Composition* (*Jaffee* 1973)

The somewhat higher density of the metastable β alloys is offset by their ability to strengthen to higher levels than the $\alpha+\beta$ class while retaining toughness. This is achieved essentially by stabilising the β phase sufficiently so that it may be retained in a metastable form at room temperature, followed by an age-hardening treatment in which the α phase precipitates in a fine, uniform distribution. The β stabilising additions are Mo, V, Cr or Fe. While the eutectoid-formers are strong β strengtheners, they also tend to embrittle the alloy by precipitating intermetallic compounds on aging. Cr or Fe, however, may be utilised as β stabilisers since they are sluggish eutectoid formers. Aluminium and tin are present to control the $\beta \rightarrow \alpha$ transformation characteristics and may also strengthen the α precipitate.

5.2 *Processing and heat treatment* (*Froes et al* 1980; *Williams et al* 1980)

The stabilising of the β phase through alloying introduces additional metastable phases which complicate the simple transformation characteristics of the $\alpha+\beta$ alloys. The most typical of these is the ω phase (figure 11a) which forms as a fine spherical or cuboidal dispersoid during the isothermal aging of such alloy compositions. The kinetics of the ω and α transformations are competitive as shown in a typical TTT diagram in figure 11b with α phase formation predominating at higher temperatures. Since the ω phase tends to embrittle the alloy, the metastable β alloys are aged above the ω transformation temperatures. Aluminium and tin in this respect are important additions since they (i) accelerate α transformation kinetics and therefore (ii) retard ω phase formation, and finally (iii) promote uniform α nucleation.

The strength of the aged alloy is controlled by varying the aging temperature and time in the α formation regime. It has also been reported that careful adjustment of ω spacing can lead to alloys of very high strength but with some ductility. In addition, the tendency of the α phase to nucleate on ω can be utilised to obtain an extremely fine dispersion through a step-aging treatment indicated in figure 11b. However, the rapid kinetics of the ω reaction makes it difficult to achieve sufficient control over these steps in a production sequence at present.

The low β transus and high cold-formability of the metastable β alloys offer the possibility of thermomechanical treatment to further enhance strength. Heterogeneous nucleation sites in the form of dislocations may be introduced within the β grains to accelerate α formation kinetics and obtain uniform α precipitation, and to eliminate the tendency for α to nucleate on grain boundaries (with subsequent embrittlement). This may be achieved by subtransus warm-working and solution treatment, *i.e.* processing below the recrystallisation temperature, or cold-working following solution treatment.

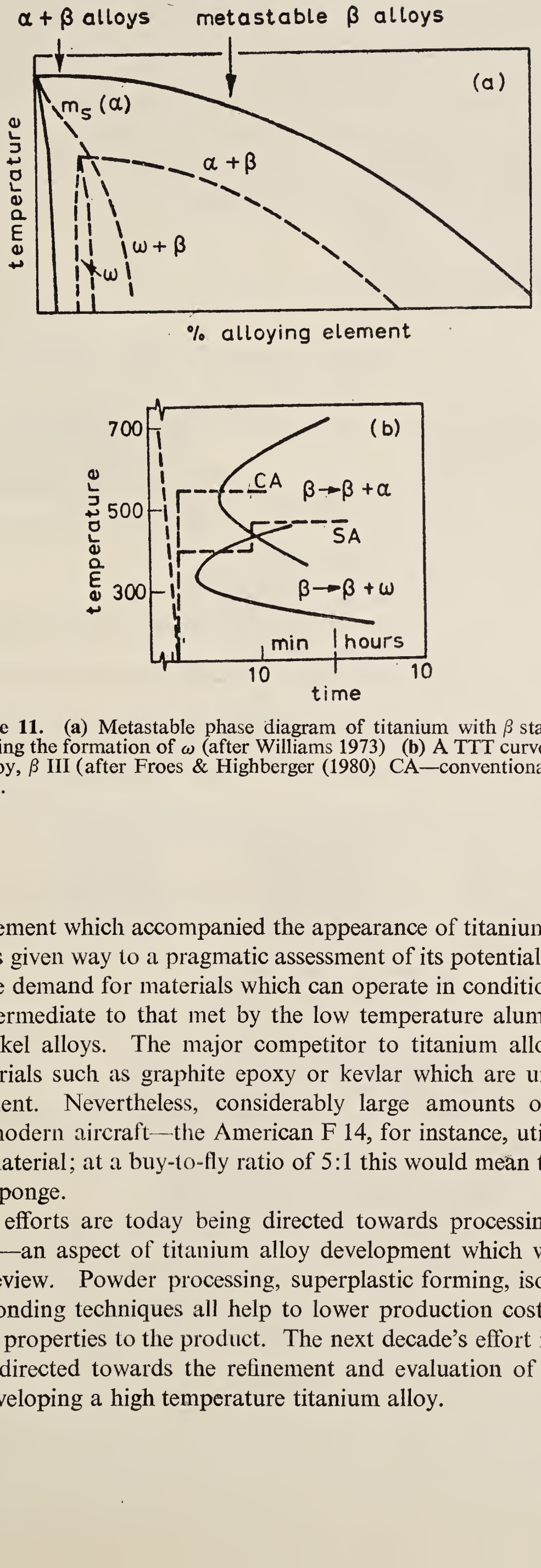

Figure 11. **(a)** Metastable phase diagram of titanium with β stabilising additions, showing the formation of ω (after Williams 1973) **(b)** A TTT curve of the metastable β alloy, β III (after Froes & Highberger (1980) CA—conventional aging; SA—step aging.

6. Conclusion

The initial excitement which accompanied the appearance of titanium on the technological scene has given way to a pragmatic assessment of its potentialities. Titanium alloys satisfy the demand for materials which can operate in conditions of stress and temperature intermediate to that met by the low temperature aluminium and high temperature nickel alloys. The major competitor to titanium alloys are the new composite materials such as graphite epoxy or kevlar which are under a phase of rapid development. Nevertheless, considerably large amounts of titanium find their way into modern aircraft—the American F 14, for instance, utilises about 3000 kg of finished material; at a buy-to-fly ratio of 5:1 this would mean the consumption of 15000 kg of sponge.

Considerable efforts are today being directed towards processing techniques to near net-shapes—an aspect of titanium alloy development which we have not discussed in this review. Powder processing, superplastic forming, isothermal forging and diffusion-bonding techniques all help to lower production costs and may even impart superior properties to the product. The next decade's effort in titanium technology will be directed towards the refinement and evaluation of these processes, and towards developing a high temperature titanium alloy.

The authors are grateful to Dr V S Arunachalam and Dr S N Tewari for several valuable suggestions regarding the style and content of the article and to Messrs Bhaskar Sarma, W Krishnaswamy, D Mukherjee, K Bose, R L Saha and Dr N C Birla for permission to reproduce micrographs from their unpublished work in figures 4 and 5. The authors also wish to express their gratitude to Prof. J. C. Williams for a critical reading of the manuscript and for comments on some aspects of deformation and strengthening of the α phase.

References

Arunachalam V S & Banerjee D 1980 4th International Conference on Titanium Alloys (Japan)
Banerjee D 1979 Contract Report to ARDB Project RD—134/100/10/77-78/200, Phase I–II
Bhat T B & Arunachalam V S 1980 *Proc. Indian Acad. Sci.* (*Engg. Sci.*) **2** 275
Blenkinsop P A, Neal D F & Goosey R E 1976 3rd International Conference on Titanium Alloys (Moscow)
Chesnutt J C, Rhodes C G & Williams J C 1976 ASTM STP 600 (Philadelphia: ASTM) p. 99
Eylon D, Hall J A, Pierce C M & Ruckle D L 1976 *Metall. Trans.* **A7** 1817
Froes F H, Yolton F, Capenos J M, Wells M G H & Williams J C 1980 *Metall. Trans.* **A11** 21
Froes F H & Highberger W T 1980 *J. Met.* **32** 57
Greenfield M A & Margolin H 1972 *Metall. Trans.* **3** 2649
Hall I W & Hammond C 1978 *Mater. Sci. Engg.* **32** 241
Hall J A, Pierce C M, Ruckle D L & Sprague R A 1972 *Mater. Sci. Engg.* **9** 197
Hirth J P & Froes F H 1977 *Metall. Trans.* **A8** 1165
Jaffee R I 1973 *Titanium science and technology* eds R I Jaffee and H M Burte (New York: Plenum) p 1665
Kornilov I I 1970 *The Science, technology and application of titanium* eds R I Jaffee and N E Promise (New York: Pergamon) p 408
Krishnan R V, Rangaraju R & Arunachalam V S 1976 3rd International Conference on Titanium Alloys (Moscow)
Lipsitt H A, Schechtman D & Schafrik R E 1975 *Metall. Trans.* **A6** 1991
Lipsitt H A, Schechtman D & Schafrik R E 1980 *Metall. Trans.* **A11** 1369
Lutjering G & Weissmann S 1970 *Acta Metall.* **18** 785
Mahoney M W, Paton N E, Parris W M & Hall J A 1977 AFML-TR-77-56 p. 42
Margolin H, Greenfield M A & Greenhut I 1973 *Titanium science and technology* eds R I Jaffee & H M Burte (New York: Plenum) p 1709
Rhodes C G & Paton N E 1979a *Metall. Trans.* **A10** 209
Rhodes C G & Paton N E 1979b *Metall. Trans.* **A10** 1753
Rhodes C G & Williams J C 1975 *Metall. Trans.* **A6** 2103
Rosenberg H W 1970 *The science, technology and application of titanium* eds. R I Jaffee & N E Promisel (New York: Pergamon) p 851
Sankaran K K, Sastry S M L & Rao P S 1980 *Metall. Trans.* **A11** 196
Versnyder F L & Gell M 1977 *Fundamental aspects of structural alloy design* eds R I Jaffee & B A Wilcox (New York: Plenum) p 209
Williams J C 1973 *Titanium science and technology* eds R I Jaffee & H M Burte (New York: Plenum) p 1453
Williams J C, Froes F H & Yolton C G 1980 *Metall. Trans.* **A11** 356
Wood R A 1972 Metal and Ceramics Information Centre, Report 72-11, p 4
Yoder G R, Cooley L A and Cooker T W 1979 *J. Engg. Mater. Tech.* **99** 313

Plate 1

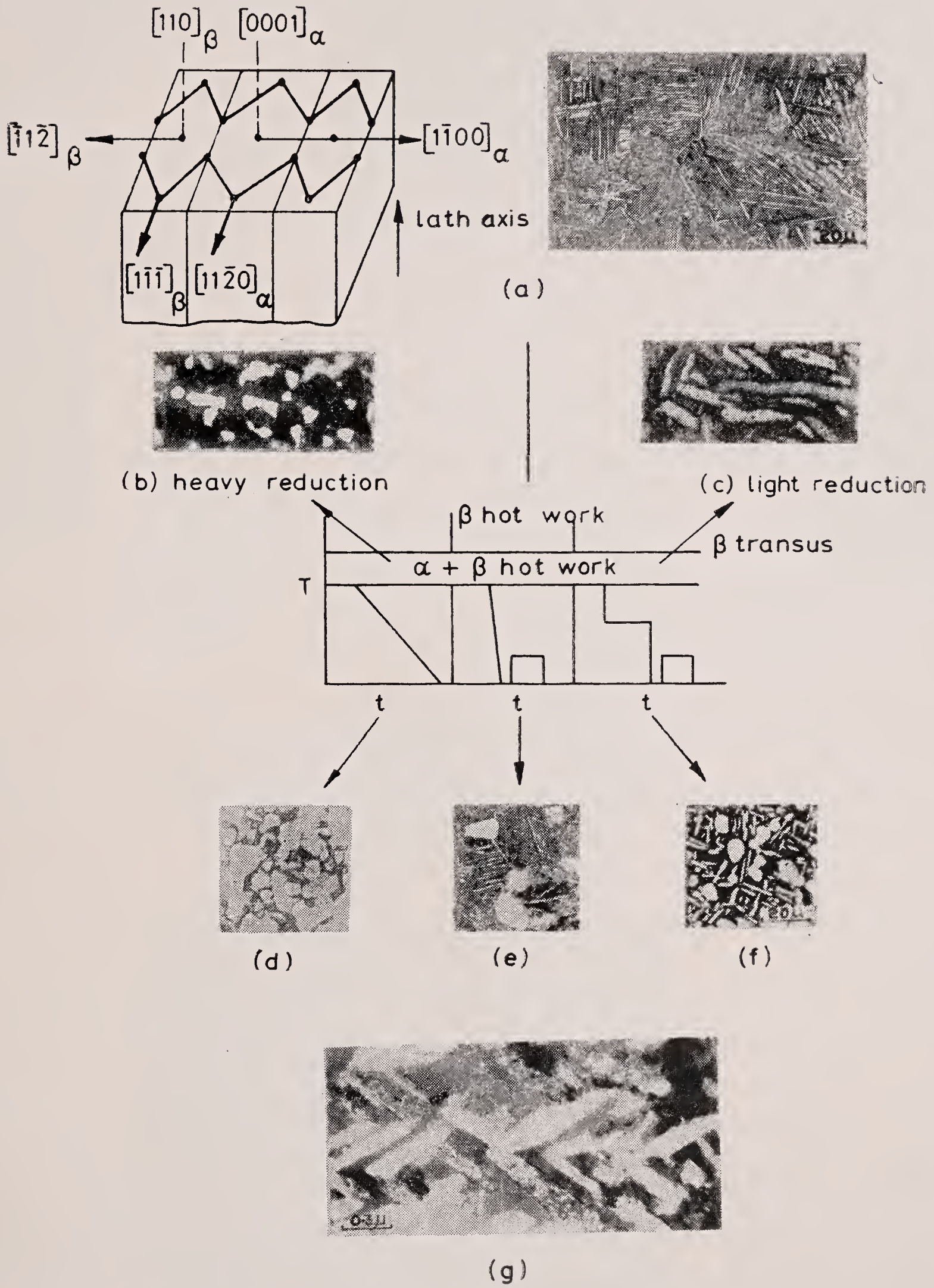

Figure 4. The relationship of processing to structure in $\alpha + \beta$ titanium alloys. **(a)** $\alpha : \beta$ crystallography and transformed β structure. **(b)** - **(f)** subtransus processed structures **(c)** TEM of α precipitates in a metastable β alloy.

Plate 2

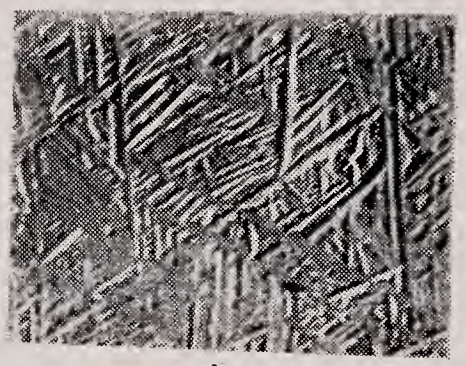

creep and fatigue strength, high toughness
low tensile strength

high strength
high ductility
low toughness

20 μ

high strength
high toughness
low ductility

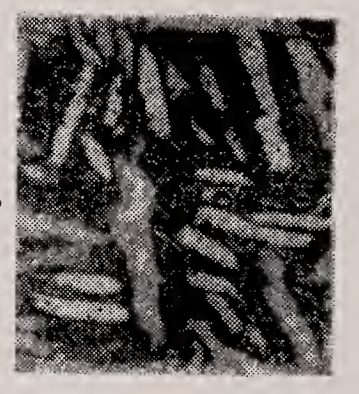

optimised
strength ductility toughness

Figure 5. The relationship of structure to properties in $\alpha+\beta$ titanium alloys.

Plate 3

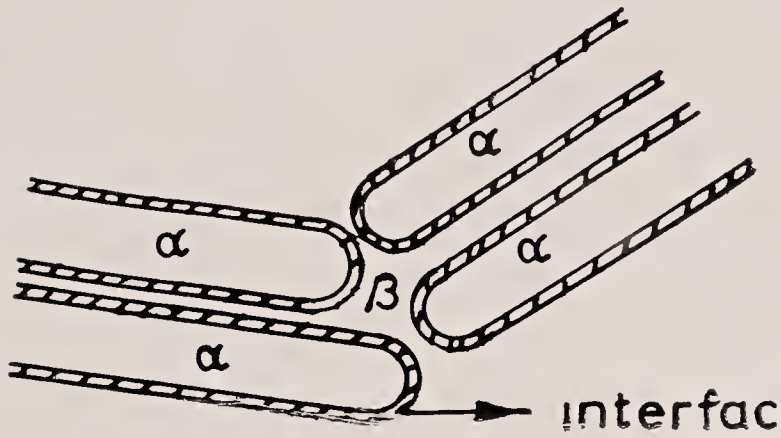

(a)

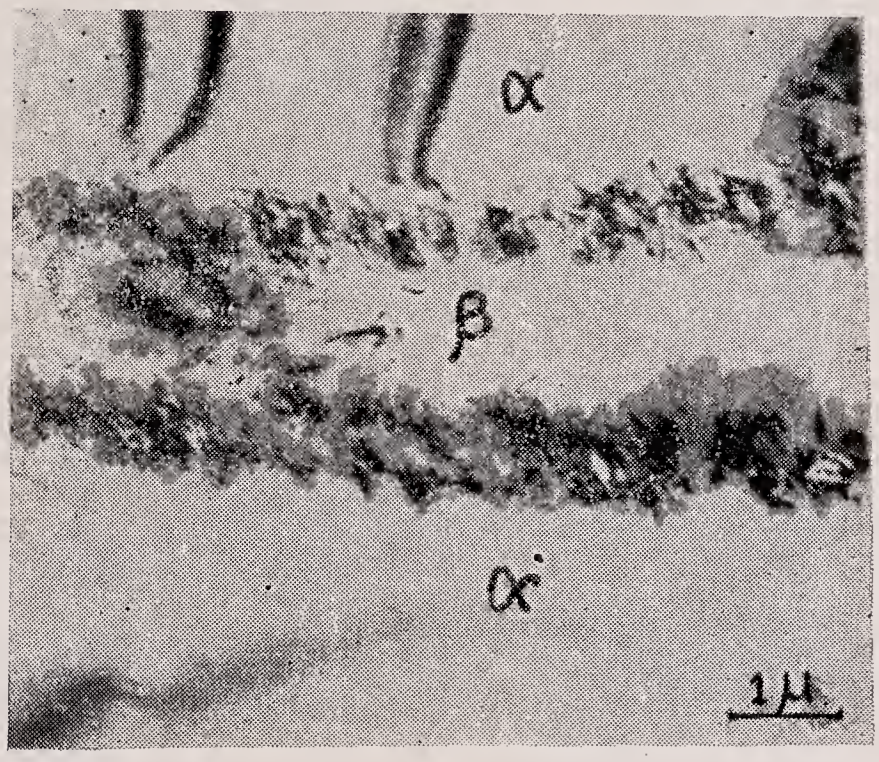

(b)

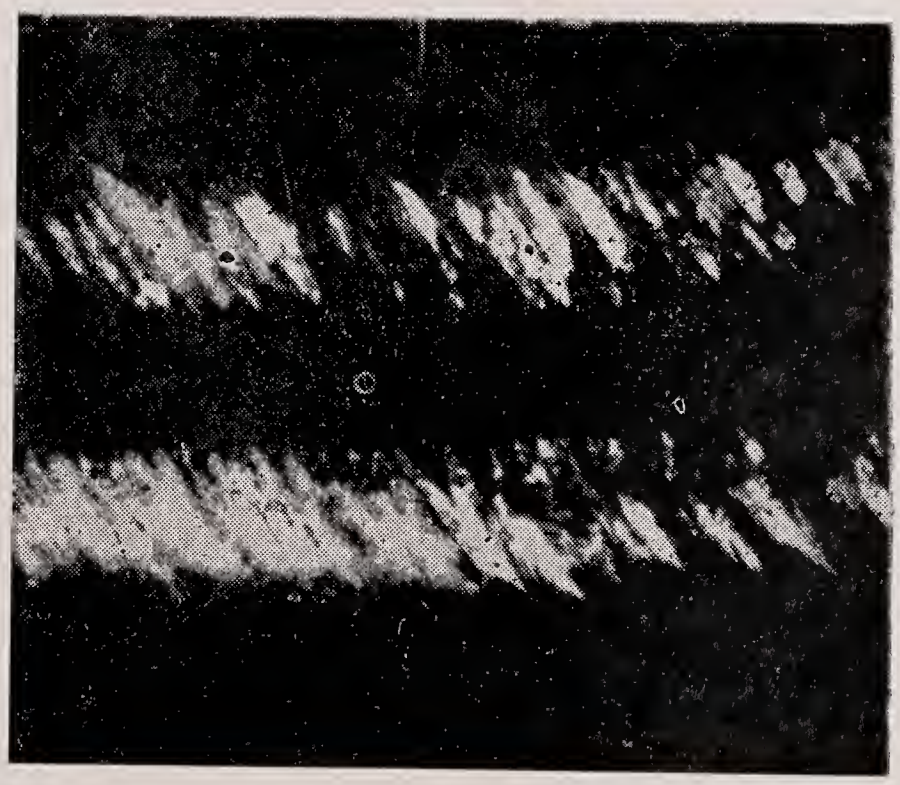

(c)

Figure 7. The interface phase in $\alpha + \beta$ titanium alloys. **b** and **c** are bright field and dark field micrographs of an fcc phase at the α/β interface of IMI 685 (Banerjee 1979).

Plate 4

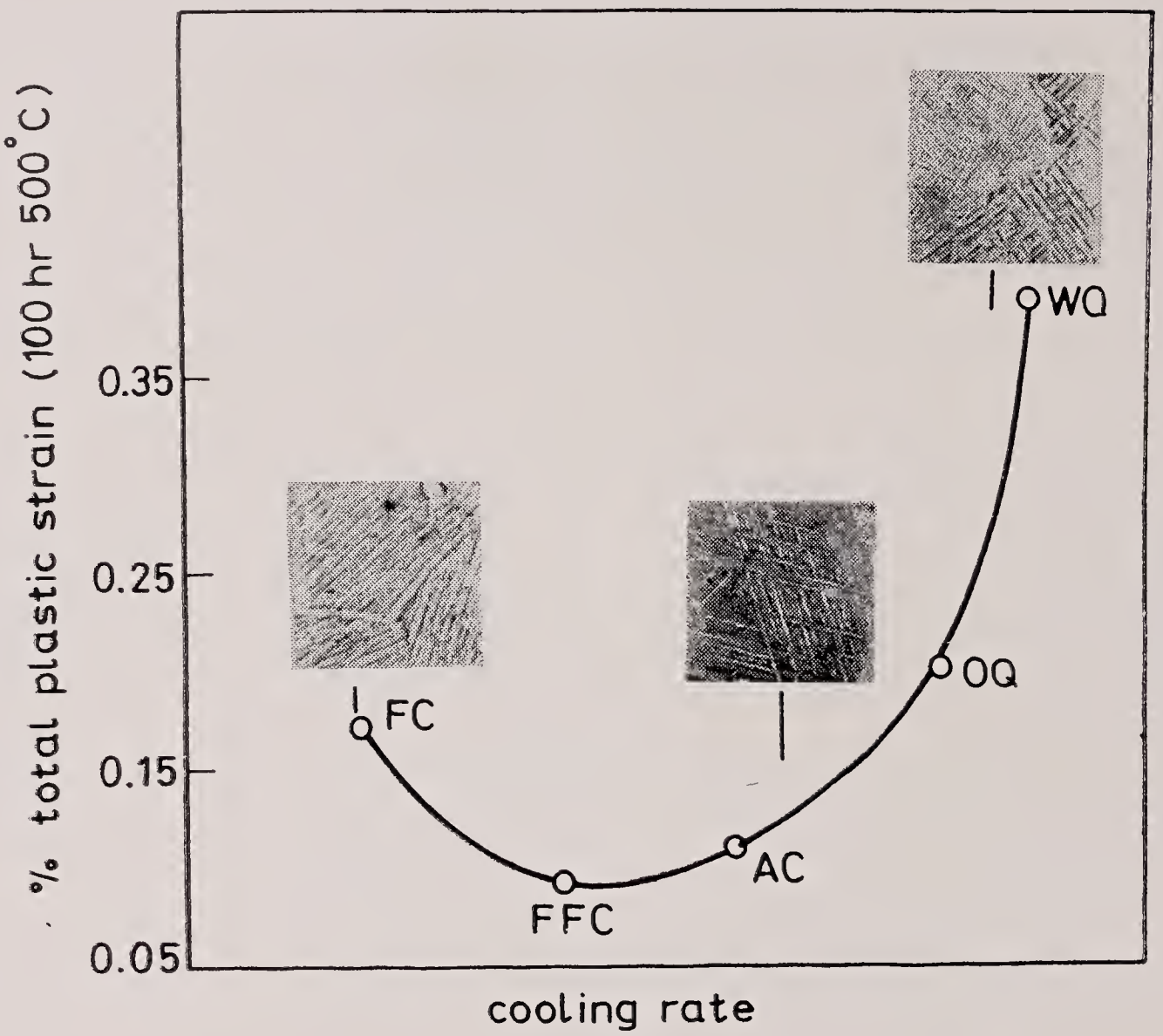

Figure 9. The effect of cooling rate after β solutionising on creep strain in IMI 685, after Blenkinsop *et al* (1976). FC—furnace cooled; FFC—fast furnace cooled: AC—air cool; OQ—oil quench; WQ—water quench.

Plate 5

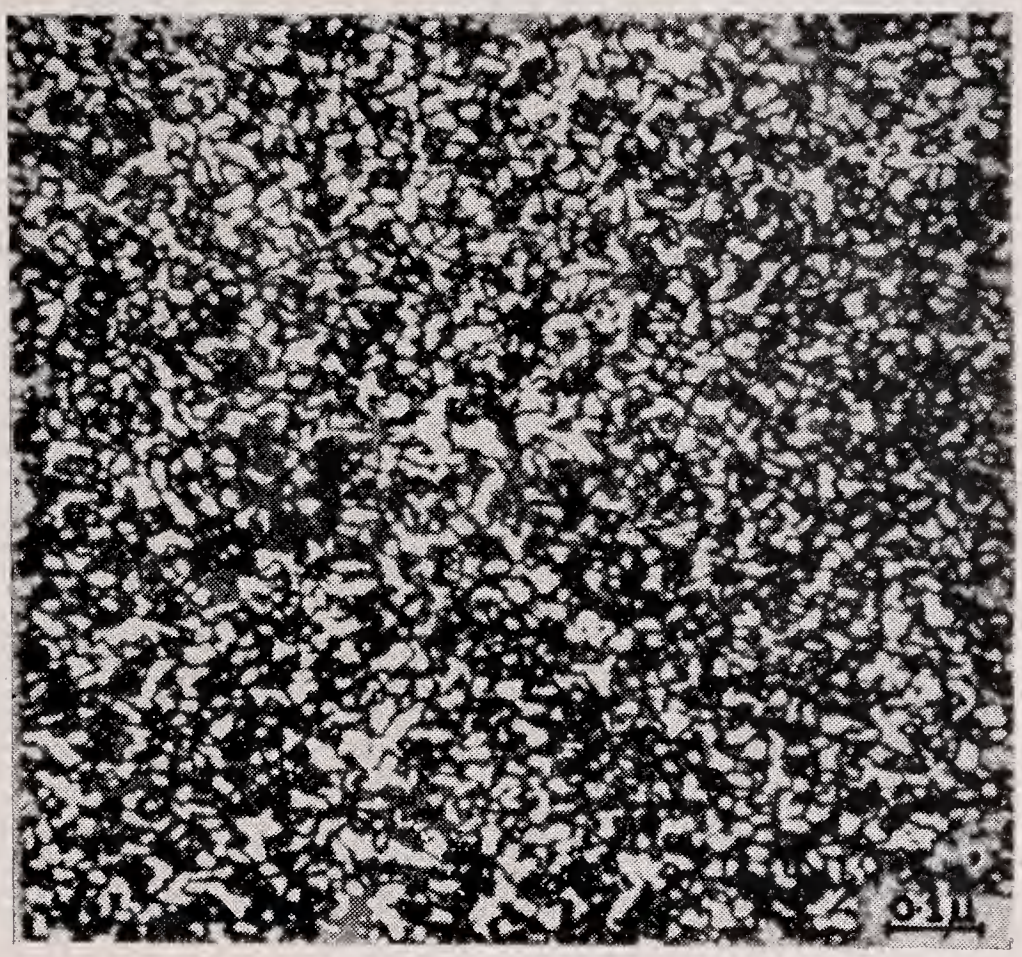

Figure 10. α-Titanium strengthened by second phases (**a**) TEM of Ti_3Al precipitates in a Ti-9wt% Al alloy (Banerjee & Mukherjee, 1980, unpublished research). (**b**) TEM of yttria particles in recrystallising α—Ti in a titanium-yttrium alloy hot-rolled and annealed at 900°C for 1 hr (Krishnan *et al* 1976).

Zirconium alloys in nuclear technology

R KRISHNAN and M K ASUNDI
Metallurgy Division, Bhabha Atomic Research Centre, Trombay, Bombay 400 085

MS received 17 October 1980

Abstract. This paper describes the historical development of zirconium and its alloys as structural materials for nuclear reactors. The various problems encountered in the early stages of the development of zircaloys and their performance in reactors operating presently are described in detail. The development of Zr-2·5% Nb alloys for pressure tube applications is discussed. The paper concludes with a detailed discussion on the development potential of zirconium alloys for high temperature applications and a brief account of the work carried out at Trombay in this field.

Keywords. Zirconium; zirconium alloys; structural materials; nuclear reactors; corrosion; high strength alloys.

1. Introduction

The development of zirconium metallurgy is essentially due to the nuclear industry, where zirconium alloys have come to be regarded as the proven structural material. This is primarily because of their unique combination of good corrosion resistance in water near 300°C and low capture cross-section for thermal neutrons (Douglass 1971). It is quite likely that the application of zirconium in the nuclear industry will remain its dominant use. This paper begins with an account of the present day use of zirconium alloys in the nuclear industry mainly to acquaint non-nuclear technologists with the various sizes, shapes and functions of such structural materials. Then the history of the development of presently accepted zirconium alloys—zircaloy-2 and zircaloy-4—is given some consideration. A discussion on the development of high-strength zirconium alloys follows and the paper concludes with a brief account of the work being done at Trombay.

2. Current applications

There are two types of water-cooled power reactors. In the first, the whole reactor core is enclosed in a large steel pressure vessel in which one fluid, usually ordinary water, is both the heat transfer medium and neutron moderator. Such a reactor is based on the pressurised water reactor (PWR) and boiling water reactor (BWR) concepts, where zirconium is used for the cladding tubes which encase the uranium dioxide fuel pellets. The reactor operating at Tarapur near Bombay is an example of the BWR reactor.

In the second, the pressure vessel is replaced by a large number of tubes each conveying either light or heavy water coolant over an individual fuel element. These

pressure tubes pass through a calandria tank containing cool, heavy water moderator. The pressure tube is separated from the surrounding calandria tube by a gas gap which insulates the moderator from the hot coolant. Operating reactors of this type are the pressurised heavy water-cooled CANDU-PHW and the boiling light water-cooled CANDU-BLW and the British steam-generating heavy water reactor SGHWR. The nuclear power station at Rana Pratap Sagar at Kota in Rajasthan is an example of the CANDU-PHW system. In these reactor systems, the fuel-cladding tubes, the pressure tubes and sometimes the calandria tubes are all made of zirconium alloy.

Fuel-cladding tubes are thin-walled (0·4 to 0·8 mm) and experience a complex sequence of heterogeneous tensile, creep and recovery strains during their operating life of 15,000 to 30,000 hr. The pressure tubes in CANDU reactors are 103 mm ID and the minimum wall thickness is in the range of 2·4 to 5·1 mm depending on the strength of the alloy and the operating conditions (Ross-Ross 1968). Tubes for the SGHWR are of 130 mm ID and a minimum wall thickness of 5 mm (Watkins & Cockady 1965). These pressure tubes are subjected to the full coolant pressure (55–60 bar in SGHWR, CANDU-BLW and 85–90 bar in CANDU-PHW) and coolant temperature of 200–300°C. Unlike the fuel-cladding tubes, these tubes experience a simple biaxial stress system with a hoop-to-axial stress ratio of approximately 2:1. The tubes must have very high integrity throughout a plant life perhaps exceeding 200,000 hr. Although failure can be tolerated and faulty tubes replaced, it is very expensive.

The zircaloy calandria tubes typically have a wall thickness of 1·24 mm and 107·7 mm ID, in a CANDU-PHW system. These tubes are generally fabricated from rolled sheets by seam welding. The demands made on zircaloy calandria tubes are less exacting than those made on fuel or pressure tubes (Cheadle 1977).

3. Historical development

The decision to use zirconium in a nuclear reactor was essentially due to Admiral Rickover of the US Navy (Rickover 1975). He was in charge of the development of nuclear-propelled ships and submarines. The reactor for navigation had necessarily to be compact and had to operate when the ship was rolling or pitching or at an angle, when the submarine was diving or surfacing. Thus a pressurised water reactor (PWR) was envisaged, and hence a metal which would withstand corrosion at high temperatures for long periods of time, which would maintain its integrity in an environment of intense radiation and which would not absorb neutrons required for the nuclear reaction, was needed. The availability of the metal in sufficient quantities and at reasonable cost would be the additional consideration. Stainless steel, beryllium and aluminium all had disadvantages which weighed against their use. Zirconium also did not appear promising as it was expensive and not produced in quantity. Initial tests with zirconium showed that it absorbed neutrons needed for the fission process. It was discovered later that naturally-occurring zirconium contained about 2% by weight of hafnium, which gave zirconium the high level of absorption cross-section for neutrons. Kaufman at MIT and Pomerance at Oak-Ridge came out with laboratory successes in separating hafnium from zirconium and showed that zirconium in its pure form absorbed only a few neutrons. These early promises

led Admiral Rickover to decide that zirconium would be the reference core structural material for the Mark I PWR in the Idaho prototype and for the Mark II reactor being built for the nuclear submarine, Nautilus.

Though the decision was taken by the U. S. Navy to use zirconium as the reactor structural material, no technical specifications had been elaborated. The only thing they knew was that the metal should be ' as pure as possible ' and the minimum strength limits were to be ' as strong as possible without increasing the hardness '.

Naturally, the choice fell on the crystal-bar process (also called the Van-Arkel-DeBoer Process) for the production of high-purity zirconium. This process is essentially a refining rather than a metal reduction technique. In this process zirconium tetra-iodide is formed at the surface of a bed of impure metallic zirconium maintained at low temperature (approximately 400°C) by reaction with free iodine and is decomposed at the surface of a hot (approximately 1400°C) filament, depositing pure zirconium on the filament and liberating iodine vapour to react again with the impure zirconium. The end product was designated as the ' crystal bar ' because of the bright surface and the external shape of the grains that grew on the filament.

When crystal bar zirconium was corrosion-tested in high temperature water autoclaves, it was found that corrosion-resistant material became black after testing, while non-corrosion resistant samples became white, the different appearances being related to the thickness and physical nature of the zirconium oxide corrosion product film. Initial experiments with crystal bar zirconium showed a bewildering variety of corrosion test behaviour. This led to the problem of detecting and measuring the culprit impurity elements in zirconium. It was found that if the refining process could be carried out under sufficiently ' antiseptic ' conditions, a reproducible high level of corrosion resistance could be obtained.

At this stage, the decision was taken to use a purer grade of sponge zirconium as the raw material (for crystal bar), which had then become possible by the Kroll process. In the Kroll process, zirconium tetrachloride vapour, prepurified by sublimation, is brought into contact with the reductant, molten magnesium, using precautions to exclude air during all critical operations. The use of this high-purity raw material coupled with improved operating practices and procedures resulted in an improved yield of corrosion-resistant product.

Every one connected with zirconium technology knew that continued purification of the product was not necessarily the correct path. In fact, it was then observed that the crystal bar stock received from two different sources did not behave in a similar manner. Contrary to expectations, it was found that the corrosion resistance of the purer material was lower than that of the impure crystal bar. It was argued that the pick-up of impurity elements like iron, chromium and nickel might be helpful in imparting corrosion resistance to zirconium. Even with intentional additives, zirconium showed poor corrosion resistance in the presence of nitrogen. It was ultimately decided that refining the Kroll sponge into crystal bar zirconium might not be the right step and thus the programme of development of Kroll-process sponge-base alloys was started.

4. Development of zircaloys

The first stage in the development of zirconium alloys was to identify those elements which improved the corrosion behaviour of Kroll sponge zirconium to a level apparently equivalent to that of the good quality crystal bar. These elements were tin, tantalum and niobium, which, in decreasing order of effectiveness, circumvented the damaging effect of the impurities present in the sponge then available. Tin as an alloying addition was selected for intensive investigation because it was most effective in imparting corrosion resistance without seriously affecting the neutron economy. The level of addition which at one time was as high as 5 wt% was reduced to 2·5 wt%, as a good compromise between corrosion resistance, strength and fabricability. This alloy was designated as zircaloy-1. Samples of zircaloy-1 were subjected to long-term high temperature water corrosion testing and soon a disturbing trend became noticeable. Instead of continuing to corrode at a decreasing rate with increasing time, the corrosion rate at a specific time (breakaway or transition time) increased and remained essentially constant thereafter. This transition time for zircaloy-1 was not much greater than the time at which unalloyed sponge would begin to show white non-adherent oxide corrosion product. Thus an immediate halt was called to the processing of zircaloy-1 and an urgent search for an alternative was started.

Around that period, the important effect of iron additives on the corrosion behaviour of zirconium had been established. In fact a melter in the Bettis fabrication shops had melted a zircaloy-1 ingot which had become contaminated with stainless steel and the resultant material proved to have an outstanding corrosion resistance. Subsequent experiments with nickel additives also confirmed its beneficial effect. Thus the next step was to choose an alloy composition that would confer major corrosion resistance and permit the use of the fabrication experience gained with zircaloy-1. Thus in selecting the composition, the iron content was nominally set at 0·15% mainly because of the range of iron present in the then available Kroll sponge. A nominal nickel level of 0·05% was chosen because of the beneficial effect of nickel on high temperature corrosion resistance. Chromium is picked up as an impurity from the stainless steel reacting vessels and thus its content was kept at 0·10%. For tin, unlike in zircaloy-1, a nominal level of 1·5%, which was found to be adequate to counteract the deleterious effects of nitrogen, was suggested. This new alloy composition, designated zircaloy-2, was found to have tensile properties equal to those of zircaloy-1 but much better high temperature corrosion resistance. Table 1 gives the alloying additions in zircaloys.

Table 1. Compositions of zircaloys

Alloy	Mean composition in weight %			
	Sn	Fe	Cr	Ni
Zircaloy-1	2·5	—	—	—
Zircaloy-2	1·5	0·12	0·10	0·05
Zircaloy-3	0·25	0·25	—	—
Zircaloy-4	1·50	0·22	0·10	—

Though zircaloy-2 performed satisfactorily, there was a fear that with increase in reactor core lifetimes, the detrimental effect of the high tin content of zircaloy-2 would reveal itself. In fact tin was originally added in zircaloy-1 with the belief that it was a good corrosion inhibitor, but this belief proved ill-founded. Thus it was decided to limit the tin content to the amount just necessary to counteract the nitrogen levels present in the sponge, as well as to tramp nitrogen levels picked up during melting. So Zr with 0·25% Sn and 0·25% Fe was recommended as the most corrosion resistant composition in the family of zirconium alloys. This alloy was designated as zircaloy-3.

During corrosion testing, zircaloy-3 showed a network of fine white corrosion indications, which were identified as stringers of Fe-Cr intermetallic compounds. The stringers formed as a result of the fabrication of the material in the two-phase alpha plus beta region which exaggerated the agglomeration of the intermetallic phases. Though the formation of stringers could be avoided by altering the fabrication temperatures, it was found that with the introduction of the vacuum arc melting of zirconium (as compared to the induction melting practised earlier), the stringers vanished totally. However, the lower mechanical properties of this alloy compared to zircaloy-2 contributed to its abandonment.

Right at that time, the far-reaching effect of hydrogen on the mechanical properties of zirconium and its alloys became more evident, when notched bar impact testing was initiated. Samples that yielded low impact values showed the presence of crystallographically-oriented zirconium hydride platelets which were absent in normally behaving samples. Analysis of zircaloy specimens showed the inter-relations between hydrogen content and embrittlement in notched impact tests. It was estimated that the tolerance level of hydrogen in zirconium could be around 250 ppm. During investigations on eutectic diffusion bonding techniques for the development of plate type fuel elements, it was found that when zircaloy-2 sheets were coated with nickel, hydrogen absorption increased considerably. A suggestion was then made to eliminate the 0·05% nickel addition in zircaloy-2 and this alloy then came to be referred to as ' nickel-free zircaloy-2 '. This alloy was however found to have inadequate corrosion resistance. The choice was then to increase the iron content. Thus a new composition of the alloy with 0·18 to 0·24% Fe, 0·10% Cr and 1·5% Sn was arrived at and this was designated as zircaloy-4. It was found to retain almost as good steam corrosion resistance as zircaloy-2 while exhibiting one-half of the hydrogen absorption.

5. Performance of zircaloys

The zirconium alloys—zircaloy-2 and zircaloy-4 have become the widely accepted structural material in operating reactors at present. Typical properties of zircaloy-2 at 300°C are shown in table 2 (McDonald 1971). The differences in the ratios of yield-to-tensile, transverse-to-longitudinal, and transverse-to-biaxial strengths partly reflect differences in the crystallographic textures of these alloys. The highly anisotropic deformation behaviour of zirconium leads to pronounced textures in fabricated components, depending on the alloy and the fabrication and heat-treatment history. For zircaloy tubes, the texture is such as to inhibit wall-thinning during biaxial stressing, resulting in large circumferential expansion and some axial contraction prior to

Table 2. Typical tensile and burst properties of zircaloy-2 pressure tube material at 300°C

Alloy autoclaved 72 hr, 400°C	Test	0·2% yield stress 10^3 psi	UTS 10^3 psi	Elongation %
15–20% cold drawn zircaloy-2 103 mm diameter	Long.	45	54	26
	Trans.	50	52	23
	Burst	60	63	26–36
30% cold drawn zircaloy-2 130 mm diameter	Long	51	54	20
	Trans.	48	50	20
	Burst	—	67	20

failure. Thus the texture developed in zircaloys is beneficial to biaxial ductility and to biaxial relative to uniaxial strength. This implies that the fuel tube with such a texture will bulge considerably before it fails. As a result, considerable progress has been made in elucidating the formation of textures and their role in deformation behaviour. However, the desired degree of control of texture formation appears to be difficult.

The major problem in the use of zirconium alloys is hydrogen absorption (from the metal/water reaction) and consequent embrittlement (Ells 1968). It was believed that this could impose the main design limit on zirconium alloys. However, it is now clear that severe embrittlement under tensile loading conditions is observed mainly near room temperature and when the hydride plates are oriented near normal to the applied stress. The conditions producing preferential orientation of plates have been identified and can be controlled. In tubes, circumferential alignment of plates parallel to the operating hoop stress is ensured by avoiding unsupported sinking operations during fabrication. However, a desire to limit the total hydrogen uptake to 300–400 ppm is still a consideration in the selection and processing of zirconium alloys. In this context, it should be stated that stress-assisted hydride precipitation (in service) may lead to severe embrittlement problems at room temperature.

Zirconium alloys harden under irradiation and the extent of hardening depends on the prior metallurgical structure, including dislocation arrangements and the nature and distribution of second-phase precipitates (Williams 1970). The main manifestation of embrittlement by hydride and irradiation, is in a loss of fracture toughness of notched, impacted specimens. The transition temperature from low to high energy absorption is shifted from below room temperature to 200–300°C.

The most important effect of fast neutron irradiation on zircaloys is the increase of the secondary creep rate at 220–350°C by 5 to 10 times. This phenomenon had not been recognised in the PWR pressure tube design but has been studied in great detail in recent years (Nicohls & Watkins 1968; Watkins 1970; Ibrahim 1969).

6. Development of Zr-Nb alloys

In the development of improved alloys for 300°C application, a fair amount of success has been achieved with Zr-2·5 wt% Nb alloy, particularly for pressure tube

applications. It has been used in two conditions (Douglass 1971; Watkins & Cockady 1965), hot extruded at 840°C, then cold-drawn 15–20% or hot extruded, quenched from 880°C, cold-drawn 3–15% and aged for 24 hr at 500°C. In the latter form, it is the strongest of the established zirconium alloys. However, unlike zircaloy-2, in which texture strengthening has played a decisive role by increasing circumferential ductility under biaxially stressed conditions, in Zr-2·5 Nb alloys, the texutres developed in the two conditions appear less attractive and in fact can nullify some of the gain from their higher uniaxial strengths. In this case, wall-thinning is enhanced during biaxial stressing and failure occurs at low circumferential strain. Further, Zr-2·5 Nb solution treated and quenched from the beta phase field is particularly susceptible to irradiation embrittlement (Ells & Williams 1969). Another observation is that the heat-treated Zr-2·5 Nb tubes creep in-pile almost twice as fast as the cold-worked material, in spite of higher uniaxial and biaxial strengths and slower out-of-pile uniaxial creep. This is an important consideration in alloy development. This observation is explained on the basis of texture in these tubes (Ibrahim 1969): grains have basal plane poles parallel to the tube axis, which is absent in the cold-worked tubes. In addition to the texture effect, the neutron flux appears to have a greater effect on heat-treated as compared to cold-worked Zr-2·5 Nb. Since deformation by irradiation creep and growth is known to be dependent on the metallurgical structure (texture, dislocation density and grain structure) of the pressure tubes, ways of altering the structure by modifying the fabrication route and heat treatment schedules have to be found, to improve the stability of the alloy under irradiation (Fleck 1969).

7. High temperature applications

Considering the performance of zircaloy-2 and 4, and Zr-2·5Nb, in presently operating reactors, it is very unlikely that these alloys can be surpassed in either corrosion resistance or neutron capture cross-section at 300°C. The creep strength of these alloys however diminishes rather rapidly with increasing temperature and above 350°C becomes the criterion for selecting a design stress. To improve the station efficiency and the capital cost, the temperature of the coolant tube must be raised significantly to temperatures above 450°C. The prospects for development of zirconium alloys for high temperature applications are quite promising and attempts are being made in several laboratories to develop such high temperature alloys both for cladding and pressure tube applications.

For pressure tube applications, it is necessary to have an alloy which has the following properties at a temperature of at least 450°C (Thomas 1969)

(i) a minimum stress of 210 to 280 MPa (34 to 45 kpsi) as one third of the UTS,
(ii) a maximum creep rate of 10^{-7} hr^{-1} after 5000 hr at a stress of 62 to 74 MPa (10 to 12 kpsi),
(iii) a minimum of 155 MPa (25 kpsi) as the stress to rupture in 100,000 hr,
(iv) a neutron capture cross-section not significantly greater than that of zircaloy-2.

However, most of the high-strength zirconium alloys have poor corrosion resistance and it would be necessary to clad these with a corrosion resistant alloy. This

would obviously mean complex production processes and costs but then this would have to be balanced against the rewards of higher efficiency.

There are many similarities between the physical properties and metallurgy of titanium and zirconium and their alloys. Alpha titanium has a higher shear modulus than alpha zirconium. The Young's modulus values also show an advantage over titanium. These differences indicate that titanium alloys may develop slightly higher tensile and creep strengths than zirconium alloys. The other important parameter to be considered is the self-diffusion coefficient. Calculated diffusivities suggest that alpha zirconium may have a higher creep resistance than alpha titanium in the temperature range where steady-state creep occurs by dislocation climb, a diffusion-controlled process. However, such comparisons are only of limited value when alloying additions are made to the metal, and structural differences are introduced by fabrication processes. However, the data support the view that zirconium alloys should be capable of providing mechanical properties similar to those of titanium alloys.

Initial experiments on the effect of several alloying additions on the properties of zirconium have shown that to achieve high yield strength at 500°C, the most effective additives are the alpha stabilisers Al and Sn and the beta stabilisers Mo and Nb. Al and Sn are reasonably soluble in zirconium compared with other alloying elements and provide solution strengthening upto about 850°C. Mo and Nb have only a limited solubility in zirconium and their strengthening effect is due to a dispersion of fine precipitates which can be achieved by quenching and ageing treatments. Increased strengthening is obtained in ternary alloys containing combinations of alpha+beta stabilizing additions so that both solution and precipitation hardening contribute. Table 3 gives the tensile properties of some selected ternary and quarternary alloys of zirconium and indicates the systems worth studying (Thomas 1969). It appears that the required objectives may be reached by the ones containing 3 to 4 wt% Sn and 1 to 2 wt% Mo or the ones containing 1 to 2 wt% Al and 0·5 to 1·5 wt% Mo. The creep behaviour of these will have to be taken into account in the final selection.

The alloying additions that can be made to zirconium have to face the constraint of not increasing the neutron capture cross-section. The increment in cross-section for each 1% of alloying addition (Thomas 1969) indicates the penalty in neutrons associated with each element (table 4).

In the development of a new alloy, in addition to strength requirements, one major concern is corrosion resistance. Thus even though Al is a more effective strengthener

Table 3. Tensile properties of various zirconium alloys, normalised to 450°C

Alloy composition wt%	Treatment	UTS kpsi	% Elongation
Zr-3 Al-3 Sn	Annealed at 650°C	82	10
Zr-3 Sn-1·5 Mo	Air cooled from 900°C	96	10
Zr-3·7 Sn-2 Mo	β-quenched/aged	110	10
Zr-5Nb-2 Sn	($\alpha+\beta$) quenched/aged 8 hr at 482°C	130	5
Zr-1·5 Al-1·5 Mo	Hot worked and annealed at 790°C	70	20
Zr-3 Al-1·5 Sn-1·5 Mo	Hot worked and annealed at 790°C	90	20
Zr-1·5 Al-0·5 Mo	($\alpha+\beta$) quenched	112	2

Table 4. Increase in thermal neutron capture cross-sections of zirconium due to 1 wt% alloy addition

Element	Cross-section increase Σ_c cm² per cm³
Sn	0·00019
Mo	0·00089
Nb	0·00037
V	0·00335
Sb	0·00174
Si	0·00114
Al	0·00012

than Sn, zirconium alloys containing Al have extremely poor corrosion resistance. (In fact, the composition specifications of zircaloys indicate a maximum permissible level of 75 ppm for aluminium). Thus a Zr-Sn alloy could be a preferred base. Further, limits set by neutron capture cross-section, solubility limits of the individual elements and the prospect that good creep strength would be promoted by a combination of alloying elements that give rise to intermetallic compounds, has led the Canadian Group to suggest the following range of alloys for testing as pressure tube materials: Zr with 2 to 4 wt% Sn, 0·5 to 1·5 wt% Mo, 0·5 to 2 wt% Nb, 0·5 to 1·5 wt% Al and 0·5 wt% Si. The precaution to be taken in this case is that such alloys cannot be used unclad.

It would be appropriate at this stage to refer to the work of scientists from UK and Scandinavia on the development of new zirconium cladding alloys (the ' SCANUK ' alloys) (Tyzack *et al* 1977). The reasons given by them for their choice of alloy composition and the results obtained by them can be stated as follows:

Improvements in corrosion resistance and mechanical properties would be obtained by alloying zirconium with elements selected from group V A and VI A and possibly group VIII A of the Periodic Table. Another alloying element of proven worth in the context of 300°C fuel element operation is tin, particularly in counteracting the effects of nitrogen. Tin appears to maintain a mildly beneficial influence on corrosion upto $\sim$350°C but in 450°C steam and at higher temperatures, particularly at high pressures, its presence becomes significantly detrimental. The binary alloy systems of zirconium with the elements of the above 3 groups are either of the form in which the β phase extends over the whole composition range with no intermetallic phases (*e.g.* Nb, Ta) or of the eutectoid type including intermetallic phases (*e.g.* V, Cr, Mo, W, Fe, Co, Ni, Cu). The solubility of these elements in alpha zirconium is very limited and the likelihood of appreciable solid solution hardening is very small. However, one could take advantage of the possibility of dispersion strengthening by eutectoid decomposition since both the tensile strength and creep resistance can be improved at temperatures $\leqslant$ 500°C by precipitation of finely-dispersed intermetallic phases. The hardening introduced in this way can be greater than that due to solid solution. A further approach would be to base the strengthening process upon a martensitic transformation. It is thus possible to produce the desired tensile or creep strength by controlling the range of alloying additions, but designing for ductility is much more difficult and a reasonable balance between tensile strength and ductility is to be made. Another aspect which should be borne in mind is that any high

temperature homogenising treatments followed by quenching and tempering should be done at the billet stage rather than on the tubing to avoid distortions in the finished product.

The ' Scanuk ' alloy compositions are shown in table 5. The texture of the Scanuk alloy tubes was similar to that of commercial zircaloy-2 tubes. The UTS values at 25°C for the different alloys are also given in table 5. One can see that the mechanical properties of ' Scanuk ' alloys compared favourably with those of zircaloy-2 and in some respects represented an improvement. These alloys had higher strengths than zircaloy-2 in the temperature range of 250–400°C and the decrease in strength with increase in temperature was much less severe—alloys 3 and 4 were the best in the sense that their strength at 300–400°C exceeded that of zircaloy-2 by some 15–25%. Alloy 4 showed more resistance to hydrogen absorption than zircaloy-2. The hydride precipitates were very small and were found to be circumferentially oriented. All these alloys showed markedly lower oxidation rates than zircaloy-2. It may be possible to improve the ' Scanuk ' alloys with further study and optimisation.

8. Zirconium metallurgy at Trombay

The Metallurgy Division, Bhabha Atomic Research Centre, Trombay, Bombay has been carrying out programmes on zirconium and its alloys, mainly to understand the physical and mechanical properties of pure zirconium and its alloys, which would lead to the development of newer alloys with improved properties for nuclear applications (Asundi 1973). A brief resume of the work carried out at Trombay is given below.

In zirconium alloys, microstructural control by thermal and mechanical processing is of particular importance since the selection of alloy composition is severely restricted by neutron absorption considerations. In general, the most suitable mode of strengthening for a given alloy system is dictated largely by the relevant phase diagram. Thus age hardening could be employed in systems where the solid solubility is strongly temperature-dependent, martensitic strengthening in alloys which undergo an allotropic transformation, hardening through the creation of the numerous interfaces associated with a two-phase lamellar aggregate in eutectoid systems, and order hardening in systems where an ordering reaction occurs. Fortunately, it is possible to invoke one or the other of the known methods of microstructural strengthening in

Table 5. Scanuk alloy compositions and UTS values at 25°C

Alloy	Nb	Fe	Sn	Cr	Mo	Ni	Oxygen	UTS at 25°C kg/mm²
1	0·91	0·026	—	0·01	0·005	0·005	0·100	47
2	0·93	0·038	0·073	0·01	0·005	0·005	0·096	45
3	1·12	0·045	0·060	0·49	0·005	0·005	0·126	50
4	0·52	0·036	0·060	0·49	0·004	0·005	0·134	47
5	0·49	0·037	0·047	0·01	0·280	0·005	0·097	47
6	0·58	0·044	0·060	0·32	0·220	0·005	0·125	48

dilute zirconium alloys of compositions compatible with nuclear applications. The wide variety of microstructures that can be produced in a number of zirconium base systems has been examined in our laboratory and the influence of these structures on the mechanical properties has also been investigated.

Zirconium-rich alloys undergo a martensitic transformation during quenching from the high temperature beta phase. The morphology and the fine structure of the martensite has been found to be strongly dependent on the alloy composition and the transformation temperature. In our laboratory, the microstructure associated (figures 1 and 2, plate 1) with the martensitic transformation has been analysed for zirconium of different levels of purity and of a host of binary systems like Zr-Nb (Banerjee & Krishnan 1971), Zr-Ti (Banerjee & Krishnan 1973), Zr-Ta (Mukhopadhyay *et al* 1978), Zr-Al (Mukhopadhyay *et al* 1979a) Zr-Cu (Wadekar *et al* 1979) and Zr-Cr (Mukhopadhyay *et al* 1979 b). These studies have revealed that the M_s temperature is the most important parameter in determining the nature of the martensite product in terms of morphology and substructure. It has been possible, on the basis of the extensive work carried out in our laboratory, to propose a generalisation that in zirconium base alloys a lath morphology and a dislocated substructure result when the M_s temperature exceeds 650–700°C, while lower M_s temperatures lead to the formation of internally-twinned acicular martensites. The amount of a particular alloying addition necessary to bring about the transition naturally depends on the effectiveness of that particular element in depressing the M_s temperature. Mechanical property investigations have revealed that though both types of martensites are characterised by high densities of interfaces, only the internally twinned plate martensite could lead to a very substantial strengthening due to the martensite microstructure *per se* (Banerjee *et al* 1978). This is because in lath martensites, the lath boundaries are small angle boundaries which do not act as effective barriers to the propagation of deformation fronts.

Even when a martensitic structure enhances the strength of an alloy, it is important to examine the temperature regime over which this strengthening is effective. To test this, the martensites obtained in the various alloys studied have been tempered at different temperatures, including those pertinent to reactor operation. It has been found that in most cases, the martensite structure remains more or less unaltered upto about 500°C and contributes to the strength of the alloy (Banerjee *et al* 1976). Moreover, precipitation (whether of an intermetallic phase or of the beta phase) occurs preferentially along the martensitic interfaces during tempering so that even when the martensite undergoes recovery and recrystallisation, the distribution of closely spaced precipitates continues to act as a barrier to the propagation of slip and twinning (figures 3 and 4, plate 1).

While studying the precipitation of the beta phase in Zr-Nb martensites during tempering, an anomaly has been observed in that at temperatures close to but below the monotectoid temperature, a non-equilibrium zirconium-rich, bcc phase precipitates in preference to the equilibrium, niobium-rich bcc phase. A similar observation has also been made in the Zr-Ta system which also shows a monotectoid reaction. To resolve this anomaly, extensive computer calculations have been made to generate free energy versus composition data (Menon *et al* 1979). With the aid of these, a thermodynamic rationale has been arrived at for explaining the apparently anomalous precipitation behaviour. In fact it has been possible, on the basis of these calculations, to predict the complete sequence of phase transformations, over the entire

composition range, for Zr-Nb alloys (Menon *et al* 1978). The correctness of these predictions has been verified by experiments conducted here and elsewhere.

It has been mentioned earlier that apart from producing a martensitic structure, another promising method of generating-numerous closely spaced interfaces in zirconium alloys would involve the occurrence of the eutectoid transformation on a fine scale. The eutectoid reaction has been studied in the Zr-Cu (Mukhopadhyay *et al* 1979c) and the Zr-Cr systems (Mukhopadhyay *et al* 1979d). The former, where a phase separation cannot be prevented even during rapid beta quenching, is the prototype of a class of eutectoid systems known as active eutectoids (figure 5, plate 2). These are quite prevalent in zirconium and titanium alloy systems. On the basis of the work carried out in our laboratory, a viable mechanism for the active eutectoid decomposition, invoking the formation of an ordered transient phase, has been proposed.

There has been strong emphasis recently on considering the feasibility of alloys based on the intermetallic phase Zr_3 Al for reactor applications. The microstructural features associated with Zr_3 Al formation in Zr-Al alloys have been studied in our laboratory (Mukhopadhyay *et al* 1979e). In the course of these investigations, it has been possible to establish that the formation of equilibrium Zr_3Al in hypostoichiometric alloys is preceded by the formation of a metastable ordered phase which has a hexagonal crystal structure. The precipitation mode of the equilibrium Zr_3Al phase in beta quenched and aged alloys has been found to be of the discontinuous type (figure 6a–c, plate 2). The mechanical properties associated with different types of matrix-precipitate aggregates have been examined and analysed (Raman *et al* 1978).

Zirconium alloys have been investigated extensively by internal friction studies mainly to understand the behaviour of interstitial and substitutional solutes in the lattice (Mishra & Asundi 1972). These studies have shown that the activation energy for the jump of an oxygen atom from one octahedral position to the other is dependdent upon the size of the substitutional solute. The larger the difference in size between the solute and the solvent atom, the smaller the activation energy. This indicates that the elastic interactions between the various species of atoms are far more predominant than the electronic interactions. It also suggests that oxygen, though easily soluble in zirconium, has a tendency to cluster around the substitutional solute, presumably to minimise the local elastic distortions accompanying such point defects (Mishra & Asundi 1970). The behaviour of nitrogen is rather interesting. Only substitutional solute atoms which are larger than the zirconium atom can cause internal friction peaks. This again shows that clustering around the substitutional solutes occurs because the nitrogen atom is larger than the oxygen atom. It is apparent that those solute atoms which are larger than the zirconium atom have a tendency to attract nitrogen atoms for the minimisation of the elastic distortion. By a purely elastic interaction phenomenon, one can explain the role of tin in zirconium, in counteracting the deleterious effect of nitrogen on corrosion by a scavenging mechanism.

Irradiation-hardening studies have been conducted on an experimental alloy, Zr-0·5% Nb-1·0% Cr upto a fluence of 10^{18} to 18^{19} n/cm^2. The recovery of radiation hardening has been found to take place in the range of 200–400°C in well-annealed specimens, while for the quenched and aged alloy, this range was pushed upto 500–700°C. The microstructure of the quenched and aged alloy showed precipitation of chromium (Ray & Sharma 1967).

9. Conclusion

Zircaloy-2 has proved its worth as an excellent structural material particularly in pressurised reducing conditions. Under oxygenated boiling conditions, however, it appears to be susceptible to localised accelerated attack particularly in regions of flow discontinuity. Considering the excellent performance of zircaloy-2 is it possible to develop an alternate material which would find ready adoption? This might happen if some major improvements in alloy properties are achieved. On the other hand, it seems more likely that a change could be based on a study of some serious operational shortcomings in the properties of zircaloy-2.

Efforts have been made to develop high temperature zirconium alloys; but it appears now that all ideas of using nuclear superheated steam appear to have been abandoned. As such, R & D activities in this area do not find much support.

Finally, fibre reinforcement is the subject of active materials research but has not yet made a significant impression on zirconium metallurgy. Efforts in this direction may prove useful.

If one looks at the research being carried out by material scientists in areas like ion-implantation and laser glazing, it appears that it may be possible to develop high-strength zirconium alloys which could be laser-treated to have an outer amorphous layer which could lead to improved corrosion resistance. However, it may be necessary to restrict the operating temperature to say less than 550°C, to avoid crystallisation of the amorphous layer.

The authors would like to take this opportunity to thank Sri C V Sundaram, Head, Metallurgy Division, for his keen interest and encouragement in the programmes pertaining to zirconium metallurgy.

References

Asundi M K 1973 *The Banaras Metall.* **5**
Banerjee S & Krishnan R 1971 *Acta Metall.* **19** 1317
Banerjee S & Krishnan R 1973 *Metall. Trans.* **4** 1811
Banerjee S, Vijayakar S J & Krishnan R 1976 *J. Nuclear Mater.* **62** 229
Banerjee S, Vijayakar S J & Krishnan R 1978 *Acta Metall.* **26** 1815
Cheadle B A 1977 in *Zirconium in the nuclear industry* ASTM-STP 633, American Society for Testing Materials
Douglass D L 1971 *The metallurgy of zirconium*, Atomic Energy Review Supplement
Ells C E 1968 *J. Nuclear Mater.* **28** 129
Ells C E & Williams C D 1969 *Trans. Met. Soc. AIME* **245** 1321
Fleck R G 1979 *Can. Met. Q.* **18** 65
Ibrahim E F 1969 in *Applications related phenomena in Zr and its alloys* ASTM-STP 458, American Society for Testing Materials
McDonald N R 1971 *Proceedings of the Australian Institute of Metals Conference*
Menon E S K, Banerjee S & Krishnan R 1978 *Metall. Trans.* **A9** 1213
Menon E S K, Mukhopadhyay P, Banerjee S & Krishnan R 1979 *Z. Metallkunde* **10** 168
Mishra S & Asundi M K 1970 BARC Report No. 458
Mishra S & Asundi M K 1972 *Can. Met. Q.* **11** 69
Mukhopadhyayay P, Menon E S K, Banerjee S & Krishnan R 1978 *Z. Metallkunde* **69** 728
Mukhopadhyay P, Raman V, Banerjee S & Krishnan R 1979a *J. Nuclear Mater.* **82** 227

Mukhopadhyay P, Raman V, Banerjee S & Krishnan R 1979b *J. Mater. Sci.* **14** 1389
Mukhopadhyay P, Menon E S K, Banerjee S & Krishnan R 1979c *Metall. Trans.* **A10** 1071
Mukhopadhyay P, Raman V, Banerjee S & Krishnan R 1979d *J. Mater. Sci.* **14** 1398
Mukhopadhyay P, Raman V, Banerjee S & Krishnan R 1979e *J. Nucl. Mater.* **82** 227
Nichols R W & Watkins B 1968 *Proceedings of the Conference on SGHWR*, British Nuclear Society, London
Raman V, Mukhopadhyayay P & Banerjee S 1978 *Mater. Sci. Engg.* **36** 105
Ray S & Sharma B D 1967 BARC Report No. 300
Rickover H G 1975 in *History of development of zirconium alloys for use in nuclear reactors*, United States Energy Research and Development Administration NR:D
Ross-Ross P A 1968 Atomic Energy of Canada Limited AECL-3136
Thomas W R 1969 Atomic Energy of Canada Limited AECL-3362
Tyzack C, Hurst P, Slattery G F, Trowse F W, Garlick A, Sumerling R, Stuttard A, Videm K, Lunde L, Warren M, Tolksdorf E, Tarkdea P & Forsten J 1977 *J. Nuclear Mater.* **66** 163
Wadekar S L, Raman V & Mukhopadhyay P 1979 *J. Mater. Sci.* **14** 407
Watkins B 1970 UKAEA Report TRG 1966 (C)
Watkins B & Cockady R E 1965 UKAEA Report TRG 998 (C)
Williams C D 1970 *Reactor Technol.* **13** 147

Plate 1

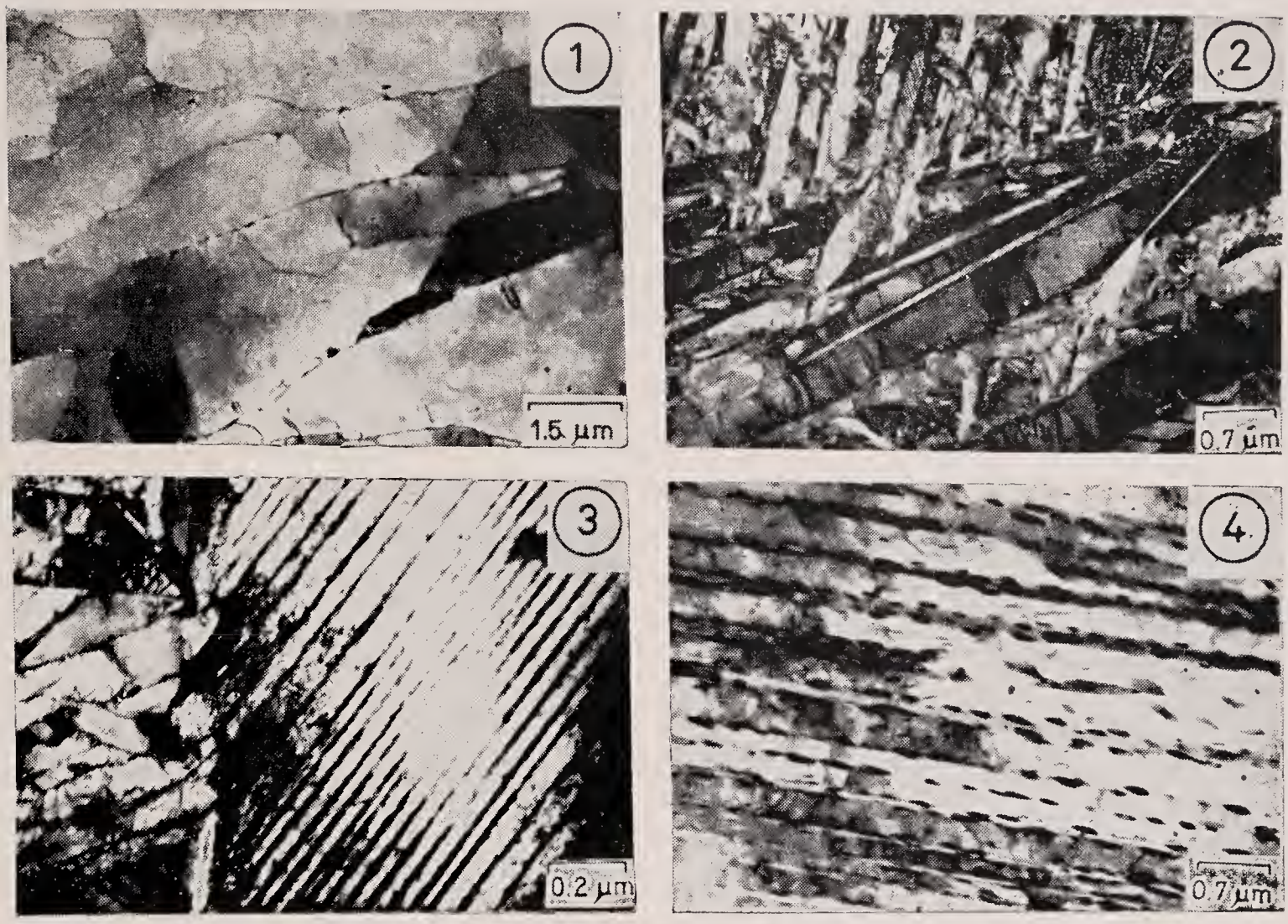

Figures 1 to 4. **1.** Lath martensite structure in β quenched Zr-0·1 Cu alloy. **2.** Acicular martensite structure in β quenched Zr-15 Ti alloy. **3.** Internally twinned plate martensite in β quenched Zr-2·5 Nb alloy. **4.** Precipitation along twin boundaries in tempered Zr-2·5 Nb alloy martensite.

Plate 2

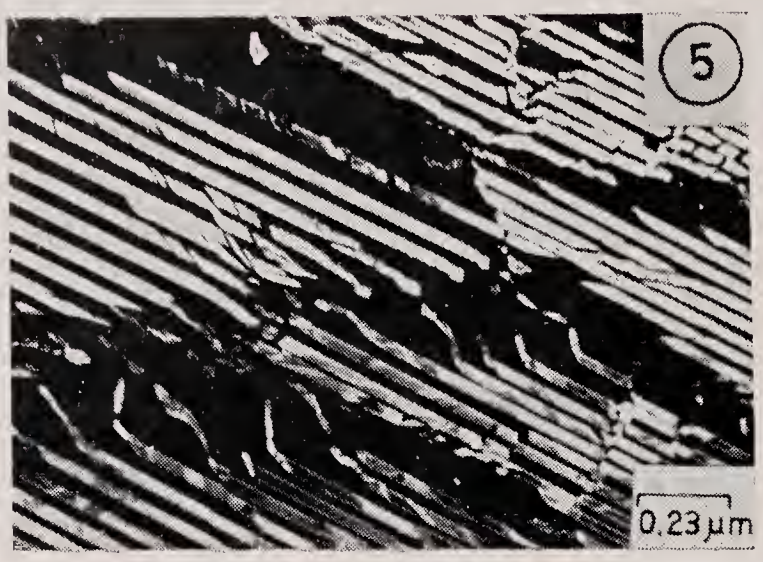

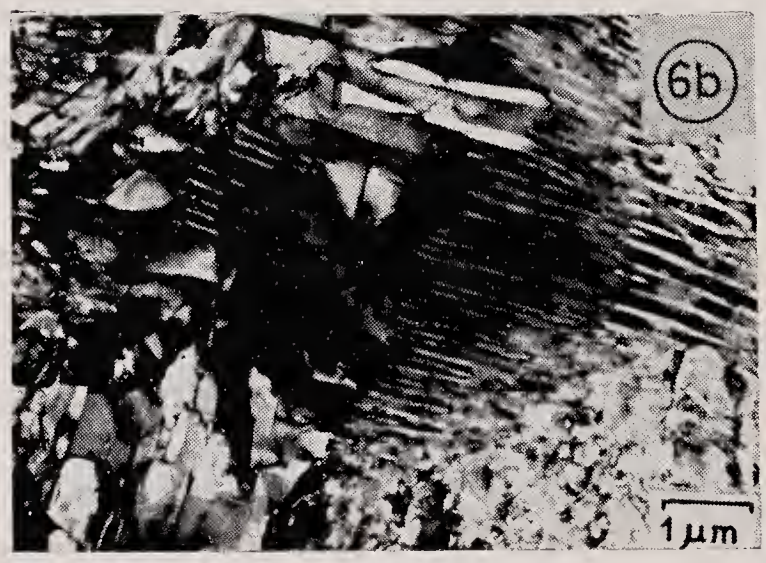

Figures 5 and 6. **5.** Lamellar two phase structure in β quenched Zr-1·6 Cu alloy (dark field). **6.** **(a)** Dislocated lath martensite in β quenched Zr-4·6 Al Alloy. **(b)** Lamellar structure comprising α and Zr_3 Al lamellae in Zı-4·6 Al alloy after ageing. **(c)** Two-phase structure comprising α grains and spheriodised Zr_3 Al crystals in Zr-4·6 Al alloy after prolonged ageing.

AUTHOR INDEX

SUBJECT INDEX

ACADEMY PUBLICATIONS IN ENGINEERING SCIENCES

General Editor: R. Narasimha

Volume 1. The Aryabhata Project
Edited by U. R. Rao, K. Kasturirangan

Volume 2. Computer Simulation
Edited by N. Seshagiri, R. Narasimha

Volume 3. Rural Technology
Edited by A. K. N. Reddy

Volume 4. Alloy Design
Edited by S. Ranganathan, V. S. Arunachalam, R. W. Cahn